



## **Biomass properties and enzyme-lignin interactions in the enzymatic cellulose degradation of hydrothermally pretreated lignocellulosic grass feedstocks**

**Djajadi, Demi Tristan**

*Publication date:*  
2018

*Document Version*  
Publisher's PDF, also known as Version of record

[Link back to DTU Orbit](#)

*Citation (APA):*

Djajadi, D. T. (2018). Biomass properties and enzyme-lignin interactions in the enzymatic cellulose degradation of hydrothermally pretreated lignocellulosic grass feedstocks. Kgs. Lyngby: Technical University of Denmark (DTU).

---

### **General rights**

Copyright and moral rights for the publications made accessible in the public portal are retained by the authors and/or other copyright owners and it is a condition of accessing publications that users recognise and abide by the legal requirements associated with these rights.

- Users may download and print one copy of any publication from the public portal for the purpose of private study or research.
- You may not further distribute the material or use it for any profit-making activity or commercial gain
- You may freely distribute the URL identifying the publication in the public portal

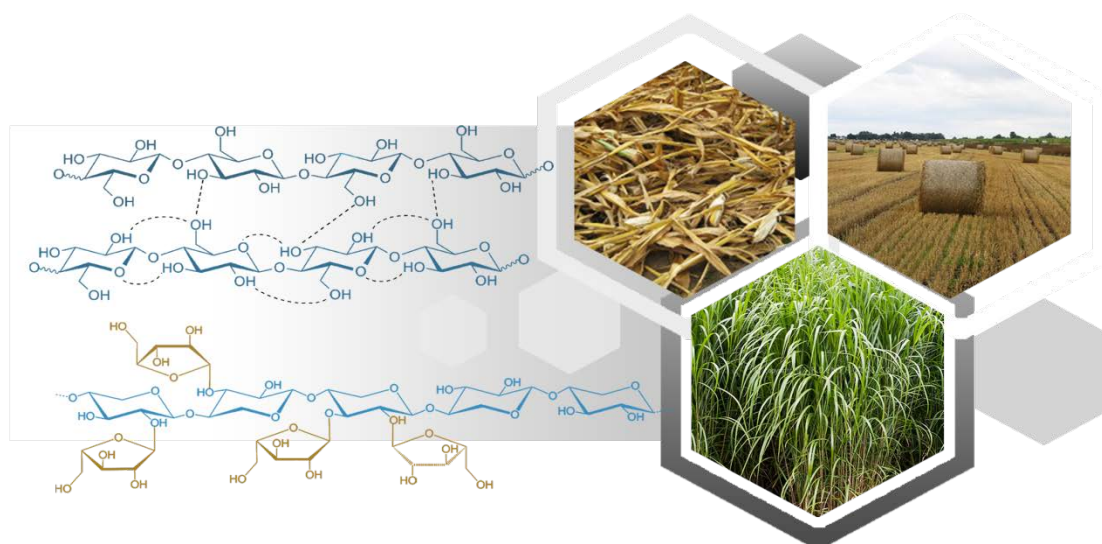
If you believe that this document breaches copyright please contact us providing details, and we will remove access to the work immediately and investigate your claim.

---

Biomass properties and enzyme-lignin interactions in the enzymatic cellulose degradation of hydrothermally pretreated lignocellulosic grass feedstocks

Demi Tristan Djajadi

April 2018



## Supervisors

Professor Anne S. Meyer

Center for Bioprocess Engineering (BioEng)

Department of Chemical and Biochemical Engineering,

Technical University of Denmark

Associate Professor Manuel Pinelo

Center for Bioprocess Engineering (BioEng)

Department of Chemical and Biochemical Engineering,

Technical University of Denmark

Associate Professor Henning Jørgensen

Section for Plant and Soil Sciences

Department of Plant and Environmental Sciences

University of Copenhagen

## **Department of Chemical and Biochemical Engineering**

Center for Bioprocess Engineering (BioEng)

Technical University of Denmark

2800 Kongens Lyngby

Denmark

## **Preface**

The thesis is submitted as to fulfil the prerequisite in accomplishing the PhD education and training at Technical University of Denmark (DTU). The work is supported by BioValue SPIR, Strategic Platform for Innovation and Research on value added products from biomass, which is co-funded by The Innovation Fund Denmark, case no: 0603 - 00522B. The work presented in the thesis was conducted largely at the Center for Bioprocess Engineering (BioEng), Department of Chemical and Biochemical Engineering, DTU, during the periods of February 2015 – April 2018. Part of the thesis work was conducted during external research stay for three months at Biomass Processing Technologies Team, Technical Research Center of Finland (VTT).

I am most grateful for the thorough supervision by my main supervisor Professor Anne S. Meyer which has been a great impetus towards the grand finale. Her persevering pursuits in testing of hypotheses and data interpretation as well as breadth of scientific aptitudes have been great sources of inspiration during the study. I am also very thankful for the welcoming support by Henning Jørgensen who had been my initial main supervisor and has continued to provide many insights in the work with his superb analytical mind. Similarly, I am also very thankful for the supervision and support by Manuel Pinelo who has been providing many excellent suggestions to the work, but importantly also for showing me how to be an exemplary teacher in the class.

I would also like to extend my gratitude to many of my co-authors and co-workers throughout the study, many of whom were from the BioValue SPIR network. From University of Copenhagen (KU), I would like to thank Anders Jensen, Aleksander R. Hansen and Lisbeth Thygesen for introducing me to new analytical methods and productive discussion resulting in the published works. From Aarhus University (AU), I would like to thank Mads M. Jensen and Marianne Glasius for the many analytical works and insights as well as the fruitful collaboration

with the lignin work. From VTT, I would express my earnest gratitude to Jenni Rahikainen, Kristiina Kruus and Ville Pihlajaniemi for kindly hosting the research stay and for being involved in planning of the work. Miriam Kellock from VTT is also thanked for providing the spruce lignin. I also thank my Erasmus master's thesis students, Marlene Oliveira and Rita Couto, who were very helpful in both advancing the PhD study and preparing me to supervise others.

I would also thank the BioValue SPIR for providing strategic network for exchange of knowledge, especially under the management and coordination of Jane Lindedam from KU in the platform and Anne Stenbæk from Novozymes A/S in Project 3. For technical support, I would thank the many scientists, technicians and lab trainees I have come across in the past years. Annette E. Jensen was particularly helpful with the HPLC system used in the study. I also thank Biomass Science and Technology group at KU of Professor Claus Felby which hosted me during the collaborative works and provided both engaging discussions as well as cordial hospitality.

Furthermore, I would also thank the colleagues from DTU BioEng for creating conducive working environment inside office and lab, while refreshing outside. I would also thank friends and communities in Copenhagen area, especially CAYAC, COMPANIONS and PPI DK, for providing support in various aspects of life in Denmark. I am also grateful for the focal support from Emeritus Professor Liisa Viikari which has launched and supported me on the research track since the master's studies in Finland. Last but not least, I am indebted to my family for their endless support during the PhD study, especially from my mother Cendrawati and sister Della Djajadi. I dedicate this work to my late father Iqbal Djajadi, a paragon of idealist researcher.

*-Ad maiorem Dei gloriam-*

Kongens Lyngby, April 2018

Demi T. Djajadi

## Table of Contents

Preface.....	ii
Table of Contents.....	iv
Summary.....	vi
Dansk sammendrag.....	x
List of publications.....	xiii
List of abbreviations.....	xiv
Chapter 1 – Introduction and literature review.....	1
1.1 Drivers for research and development in bioprocessing of lignocellulosic biomass.....	1
1.2 Lignocellulosic biomass and its recalcitrance.....	2
1.3 Hydrothermal pretreatment and its effect on lignocellulosic biomass components.....	6
1.4 Cellulolytic enzymes and enzymatic cellulose degradation.....	9
1.5 Adsorption of cellulases and cellulolytic enzyme mixture components on lignocellulose.....	12
1.6 Retardation of enzymatic cellulose degradation by lignin.....	17
Chapter 2 – Background, hypotheses and objectives.....	21
2.1 Overall background, aim and hypothesis.....	21
2.2 Specific background, hypotheses and objectives.....	22
Chapter 3 – Materials and methods.....	25
3.1 Biomass feedstocks and lignocellulosic substrate.....	25
3.2 Cellulolytic enzymes.....	25
3.3 Isolation of lignin-rich residues (LRRs).....	26
3.4 Hydrolysis experiments.....	26

3.5 Adsorption experiments .....	26
3.6 Analytical methods in biomass and lignin characterization.....	27
3.7 General overview of the PhD study .....	29
Chapter 4 – Biomass properties that correlate to the digestibility of hydrothermally pretreated grass biomass feedstocks (Paper I) .....	31
4.1 Hypotheses .....	31
4.2 Experimental considerations .....	31
4.3 The digestibility of hydrothermally pretreated grass biomass feedstocks .....	32
4.4 Changes in bulk composition of biomass after hydrothermal pretreatment .....	33
4.5 Changes in surface properties of biomass after hydrothermal pretreatment.....	35
4.6 Correlating biomass digestibility with bulk composition and surface properties.....	37
4.7 Concluding remarks and significance of study .....	38
Chapter 5 – The role of lignin from hydrothermally pretreated grass biomass feedstocks in retarding enzymatic cellulose degradation (Paper II).....	40
5.1 Hypotheses .....	40
5.2 Experimental considerations .....	40
5.3 Changes in the physical and chemical properties of the lignin after HTP .....	42
5.4 Role of lignin in retarding enzymatic cellulose degradation by inducing irreversible non-productive adsorption.....	45
5.5 Role of lignin in retarding enzymatic cellulose degradation by acting as a physical barrier ..	46
5.6 Concluding remarks and significance of study .....	48
Chapter 6 – The nature of the binding of monocomponent cellulases on lignin isolated from hydrothermally pretreated lignocellulosic biomass (Paper III).....	50
6.1 Hypotheses .....	50

6.2 Experimental considerations .....	50
6.3 Binding affinity of the monocomponent cellulases on LRRs .....	51
6.4 Reversibility of the adsorption of the monocomponent cellulases on LRRs .....	53
6.5 Competitive binding of the monocomponent cellulases on LRRs.....	56
6.6 Concluding remarks and significance of study .....	58
Chapter 7 – Synthesis and reflection.....	59
7.1 Biomass properties and digestibility .....	59
7.2 Enzyme-lignin interaction.....	62
7.3 Lignin as physical barrier.....	67
Chapter 8 – Conclusions and future perspectives .....	72
8.1 Conclusions.....	72
8.2 Future perspectives .....	73
References.....	74
Appendix A .....	95
Appendix B .....	98
Appendix C .....	99
Appendix D.....	102
Appendix E .....	104

PAPERS

Paper I

Paper II

Paper III



## Summary

Utilization of lignocellulosic biomass as renewable source of fuels, chemicals and materials under the biorefinery scheme offers sustainable option as compared to total reliance on using fossil fuels, which has been pointed as the culprit behind global warming and climate change. Hydrothermal pretreatment (HTP) of lignocellulosic biomass followed by enzymatic hydrolysis to produce monosaccharides have been developed mainly to produce fuel ethanol, yet the process is also meant to initiate the biorefining of biomass to produce platform monosaccharides and other chemicals. However, the process still suffers from the need to use high enzyme loading to produce reasonable product yield due to the inherent recalcitrance of lignocellulosic biomass. Research in optimizing the utilization lignocellulosic biomass is important to support the growing world's population.

This PhD study aimed to understand the factors that affect enzymatic cellulose degradation of lignocellulosic biomass that were processed using the latest technology. Biomass properties and enzyme-lignin interactions were of particular focus. Hydrothermally pretreated key grass biomass feedstocks (corn, *Miscanthus*, wheat) were investigated for their biomass properties to find correlation with the ensuing enzymatic digestibility using commercial cellulolytic enzyme mixture (**Paper I**). The corresponding lignin-rich residues (LRRs) from these pretreated biomass feedstocks were characterized for chemical and physical characteristics and studied for enzyme-lignin interaction and to assess the factors that retard enzymatic cellulose degradation (**Paper II**). A selected grass LRR from the previous work (wheat straw) and another LRR from hydrothermally pretreated softwood (spruce) were used to investigate the adsorption kinetics of monocomponent cellulases on lignin (**Paper III**).

The tested grass biomass feedstocks had different digestibility after HTP at different severity levels (**Paper I**). However, these differences were not reflected in their bulk composition,

especially the extent of hemicellulose removal after HTP. Biomass wettability correlated well with digestibility and showed that the least digestible biomass had the lowest wettability after HTP. Analyses using attenuated total reflectance-Fourier transform infrared (ATR-FTIR) spectroscopy revealed that the least digestible biomass had the highest apparent surface abundance (ASA) of hemicellulose and lignin. Therefore, surface properties correlated better to the digestibility of hydrothermally pretreated grass biomass feedstocks compared to bulk composition (**Paper I**).

The components of the commercial cellulolytic enzyme mixture adsorbed similarly on the isolated LRRs regardless of severity levels and biomass feedstocks, in agreement with minor chemical changes in lignin after HTP (**Paper II**). The LRRs also did not retard the enzymatic hydrolysis of model cellulose, suggesting reversible adsorption. The residual carbohydrates in the LRRs were not accessible to the enzymes and were not traceable to the surface of the LRRs using ATR-FTIR analysis. These data suggested that the enzymatic cellulose degradation was retarded by increasing presence of lignin in the surface of the biomass particles which can be affected by the physical properties of lignin. Thus lignin retards enzymatic cellulose degradation by acting as physical barrier rather than inducing non-productive adsorption (**Paper II**).

The radiolabeled monocomponent cellulases had different binding affinity on the tested LRRs and fitted well with Langmuir model which assumes reversible binding (**Paper III**). Adsorption experiments with dilution at early and late time points revealed that the adsorption of the enzymes did not exhibit hysteresis. Kinetic modelling of the experiments showed that reversible adsorption behavior can fully explain the observed data, though pointed at extended reaction time and elevated temperature (40-50°C) the binding can turn irreversible. Furthermore, the adsorption parameters  $K_{ads}$  and  $B_{max}$  from both Langmuir fitting and kinetic modelling were in agreement. Simultaneous adsorption of different cellulases displayed competition and fitted well with

Langmuir model. These observations gave compelling evidence of reversible binding of cellulases on lignin (**Paper III**).

All in all the results above provided new understandings of biomass surface, lignin, and the interactions of cellulases with biomass, which should be considered and pursued further in order to advance the understanding in lignocellulosic biomass conversion.

## Dansk sammendrag

Brug af lignocellulosisk biomasse som en vedvarende kilde til produktion af brændsel, kemikalier og materialer i bioraffinaderi systemer er mere bæredygtigt end brug af fossile brændstoffer, som desuden har ført til global opvarmning og klima forandringer. Hydrotermisk forbehandling (HFB) af lignocellulosisk biomasse efterfulgt af enzymatisk hydrolyse til produktion af monosaccharider er primært udviklet med henblik på at producere ethanol, men er også udgangspunkt for bioraffinering af biomassen til produktion af platform monosaccharider og andre stoffer. Imidlertid kræves en stor mængde enzymer til fremstilling af et rimeligt udbytte af produkter på grund af den lignocellulosiske biomasses evne til at modstå nedbrydning. Optimering af udnyttelsen af lignocellulosisk biomasses er vigtig for at støtte verdens befolknings vækst.

Dette ph.d.-studie havde til formål at forstå de faktorer som påvirker enzymatisk cellulose nedbrydning af (hydrotermisk forbehandlet) lignocellulosisk biomasse. Studiet var fokuseret på biomassens egenskaber og enzym-lignin interaktioner. Hydrotermisk forbehandlede biomasser fra vigtige græstyper (majs, *Mischantus*, hvede) blev undersøgt for at identificere de biomasse-egenskaber som korrelerer med enzymatisk nedbrydning under brug af en kommerciel cellulolytisk enzymblanding (**Artikel I**). De korresponderende lignin-rige restprodukter (LRRer) fra disse forbehandlede biomasser blev karakteriseret for at evaluere deres kemiske og fysiske egenskaber og undersøgt for at identificere deres interaktioner med enzymer og for at forstå, hvordan lignin forsinker enzymatisk cellulose nedbrydning (**Artikel II**). LRR fra hvedestrå og et andet LRR fra hydrotermisk forbehandlet nåletræ (gran) blev undersøgt at udrede adsorptionskinetikken for monokomponente cellulaser på lignin (**Artikel III**).

De undersøgte græs-biomasser blev nedbrudt enzymatisk i forskellig grad efter hydrotermisk forbehandling med forskellige severity-grader (**Artikel I**). Til gengæld blev disse

forskelligheder ikke afspejlet i biomassernes bulk sammensætning, herunder især ikke i graden af hemicellulosefjernelse efter HFB. Biomassernes befugtningsgrad korrelerede fint med den enzymatiske nedbrydning og viste, at den mindst fordøjelige biomasse havde den laveste befugtningsgrad efter HFB. Analyser med Fourier transform infrarød (FTIR) spektroskopi viste, at den mindst fordøjelige biomasse havde de højeste mængder hemicellulose og lignin på overfladen. Derfor korrelerede overfladens egenskaber bedre med fordøjelighed af de forbehandlede græs-biomasser end bulk sammensætningen (**Artikel I**).

De enzym-komponenter fra den kommercielle cellulolytiske enzymblanding adsorberede på samme måde på de isolerede LRRer uafhængigt af severity-grad og biomassetype, hvilket passede med, at der kun var små ændringer i ligninen efter den hydrotermiske forbehandling (**Artikel II**). Tilstedeværelsen af LRRer forsinkede ikke den enzymatisk hydrolyse af model cellulose, hvilket kunne indikere reversibel adsorption af enzymerne på lignin. De resterende kulhydrater i LRRer var ikke tilgængelige for enzymerne og kunne ikke spores til overfladen af LRRerne ved anvendelse af FTIR analyse. Disse data tydede derfor på forsinkelse af enzymatisk cellulose nedbrydning som resultat af stigende lignin indhold på overfladen af biomasse partiklerne, og dermed en påvirkning fra lignins fysiske egenskaber. Derfor forsinkes lignin enzymatisk cellulose nedbrydning ved at fungere som fysisk barriere og ikke ved at inducere non-produktiv enzym-adsorption (**Artikel II**).

Radioaktivt mærkede monokomponente cellulaser havde forskellige bindingsaffiniteter på de undersøgte LRRer hvilket passede godt med en Langmuir adsorptions model som antager reversibel adsorption (**Artikel III**). Adsorptions-eksperimenter med fortynding på tidlige og sene tidspunkter under inkuberingen af enzymerne med LRRerne viste at adsorptionen af enzymerne ikke udviste hysteresis. Kinetisk modellering af resultaterne viste, at reversibel adsorption kunne forklare de observerede data. Dog tydede data på, at adsorption kan blive

irreversibel over forlænget reaktionstid ved høj temperatur (40-50°C). Ydermere var adsorptionsparametre ( $K_{ads}$  og  $B_{max}$ ) fra både Langmuir isotherm og kinetisk modellering i overensstemmelse. Samtidig adsorption af forskellige cellulaser udviste konkurrence og fittede godt med Langmuir modellering. Disse observationer blev tolket som overbevisende bevis på, at cellulaser adsorberer reversibelt på lignin (**Artikel III**).

Alt i alt gav resultaterne ny forståelse af betydningen af biomassens overflade, lignin, og cellulasers interaktion med biomasse, som bør overvejes og forfølges yderligere for at fremme forståelsen af enzymatisk omdannelse af lignocellulosisk biomasse.

## List of publications

The thesis is based on the following original research papers which are referred to in the text as **Papers I-III**. **Papers I** and **II** are open access articles and reproduced under Creative Commons Attribution License 4.0. Unpublished manuscript of **Paper III** is also presented.

- I. **Djajadi DT**, Hansen AR, Jensen A, Thygesen LG, Pinelo M, Meyer AS, Jørgensen H. Surface properties correlate to the digestibility of hydrothermally pretreated lignocellulosic Poaceae biomass feedstocks. *Biotechnol. Biofuels* 2017; 10:49.
- II. **Djajadi DT**, Jensen MM, Oliveira M, Jensen A, Thygesen LG, Pinelo M, Glasius M, Jørgensen H, Meyer AS. Lignin from hydrothermally pretreated grass biomass retards enzymatic cellulose degradation by acting as a physical barrier rather than by inducing non-productive adsorption of enzymes. *Biotechnol. Biofuels* 2018; 11:85.
- III. **Djajadi DT**†, Pihlajaniemi V†, Rahikainen J, Kruus K, Meyer AS. Cellulases adsorb reversibly on biomass lignin. Submitted to *Biotechnol. Bioeng.*

†: Equal contribution

Other publications which are not included in the thesis:

- IV. Jensen MM, **Djajadi DT**, Torri C, Rasmussen HB, Madsen RB, Venturrini E, Vassura I, Becker J, Iversen BB, Meyer AS, Jørgensen H, Fabbri D, Glasius M. Hydrothermal liquefaction of enzymatic hydrolysis lignin – Biomass pretreatment severity affects lignin valorization. *ACS Sustain. Chem. Eng.* DOI: 10.1021/acssuschemeng.7b04338.
- V. Wilkens C, Holck J, **Djajadi DT**, Brask J, Pilgaard B, Krogh KBRM, Meyer AS, Lange L. Discovery of a new bacterial xylanolytic triple domain enzyme complex targeted at feruloylated arabinoxylan degradation. Submitted to *Biotechnol. Bioeng.*

## List of abbreviations

ANOVA	analysis of variance
ASA	apparent surface abundance
ATR-FTIR	attenuated total reflectance – Fourier transform infrared
BGL	$\beta$ -glucosidase
CAM	contact angle measurement
CBH	cellobiohydrolase
CoMPP	comprehensive microarray polymer profiling
CS	corn stover
DM	dry matter
EG	endoglucanase
GPC	gel permeation chromatography
HPLC	high performance liquid chromatography
HSQC	heteronuclear single quantum coherence
HTP	hydrothermal pretreatment
LRR	lignin-rich residues
MS	<i>Miscanthus</i> $\times$ <i>giganteus</i> stalks
M <sub>w</sub>	molecular weight
NMR	nuclear magnetic resonance
Py-GC-MS	pyrolysis – gas chromatography – mass spectrometry
SDS-PAGE	sodium dodecyl sulfate – polyacrylamide gel electrophoresis
UV	ultraviolet
WS	wheat straw



## **Chapter 1 – Introduction and literature review**

### ***1.1 Drivers for research and development in bioprocessing of lignocellulosic biomass***

Utilization of lignocellulosic biomass for bioenergy and other (biorefinery) products offers an alternative to the use of fossil fuels that are considered as the culprit behind global warming and climate change issues. Unlike crude oil, lignocellulosic biomass is abundant in wide range of geographical distribution, mostly in the form of terrestrial plants and products derived from them. Furthermore it is renewable and its use recycles carbon in the atmosphere instead of adding those locked in Earth's crust for many geological periods. Fuel ethanol produced from thermochemical pretreatment and biological processing lignocellulosic biomass has been championed as a solution for the problem with high oil price [1,2]. It has lower carbon emissions than gasoline and can be blended with gasoline for use in current distribution infrastructure and internal combustion engines of road vehicles [1]. A typical setup of operation in producing lignocellulosic ethanol involves pretreatment of lignocellulosic biomass by steam. This is then followed by enzymatic digestion to release the monosaccharides constituent in the biomass. The monosaccharides, especially glucose, are then fermented by yeast to produce ethanol which is then purified prior to use [3,4].

Nowadays, several commercial lignocellulosic ethanol plants have been built and have been operating [5]. However, many were recently forced to shut down due to the plummeting price of crude oil, though the constructions began at the time when the price of crude oil was high [6]. In order to be cost competitive with the low oil price, several improvements need to be made. An inherent challenge in the process is the slow and energy intensive processing of lignocellulosic biomass due to its natural recalcitrance towards degradation [7]. In the currently applied technology at commercial scale, one key challenge is the huge enzyme loading that is still needed to degrade biomass to monosaccharides [8], which impacts to the cost of ethanol or any resulting products.

Nevertheless, apart from liquid fuels, the growing society also need food, chemicals and materials without relying too much on fossil fuels which can also affect the environment negatively. In this case, lignocellulosic biomass has the great potential to be used as substrate in biorefinery process where multiple array of products can be produced in equivalence to that of classical oil refinery [9]. This is especially true in agricultural and forestry sectors where the lignocellulosic wastes produced are not yet being utilized optimally. Such utilization will allow improved economy and resource efficiency, as in principle, no waste will ever be produced in a given economic process, a term now known as circular economy [10]. In an ideal futuristic circular economy, a standard farm does not only produce the intended crops or food products, but also energy, fuels, chemicals and materials. In order to achieve what seemingly look like utopian self-sufficient societies, more research and development are needed in the processing of lignocellulosic biomass. Otherwise, reality will give a hard hit as humankind enters 22<sup>nd</sup> century with abundant population yet meagre resources.

### ***1.2 Lignocellulosic biomass and its recalcitrance***

Lignocellulosic biomass, largely in the form of terrestrial plant cell wall, is the most abundant organic material on Earth with approximate annual production of 150-170 x 10<sup>9</sup> Mg. Yet only about 2% of this amount being used annually worldwide, mostly in the form of wood for energy, timber, pulp and paper [11]. Being also renewable, it makes an excellent raw material for production of fuels, chemicals and materials. Lignocellulosic biomass comprises of woody plants along with the wood products formed such as hardwood, softwood, chips, pellet, briquette, sawdust as well as herbaceous and agriculture residues such as grasses, straws, husks, hulls, stalks, cobs, bagasse [12].

Agricultural residues from cereal crops are of most interest since they are produced as part of the food production process and residue per crop ratio of most of them is one or above [13].

This means a lot of residues were produced in the processing of crops. Among the many cereal crops cultivated, corn and wheat are the ones with the more equal geographic distribution. Oat and barley are more predominant in Europe, sugarcane in Asia and South America, whereas rice is almost exclusively grown in Asia [13]. Alternatively, fast growing perennial grasses with C4 metabolic pathway such as *Miscanthus* and switchgrass are also attractive feedstocks being studied across the globe, especially for fuel ethanol. This is due to their ability to grow in marginal lands, requiring little water and fertilization while they can be harvested whole year round with high yields [14]. They have been suggested as ideal feedstocks for sustainable cellulosic biofuels production with minimal environmental impacts when grown as native species in marginal lands [15]. Despite their differences, all lignocellulosic biomasses share common features in their cell wall.

The plant cell wall of lignocellulosic biomass exists in several layers known as primary wall, middle lamella and secondary wall [16,17] (Fig. 1.1). Primary walls are formed during cell growth while secondary walls are formed after growth ceased. The plant cell walls are bound and connected by the middle lamella [11,17]. The composition and formation of the layers depend on the plant species. In woody biomass, the primary wall is degraded before the formation of secondary wall. In grasses, the secondary wall is deposited inside the primary wall [18]. Regardless, due to its thickness, the secondary walls comprise the bulk of plant cell wall, especially in woody plants [11]. However, they constitute at least 50% of cell wall mass in stems and leaves of grasses [18]. The major components of plant cell wall of lignocellulosic biomass are cellulose (40.6-51.2%), hemicellulose (28.5-37.2%) and lignin (13.6-28.1%) [11].

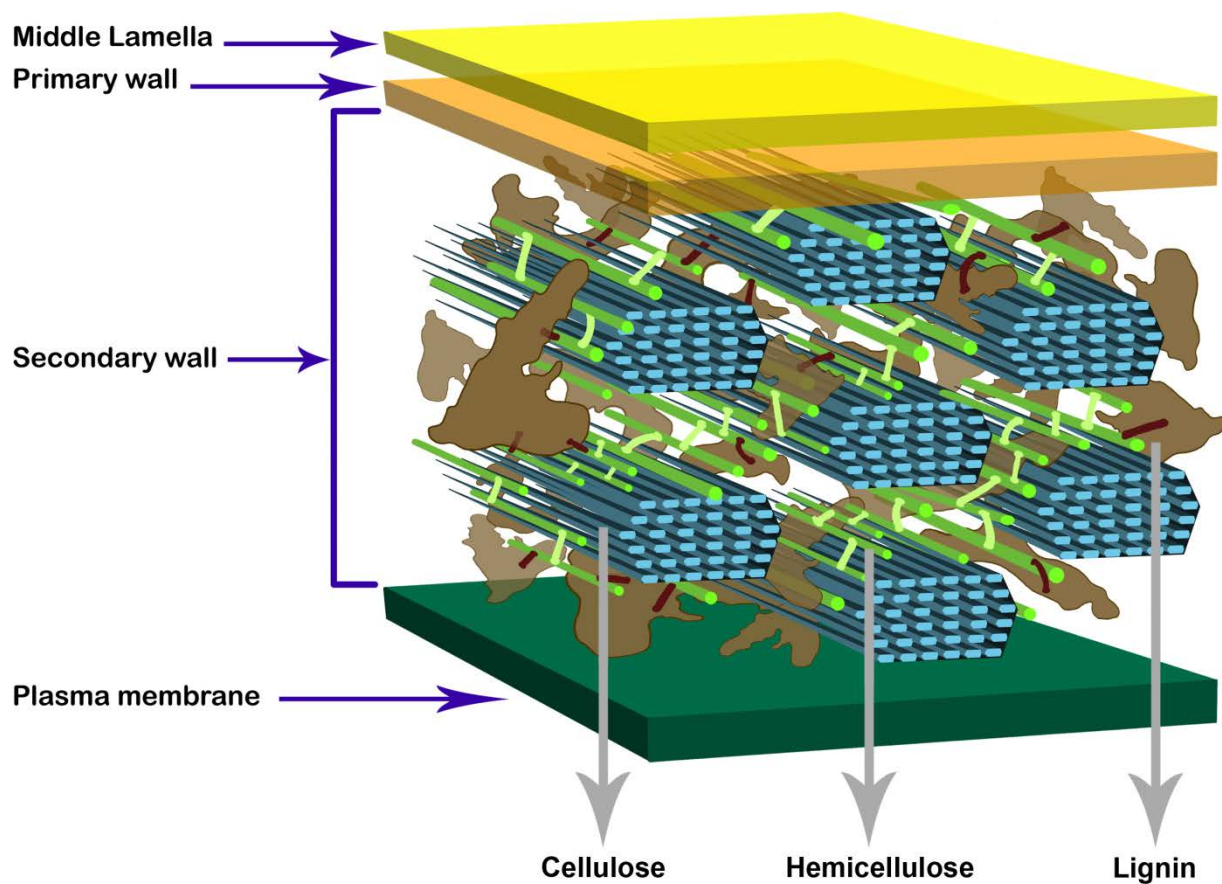


Fig. 1.1 Simplified structure of plant cell wall in grasses, highlighting the layers and the major components in the secondary wall. The cross-links between hemicellulose chains and between hemicellulose and lignin, which form parts of lignin-carbohydrate complexes (LCCs), were shown in different colors. Figure adapted based on information and depiction from references [19–21].

Cellulose is a linear homopolymer of  $\beta$ -D-glucose units with  $\beta$ -1,4 glycosidic linkages. About 24-36 of the glucan chains are packed together and aggregated to form cellulose microfibrils of 2.4-5 nm through intra- and intermolecular hydrogen bonds [17,19,22]. The arrangement has made cellulose to be highly crystalline, insoluble and resistant to enzymatic attacks with a native degree of polymerization in the order of  $\sim$ 5000-15,000 [23]. In nature, crystalline cellulose is known to exist as two variants of polymorphs, one-chained triclinic  $I_{\alpha}$  and two-chained

monoclinic  $I_{\beta}$  that are packed in parallel arrangement [24]. During the growth process, microfibrils associate with hemicelluloses and lignins in bundles, forming cell wall layers [19].

Hemicelluloses are branched heteropolymers of various monosaccharides with  $\beta$ -1,4-linked backbones of glucose (glucans), mannose (mannans), glucose and mannose (glucomannans) or xylose (xylans) with degree of polymerization of  $\sim$ 70-200 [23,25]. The backbones with specific chains are then grouped separately. For example, glucans with xylosyl residues are termed xyloglucans (XG), while xylans with arabinofuranosyl residues and glucuronic acid are termed glucuronoarabinoxylans (GAX) [25]. The composition of hemicelluloses varies in different types of lignocellulosic biomass. Hardwoods contain mostly xyloglucans and glucuronoxylans, whereas galactoglucomannans and glucuronoarabinoxylans are the predominant constituent of softwoods and grasses, respectively [18,25]. A unique feature in GAX of grasses is the esterified ferulic acid which can present in some of the arabinofuranosyl residues [18,25].

Lignins are recalcitrant heterogenous insoluble aromatic polymers that are composed of phenylpropanoid units, mainly of *p*-hydroxyphenyls (H), guaiacyls (G) and syringyls (S) moieties. They are synthesized from the aromatic alcohols precursors (monolignols), i.e. *p*-coumaryl, coniferyl and sinapyl alcohols [26]. Lignin composition differs not only depending on the plant source, but also on cell type and cell wall layer, as well as on growth stage [27]. However, it is known that lignins in hardwoods mostly consist of G and S units with minor amount of H units, whereas softwoods contain predominantly G units. Grasses have similar amounts of G and S units, but a higher amount of H units compared to hardwoods [23,27,28]. The nature of lignin polymer is difficult to discern due to its high insolubility which prevents extensive analysis. Traditionally lignin has been depicted as highly branched polymer although recently it is suggested to be more linear [29]. The lignin units are connected through covalent linkages by combinations of C-C and C-O (ether) bonds formed during lignin synthesis [23,26,27]. The C-C linkages such as  $\beta$ -5 and 5-5

are more thermochemically stable compared to the ether  $\beta$ -O-4 linkages [30,31]. In grasses, lignin is also associated with hydroxycinnamates, i.e. ferulic acid and p-coumaric acid [18].

Cellulose, hemicellulose and lignin form a complex network that makes the plant cell wall resistant towards depolymerization. Hemicelluloses form networks with cellulose microfibrils through hydrogen bonding either longitudinally or in transversal direction, connecting different microfibrils with other hemicellulose chains through ester cross-linking [17,32]. Hemicelluloses can be connected to lignin by the side groups or chains forming ester or ether bonds. In grasses, the esterification network is formed through ferulic and *p*-coumaric acids [18]. In wood, lignin is covalently linked with the main hemicellulose, i.e. glucuronoxylan or galactoglucomannan [33]. Lignin is considered the most recalcitrant of the polymers and a major source of recalcitrance to the whole lignocellulosic biomass itself [34,35]. This is due to the role of lignin as “gluing agent” due to its direct connection with hemicelluloses while filling the space in between cellulose microfibrils [19,23]. The aggregated polymers are collectively termed lignin-carbohydrate complexes (LCCs) which organize themselves as inclusion complexes that expel water and prevent degradation of both lignin and polysaccharides [36]. Ultimately this prevented the enzymatic degradation of cellulose, the main target for producing platform monosaccharides. Cellulose accessibility is thus the most important parameter for efficient processing of lignocellulosic biomass [37,38]. In order to break the complexity of the network and render the cellulose accessible for enzymatic hydrolysis, different thermochemical pretreatments have been developed.

### ***1.3 Hydrothermal pretreatment and its effect on lignocellulosic biomass components***

Pretreatment of lignocellulosic biomass is an essential step in reducing its recalcitrance prior to enzymatic digestion. Ultimately the goal of pretreatment is to improve the accessibility and thus the digestibility of cellulose to be amenable for ensuing downstream processing. Various pretreatment

methods have been developed for the purpose with different advantages and disadvantages [39–41]. Hydrothermal pretreatment (HTP) is a pretreatment method that has been developed and recently employed in various demonstration and commercial scale 2G ethanol plants [3,4,42]. In HTP, biomass was treated with steam from water without any catalyst added. This contributes to both lower operation and capital cost as inexpensive steel alloys can be used for construction [4]. The process works by heating water under pressure in a reactor until it reaches the subcritical temperature region (100-374°C) [8,43]. In this condition, water is auto-ionized, forming hydronium ions ( $\text{H}_3\text{O}^+$ ). The ions act as catalyst by cleaving glycosidic bonds and also release organic acids in the biomass which in turn perform similar catalytic function as well [43,44].

During HTP, polysaccharides (mainly hemicellulose) are solubilized and lignin is redistributed, contributing to improved digestibility due to increased cellulose accessibility [45,46]. Although HTP technically can be operated around the subcritical temperature region, the typical operating conditions such as in Inbicon demonstration plant are 180-200°C for 10-20 min [4]. It is an act of balancing the water and energy consumption, improvement of cellulose enzymatic digestibility and loss of monosaccharides due to degradation of polysaccharides. An empirical model equation that is widely used to measure the intensity of HTP is the severity factor developed by Overend and Chornet (Eq. 1) [47]. At higher severity conditions, more degradation products from polysaccharides can be formed and these can be inhibitory to subsequent enzymatic and biological processes [48,49]. Therefore, testing the optimal HTP severity levels of the biomass feedstocks are important to establish process operations.

$$\log R_0 = \log \left[ t \text{ (min)} \times \text{EXP} \left( \frac{T(^{\circ}\text{C}) - 100}{14.75} \right) \right] \quad (1)$$

HTP improves the enzymatic digestibility of cellulose by affecting the lignocellulose components differently. First and foremost, the glycosidic bonds of hemicellulose were cleaved by the formed  $\text{H}_3\text{O}^+$  ions and released organic acids during HTP. The released oligosaccharides, monosaccharides and degradation products are then solubilized into the liquid fraction which can be separated from the fiber fraction, depending on process configuration [8,43]. Decorations of hemicellulose such as acetyl groups and uronic acid are also removed after HTP [43,50]. Arabinosyl residues and acetyl groups which are predominant in straws are known to be easily removed from xylan [43]. The extent of hemicellulose degradation is affected by the intensity of HTP as reflected by severity factor ( $\log R_0$ ). Studies have reported that the removal of hemicellulose at increased severity factor correlates to the improved enzymatic digestibility of cellulose [46,51–53]. Hence it is normally observed that hemicellulose content in the biomass decreases after HTP with increasing severity.

Lignin has been reported to be redistributed after HTP, redeposited in the surface of pretreated material as droplets [45,54]. This is due to its physical properties in which it will melt into a fluid-like state above its glass transition temperature ( $T_g$ ) [55]. The  $T_g$  of lignin varies across biomass and difficult to determine since it can be affected by various factors, including state of water and thermochemical pretreatments [56]. Generally the range of  $T_g$  in lignin is reported to be around 70-170°C [55,57]. In wheat straw lignin, values as low as 53 or 63°C depending on extraction by *n*-hexane [58] or values between 50-80°C depending on water saturation and HTP [59] have been reported. In *Miscanthus sinensis* lignin after HTP it was reported to be 116.4°C [60], while in organosolv lignin from switchgrass it was 118 or 128°C depending on severity [61]. For hydrothermally pretreated mixed hardwood chips, the reported  $T_g$  was 172-180°C; the value increased with pretreatment severity levels [62]. After HTP, molten lignin will turn hard and stiff as it cools and relocates after migration. The relocation of lignin is thought to expose more cellulose [45], although there were reports that the droplets also provide steric hindrance and to the enzymes



and can bind them [63,64]. At very high severity levels and with flowthrough configuration, a significant fraction of lignin can be removed [8,51]. Indeed the acidic reaction conditions during HTP can cleave mainly the  $\beta$ -O-4 aryl ether linkages in lignin, leading to depolymerization and potentially reduced molecular weight ( $M_w$ ) [65]. However, competing repolymerization reactions at high severity which leads to condensation can offset depolymerization reactions, leading to stable if not increased  $M_w$  after HTP [65,66]. Other chemical changes after HTP include increase of phenolic OH groups, formation of carboxylic groups along with decrease of aliphatic OH groups [65,67].

Cellulose on the other hand remains relatively stable at typical HTP operating conditions, although some degradation might occur depending on the severity. If occurred, cellulose degradation reduces the degree of polymerization and improves digestibility [8,20]. However, the crystallinity of cellulose was found to increase after HTP, which is thought to occur due to the removal amorphous regions [20,68,69]. This seemingly against the idea of reducing recalcitrance since higher crystallinity is also known to retard cellulose degradation [70]. Nevertheless, the effect is also being counterbalanced by the removal of hemicellulose and redistribution of lignin which increases accessibility of cellulose to enzymes [8,45,46,71]. Microscopic observations also showed that there was partial defibrillation effect after HTP, separating individual cellulosic fibers [45].

#### ***1.4 Cellulolytic enzymes and enzymatic cellulose degradation***

Non-complexed cellulases from *Trichoderma reesei* (teleomorph: *Hypocrea jecorina*) have been used as model for fungal cellulase system widely employed in biomass degradation studies [72]. The system was termed non-complexed since the individual enzyme components are freely released compared to the complexed multidomain bacterial cellulase system in which the individual enzyme components are clustered in scaffoldings [73]. The complexed bacterial cellulolytic system has been termed “cellulosome” as observed on studies in clostridia and ruminal bacteria, in particular

*Clostridium thermocellum* [73]. Cellulases of *T. reesei* have been traditionally divided into three major components: cellobiohydrolases (CBHs), endoglucanases (EGs) and  $\beta$ -glucosidases (BGLs). Thus far, 2 CBHs, 5 EGs and 2 BGLs have been characterized in *T. reesei* up to protein level [74]. Based on the classification using Enzyme Commission (EC) number, the three major components of cellulases belong to the hydrolase group (EC 3) which perform the hydrolysis of ( $\beta$ -1,4) glycosidic bonds (EC 3.2) of O- and S-glycosyl compounds (EC 3.2.1) [73].

Cellulases typically consist of two domain structures, namely a carbohydrate-binding module (CBM) and a catalytic domain (CD). CBM is suggested to be non-catalytic and has the main role in polysaccharide recognition and binding [75,76]. All CBMs in fungal cellulases are classified as Type A surface-binding CBM with flat (planar) surface and family 1 CBM [75,76]. CBM is found in the CBHs and most EGs of *T. reesei* cellulases [76]. The CBMs in *T. reesei* cellulases consist of about 33 amino acids with 4 conserved cysteine residues forming 2 disulfide bridges. They are attached to the N- or C-terminus of the CD through a flexible chain-like O-glycosylated linker region of about 26-44 amino acid residues rich in proline, serine and threonine [77]. The CD of the cellulases contains the active site in which the hydrolysis of glycosidic bonds occurs. The active site contains catalytic amino acid residues, at least a proton donor and a nucleophile, which facilitate hydrolysis reaction via acid-base catalysis [72,73]. Different topologies of the active sites are observed in different cellulase components of *T. reesei*. In CBHs active sites are known to be tunnel-shaped with a length of 50 Å in *TrCel7A* (CBHI) [78,79] and 20 Å in *TrCel6A* (CBHII) [80]. Endoglucanases, e.g. *TrCel7B* (EGI) and *TrCel5A* (EGII) have an open substrate-binding site with the shape of a cleft [72,81].

Cellulose can be completely degraded into its glucose monomers by the distinctive yet concerted actions of cellulase components [72,73]. EGs (EC 3.2.1.4) cleave  $\beta$ -bonds randomly in the internal-amorphous region of cellulose, producing cello-oligosaccharides of various lengths,

cellobiose, glucose and new chain ends for CBHs to attack. CBHs (EC 3.2.1.91) release mostly cellobiose and glucose by processively degrading crystalline cellulose chain from the reducing (*TrCel7A*) or non-reducing end (*TrCel6A*). Processive CBHs, unlike EGs, remain attached to the polymeric substrate while continuously threading and performing multiple successive catalyses before dissociating [72,73]. BGLs complete the hydrolysis of cellulose by releasing glucose from cellobiose and soluble short-chained cello-oligosaccharides. However, cellulases are known to suffer from end-product inhibition; BGL is strongly inhibited by glucose whereas CBHs and EGs are both inhibited by cellobiose [82]. Thus, glucose inhibition of BGL has been considered rate-limiting and the alleviation of cellobiose inhibition in CBHs and EGs is important for efficient hydrolysis. CBHs are more prone to cellobiose inhibition compared to EGs [83]. CBHs and EGs have also been found to be inhibited by glucose with varying degree of sensitivity. *TrCel6A* is more inhibited by glucose compared to *TrCel7A* and *TrCel7B* whereas *TrCel5A* seems to be the least sensitive to glucose inhibition. Nevertheless, inhibition of CBHs and EGs by cellobiose is still found to be significantly stronger than glucose [83].

In enzymatic cellulose degradation, cellulases act synergistically so that the combination of different enzymes (i.e. CBHs and EGs) results in higher total hydrolysis yield compared to that of the sum of individual enzymes [72,84]. The phenomenon has been well-documented to occur among CBHs and EGs as well as between CBHs and known as endo-exo and exo-exo synergism, respectively [72,84]. Stalling of processive *TrCel7A* by obstacles in the substrate was found to be the rate-limiting factor in the hydrolysis, especially given the slow dissociation of the enzyme from the substrate [85,86]. Thus the presence of endo-acting EGs that are less prone to stalling was found to increase the hydrolysis rate by preventing *TrCel7A* from stalling by removing the less ordered amorphous regions [86,87]. *TrCel6A* along with EGs was also found to remove the amorphous regions and aggregates of microcrystals, thus exposing and clearing the microfibril for the

processive attack by *TrCel7A* [88]. Furthermore, *TrCel6A* is also suggested to create new attack sites for *TrCel7A* causing the exo-exo synergism during crystalline cellulose hydrolysis [89].

Nowadays, the fungal cellulolytic system has been expanded due to recent discovery of the oxidative enzymes known as lytic polysaccharides monooxygenases (LPMOs) which have also been found to play a role in crystalline cellulose degradation [90]. The suggested mechanism involves oxidative cleavage of cellulose at C1 and C4 positions involving oxygen and electron donor, releasing aldonic acids. The oxidized positions then open up new attack site for CBHs [90]. In that respect, the term “cellulose hydrolysis“ might not be appropriate when referring to cellulose degradation using newer commercial enzyme mixture where LPMOs are present [91]. However, the term “hydrolysis” which traditionally has been used to refer subjecting cellulose to enzymatic degradation mainly using cellulases is still maintained. In any case, even the term LPMO might need to be revised since it is suggested that their action is more dependent on hydrogen peroxide rather than oxygen [92]. Other groups of enzymes that are beneficial to support cellulolytic activity are the hemicellulases. Addition of hemicellulases such as xylanase,  $\beta$ -xylosidase,  $\alpha$ -arabinofuranosidase and  $\alpha$ -glucuronidase alongside minimal cellulases cocktail is found to improve its cellulolytic activity better than commercial enzyme mixture [93].

### ***1.5 Adsorption of cellulases and cellulolytic enzyme mixture components on lignocellulose***

In order to perform their catalytic function, cellulases need to a certain extent adsorb on their insoluble cellulose substrate. This is especially true for the processive CBHs that compose the majority of *T. reesei* secretion [94]. The binding of CBHs is thought to be modulated by their CBM since its removal resulted in reduced adsorption and hence activity on crystalline cellulose [95,96]. The planar side of CBM of *TrCel7A* has conserved amino acids shared with over 250 family 1 CBMs which suggested that they share common mechanism [97]. The planar surface on the CBM

of CBHs has conserved hydrophobic aromatic amino acid residues (Y5, Y31, Y32 for *TrCel7A* and W7, Y32, Y33 for *TrCel6A*). This led to the hypothesis that hydrophobic interaction might play an important role in binding with cellulose [96], especially since *TrCel7A* was shown to hydrolyze crystalline cellulose exclusively on the hydrophobic surface [98]. Further studies and simulations though suggested that in the CBM of *TrCel7A*, polar residues Q7 and N29 were also involved. Along with Y5 and Y32 they are suggested to bind glucose residue in the cellulose chain through hydrogen bonding and aromatic ring stacking via tyrosine residues [97]. The binding thus is suggested to involve combined mechanisms where partial exclusion of water due to hydrophobic effect bring the CBM closer to cellulose in order to form hydrogen bonds [99].

The binding of cellulases however, is also thought to involve their CD. The CDs of both *TrCel7A* [78,79] and *TrCel6A* [100] contain tryptophan residues in the entrance and inner lining of the tunnel. These amino acid residues (W40 for *TrCel7A* and W272 for *TrCel6A*) were thought to play role in the hydrolysis through aromatic ring stacking interaction with glucose residue in the cellulose chain. Mutations of W40 [101] and W272 [100] resulted to substantially reduced activity against crystalline cellulose, and in the case of W40A mutant of *TrCel7A*, the binding and processive movement were impaired [101]. The W40A mutant without CBM was shown to bind only weakly to the substrate. Thus, W40 is thought to contribute to binding, but the binding was dominated by the CBM [102]. Apart from initial binding, W40 was found to be necessary in positioning and loading the cellulose chain to the tunnel leading to processive catalysis [102]. However, studies at high consistency cellulose hydrolysis revealed that cellulases with and without CBM had similar yield. Cellulases without CBM were found to be mostly desorbed (60-90%) after 48 h hydrolysis as opposed to intact cellulases which remained mostly adsorbed [103,104]. Work at large scale showed that despite the high desorption, high glucose and ethanol yields were obtained using CBHs without CBM in processing of industrially pretreated biomass

feedstocks, allowing efficient recycling of enzymes [105]. Thus at increased dry matter (DM) content, increased enzyme binding through modulation by CBM seems to be not necessary.

Another study in progress on the binding of cellulases is their propensity to bind other components in lignocellulosic biomass, notably lignin. Not so much is known about the binding of cellulases on hemicellulose although they have been reported to adsorb on xylan and mannan [106]. The critical concern is that the binding of cellulases on lignin renders them unable to perform their catalytic function. Such binding has been termed as non-productive adsorption and is considered a major factor in retarding the enzymatic cellulose degradation [7,34,107,108]. Numerous studies have found that cellulolytic enzyme mixtures [109–114] and monocomponent cellulases [115–120] adsorbed on lignin isolated from a wide range of pretreated biomass feedstocks. Consequently the adsorption on lignin is tied to the observed reduction in the rate and extent of model cellulose substrate in the presence of the isolated lignin. In the case of retardation by hemicelluloses, supplementation of different hemicellulases can alleviate the problem [121]. However, it is less straightforward in the case of lignin. Before detailed review on the mechanism of how enzymatic cellulose degradation is retarded by lignin, it is important to assess the factors affecting adsorption. Several studies indicated that the enzyme-lignin interaction occurred mainly through hydrophobic interaction [111,119], electrostatic interaction [118,122] or hydrogen binding [109,123]. However, others indicated that combination of multiple interactions can be involved [67,124–126]. Other factors that were found to affect adsorption of cellulases on lignin includes temperature [111,112], pretreatment and lignin chemistry [114,117], CBM [117,118] and biomass [117,118,127].

Hydrophobic interaction is conceivably a major interaction due to the hydrophobic amino acid residues in the CBM and CD of cellulases [78,79,96,97,100] and the hydrophobic nature of cell wall lignin [20,111,116,128]. The presence of CBM was indeed reported to increase the binding of monocomponent cellulases on lignin [117,118]. A study using a wide range of proteins

including *TrCel7A*, other enzymes and bovine serum albumin (BSA) found a linear correlation between hydrophobic patch score and adsorption on lignin [119]. Surface charge however, did not provide a good correlation. It is interesting to note that BSA had significantly higher hydrophobic patch score than others [119]. Accordingly, BSA was previously proposed as “lignin-blocking agent” in order to reduce the retardation of enzymatic cellulose degradation [129]. The correlation was less clear-cut in another lignin adsorption study using monocomponent cellulases and a xylanase [120]. The CBM and CD of different enzymes were found to have different hydrophobic patch score and it alone cannot fully explain the differences in the adsorption profile.  $M_w$  and surface charge of the enzymes were also found to have some role [120].

Electrostatic interaction is also suggested to have major contribution in the adsorption of cellulases on lignin. Increased pH ranges were found to significantly reduce the binding of a monocomponent cellulase [118] and components of a commercial cellulolytic enzyme mixture [126]. Consequently another study testing commercial cellulolytic enzyme mixtures on the hydrolysis of woody biomass with different pretreatments found an optimum pH range of 5.2-6.2 [122]. The electrostatic interaction is tied to the isoelectric point (pI) of the enzyme and the net negative charge of lignin at the experimental pH. The higher the reaction pH, the more likely that the enzymes to be more negatively charged. At increasing reaction pH, lignin substrates isolated from spruce and wheat straw were also found to be more negatively charged [118]. These conditions promote Coulombic repulsion between enzyme and lignin, therefore reducing adsorption. Engineering cellulase with highly increased negative charge was indeed found to improve their hydrolytic performance in the presence of lignin [130].

Hydrogen bonding is correlated more to the functional groups in lignin following pretreatment, especially the formation of phenolic hydroxyls. They are thought to bind cellulases through hydrogen bonding and their increased formation after pretreatment correlated to increased

enzyme adsorption and retardation of cellulose degradation [109,123,131]. Blocking of phenolic hydroxyl groups by hydroxypropylation was indeed found to reduce the effect of lignin on enzymatic cellulose degradation [109,131]. Pretreatment on its own was indeed found to increase the adsorption of cellulases on lignin. The lignins isolated from steam pretreated spruce and wheat straw bound more *TrCel7A* compared to those isolated from untreated biomass. This was followed by the formation of more phenolic hydroxyls, condensed lignin units and reduction of S/G ratio [117]. Increasing pretreatment severity was also found to increase the binding of a commercial cellulolytic enzyme mixture on hydrothermally pretreated hardwoods. Furthermore lignin with higher G units was found to adsorb more enzymes [114]. Although variation in the adsorption of enzymes on lignin isolated from different biomass feedstocks has been expected, the explanation remains still unclear. It is nevertheless well-known that lignin isolated from softwood adsorb more than those from hardwood and grass [117,118,127]. Yet changes in phenolic hydroxyls seemed to be similar in both spruce and wheat straw after steam explosion [117], leaving the inherent difference in the S/G ratio. Softwood lignin which consists exclusively of G units [23,27,28] is indeed reported to retard enzymatic cellulose degradation more than others [120,127,132].

The adsorption kinetics of cellulases on lignin are also still largely unknown. In the case of the adsorption of cellulases on cellulose, studies have shown that the enzymes adsorb reversibly [133–135]. Generally, adsorption of protein on solid surface is known as a dynamic process involving partial exchange of adsorbed and desorbed states. During the process however, the constant conformational rearrangements between the two states can compromise the structural integrity of the protein, leading to irreversible structural change(s) that can affect subsequent adsorption behavior [136]. It has been reported that the binding of cellulases on lignin increased with temperature [111,112]. The increased binding over time led to reduction of recoverable activity and retardation of enzymatic cellulose degradation of model cellulose, especially at



elevated temperature used in hydrolysis reaction (45°C as opposed to 4°C used in many adsorption studies). Therefore it was suggested that during the intensified binding, the protein structure denatured after successive conformational rearrangements and became irreversibly bound on lignin, losing its activity [112]. In general, the binding of enzymes on lignin is considered to be irreversible [108]. Nevertheless Langmuir adsorption model has been used to describe the binding of cellulases on lignin [111,116,118], although the model itself assumes the binding to be reversible [137].

### ***1.6 Retardation of enzymatic cellulose degradation by lignin***

There are three mechanisms involved in explaining the retardation of enzymatic cellulose degradation by lignin, especially when considering the whole biomass slurry after pretreatment. They are inhibition by soluble compounds, non-productive adsorption and steric hindrance or physical barrier. Depending on the pretreatment severity, various degradation products can be formed from the lignocellulose components [48,49]. These degradation products can be inhibitory to enzymes and microbes in the subsequent downstream processing. Phenolic compounds from lignin degradation products for instance were found to be significantly inhibiting or deactivating cellulases [138]. However, this aspect will not be discussed further since phenolic compounds can also be derived from polysaccharides [49,139] and process configurations such as washing or detoxification can be implemented to reduce the effect [48]. In many studies, this effect can be excluded by excessive washing after pretreatment and during lignin isolation procedure. Hence this step enables researcher to focus on insoluble part of lignin which still remains after pretreatment using hydrothermal or steam pretreatment.

The non-productive adsorption of cellulases on lignin is considered the major cause of retardation of enzymatic cellulose degradation by lignin [7,34,107,108]. Normally it is studied by isolating lignin from pretreated biomass, then performing hydrolysis of model cellulose substrate in

the presence of the isolated lignin. Series of adsorption experiments are usually also performed alongside the former in order to explain the observed trends and ultimately to pinpoint the existence and intensity of the non-productive adsorption. Although there are numerous methods to isolate lignin, the lignin-rich residue (LRR) isolated through extensive cellulose hydrolysis followed by protease treatment is considered to be representative as it contains the majority of the original lignin [127]. Furthermore it is also thought to exert the least chemical changes [31].

Numerous studies using wide range of biomass feedstocks with hydrothermal or steam pretreatments reported varying degree of reduction in the rate and extent of model cellulose hydrolysis in the presence of isolated LRRs [112,120,127,132,140–142]. LRRs from softwood retarded the enzymatic cellulose hydrolysis more significantly than those from hardwood and grasses [120,127,132]. Yet, there was no retardation of enzymatic cellulose degradation observed when using LRRs from grasses [127,141,142]. More importantly, the direct connection between adsorption on lignin and reduction in the degradation of model cellulose has not been clearly established. One plausible theory was the thermal denaturation of protein during adsorption on lignin, resulting in the loss of recoverable cellulases activity [112]. However, there are also reports that cellulases, especially BGLs, were still active while being highly bound on lignin [143], even more than other components in commercial cellulolytic enzyme mixture [126]. In another study, the total recoverable activity of enzymes was not affected by adsorption on lignin [144]. Therefore, in a way these findings question the term “non-productive adsorption” itself, if the enzymes are still productive despite binding on lignin.

The role of lignin as physical barrier is naturally understandable given its location and function in the native plant cell wall [17,18,27,145]. However, in the actual hydrolysis reaction it is difficult to discern due to lack of quantitative information. This is especially true when comparing different biomass feedstocks or pretreatment methods in order to assess recalcitrance or enzymatic

digestibility. Furthermore, lignin was also shown to be redistributed after hydrothermal or steam pretreatment. This redistribution allegedly improve hydrolysis of pretreated biomass by increasing cellulose accessibility [45,54,71]. However, the remaining lignin after pretreatment can still provide physical barrier for the enzymes to access cellulose to a certain extent. Several studies found considerable improvement in enzymatic cellulose degradation after performing delignification of hydrothermally or steam pretreated biomass [140,146,147]. The results were striking in the case of softwood which has been deemed as the “worst-case scenario” substrate [148], although the lignin has been pointed to also promote significant non-productive adsorption [112,120,127,132]. In one study, the removal of lignin doubled the extent of enzymatic hydrolysis of steam pretreated spruce and its residue which has been enzymatically digested previously [147]. In another study, adding the isolated LRRs from steam pretreated spruce to its delignified counterpart only resulted in meagre retardation of enzymatic cellulose degradation [140]. However, as shown in another study with wheat straw, if lignin and hemicellulose were to be almost entirely removed after severe series of pretreatments, it can instead hamper enzymatic cellulose degradation due to collapse of porous structure [146]. These results indicate that lignin still plays a role as physical barrier to a certain extent, despite the redistribution after pretreatment.

Other studies utilizing surface analyses and imaging techniques also showed the importance of lignin as physical barrier. A study monitoring the hydrolysis of specific tissues from wheat straw that has been hydrothermally pretreated using microscopy and attenuated total reflectance-Fourier transform infrared (ATR-FTIR) analyses revealed increasing surface lignin over time as the rate of hydrolysis decreased [149]. Another study investigating pulps found that higher lignin content corresponded to higher surface lignin coverage measured with X-ray photoelectron spectroscopy (XPS) and accordingly lower degree of hydrolysis [150]. Time-of-flight secondary ion mass spectrometry (ToF-SIMS) is another method developed to understand the surface chemistry of

lignocellulosic biomass [151]. When comparing the lignin contents of untreated, ammonia- and organosolv-pretreated poplar, ToF-SIMS revealed slightly higher variation than the bulk chemical analysis [152]. In study comparing wheat straw with series of HTP, NH<sub>3</sub> extractions and their combination, samples with lower lignin content were found to be less enzymatically digestible than those with higher lignin content. Apparently, application of more extensive treatments that removed more lignin increased the lignin surface area as measured by dye adsorption. The increase of lignin surface area correlated better to biomass digestibility [71].

Various advanced microscopy and imaging techniques have been developed to visualize lignocellulose components in the plant cell wall compartments before and after pretreatment at high resolution [153]. One study used fluorescence lifetime imaging microscopy (FLIM) to monitor lignin structure on poplar cell walls. The study found that pretreatment removed the loosely packed easily and with increasing severity, more of the densely packed lignins were removed [154]. Imaging techniques can indeed provide rich information on both compositional and structural level of biomass, although extracting quantitative information can sometimes difficult [153]. Recently, it has become clear that advanced imaging techniques and sensitive surface chemical analyses may be needed to study the surface distribution of lignin on lignocellulosic biomass substrates [67].

## **Chapter 2 – Background, hypotheses and objectives**

### ***2.1 Overall background, aim and hypothesis***

The PhD study departed from the need to understand factors that affect the efficiency of enzymatic cellulose degradation. A particular focus benchmark in the study is the currently used state of the art technology in large scale lignocellulosic ethanol plant, i.e. HTP followed by enzymatic hydrolysis. Even though the goal of the operation was confined mostly to production of fuel ethanol, it also aimed to valorize the lignin-rich bioprocess residue which has been underutilized as solid fuel. However, the presence of lignin itself has been pointed as one of the major obstructions in attaining efficient enzymatic conversion, notably by inducing non-productive adsorption of enzymes. As multiple biomass feedstocks are being explored for utilization, it is important to identify key factors that correlate to their digestibility. Several main research questions are:

- How do different biomass feedstocks respond to HTP at different severity levels?
- What are the changes in the biomass feedstocks after HTP that correlate to enzymatic cellulose degradation?
- How does lignin retard enzymatic cellulose degradation?
- What are the characteristics of enzyme-lignin interactions?

Therefore the study aims to identify biomass properties and subsequent interaction with enzymes that affect enzymatic cellulose degradation. It is hypothesized that these factors, i.e. lignocellulose components and enzyme-lignin interactions, affect enzymatic cellulose degradation negatively. This means that higher abundance of non-cellulosic lignocellulose components (i.e. hemicellulose and lignin) and higher intensity of enzyme-lignin interaction contribute to lower rate and extent of enzymatic cellulose degradation.

## ***2.2 Specific background, hypotheses and objectives***

The specific background along with hypotheses and objectives are organized based on the publications pertained to the PhD thesis. The specified hypotheses are presented again in the beginning of Chapters 4, 5 and 6; each of which outlines **Papers I, II and III**, respectively.

### **Paper I**

Background:

Hydrothermal pretreatment (HTP) is known to improve the digestibility of lignocellulosic biomass by partial removal of hemicellulose and redistribution of lignin that increases cellulose accessibility. Many studies found good correlation between hemicellulose removal and the enzymatic digestibility of cellulose after HTP. However, the reasons and mechanisms responsible for quantitative differences in enzymatic digestibility of various biomass feedstocks in response to the pretreatment severity factor are still not sufficiently understood.

Hypotheses:

- Biomass feedstocks of diverse botanical origins respond differently to HTP in terms of digestibility and changes in the composition.
- Composition of lignocellulosic biomass and the changes after HTP (particularly hemicellulose profile) correlate to digestibility.

Objectives:

- To evaluate the digestibility of key lignocellulosic biomass feedstocks that were hydrothermally pretreated at different severity levels.
- To analyze the changes in the composition of lignocellulosic biomass feedstocks after HTP at different severity levels.

- To assess whether the composition of lignocellulosic biomass feedstocks and the changes after HTP (particularly hemicellulose profile) correlate to digestibility.

## **Paper II**

### Background:

Lignin has been considered as one of the major factors that hinder enzymatic cellulose degradation. In that context, lignin has been studied in its isolated form. One of the most frequently studied isolated forms is lignin-rich residues (LRRs) which are isolated through extensive cellulose hydrolysis. The non-productive binding of cellulolytic enzymes on LRRs has been considered an important mechanism in the retardation. Multiple studies have reported that the enzymatic degradation of cellulose was retarded in the presence of LRRs.

### Hypotheses:

- Lignin substrates isolated from hydrothermally pretreated lignocellulosic biomass feedstocks (in the form of LRRs) retard enzymatic cellulose degradation by inducing irreversible non-productive adsorption of enzymes.
- The extent of retardation of enzymatic cellulose degradation caused by LRRs can be correlated to the changes in physical and chemical properties of lignin polymer after HTP.

### Objectives:

- To investigate the effect of adsorption of cellulolytic enzymes on LRRs isolated from hydrothermally pretreated lignocellulosic biomass feedstocks on subsequent enzymatic cellulose degradation.
- To assess whether the exerted changes in the physical and chemical properties of lignin after HTP correlate to the observed retardation of enzymatic cellulose degradation.

### **Paper III**

#### **Background:**

The adsorption of cellulases on lignin has been perceived as irreversible, hence purportedly contributing to observed retardation of enzymatic cellulose degradation. Many efforts to curb this effect, such as supplementing various additives in the enzymatic reaction or engineering several properties of the enzymes, have been proposed. Yet, the affinity and nature of the binding on lignin is still not known for individual monocomponent cellulases.

#### **Hypotheses:**

- Monocomponent cellulases adsorb on lignin isolated from hydrothermally pretreated lignocellulosic biomass feedstocks (in the form of LRRs) with different binding affinity that can be correlated to the intrinsic properties of the enzymes.
- The adsorption of monocomponent cellulases on lignin isolated from hydrothermally pretreated lignocellulosic biomass feedstocks (in the form of LRRs) is irreversible by nature.
- Monocomponent cellulases bind competitively on LRRs where one enzyme with higher affinity would be more predominant over the other.

#### **Objectives:**

- To evaluate the binding affinity of monocomponent cellulases on LRRs of different origins.
- To assess whether intrinsic properties of monocomponent cellulases correlate to the corresponding binding affinity on LRRs of different origins.
- To study the kinetics of adsorption of monocomponent cellulases on LRRs of different origins with respect to its reversibility.
- To investigate the competition among monocomponent cellulases during adsorption on LRRs of different origins.



## Chapter 3 – Materials and methods

This chapter outlines the materials and methods used during the PhD study. Detailed descriptions are provided in the original publications **Papers I-III** which are cited throughout the text. A general overview of the whole work is presented at the end of this chapter (Subchapter 3.7).

### 3.1 Biomass feedstocks and lignocellulosic substrate

Grass biomass feedstocks, i.e. corn stover (*Zea mays* subsp. *mays* L.) (CS), *Miscanthus × giganteus* stalks (MS) and wheat straw (*Triticum aestivum* L.) (WS) were hydrothermally pretreated at three different severities: 190°C for 10 min ( $\log R_0 = 3.65$ ), 190°C for 15 min ( $\log R_0 = 3.83$ ) and 195°C for 15 min ( $\log R_0 = 3.97$ ). The pretreated biomass feedstocks were used for hydrolysis experiments and various characterizations (**Paper I**) as well as source for isolation of lignin-rich residues (**Paper II** and partly in **Paper III**). The hydrothermal pretreatment (HTP) was performed using Mini-IBUS equipment at Technical University of Denmark which mimicked the large scale Integrated Biomass Utilization System (IBUS) [3]. Therefore the substrates are expected to represent key grass biomass feedstocks processed at relevant commercial-ready technology. The spruce used to produce lignin-rich residue (LRR) in **Paper III** was hydrothermally pretreated using in-house built pretreatment equipment [155] at 200°C for 10 min ( $\log R_0 = 3.94$ ). Microcrystalline cellulose Avicel PH-101 (Sigma-Aldrich, St. Louis, MO, USA) was used in hydrolysis experiments with LRRs (**Paper II**).

### 3.2 Cellulolytic enzymes

State of the art commercial cellulolytic enzyme mixture Cellic<sup>®</sup> CTec3 was kindly provided by Novozymes A/S as part of BioValue SPIR work. The enzyme mixture was used in studies with hydrothermally pretreated grass biomass and the corresponding isolated lignin-rich residues,

presented in **Paper I** and **Paper II**, respectively. Purified monocomponent cellulases *TrCel7A*, *TrCel6A*, *TrCel7B* and *TrCel5A* were used in the study on the nature of the binding of enzymes on lignin isolated from hydrothermally pretreated biomass, presented in **Paper III**. The detailed characteristics of the monocomponent cellulases used in this study are presented in Table 6.1 (in Chapter 6 which outlines **Paper III**).

### ***3.3 Isolation of lignin-rich residues (LRRs)***

The lignin substrates used in the study (**Paper II** and **Paper III**) were isolated in the form of lignin-rich residues (LRRs). The procedure involved extensive cellulose hydrolysis at repeated high enzyme dosage, mainly using Cellic<sup>®</sup> CTec3, followed by protease treatment to remove adsorbed enzyme and freeze drying. In this way, the LRRs are expected to resemble actual lignocellulosic bioprocess residue and the procedure is expected to exert minimal changes to the lignin.

### ***3.4 Hydrolysis experiments***

Total hydrolysis of the whole pretreated biomass was performed using multiple dosages of Cellic<sup>®</sup> CTec3 to assess their digestibility (**Paper I**). Series of hydrolysis experiments were also performed using Cellic<sup>®</sup> CTec3 on Avicel as model cellulose with and without the presence of LRRs to assess the effect of lignin in retarding the enzymatic cellulose degradation (**Paper II**). The detailed schemes of the latter experiments are presented in Fig. 5.1 (in Chapter 5 which outlines **Paper II**).

### ***3.5 Adsorption experiments***

All adsorption experiments were performed to assess the interaction between cellulolytic enzymes and the isolated LRRs. In general, the procedure involved a period of incubation of mixed enzyme and LRRs in buffer solution after which centrifugation was performed. The amount of bound

enzyme was calculated by analyzing the supernatant for unbound enzyme. Analysis of the supernatant was performed using ninhydrin method to measure total protein concentration of Cellic<sup>®</sup> CTec3 (**Paper II**) or using radiolabeling technique on labeled monocomponent cellulases (**Paper III**). A simple adsorption experiment on a given protein concentration was performed on the nine isolated LRRs from CS, MS and WS (**Paper II**). A series of adsorption isotherms on broad concentration range and long adsorption experiments with dilution series to establish the binding kinetics were performed using monocomponent cellulases on LRRs from hydrothermally pretreated spruce and WS (**Paper III**). The details of the dilution experiments and kinetic modelling are summarized in Chapter 6.2 (in Chapter 6 which outlines **Paper III**).

### ***3.6 Analytical methods in biomass and lignin characterization***

Numerous analytical methods were employed to characterize the biomass (**Paper I**) and LRRs (**Paper II** and **Paper III**) used in this study. One important distinction in the methods being used is the scope of analysis which either give information relevant to the bulk or the surface of the samples' particles. A common denominator of the bulk methods is degradation or solubilization of the polymers in the biomass material to yield smaller monomers which are then separated and analyzed. Occasionally, the protocols are also comprised of high severity grinding such as ball milling. Surface methods on the other hand do not involve severe mechanical processing or deconstruction of biomass polymers. Furthermore, the information obtained during surface analysis was the result of interaction between water and infrared beam in this case, each with the surface of the biomass particles. The overview of methods being used is presented in Table 3.1.

Table 3.1 Analytical methods used for characterization of biomass and lignin in this study

Purpose of analysis	Method		Short description of the procedure	Publication
	Scope	Instrument or protocol		
Carbohydrates and lignin composition	Bulk	Strong acid hydrolysis	Two-step sulfuric acid hydrolysis of biomass or LRRs followed by analysis of the hydrolysates for monomeric sugars and the insoluble residues for Klason lignin contents [156].	Paper I, II, III
Hemicellulose decoration		2D Nuclear magnetic resonance (NMR)	Gelling of ball-milled biomass or LRRs followed by acquisition and analysis of 2D NMR spectra [157].	Paper I
Lignin interunit linkages and abundance of triclin				Paper II
Plant cell wall polymer structures, especially hemicellulose		Comprehensive microarray polymer profiling (CoMPP)	Chemical extraction of ball-milled biomass followed by high-throughput probing of the extracts using specific antibodies [158–160].	Paper I
Relative monolignols content and ratio		Pyrolysis-gas chromatography-mass spectrometry (Py-GC-MS)	Pyrolysis of the LRR samples followed by separation and identification of the pyrolysates by using GC-MS instruments [161].	Paper II
Relative molecular weight ( $M_w$ ) distribution		Gel permeation chromatography (GPC)	Solubilization of LRRs followed by separation based on size exclusion and detection of soluble compounds with ultraviolet (UV) detector [161].	Paper II
Apparent surface abundance of lignocellulosic components	Surface	Attenuated Total Reflectance Fourier-Transform Infrared (ATR-FTIR) spectroscopy	Analysis of total internal reflection of IR beams in diamond ATR crystal which is in contact with the biomass or LRR samples with limited penetration [162].	Paper I, II
Relative monolignols ratio				Paper II
Biomass wettability (surface hydrophobicity)		Contact angle measurement (CAM)	Measurement of initial contact angle formed on the biomass material by a water droplet recorded with a high-speed camera [163].	Paper I

### ***3.7 General overview of the PhD study***

All in all, the study incorporated extensive analysis of lignocellulose components from key grass biomass feedstocks that were systematically pretreated at narrow range of severity factors, yet still within the mid-range of that being used in large scale operation [4]. The fiber fraction of hydrothermally pretreated biomass was extensively analyzed for bulk composition and surface properties in order to find correlation with the digestibility of the biomass (**Paper I**). LRRs were isolated from the corresponding fiber fraction, extensively analyzed for chemical and physical properties of lignin and assessed for the enzyme-lignin interaction to clarify the role of lignin in retarding enzymatic cellulose degradation (**Paper II**). A selected LRR from WS (**Paper II**) along with another LRR from hydrothermally pretreated spruce were used to assess the nature of binding of individual monocomponent cellulases on lignin (**Paper III**). The overall scheme of the PhD study presented in this thesis is displayed in Fig. 3.1. Each of the following Chapters 4, 5 and 6 each outlines **Papers I, II and III**, respectively. Chapter 7 provides synthesis which summarizes the overall results and highlighting the generated knowledge as well as reflection and extrapolation based on previously established understanding and recent findings. Final Chapter 8 provides conclusions as responses to the previously set hypotheses and future perspectives based on the previous discussion and conclusions, both of which summarize the whole PhD study.

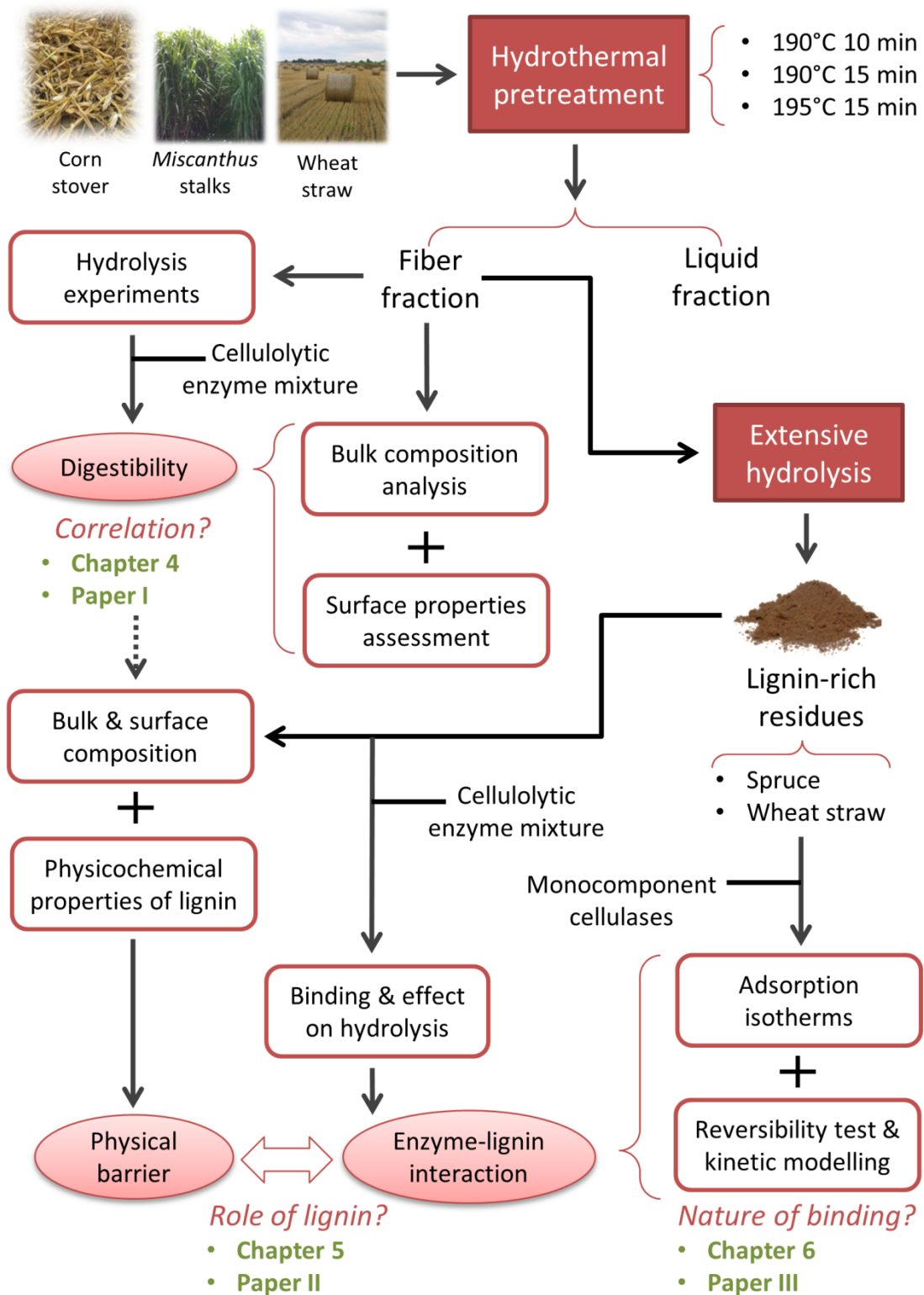


Fig. 3.1 Overall scheme of the PhD study along with aims and research questions

## **Chapter 4 – Biomass properties that correlate to the digestibility of hydrothermally pretreated grass biomass feedstocks (Paper I)**

### ***4.1 Hypotheses***

1. Biomass feedstocks of diverse botanical origins respond differently to HTP in terms of digestibility and changes in the composition.
2. Composition of lignocellulosic biomass and the changes after HTP (particularly hemicellulose profile) correlate to digestibility.

### ***4.2 Experimental considerations***

In order to assess their digestibility, the hydrothermally pretreated biomass feedstocks were subjected to enzymatic hydrolysis experiments using commercial cellulolytic enzyme mixture at multiple enzyme dosages. The hydrolysis experiments were performed on thoroughly washed biomass at low substrate concentration (1% DM) in order to minimize the influence of other factors that can be present at high consistency processing [164]. The observed digestibility is then expected to be more related to the intrinsic properties of the pretreated biomass. Assessment of the bulk composition emphasized largely on the features pertaining to the hemicelluloses moieties, i.e. their removal after HTP, their decoration and structural arrangements. This is due to the reported correlation between hemicellulose removal and cellulose digestibility in line with applied HTP severity [46,51–53]. Assessment of the surface properties covered biomass-water interaction which has also been reported as indicator of digestibility and/or efficacy of pretreatment [163,165–168]. Additionally, relative abundance of lignocellulose components in the surface was also assessed to explain the changes in the surface wettability and to ultimately find correlation with the observed digestibility. The overall work and analytical methods involved is outlined in Fig. 4.1.

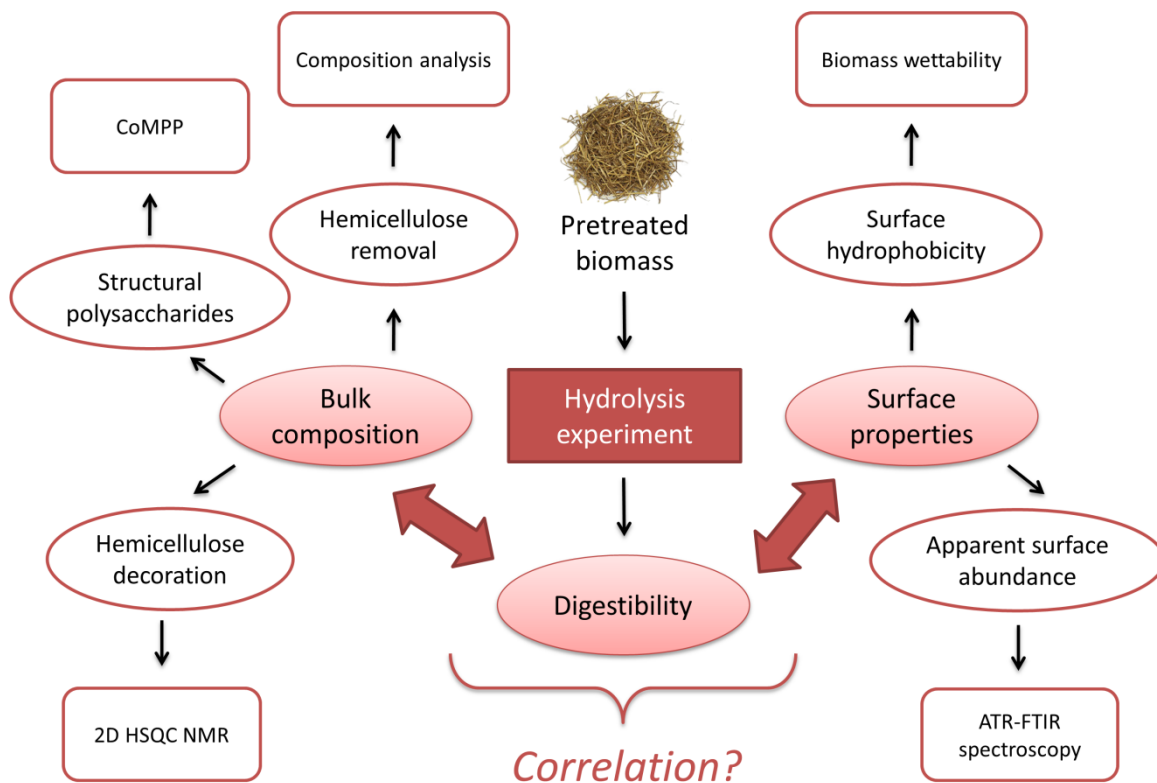


Fig. 4.1 Outline of the work in **Paper I**, highlighting the analytical methods being used.

#### 4.3 The digestibility of hydrothermally pretreated grass biomass feedstocks

Glucose release from enzymatic cellulose degradation of the hydrothermally pretreated grass biomass showed increase as response to HTP severity (Fig. 4.2). The increase however, was not linear across the multiple enzyme dosages and the varied biomass feedstocks. Corn stover (CS) and wheat straw (WS) were less affected by the pretreatment severity compared to *Miscanthus × giganteus* stalks (MS). The difference across biomass feedstocks was especially noteworthy as the glucose release from MS across corresponding severity factors and enzyme dosages were consistently lower (~24 to 67%) than CS and WS (Fig. 4.2). Based on the previous reports, increasing biomass digestibility with pretreatment severity level correlates to hemicellulose removal after HTP [46,51–53]. Therefore assuming the same observation applies to multiple biomass feedstocks, it can be expected that MS had lower hemicellulose removal after HTP than CS and



WS. Assessing the changes in bulk composition and surface properties of the biomass after HTP is therefore expected to shed light in understanding of the factors that correlate to digestibility.

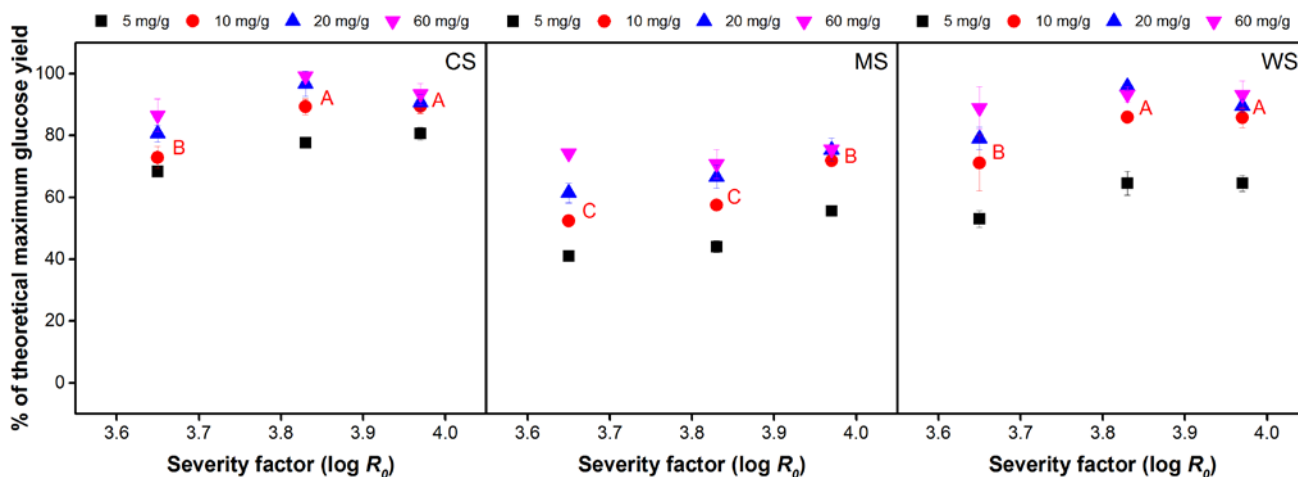


Fig. 4.2 Glucose release after 72 h enzymatic hydrolysis of 1% DM hydrothermally pretreated corn stover (CS), *Miscanthus × giganteus* stalks (MS) and wheat straw (WS) at different severity factors ( $\log R_0$ ) and enzyme dosages (mg/g). Data points represent average and standard deviation from three experimental replicates. Different letters indicate significant statistical difference based on ANOVA ( $p \leq 0.05$ ) for 10 mg/g enzyme dosage series.

#### 4.4 Changes in bulk composition of biomass after hydrothermal pretreatment

In accordance to the previous studies on HTP of lignocellulosic biomass [46,51–53], the hemicellulose (xylan) content of pretreated biomass decreased with increasing severity level. The cellulose (glucan) and lignin contents on the other hand remained relatively stable (Fig. 4.3). The pretreated biomass feedstocks had relatively similar carbohydrates composition. In contrast, the lignin content was lower on CS compared to the others, but was similar for both MS and WS (Fig. 4.3). Regardless, the extent of hemicellulose removal (relative to the untreated biomass feedstocks) revealed similar degree of arabinose and xylose release for each corresponding severities where an increasing trend can be seen (**Paper I**: Fig. 1). This indicated that all the pretreated biomass

feedstocks were subjected to the same extent of HTP severity factors regardless of their botanical origin and other inherent differences, confirming the versatile use of the severity factor [47]. Further investigation also showed that the applied HTP severity removed hemicellulose decorations, e.g. acetylations (**Paper I**: Table 2) and the arabinoxylan structure (**Paper I**: Fig. 3). The removal occurred to the same extent across biomass feedstocks and was increased with severity level. Thus bulk composition analyses indicated that the changes due to HTP affected all the tested feedstocks similarly. They were not able to provide the explanation on the observed differences in the digestibility of the different biomass feedstocks where MS was the lowest (Fig. 4.2).

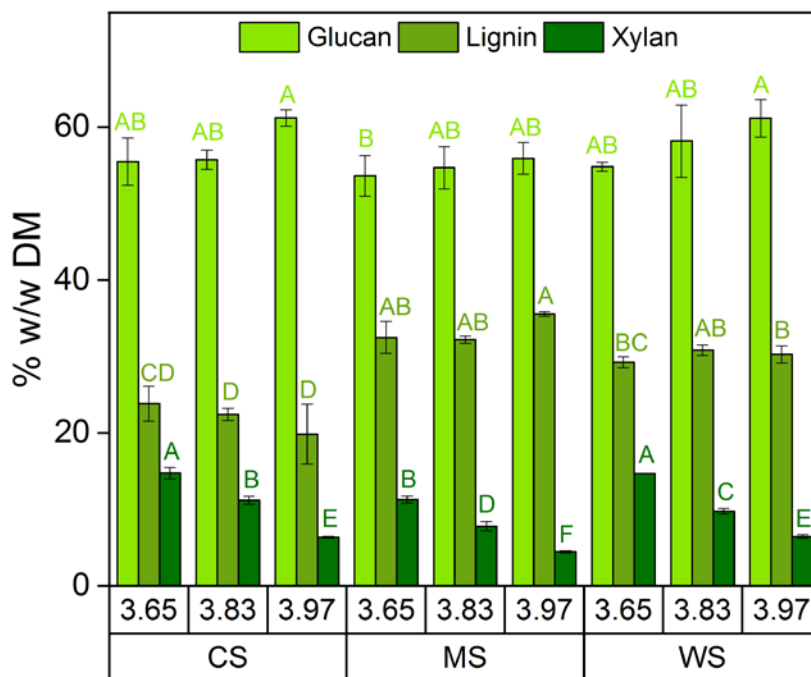


Fig. 4.3 Composition of hydrothermally pretreated corn stover (CS), *Miscanthus × giganteus* stalks (MS) and wheat straw (WS) at different severity factors ( $\log R_0$ ). Data points represent average and standard deviation from triplicate measurements. Different letters indicate significant statistical difference based on ANOVA ( $p \leq 0.05$ ).

#### ***4.5 Changes in surface properties of biomass after hydrothermal pretreatment***

Since none of the changes in bulk composition can correlate or provide explanation to the observed difference in the digestibility of the hydrothermally pretreated feedstocks, changes in surface properties were assessed. Initial water contact angle measurement revealed that the wettability of biomass improved as a result of HTP (Fig. 4.4A), which is in agreement with previous reports [163,168,169]. The applied severity levels improved further the wettability of CS and WS. However, this was not the case of MS where the wettability was consistently lowest for each corresponding severity factors (Fig. 4.4A). Overall, the wettability data correlated well with the glucose release of the pretreated biomass feedstocks (Fig. 4.4B). Further investigation was performed with ATR-FTIR spectroscopy which probed the apparent surface abundance (ASA) of lignocellulose components relative to cellulose. The method is considered pertaining to the surface of the biomass particles due to its limited depth of penetration (**Paper I**: Table 5). ATR-FTIR analysis revealed that the ASA of hemicellulose was reduced after HTP and with the applied severity factors (Fig. 4.5A). This is in agreement with the observed removal of hemicellulose after HTP (**Paper I**: Fig. 1). On the other hand, the ASA of lignin was increased after HTP and with the applied severity factors (Fig. 4.5B); possibly denoting the redistribution of lignin previously observed as droplets [45,54,63]. Yet, it is noteworthy to mark that MS had the highest values on the ASA of hemicellulose and lignin, both before and after HTP (Fig. 4.5). This correlated to both the consistently lower wettability (Fig. 4.4B) and digestibility (Fig. 4.2) of MS compared to others.

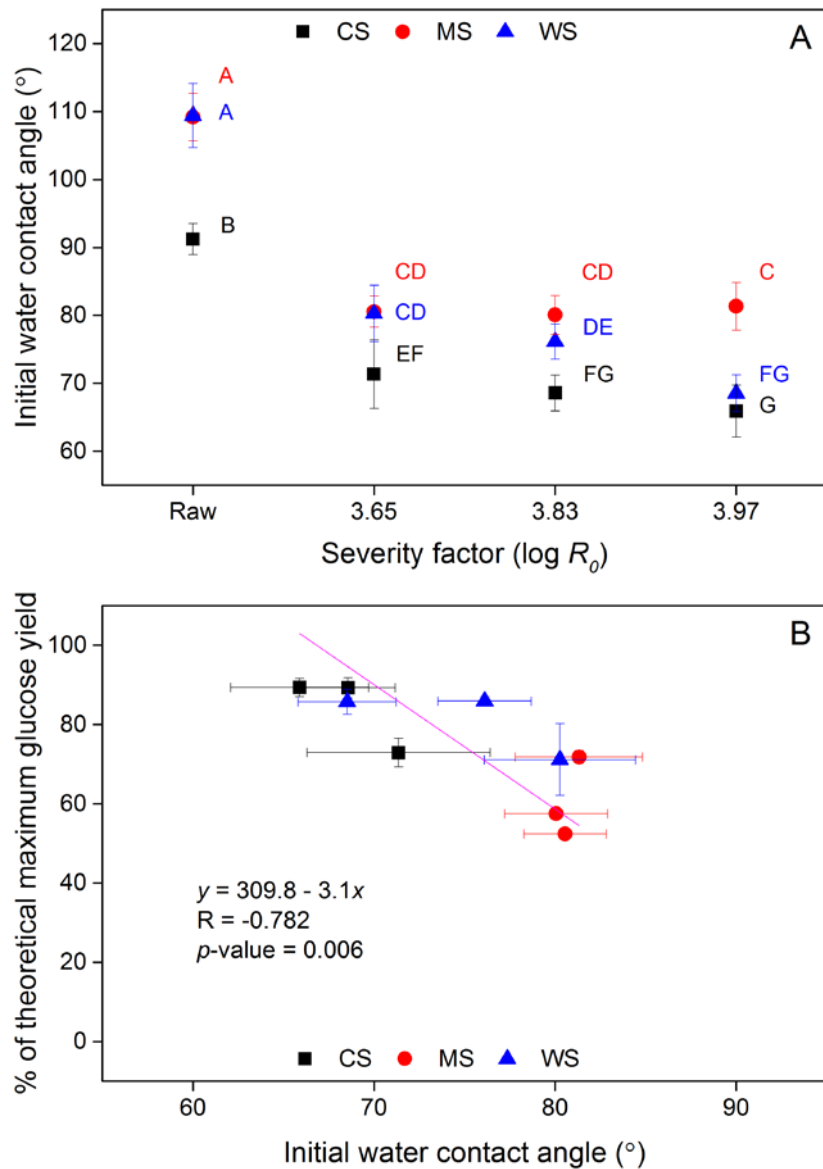


Fig. 4.4 Initial water contact angle (A) of raw and hydrothermally pretreated corn stover (CS), *Miscanthus × giganteus* stalks (MS) and wheat straw (WS) at different severity factors ( $\log R_0$ ). Data points represent average and standard deviation from five technical replicates. Different letters indicate significant statistical difference based on ANOVA ( $P \leq 0.05$ ). Scatter plot (B) of glucose release after 72 h enzymatic hydrolysis at 10 mg/g dosage for pretreated CS, MS and WS at three severity factors with corresponding initial water contact angle prior to hydrolysis. The strength of linear relationship between paired data is indicated by Pearson's correlation coefficient (R) and  $t$ -test of the regression slope (significant if  $p$ -value  $< 0.05$ ).

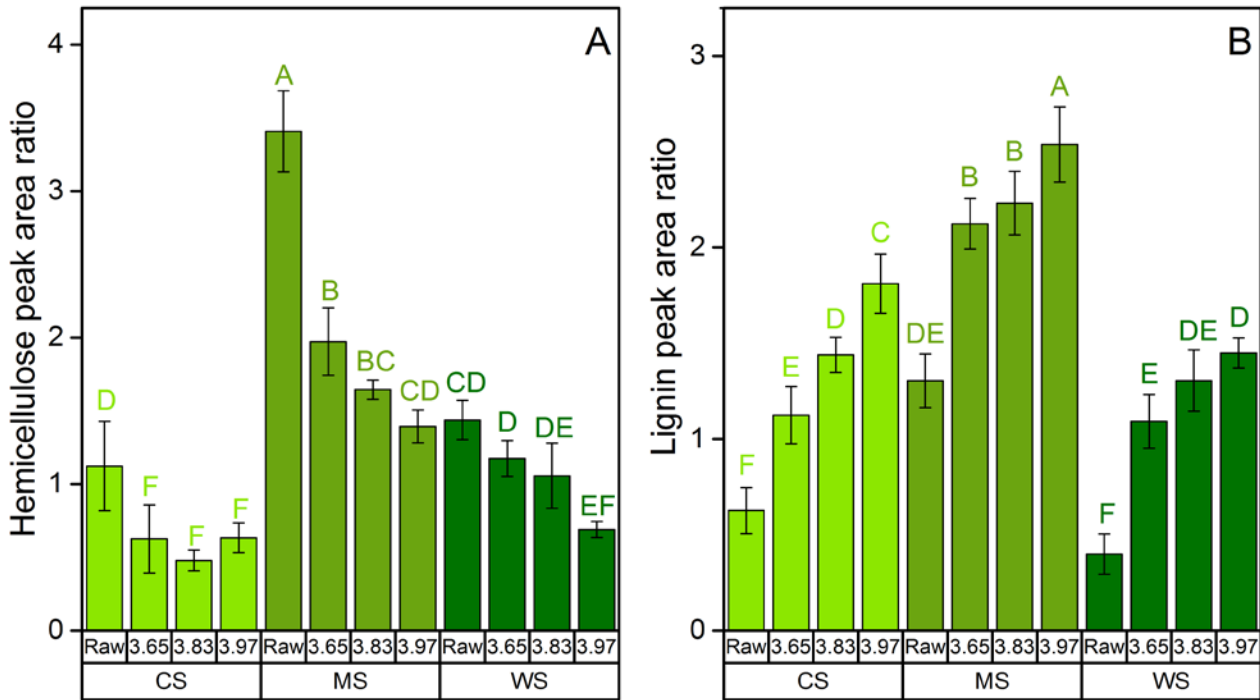


Fig. 4.5 ATR-FTIR peak area ratio of wavenumbers representing (A) hemicellulose ( $1732\text{ cm}^{-1}$ ) and (B) lignin ( $1508\text{ cm}^{-1}$ ), each relative to that of holocellulose ( $895\text{ cm}^{-1}$ ) for untreated (raw) and hydrothermally pretreated corn stover (CS), *Miscanthus × giganteus* stalks (MS) and wheat straw (WS) at different severity factors ( $\log R_0$ ). Data points represent average and standard deviation from five experimental replicates. Different letters indicate significant statistical difference based on ANOVA ( $p \leq 0.05$ ).

#### 4.6 Correlating biomass digestibility with bulk composition and surface properties

In general, factors pertaining to the surface properties of biomass correlated better to digestibility compared to those pertaining to the bulk composition of biomass (**Paper I**: Table 3). A key merit was that the methods assessing surface properties were able to distinguish MS from the other feedstocks in correlation with digestibility (Fig. 4.4 and Fig. 4.5). In contrast, hemicellulose content and removal based on bulk composition did not correlate well with digestibility (**Paper I**: Table 3).

This showed that changes in bulk composition were not good indicator of digestibility across biomass feedstocks despite being a good indicator for a single feedstock that was pretreated with different severity factors. ASA of hemicellulose on the other hand showed excellent correlation with digestibility (**Paper I**: Table 3). The method thus plausibly provides sound assessment on the removal of the extent of hemicellulose moieties that obstruct the access to cellulose. Accordingly the bulk cellulose content also correlated to digestibility (**Paper I**: Table 3) and the digestibility of cellulose in pretreated biomass is indeed pertained to its accessibility [37,38]. The correlation however, was not evident both in the case of bulk and surface assessment of lignin (**Paper I**: Table 3). A marked difference between the two methods was that bulk composition showed that the lignin content remained constant across severity (Fig. 4.3), whereas the surface assessment showed increase with each applied severity factor (Fig. 4.5B). This increased ASA of lignin, which correlated positively with increased digestibility across severity levels (Fig. 4.2), is suggested to be an artifact. The artifact occurred along with other presumably more significant changes that increased cellulose digestibility. Assessing the contribution of single lignocellulose components can be difficult due to possible interactions among them that may also affect digestibility. Regardless, the work ultimately showed that methods assessing surface properties were able to indicate the digestibility of pretreated multiple biomass feedstocks of diverse botanical origins.

#### ***4.7 Concluding remarks and significance of study***

Based on the previously set hypotheses (Subchapter 4.1), it can be concluded that:

1. Even though biomass feedstocks of diverse botanical origin responded differently to HTP in terms of digestibility, the changes in their bulk composition after HTP were similar across the pretreated feedstocks. However, the changes in the surface properties of biomass after HTP were different across the pretreated feedstocks.

2. Factors pertaining to surface properties correlated better to digestibility rather than those pertaining to bulk composition in case of hydrothermally pretreated lignocellulosic biomass.

Since pretreatment is important to improve the digestibility of lignocellulosic biomass feedstocks, a comprehensive understanding of the process is required. Many reactions and redistributions of different lignocellulose components occurred during pretreatment, thus contributing to the complexity of the process. This made assessing the digestibility of pretreated biomass based on the changes of lignocellulose components challenging. Nonetheless, understanding the changes in the lignocellulose components that correlate to digestibility is important to pinpoint the factors which can be used as input to further optimize pretreatment methods. This study showed that bulk methods, which extensively map the composition of biomass quantitatively, were not able to indicate changes in lignocellulose components that correlate to digestibility of multiple biomass feedstocks. Methods that assess surface properties of biomass, in particular assessment of ASA of lignocellulose components using ATR-FTIR spectroscopy provided fast and semi-quantitative information that correlated to digestibility of multiple biomass feedstocks (**Paper I**: Table 3). This brought further understanding on the role of non-cellulosic lignocellulose components as microscale barrier impeding cellulose degradation. Furthermore, it also emphasized the need to understand the biomass pretreatment and degradation as a surface phenomenon since enzymes and biomass interact in the surface level. All in all, this points the need for integrated understanding of multi-component changes in the biomass during pretreatment and subsequent interaction with enzymes at the surface.

## **Chapter 5 – The role of lignin from hydrothermally pretreated grass biomass feedstocks in retarding enzymatic cellulose degradation (Paper II)**

### ***5.1 Hypotheses***

1. Lignin substrates isolated from hydrothermally pretreated lignocellulosic biomass feedstocks (in the form of LRRs) retard enzymatic cellulose degradation by inducing irreversible non-productive adsorption of enzymes.
2. The extent of retardation of enzymatic cellulose degradation caused by LRRs can be correlated to the changes in physical and chemical properties of lignin polymer after HTP.

### ***5.2 Experimental considerations***

The isolation of lignin from the hydrothermally pretreated grass biomass feedstocks was done by performing extensive cellulose hydrolysis. In this way, the resulting lignin-rich residues (LRRs) are expected to resemble the actual bioprocess residue from lignocellulosic ethanol plants, i.e. that of Inbicon [4]. Furthermore the procedure is also expected to exert minimal changes to the structure of lignin. The effect of adsorption of cellulolytic enzymes on isolated LRRs on subsequent enzymatic cellulose degradation is an important investigation in this work. The investigation was performed in a series of three interconnected experimental works, i.e. adsorption experiment, Experiment I and Experiment II. Low enzyme dosage which is on par with that being used in large scale process [3] was used throughout the experiments.

The series of experimental works was designed to prove that the retardation of enzymatic cellulose degradation is attributed primarily to the loss of activity due to irreversible non-productive adsorption. A key feature in both Experiments I and II is the pre-adsorption of the enzymes on LRRs that was performed with same conditions as in an integrated adsorption



experiment. This scheme enables thorough examination of the enzymes' activity during and after adsorption (Fig. 5.1). Experiment I assessed the activity of enzymes that were both bound on lignin and unbound by adding model cellulose (Avicel) suspension on top of mixture of enzymes pre-adsorbed on LRRs. The latter addition of cellulose served as well to reveal whether the non-productive adsorption on lignin is irreversible. Experiment II assessed only the activity of enzymes that were unbound. This was done by performing centrifugation on the mixture of enzymes pre-adsorbed on LRRs and transferring the supernatant containing unbound enzymes to a fresh model cellulose suspension. If the adsorption of the enzymes on lignin was irreversible and non-productive, a similar decrease of activity should be expected in both Experiments I and II.

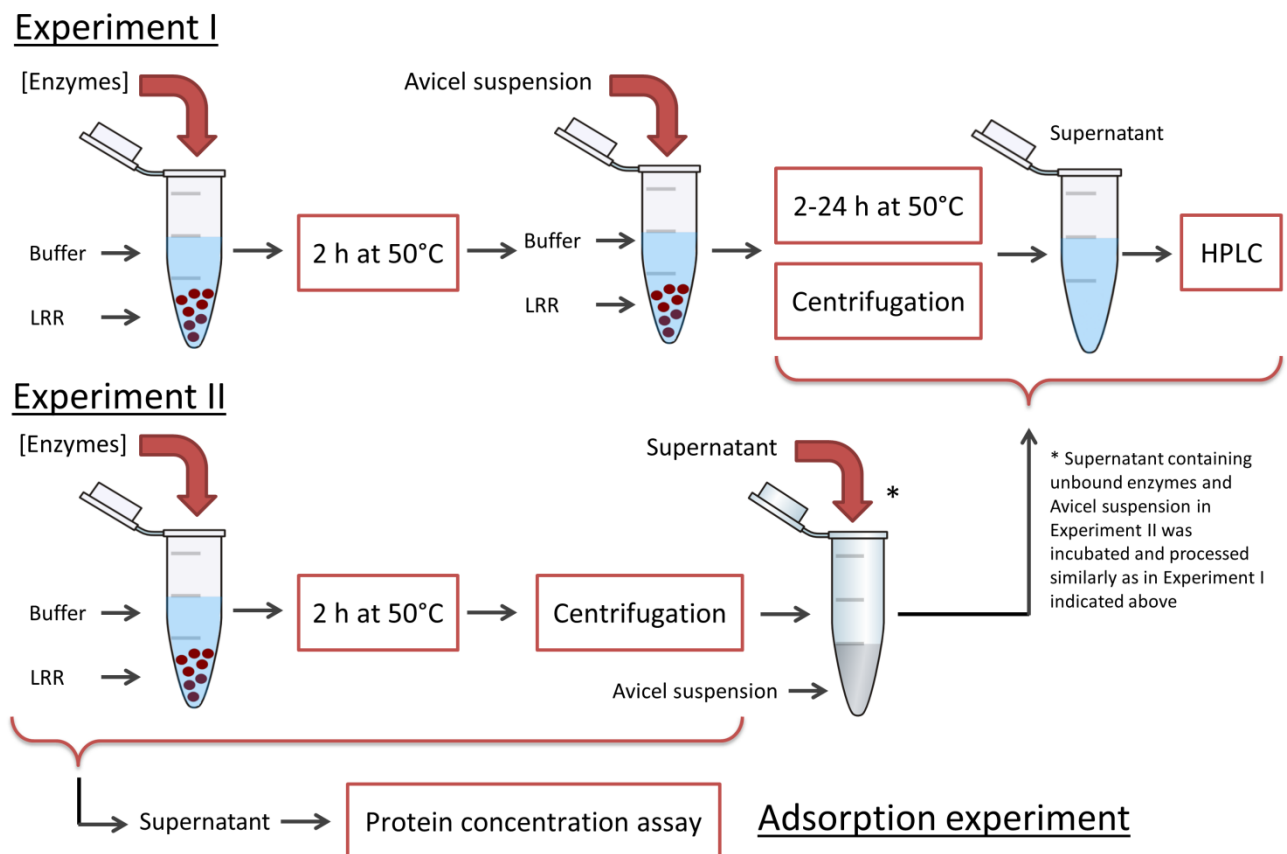


Fig. 5.1 Outline of Experiment I and Experiment II along with the integrated adsorption experiment.

### ***5.3 Changes in the physical and chemical properties of the lignin after HTP***

2D NMR spectroscopy was performed to assess the relative abundance of inter-unit linkages in the lignin polymer of the LRRs after HTP. The results revealed that there was only a minor decrease of  $\beta$ -O-4 linkage in all biomasses with each elevated severity level, corresponding to only 4-13% signal reduction in the contour integration values (**Paper II**: Table 2). Py-GC-MS analysis was performed in order to assess the composition of the monolignols of the LRRs. The results revealed no differences on the relative monolignols contents and ratios after HTP in the case of each biomass (Fig. 5.2). However, the relative monolignols contents differed among biomass feedstocks. CS had higher S/G ratio compared to MS and WS (Fig. 5.2). The monolignols ratios were also determined by ATR-FTIR spectroscopy, yielding similar results as those of Py-GC-MS (**Paper II**: Fig. 4). Thus the results showed that the applied HTP severity levels did not change the chemical composition of lignin significantly, yet variation across biomass feedstocks was present.

Assessment of the molecular weight ( $M_w$ ) distribution of the lignin polymer in the LRRs on the other hand revealed several changes across the applied HTP severity levels. The changes however, differed across the tested grass biomass feedstocks (Fig. 5.3). In CS and MS, there were negligible changes in the  $M_w$  fractions except at the highest severity level tested where low  $M_w$  fractions appeared. In the case of WS, there were more substantial increase of fractions with lower  $M_w$  that appeared with each severity level applied (Fig. 5.3). Therefore, it can be said that there were greater extent of depolymerization reactions that occurred in WS lignin compared to CS and MS. However, this was not evident from the reduction of  $\beta$ -O-4 linkages since the extents of reduction were similarly minor in all biomass (**Paper II**: Table 2). Tricin content was previously suggested to retard repolymerization reactions in lignin during HTP [31]. Accordingly, in this work, triclin had a more pronounced presence in raw (untreated) WS rather than CS and MS (Appendix A: Figures A.1-A.3; Table A.1), thus possibly explaining the difference in the changes of  $M_w$  fractions.

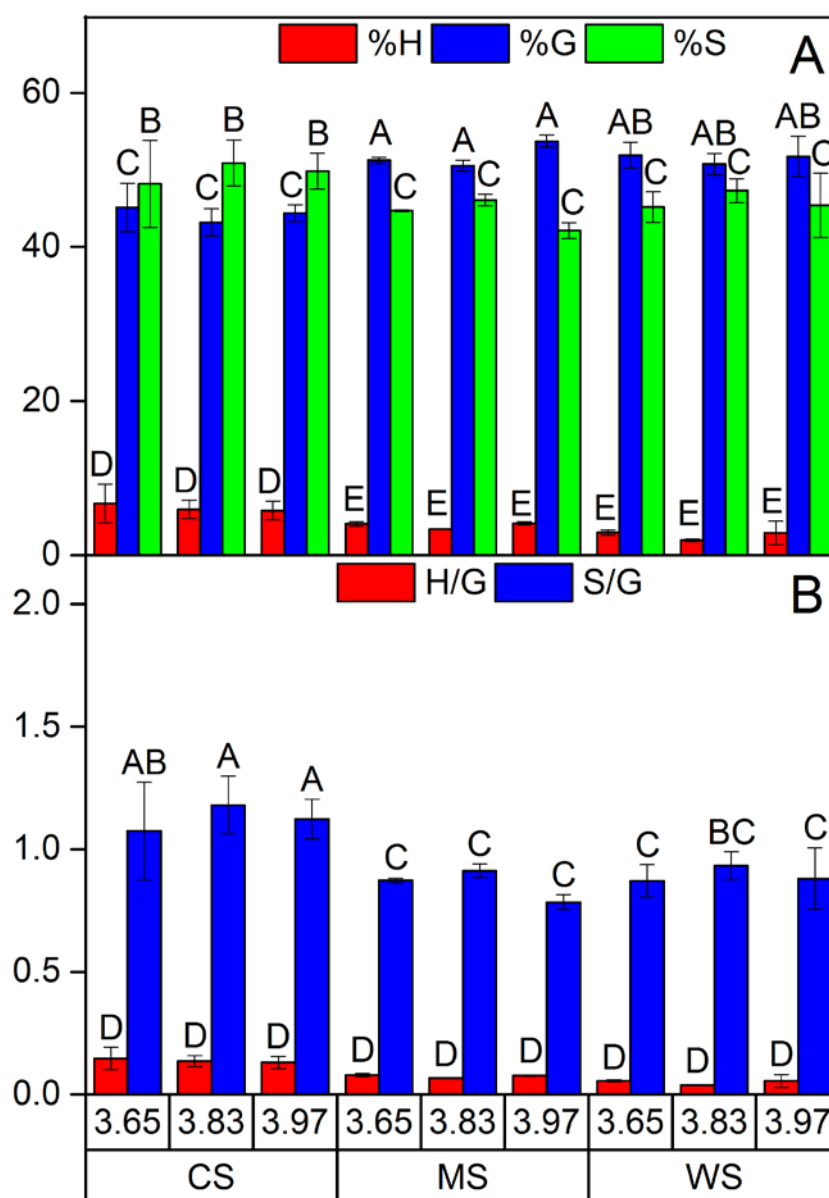


Fig. 5.2 The relative abundance of monolignols, namely *p*-hydroxyphenyl (H), guaiacyl (G) and syringyl (S) units (A) and the corresponding monolignols ratio (B) based on Py-GC-MS results of the lignin-rich residues (LRRs) from corn stover (CS), *Miscanthus × giganteus* stalks (MS) and wheat straw (WS). Data points represent average and standard deviation from two replicates. Different letters indicate significant statistical difference based on ANOVA ( $P \leq 0.05$ ).

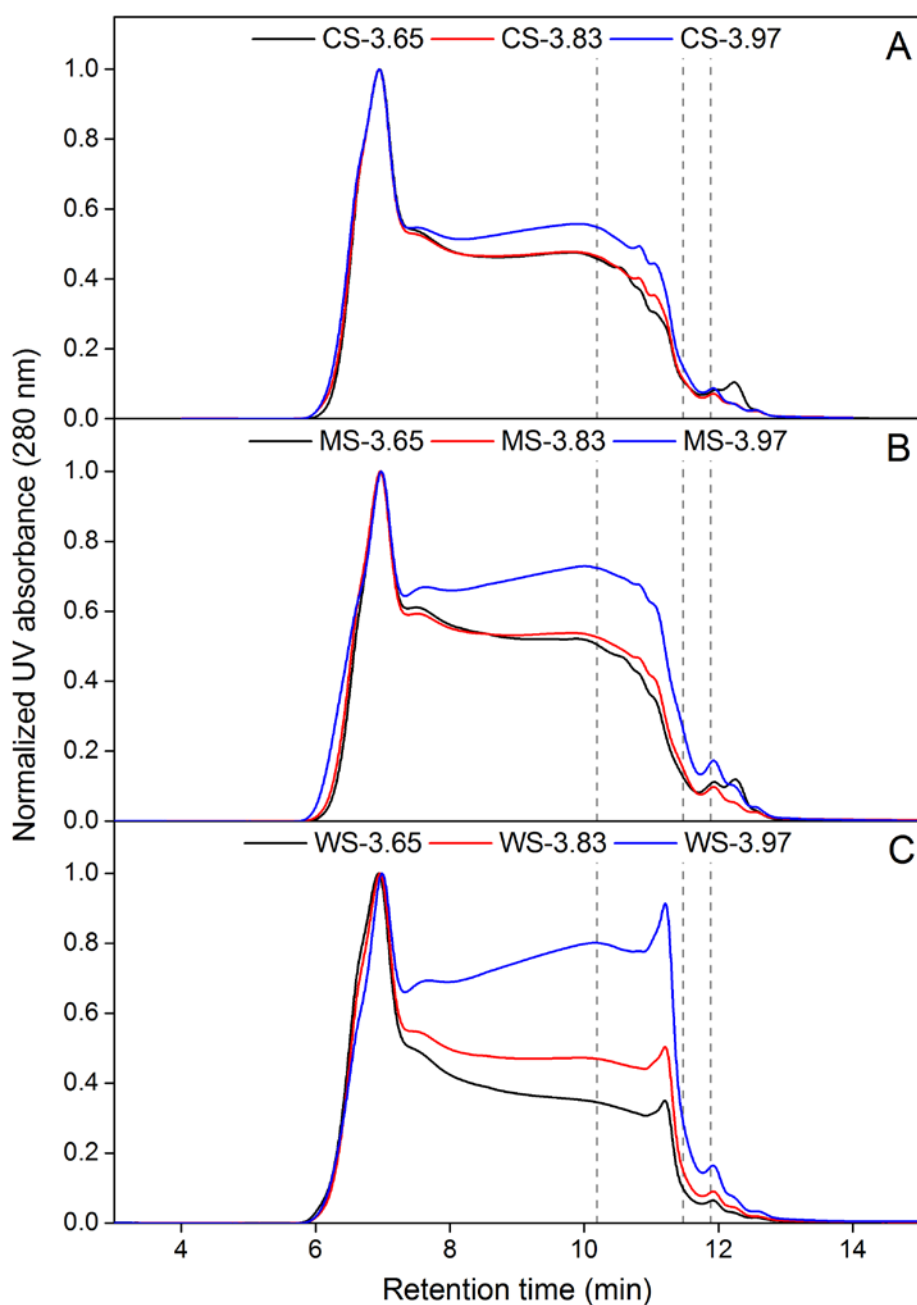


Fig. 5.3 Chromatograms from GPC analysis of lignin-rich residues (LRRs) from corn stover (CS) (A), *Miscanthus x giganteus* stalks (MS) (B) and wheat straw (WS) (C) hydrothermally pretreated at different pretreatment severity factors ( $\log R_0$ ). Peaks appearing at higher retention time correspond to fractions with lower molecular weights ( $M_w$ ). The vertical lines represent standards with  $M_w$  of 1701, 320 and 152 Da appearing at 10.19, 11.47 and 11.88 min, respectively.

#### ***5.4 Role of lignin in retarding enzymatic cellulose degradation by inducing irreversible non-productive adsorption***

The results of adsorption experiment showed that there were no evident consistent trends across all of the LRRs regardless whether it was based on biomass feedstocks or severity factors (**Paper II**: Fig. 1). This is correlated to the minimum changes in the chemical structure of lignin after HTP at different severity levels despite differences in biomass feedstocks (**Paper II**: Table 2; Fig. 5.2). Despite 34-47% of total protein being adsorbed, Experiment I (**Paper II**: Fig. 1) showed that after the pre-adsorption of enzymes on LRRs, the rate and extent of glucose release from the added Avicel were not retarded. There was also no effect of variation in biomass feedstocks or the applied severity levels (Fig. 5.4A-C) as in the results of adsorption experiment (**Paper II**: Fig. 1). On the other hand, Experiment II showed that as the result of enzymes adsorption on LRRs, the glucose release from Avicel by the unbound enzymes was reduced by 19-57% (Fig. 5.4D-F). This indicated the activity of unbound enzymes alone was not enough to degrade the added Avicel to the same rate and extent as that of the control mixture. Most importantly, by showing negligible difference in the glucose release (Fig. 5.4A-C), the results of Experiment I gave strong indication that the binding on lignin is reversible. It can be expected that the enzymes adsorbed on LRRs were able to desorb and catalyze the added cellulose, a phenomenon that has been suggested previously [170]. Due to the strong indication that the enzymes adsorb reversibly on lignin, it is unlikely that non-productive adsorption contribute significantly on enzymatic cellulose degradation. This is especially true when taking into account the previous work on **Paper I**. MS which was found to be the least digestible (Fig. 4.2) did not have a lignin which bound more enzymes (**Paper II**: Fig. 1) and retarded the cellulose degradation more significantly than other (Fig. 5.4).

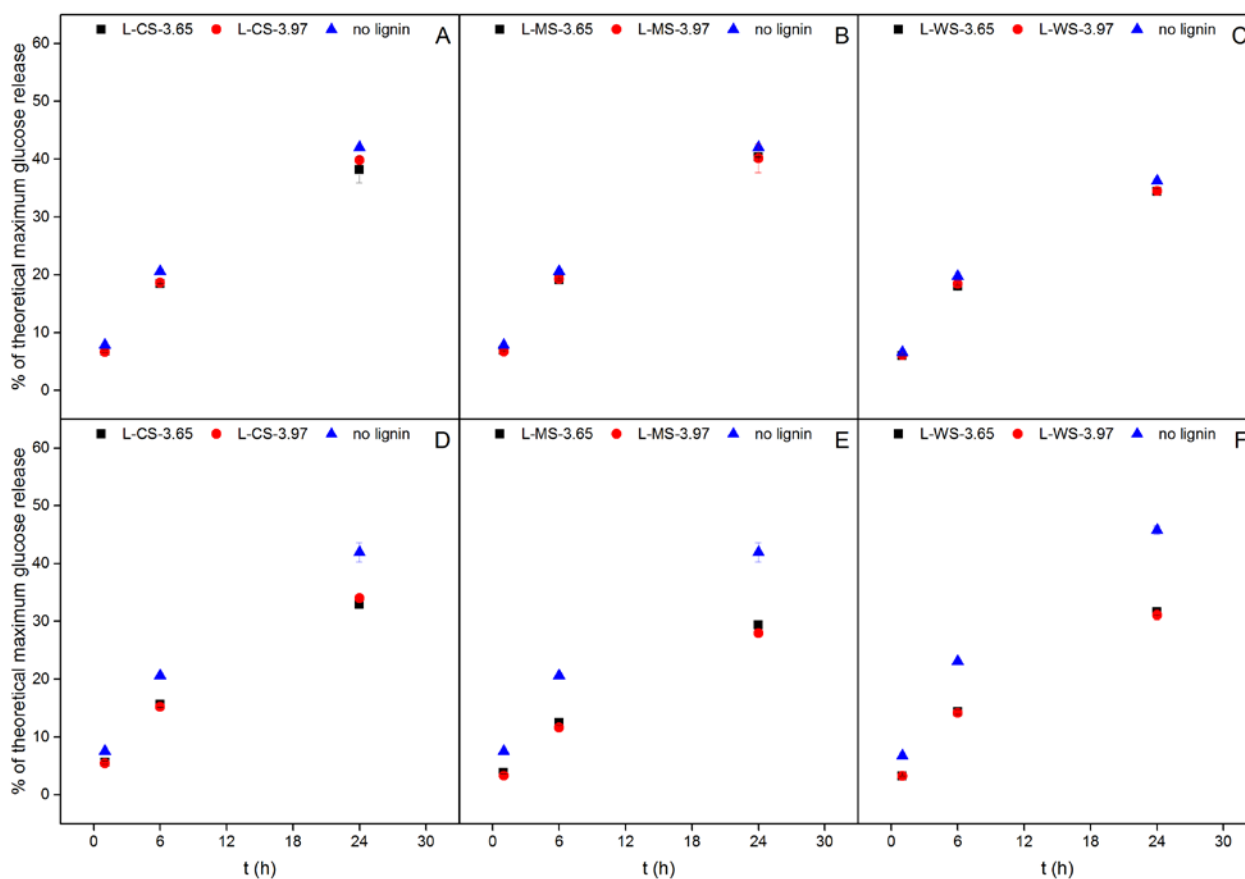


Fig. 5.4 Glucose release from 2% DM Avicel hydrolysis after adsorption experiment of Cellic<sup>®</sup> CTec3 in the presence of lignin-rich residues (LRRs) as in Experiment I (A-C) or by supernatant containing unbound enzymes after incubation with LRRs in Experiment II (D-F). LRRs were isolated from corn stover (L-CS) (A & D), *Miscanthus × giganteus* stalks (L-MS) (B & E) and wheat straw (L-WS) (C & F) that were hydrothermally pretreated at severity factor ( $\log R_0$ ) 3.65 and 3.97. Data points represent average and standard deviation from two replicates.

### 5.5 Role of lignin in retarding enzymatic cellulose degradation by acting as a physical barrier

Attributing the retardation of enzymatic cellulose degradation to lignin therefore shifted to its inherent role as physical barrier from the perspective of plant cell wall structure. The composition of LRRs (Table 5.1) alone already suggested that the mere presence of lignin might play a role in retarding cellulose degradation. The LRR isolation method served as an exaggerated version of

enzymatic hydrolysis, reflecting digestibility by the amount of residual carbohydrates left (Table 5.1). Similar to the previous results (Fig. 4.2), MS was shown to be the least digestible by having the highest amounts of residual carbohydrates left (Table 5.1). Yet these carbohydrate moieties were not accessible to the enzymes as the release of monosaccharides from enzymatic hydrolysis of LRRs was negligible (Appendix B: Table B.1). Additionally, ATR-FTIR analysis revealed that the residual carbohydrates were not traceable to the surface of the LRRs. Oppositely, the presence of lignin in the LRRs became more pronounced after extensive hydrolysis (Appendix C: Figures C.1-C.3). These observations suggested that the progressing cellulose hydrolysis was likely to be halted by increasing presence of lignin in the surface of the biomass particles which engulfed the carbohydrates, rendering them inaccessible by the enzymes.

The agreement of monolignols ratio between ATR-FTIR (surface method) and Py-GC-MS (bulk method) results (Appendix C: Figures C.1-C.3; Fig. 5.2) further corroborated the aforementioned notion. The insights from **Paper I**, concerning ASA of lignin, were used to extrapolate the process as if it occurred during the extensive cellulose hydrolysis. Initially, prior to cellulose hydrolysis, the ASA of lignin was higher in CS and MS compared to WS (Fig. 4.5B). Since the digestibility of WS after extensive cellulose hydrolysis was higher than the other feedstocks (Table 5.1), it can be suggested that as hydrolysis reaction progressed, the advance was retarded earlier in CS and MS. Ultimately this was due to the higher presence of lignin in the surface of biomass particles in CS and MS. The greater extent of lignin depolymerization in WS (Fig. 5.3) compared to other biomass also correlated to the lower ASA of lignin before and after HTP at different severity factors (Fig. 4.5B). This indicates that the distribution of lignin after HTP can also be influenced by lignin physical properties (Fig. 5.3). Hence the state of being engulfed by lignin is likely an inherent trait in the biomass which later can also be affected by pretreatment.

Table 5.1 Composition of lignin-rich residues isolated from pretreated biomass feedstocks

Biomass – log $R_0$	Pretreated biomass feedstocks			Lignin-rich residues		
	Glucan	Xylan	Lignin <sup>1</sup>	Glucan	Xylan	Lignin <sup>1</sup>
	(% w/w DM)					
<b>CS – 3.65</b>	55.5 ± 3.1 <sup>ab</sup>	14.7 ± 0.8 <sup>a</sup>	23.8 ± 2.3 <sup>cd</sup>	20.9 ± 0.5 <sup>b</sup>	5.4 ± 0.2 <sup>a</sup>	60.4 ± 1.3 <sup>f</sup>
<b>CS – 3.83</b>	55.7 ± 1.3 <sup>ab</sup>	11.2 ± 0.5 <sup>b</sup>	22.4 ± 0.8 <sup>d</sup>	14.5 ± 0.1 <sup>d</sup>	3.2 ± 0.1 <sup>bc</sup>	75.4 ± 0.9 <sup>de</sup>
<b>CS – 3.97</b>	61.2 ± 1.1 <sup>a</sup>	6.4 ± 0.1 <sup>e</sup>	19.9 ± 3.9 <sup>d</sup>	7.2 ± 0.2 <sup>f</sup>	1.6 ± 0.0 <sup>e</sup>	79.5 ± 1.6 <sup>bc</sup>
<b>MS – 3.65</b>	53.6 ± 2.6 <sup>b</sup>	11.3 ± 0.4 <sup>b</sup>	32.5 ± 2.1 <sup>ab</sup>	33.9 ± 0.7 <sup>a</sup>	5.7 ± 0.1 <sup>a</sup>	58.5 ± 0.7 <sup>f</sup>
<b>MS – 3.83</b>	54.7 ± 2.8 <sup>ab</sup>	7.8 ± 0.6 <sup>d</sup>	32.2 ± 0.5 <sup>ab</sup>	18.9 ± 0.6 <sup>c</sup>	3.0 ± 0.1 <sup>c</sup>	73.1 ± 0.8 <sup>e</sup>
<b>MS – 3.97</b>	55.9 ± 2.1 <sup>ab</sup>	4.5 ± 0.2 <sup>f</sup>	35.6 ± 0.3 <sup>a</sup>	11.7 ± 0.5 <sup>e</sup>	1.4 ± 0.0 <sup>e</sup>	81.9 ± 0.3 <sup>b</sup>
<b>WS – 3.65</b>	54.8 ± 0.6 <sup>ab</sup>	14.7 ± 0.0 <sup>a</sup>	29.3 ± 0.7 <sup>bc</sup>	13.7 ± 0.6 <sup>d</sup>	3.4 ± 0.1 <sup>b</sup>	77.7 ± 0.7 <sup>cd</sup>
<b>WS – 3.83</b>	58.2 ± 4.7 <sup>ab</sup>	9.8 ± 0.4 <sup>c</sup>	30.8 ± 0.7 <sup>ab</sup>	7.9 ± 0.0 <sup>f</sup>	2.0 ± 0.0 <sup>d</sup>	86.2 ± 0.1 <sup>a</sup>
<b>WS – 3.97</b>	61.2 ± 2.5 <sup>a</sup>	6.5 ± 0.2 <sup>e</sup>	30.3 ± 1.1 <sup>b</sup>	5.3 ± 0.1 <sup>g</sup>	1.1 ± 0.0 <sup>f</sup>	87.8 ± 1.0 <sup>a</sup>

1: Based on acid insoluble lignin (AIL) and acid soluble lignin (ASL) contents

CS: corn stover, MS: *Miscanthus × giganteus* stalks, WS: wheat straw

Results are average and standard deviation of triplicate measurements

Different letters indicate significant statistical difference based on ANOVA ( $P \leq 0.05$ )

### 5.6 Concluding remarks and significance of study

Based on the previously set hypotheses (Subchapter 5.1), it can be concluded that:

1. The isolated LRRs did not retard enzymatic cellulose degradation by inducing irreversible non-productive adsorption of enzymes. The mere presence of lignin as physical barrier and its ensuing redistribution profile after HTP were more likely to be the cause of retardation.
2. LRRs did not retard the glucose release during enzymatic cellulose degradation. Therefore it was not possible to correlate the extent of retardation of enzymatic cellulose degradation caused by LRRs to the changes in physical and chemical properties of lignin after HTP.



However, the changes in  $M_w$  fractions of lignin in the LRRs after HTP at different severity levels correlated to the ASA of lignin and biomass digestibility, further pointing that lignin retards enzymatic cellulose degradation by acting as a physical barrier.

The study revealed that to a greater extent, the retardation of enzymatic cellulose degradation of hydrothermally pretreated biomass is more likely due to increasing presence of lignin that acts as physical barrier rather than inducing non-productive adsorption. Furthermore, the study also gave strong indication that the binding of the enzymes on lignin is reversible. This can significantly affect current understanding in viewing the role of lignin in retarding enzymatic cellulose degradation. Technically, at the same instance, the increasing presence of lignin in the surface of biomass particles as the hydrolysis progresses can reasonably adsorb more enzymes; hence exacerbating the retardation through non-productive adsorption. However, this is only the case when the adsorption is irreversible. Therefore the findings underline the importance of investigating the dynamics of non-productive binding of cellulases and its monocomponent enzymes with respect to their reversibility. Nevertheless, in order to cope with the role of lignin as physical barrier, the study points towards the need to understand the physical properties of lignin, especially with respect to its migration and modification during and after pretreatment. The study suggested that chemical and physical properties of lignin can play a role in the distribution of lignin. This would lead into suggestions of possible plant genetic modification or pretreatment process engineering to modulate the migration of lignin in order to favor better fractionation and release of lignocellulose components in biorefinery operations.

## **Chapter 6 – The nature of the binding of monocomponent cellulases on lignin isolated from hydrothermally pretreated lignocellulosic biomass (Paper III)**

### ***6.1 Hypotheses***

1. Monocomponent cellulases adsorb on lignin isolated from hydrothermally pretreated lignocellulosic biomass feedstocks (in the form of LRRs) with different binding affinity that can be correlated to the intrinsic properties of the enzymes.
2. The adsorption of monocomponent cellulases on lignin isolated from hydrothermally pretreated lignocellulosic biomass feedstocks (in the form of LRRs) is irreversible by nature.
3. Monocomponent cellulases bind competitively on LRRs where one enzyme with higher affinity would be more predominant over the other.

### ***6.2 Experimental considerations***

One primary consideration is the use of monocomponent cellulases (Table 6.1) to discern any differences in their binding and to investigate whether they have similar nature on binding. The use of radiolabeling technique is also important given to their sensitivity and specificity [118,171,172]. The LRRs used represent two extremes of biomass feedstocks, spruce and WS, which were reported to be different in their adsorption [117,118] and ensuing retardation of enzymatic hydrolysis of model cellulose [120,132]. A central key experiment in the work is the reversibility test and kinetic modelling of adsorption performed on the adsorption of *TrCel6A* and *TrCel5A* on LRRs isolated from hydrothermally pretreated spruce (L-HPS) and wheat straw (L-HPWS). The adsorption and desorption profiles of the enzymes were followed over an extended time course during which a total dilution of the system by a factor of two was introduced after 1 h (Early Dilution series) and 24 h (Late Dilution series). Three initial enzyme concentrations which covered all range of the

established adsorption isotherms were used. The work aimed to quantify the proportion of irreversible binding from the difference in desorption after early and late dilutions, thus providing data for the different models. It is assumed that longer incubation time prior to the late dilution would allow more irreversible binding to occur and lead to lower desorption of enzymes compared to the early dilution. This would allow quantification of the irreversible binding.

Table 6.1 Summary of the characteristics of monocomponent cellulases used in this study

Enzymes	Old name	EC number	Domain architecture	M <sub>w</sub> (kDa) <sup>1</sup>	pI <sup>2</sup>	Hydrophobic patch score <sup>2</sup>		
						Core	CBM	Total
<i>TrCel7A</i>	CBHI	3.2.1.91	GH7-CBM1	56.0	3.6- <u>4.3</u>	6.7	6.6	13.3
<i>TrCel6A</i>	CBHII	3.2.1.91	GH6-CBM1	56.7	5.4- <u>6.2</u>	14.1	1.9	16.0
<i>TrCel7B</i>	EGI	3.2.1.4	GH7-CBM1	51.9	4.5-4.9, <u>4.7</u>	6.2	0.8	7.0
<i>TrCel5A</i>	EGII	3.2.1.4	GH5-CBM1	48.2	<u>5.6</u>	2.6	7.0	9.6

1: Based on Várnai et al. [104].

2: Based on Kellock et al. [120]; major isoform in pI measurement is underlined.

### 6.3 Binding affinity of the monocomponent cellulases on LRRs

Adsorption isotherm was established for the monocomponent cellulases at 45°C, pH 5.0 after 1 h on L-HPS and L-HPWS. The isotherms revealed that *TrCel5A* had the highest affinity on both L-HPS and L-HPWS (Fig. 6.1). The order of the enzymes' binding affinity based on visual observation (Fig. 6.1), fitting of Langmuir adsorption model (**Paper III**: Table II) and extent of binding at the lowest concentration in the isotherm (**Paper III**: Fig. 2) was: *TrCel5A* > *TrCel6A* > *TrCel7B* > *TrCel7A*. The enzymes had higher binding affinity on L-HPS compared to L-HPWS as reported

previously [117,118]. There were no consistent correlations between the enzymes' properties, i.e.  $M_w$ , pI and hydrophobicity (Table 6.1) with the binding affinity (Fig. 6.1), suggesting that multiple interactions can contribute to the binding [67,124–126].

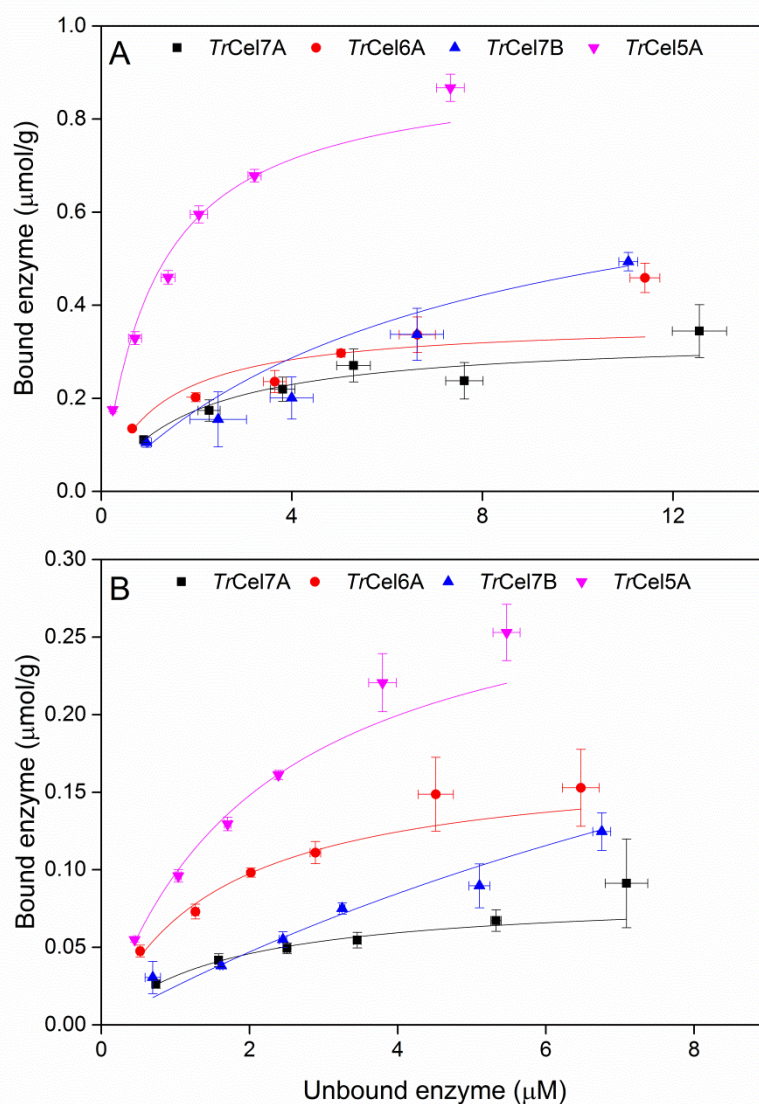


Figure 6.1 Adsorption isotherms of radiolabeled *TrCel7A*, *TrCel6A*, *TrCel7B* and *TrCel5A* on lignin-rich residues isolated from hydrothermally pretreated (A) spruce (L-HPS) and (B) wheat straw (L-HPWS) at 45°C, pH 5.0 after 1 h. Solid lines represent fitting of the Langmuir adsorption model for one binding-site to the isotherms.

#### 6.4 Reversibility of the adsorption of the monocomponent cellulases on LRRs

There were four models being used: Model 1 which describes reversible adsorption turning into irreversible (Eq. 2), Model 2 which describes separate reversible and irreversible bindings on same binding sites (Eq. 3), Model 3 which describes fully reversible adsorption (Eq. 4) and Model 4 which describes fully irreversible adsorption (Eq. 5).



Overall, the data showed that most of the adsorption has occurred within 1 h and that both enzymes, *TrCel6A* and *TrCel5A*, had similar adsorption pattern on L-HPS and L-HPWS (Appendix D: Fig. D.1). The response towards dilution however, was different where more enzymes were released after dilution in L-HPWS than L-HPS (Fig. 6.2). The lack of desorbed enzymes upon dilution in the case of L-HPS seemed to suggest irreversibility. However, the completely irreversible adsorption (Model 4) fitted poorly to the data (Appendix D: Fig. D.1) with  $R^2$  below 0.78 in each case (**Paper III**: Table III). Furthermore, no depletion of free enzymes or complete saturation of binding sites was observed and instead, equilibrium was reached at each concentration between free and adsorbed enzymes and the endpoints followed a Langmuir isotherm (Appendix D: Fig. D.2).

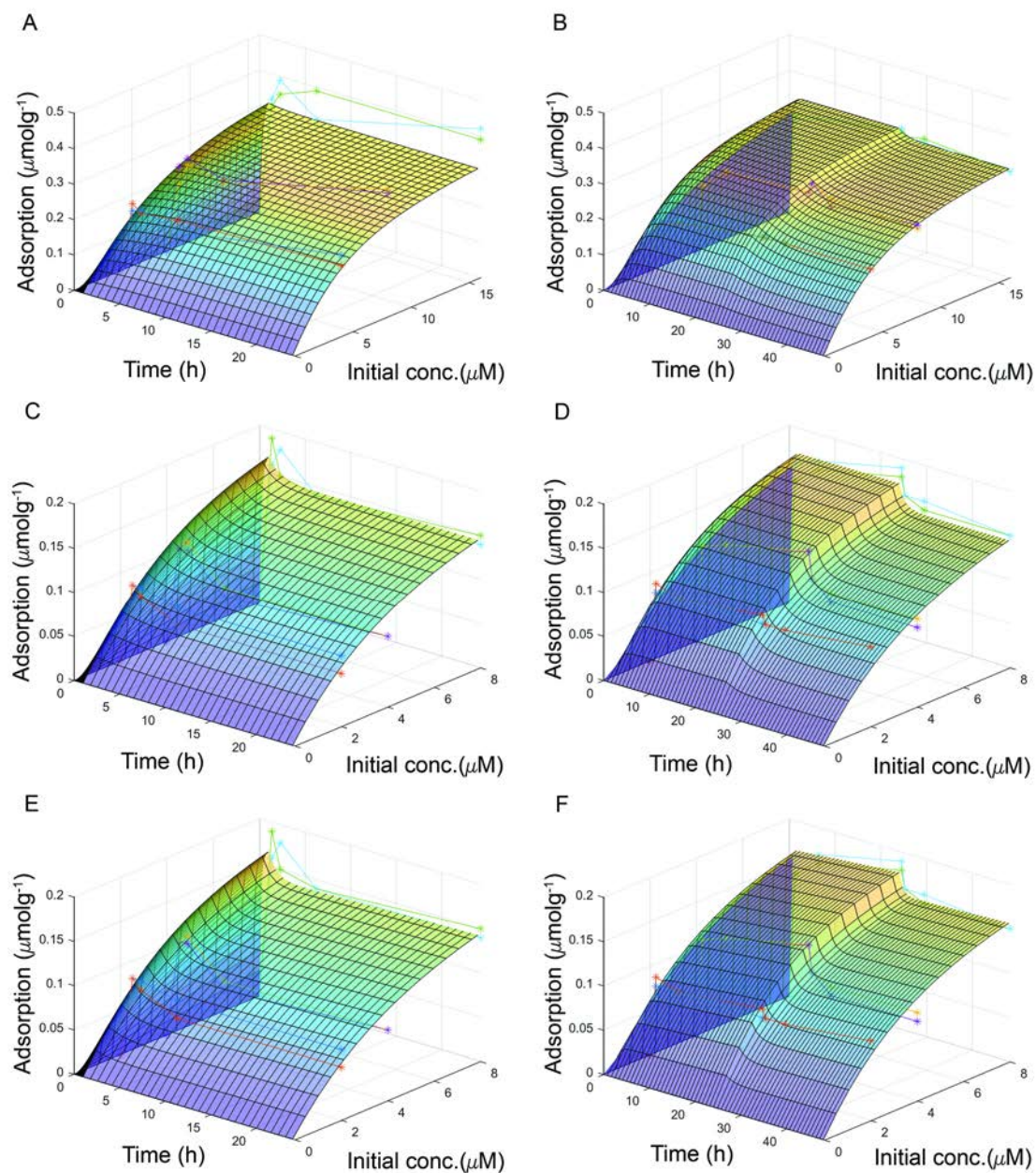


Figure 6.2 Response surface graphs displaying the fitting of experimental data of *TrCel6A* adsorption on lignin-rich residues isolated from hydrothermally pretreated spruce (L-HPS) (A & B) and hydrothermally pretreated wheat straw (L-HPWS) (C-F) modelled as reversible adsorption (A-D) and using Model 1 (E & F) with early (A, C & E) and late dilution (B, D & F).

Displaying the data from the dilution experiments as binding isotherms revealed that most of the points after dilution eventually returned to the original points prior to dilution (Appendix E: Figures E.1 and E.2). This behavior has also been described as a display of fully reversible binding during studies on the binding of monocomponent cellulases on cellulose [133,135]. The Langmuir constants  $K_{ads}$  and  $B_{max}$  determined from the kinetic modelling (**Paper III**: Table III) and adsorption isotherms data (**Paper III**: Table II) were in agreement (Fig. 6.3). These observations gave strong indication of reversible binding on lignin. The enzymes had lower binding affinity on L-HPWS than L-HPS as indicated by the lower adsorption constant ( $K_{ads}$ ) on L-HPWS compared to L-HPS of both enzymes, both in the adsorption isotherms fitting and modelling data (**Paper III**: Tables II and III). Accordingly the lower binding affinity on L-HPWS was in accordance with the higher desorption after dilution than on L-HPS (Fig. 6.2). The difference in affinity can explain previous observations where L-HPS was found to retard the enzymatic hydrolysis of model cellulose more than L-HPWS [120,132]. Finally, the models with reversible binding parameters (Models 1-3) gave good fit ( $R^2$  of 0.896–0.967) compared to the lower fitting in Model 4 ( $R^2$  of 0.570–0.784) which describes fully irreversible binding (**Paper III**: Table III). All in all, the abovementioned data and observations indicated reversible adsorption behavior can fully explain the results. The fitting and identifiability of both reversible the irreversible binding parameters were decent in Model 1 of L-HPWS, where quantification of irreversible binding was possible due to desorption after dilution. This suggested the possibility that the enzymes are first bound reversibly, followed by further interactions leading to irreversible binding. This is in agreement with the suggestion of protein unfolding taking place after binding on lignin [112,119,132].

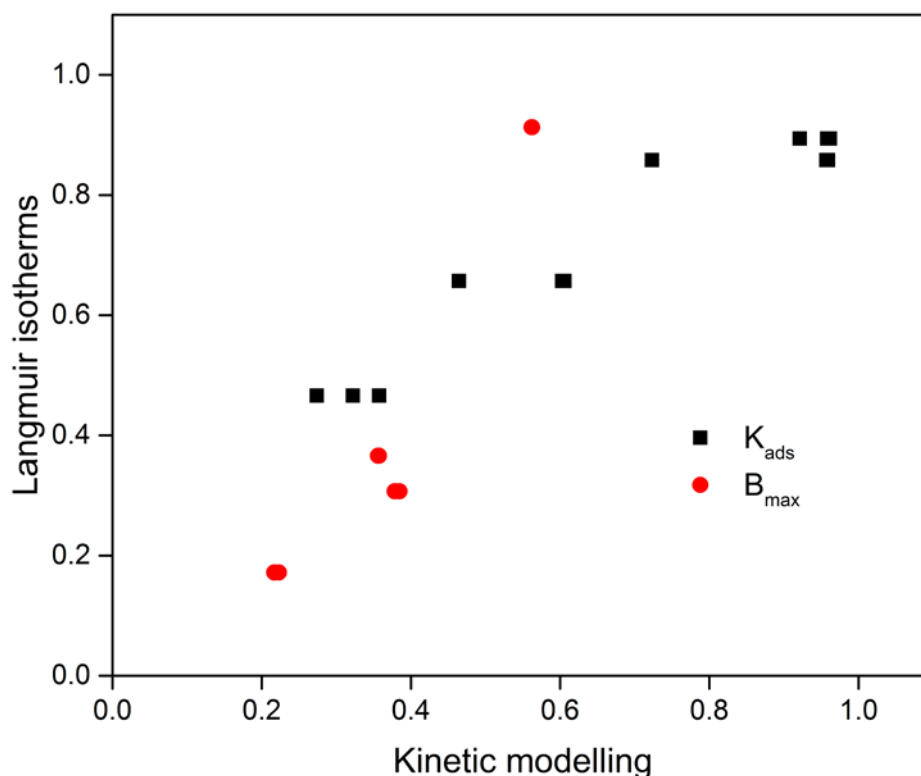


Fig. 6.3 Correlation of the Langmuir parameters determined from the adsorption isotherms and from kinetic modelling (Models 1-3) for *TrCel6A* and *TrCel5A* adsorption on lignin-rich residues isolated from hydrothermally pretreated spruce (L-HPS) and wheat straw (L-HPWS).

### 6.5 Competitive binding of the monocomponent cellulases on LRRs

Simultaneous adsorption study was performed using *TrCel6A* and *TrCel5A* where only one of them was radiolabeled, thus only the binding of the labeled one being recorded. In equimolar presence of one another, the enzymes showed competitive binding in the isotherms (Fig. 6.4). The presence of *TrCel6A* reduced the binding of labeled *TrCel5A* significantly, whereas the presence of *TrCel5A* had less pronounced effect on the binding of labeled *TrCel6A*. The reduction of the binding was clearly visible in both L-HPS (Fig. 6.4A) and L-HPWS (Fig. 6.4B). The isotherms fitted well with Langmuir adsorption model and showed that the maximum adsorption capacity ( $B_{max}$ ) was similar when both enzymes were in mixture, yet different when separated (**Paper III**: Table IV). This



indicated that both enzymes competed for similar binding sites and *TrCel6A* predominated the competitive binding albeit lower  $B_{\max}$  value. Protein size ( $M_w$ ) [173] instead of binding affinity [126] seemed to dictate the binding since *TrCel6A* had higher  $M_w$  than *TrCel5A* (Table 6.1). Nevertheless, the presence of competition between enzymes also suggested reversible binding.

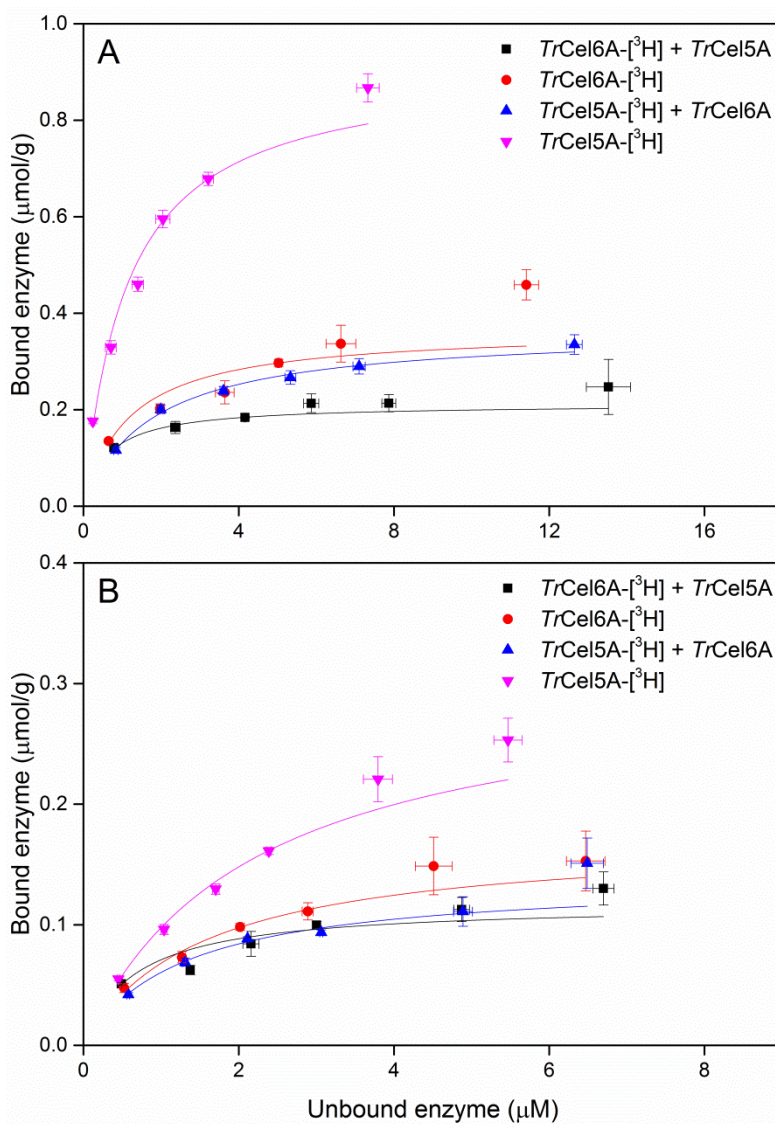


Figure 6.4 Competitive binding isotherms of *TrCel6A* and *TrCel5A* on lignin-rich residues isolated from hydrothermally pretreated (A) spruce (L-HPS) and (B) wheat straw (L-HPWS) at 45°C, pH 5.0 after 1 h. The tritium symbol ( $^3\text{H}$ ) indicates radiolabeled enzyme. Solid lines represent fitting of the Langmuir adsorption model for one binding-site to the isotherms.

## ***6.6 Concluding remarks and significance of study***

Based on the previously set hypotheses (Subchapter 6.1), it can be concluded that:

1. Monocomponent cellulases had different binding affinity on LRRs isolated from hydrothermally pretreated lignocellulosic biomass feedstocks. The binding affinity however cannot be correlated to the intrinsic properties of the enzymes.
2. Monocomponent cellulases adsorbed reversibly on LRRs isolated from hydrothermally pretreated lignocellulosic biomass feedstocks. Partial irreversible binding however may occur over extended reaction time (at 45°C).
3. Monocomponent cellulases had competitive adsorption on LRRs. However the enzyme with higher binding affinity did not predominate the binding.  $M_w$  can be the influencing factor.

Even though lignin has been considered as major factor in retarding enzymatic cellulose degradation, proper understanding of enzyme-lignin interaction that leads to reduced catalytic activity needs to be eventually clarified. The study thus showed that assuming the enzymes to bind on lignin irreversibly in the first place does not hold true. A direct exchange of adsorbed and desorbed enzyme can still occur to a certain extent even over reaction time at hydrolysis conditions. The difference in the binding affinity on lignin of different botanical origin is more likely to explain the observed difference when testing isolated lignin with model cellulose substrate. Given the different binding affinity of the monocomponent enzymes, it is important to establish the correlation between binding and activity for the individual enzyme components. However, due to the possible competition among the enzyme components in a mixture, development of methods being able to detect the activity and binding of a specific enzyme among other components would be needed.

## Chapter 7 – Synthesis and reflection

### *7.1 Biomass properties and digestibility*

The study began with key grass biomass feedstocks that were systematically pretreated using a system mimicking the latest commercial scale technology. After series of HTP at different severity levels, the bulk composition (Fig. 4.3) and the extent of hemicellulose removal (**Paper I**: Fig. 1) were similar in all biomass. Even the structure and decoration of hemicellulose and subsequent removal after HTP (**Paper I**: Fig. 3, Table 2) were also similar for all. However, after being subjected to hydrolysis using state of the art commercial cellulolytic enzyme mixture at optimized conditions, the pretreated biomass had different digestibility (Fig. 4.2). Therefore information on bulk composition cannot explain the observed digestibility among the tested biomass feedstocks.

Wettability test using CAM revealed differences among biomass feedstocks that correlated to their observed digestibility (Fig. 4.4). Given the results, it is tempting to suggest that MS is inherently less digestible than WS. One study indeed found that MS required higher pretreatment severity and released lower sugar yield than WS [174]. However, given the wide range of digestibility of various genotypes or cultivars of MS [175] and WS [176] after HTP, such justification is not necessarily universal. Nevertheless it has been stated, that switchgrass, a fast-growing grass similar to MS, is more recalcitrant compared to CS. This was especially clear in their different biomass-water interaction [166]. One established finding is that biomass-water interaction provided good indication of digestibility for various biomass feedstocks as reported in this study and previous ones [163,165,166]. Though wettability is a good indicator of digestibility; the exact structural and chemical changes that occurred after HTP and correlated to both wettability and digestibility are not well known. They will need to be pinpointed in order to understand the factors underlying biomass recalcitrance and to design effective treatments.

ATR-FTIR analysis gave both structural information pertaining to the surface of the materials and chemical information on relative abundance of lignocellulose components (**Paper I**: Table 5). Ultimately it showed that the least digestible biomass feedstock had the highest ASA of hemicellulose and lignin before and after pretreatment (Fig. 4.5). Thus the utilized surface methods provided more actual depiction of lignocellulose components than that of bulk composition, i.e. of cellulose being obstructed by other plant cell wall components which impaired enzymatic digestion. Using this approach, comparison among multiple biomass feedstocks for digestibility was feasible.

Correlation of overall data indeed showed that surface properties correlated better to biomass digestibility compared to the bulk composition. The data on hemicellulose was particularly striking since the relative surface abundance correlated excellently to digestibility as opposed to the bulk composition which did not (**Paper I**: Table 3). The consideration of the surface abundance rather than the bulk composition provided a new understanding and may even help explain previous data, where correlations between enzymatic digestibility and biomass composition have not been unequivocal. There were recent extensive studies comparing MS, WS and poplar that were steam exploded at different severity levels [177] or subjected to HTP, dilute acid and ionic liquid pretreatments [178]. In these studies, WS was obviously less recalcitrant than others. However, this was not apparent from the bulk composition, especially hemicellulose content. The final conversion of pretreated biomass across different feedstocks and pretreatments did not correlate well with it [177,178]. In that case, ATR-FTIR analysis of ASA of hemicellulose might reveal otherwise. Furthermore, it is faster to use ATR-FTIR spectroscopy when analyzing numerous samples from various genotypes or cultivars compared to performing bulk composition analysis [175,176].

The ATR-FTIR analysis therefore allowed assessment of spatial configuration that might indicate cellulose-hemicellulose interaction. It is known that HTP preferentially removed highly branched hydrophilic hemicellulose moieties [179]. Significant removal of hemicellulose

and its substitutions observed in this work (**Paper I**: Figures 1 and 3, Table 2) presumably left more hydrophobic hemicellulose moieties that can interact with cellulose and hinder digestibility. Hemicellulose with less substitutions were indeed reported to adsorb on cellulose and contribute to recalcitrance [180,181]. Recent studies utilizing both experimental and simulation data indeed showed that cellulose-hemicellulose interaction was increased at elevated pretreatment temperature and hydrophobic interaction was suggested to be the mechanism behind the process [182,183]. In this regard, although bulk composition of hemicellulose and its removal after HTP might be similar (**Paper I**: Figures 1 and 3, Table 2) across biomass feedstocks, the initial distribution and the changes in the surface might be different. Ultimately, it is this resulting migration of hemicellulose and interaction with cellulose that correlate to digestibility. Thus ATR-FTIR analysis (Fig. 4.5A) showed its novel aspect in potentially providing information on the initial distribution and redistribution of hemicellulose after HTP in the biomass surface. This points the need to understand the mobility and subsequent surface chemistry profile of residual hemicellulose after pretreatment. Pretreatment method and severity or hemicellulolytic activity in the enzyme mixture will need to be considered in order to overcome the steric hindrance provided by the residual hemicellulose.

Both bulk and surface lignin data did not correlate well, possibly pointing on the multi-component interaction in biomass. Several works have showed that the role of lignin in impeding enzymatic cellulose degradation was tied to the association of hemicellulose with lignin [184–186]. Moreover, several simulation studies did point out that the association of hemicellulose and lignin was crucial in restraining access of water to cellulose [187,188]. Accordingly, ASA of hemicellulose correlated well with wettability, although that was not the case with ASA of lignin (**Paper I**: Table 3). In this respect, along with the abovementioned suggestion, exploration of new enzymes to better hydrolyze hemicellulose moieties in the LCCs is a plausible avenue in order to improve the water constraining effect imposed by LCCs.

## 7.2 Enzyme-lignin interaction

To better understand the role of lignin in retarding enzymatic cellulose degradation, the enzyme-lignin interaction, which is also a surface phenomenon, was investigated. This is due to the possibility of the binding being non-productive. The investigation began with isolating LRRs from the hydrothermally pretreated grass biomass feedstocks (**Paper II**). Against what was initially hypothesized, the LRRs did not retard the enzymatic cellulose degradation of model cellulose substrate regardless of botanical origin of biomass and HTP severity (Fig. 5.4A-C). The elaborate experimental scheme (Fig. 5.1) showed that in the presence of LRRs, the cellulolytic enzymes were still able to catalyze the degradation of model cellulose as efficient as control experiment; even though adsorption occurred (**Paper II**: Fig. 1). Experiment II showed that the occurrence of adsorption, if irreversible by nature, did compromise the rate and extent of enzymatic cellulose degradation (Fig. 5.4D-F). However, Experiment I showed that the cellulolytic enzymes pre-adsorbed on LRRs were still able to degrade the added model cellulose substrate (Fig. 5.4A-C). As discussed previously (Chapter 5.4; **Paper II**), this gave strong indication that the binding of the cellulolytic enzymes were reversible by nature. If this were true, it would have major repercussions on the understanding of how the enzymes work in the processing of lignocellulosic biomass.

Further investigation in the adsorption on lignin therefore shifted to monocomponent cellulases (**Paper III**). If the binding is reversible in each enzyme components, it can be expected that the same is true for the enzyme mixture. Despite different affinity among the monocomponent cellulases, they fitted well with the Langmuir isotherm which assumes reversible binding (Fig. 6.1; **Paper III**: Table II). Furthermore, the kinetic modelling of dilution experiments showed better fit for models with reversible binding parameters (**Paper III**: Table III) and the adsorption constants  $K_{ads}$  and  $B_{max}$  from both modelling and Langmuir fitting were in congruence (Fig. 6.3). Even the raw data from the dilution experiments themselves showed no hysteresis as the endpoints after

dilution across different concentrations fitted with Langmuir model and eventually returning to the original isotherm line before dilution (Appendix E: Figures E.1 and E.2). All in all, these data and observations along with those in **Paper II**, provided solid proof for reversible binding of the enzymes on lignin. The simultaneous adsorption experiment which showed competition between monocomponent cellulases of different binding affinity and how they fitted with Langmuir adsorption model further sealed the verdict on the reversible nature of the binding. In the reversible binding, direct exchange between adsorbed and desorbed state of the enzyme exists in continuum. This is a paradigm-shifting finding since enzyme-lignin interaction has previously been viewed as irreversible [108] and the irreversible binding has been thought as one of the possible causes of retardation of enzymatic cellulose degradation by lignin [67]. The finding brings light to current practices and understanding, as well as points to the direction for future work.

Given the strong indication that the adsorption is reversible, it is more likely that as the hydrolytic suspension being agitated, the adsorbed enzymes can desorb and catalyze accessible carbohydrate moieties being encountered as suggested in Experiment I (Figures 5.1 and 5.4A-C). Employing the recycling of enzymes by introducing fresh substrate on top of hydrolysis residue [170] or utilizing continuous processing of biomass as in large scale operation [4], are already good strategies that have been successfully applied to a certain extent. However, as shown in the kinetic modelling of adsorption of the dilution experiments, the matter of different binding affinity still existed between spruce and WS as seen in the adsorption parameters and effect of dilution (Fig. 6.2; **Paper III**: Table III). It was indeed reported that exchange between adsorbed and desorbed enzyme was still observed even though no bound enzymes were released upon dilution during binding of monocomponent cellulases on cellulose [133]. Then one can still imagine that in the L-HPS which reduced glucose release from Avicel significantly and to a greater extent than L-HPWS, the effect could have been already apparent at early reaction time. This is possibly due to steric hindrance or

mass transfer limitation as cellulose and lignin “compete” for the binding of cellulases that can reversibly shifts in between. Previous reports indicated that although sometimes the retardation of glucose release from Avicel was obvious in the beginning, it was more pronounced at extended time and at higher reaction temperature [112,120,132]. The question is then, what actually causes the loss of cellulolytic activity over time, as previously reported in experiments using enzymatic hydrolysis of model cellulose in the presence of isolated lignin?

Further research work therefore should establish the precise mechanism of the activity loss of the enzymes during binding on lignin, the factors that influence it, how it affects different cellulases and whether increased binding promotes more activity loss. One theory that has been proposed is the protein unfolding during binding on lignin at elevated temperature (hydrolysis conditions of 45°C or higher as opposed to traditional adsorption studies at 4°C) [112,132]. The good fitting of Model 1 in this work in L-HPWS (Fig. 6.2; **Paper III**: Table III) confirmed and supported the previous suggestion. In this regard, the notion of the binding being reversible to a certain extent and might turn irreversible over time (as in Model 1) is more in line with the previous finding rather than assuming them to be irreversible from the beginning (as in Model 4). What is likely to happen is that initially the enzymes constantly change structural conformation as they adsorb and desorb reversibly. Incubation at elevated temperature increases the rate of the process and thus the binding affinity. As the process continues, eventually the protein structure unfolds and renders the enzymes to be bound irreversibly at a certain extent, losing activity. The effect of temperature on the binding affinity can also be seen in the dilution experiments since it took long time to return to original isotherm point (Appendix E: Figures E.1 and E.2) compared to other work at 4°C in the adsorption on cellulose [134]. Although L-HPS did not show good identifiability in the irreversible binding constant of Model 1 due to negligible release of enzymes after dilution (Fig. 6.2; **Paper III**: Table III), its high binding affinity on the enzymes also goes in line with the same



theory. Higher binding affinity means more likelihood and rate of adsorption-desorption, more conformational arrangements and more possibility of protein unfolding. It remains to be seen by future work whether the loss of enzyme activity and the change to irreversible binding on lignin occurred sequentially, separately or simultaneously. Finally, it is important to stress that while the binding is reversible, the loss of activity due to denaturation is irreversible.

Based on the mechanism described above, there are several possibilities to alleviate the effect of adsorption on lignin, which in this case perhaps more aptly termed “deactivating effect” rather than “inhibitory effect” of lignin. The use of additives such as BSA and surfactants which block lignin and protect against thermal denaturation [116,129] can be commended. Due to variation of lignin deriving from different biomass and pretreatment methods, it is more strategic to modify the enzymes instead of the lignin. One straightforward approach is to engineer the cellulases to be more thermostable or explore and use novel thermostable cellulases in the mixture. The latter has been demonstrated to work as the hydrolysis using thermostable enzymes were retarded less than the conventional ones [132]. Despite the reversible binding of cellulases on lignin, less binding on lignin will still be important to reduce deactivation, particularly in lignin with high affinity. One approach is to render the enzymes more negatively charged [130] or modify the pH of the reaction instead [118,122] though at the expense of potentially reduced activity. Another option is to reduce hydrophobic interaction by removing the CBM of the enzymes, since at high consistency biomass processing, cellulases with and without CBM performed equally. The CBM-less enzymes were even desorbed during the extended reaction, allowing more efficient recycling of enzymes [103–105]. In this regard, the reduction of enzymes’ adsorption on lignin, which potentially also reduces their adsorption on cellulose, seems to be a counterintuitive solution to improve cellulose hydrolysis. This brings again the age old question of whether increased binding equals to increased degradation of insoluble substrate. In the past studies with CBHs and their CBM at low substrate

concentration, the statement holds true [96,189,190]. However, with the recent works of CBM-less enzymes at high consistency process showed that was not the case [103–105]. Additionally, recent studies with processive CBHs also showed that their slow speed is likely due to their inherently slow dissociation rate constant ( $k_{\text{off}}$ ) during the processive action [85,191]. Accordingly, CBHs with less or more flexible loops covering the active site were found to be more efficient albeit lower affinity to the substrate [192,193]. Hence modifying the enzymes to have lower binding on lignin at the expense of equally lower binding on cellulose can be viable given the right circumstances.

A cautionary note to be put however, regarding the abovementioned discussion, is that inferences and discussion were drawn mainly from model systems studying the hydrolysis of model cellulose in the presence of isolated lignin. The conditions are not necessarily the same when considering the enzymatic hydrolysis of the whole pretreated biomass feedstocks. The spatial information on the arrangement of the lignocellulose components and their interactions both before and after pretreatment are certainly lost despite their significance; as previously discussed (Chapter 7.1 and in other works [45,54,71,146,182]). The lignin isolation method itself can affect the resulting lignin properties, although this latter aspect has been minimized in the work. Future investigations on activity loss in these model systems have to be particularly taken with care. Thermal deactivation itself can occur over time and denaturation of enzymes can also stem from other factors apart from the presence of lignin. Shear forces generated during agitation and exposure to air-liquid interface at low enzyme loading can also contribute significantly to that [194,195]. Soluble components present in the pretreated biomass feedstocks however, seemed to prevent that [104]. Thus the next question to be discussed is, what role does the lignin play in retarding the enzymatic degradation of actual pretreated lignocellulosic biomass feedstocks?

### *7.3 Lignin as physical barrier*

A final point to address still is the role of lignin in retarding the enzymatic cellulose degradation, to which studies in **Paper II** will be referred again with reference to **Paper I**. The LRRs isolated from the same set of hydrothermally pretreated grass biomass (**Paper I**) through extensive cellulose hydrolysis had different composition (Table 5.1). Based on the amount of residual carbohydrates left, the difference in the composition of LRRs reflected the same trend of digestibility that was observed previously (Fig. 4.2), i.e. MS was the least digestible. These residual carbohydrates in the LRRs were not accessible by cellulolytic enzymes when subjected to another hydrolysis experiment (Appendix B: Table B.1). Using ATR-FTIR analysis, the residual carbohydrates were not traceable to the surface of LRR particles either, while the presence of lignin in the surface was increasing (Appendix C: Figures C.1-C.3). These suggested that the progression of enzymatic cellulose degradation was halted by the presence of lignin, which occluded the carbohydrate moieties.

The observations from previous work which found that ASA of lignin was highest on MS and lowest on WS (Fig. 4.5B) had a good inverse correlation to the observed enzymatic digestibility (Fig. 4.2; Table 5.1), where MS was lowest and WS was highest. Thus extrapolation of the previous inferences (**Paper I**) suggested that the enzymatic degradation of cellulose was retarded earlier in the biomass feedstocks with high ASA of lignin. Furthermore, since low ASA of lignin (Fig. 4.5B) correlated to the high extent of lignin depolymerization (Fig. 5.3), this also suggested that physical properties of lignin can affect its subsequent distribution. The biomass feedstocks with high ASA of lignin and low extent of lignin depolymerization (in another way, high extent of lignin repolymerization) thus became a more potent barrier after HTP. Therefore this study along with other recent works [150,196,197] underlined the importance of lignin in retarding enzymatic cellulose degradation by acting as physical barrier.

The role of lignin in retarding enzymatic cellulose degradation as physical barrier can technically be linked tightly to the induction of non-productive adsorption, therefore exacerbating the retardation. This is especially due to the increasing presence of lignin in the surface of biomass particles during the course of hydrolysis [149,196] (Appendix C: Figures C.1-C.3). The increasing presence of lignin could have then also increased the non-productive adsorption. However, given the reversibility of binding (**Paper III**) combined with the implementation of continuous biomass processing and recycling step where a fresh substrate is constantly being introduced to progressing hydrolysis reaction, it is more likely that the enzymes can desorb from lignin to degrade cellulose. Nevertheless, the dualistic role of lignin in retarding enzymatic cellulose degradation by both acting as physical barrier and inducing non-productive adsorption can be true to a certain extent when it comes to softwood lignin with high affinity to bind enzymes. The similar rate of hydrolysis of steam pretreated spruce and its pre-digested residue seemed to suggest that accumulation of lignin itself did not retard enzymatic cellulose degradation [147]. Yet the strong indication of lignin as physical barrier in this work with grass biomass feedstocks can still actually explain another previous work on softwood and confirmed that the lignin from softwood also acted as physical barrier. In another study, adding the isolated LRRs from steam pretreated spruce back to its delignified counterpart only resulted in minor retardation of enzymatic cellulose degradation [140]. This indicated that non-productive adsorption even on lignin with high affinity is still less in magnitude of importance compared to the actual cellulose accessibility for enzymes provided by lignin removal. The near complete hydrolysis of steam pretreated delignified spruce using low enzyme dosage in the same previous study [140] also gives insight to other role of lignin as barrier.

Expanding the potential role of lignin as physical barrier, another plausible barrier effect could have already existed during the pretreatment process itself. That is the role of lignin in restricting the access of water to plant cell wall cavities, hence impairing HTP. It has indeed been

suggested before with different perspectives and emphases [37,140,198–200], yet important to underline in light of the findings in this study with respect to HTP. One series of clear connection is that lignin restricted swelling of biomass [198,200] and swelling is tied to biomass water content [37], and biomass-water interaction is correlated to digestibility [165,166]. Accordingly, in this study, the biomass which was the least digestible (Fig. 4.2; Table 5.1) had the lowest wettability after pretreatment (Fig. 4.4) and the highest ASA of lignin (Fig. 4.5B). Therefore the barrier effect deriving from surface lignin distribution as seen to be occurring in greater extent in MS (**Papers I and II**) could have been simply because lignin among others prevented efficient HTP in the first place by restricting swelling. This insight can clarify previous observations and can be applied across feedstocks. For grasses in particular, this explains the seemingly inherent higher recalcitrance of *Miscanthus* or switchgrass compared to CS or WS [166,174]. Switchgrass was indeed reported to have much lower degree of biomass-water interaction than CS and thus is considered more recalcitrant [166]. The exact explanation to the phenomenon remains to be seen and can be tied to various structural factors. However, this study presented compelling evidence that surface distribution of lignin, which correlated to wettability and ensuing digestibility profile across the multiple biomass feedstocks (**Papers I and II**), can be a strong influencing factor. In that way, the role of lignin as physical barrier has two-fold consequences, i.e. preventing access of cellulose microfibrils to both water during pretreatment, and enzymes during hydrolysis.

In order to extrapolate the abovementioned inference to other biomass feedstocks, correlation with the chemical and physical properties of the lignin will need to be assessed. It is noteworthy to mark that the extent of lignin depolymerization (Fig. 5.3) correlated to the ASA of lignin (Fig. 4.5B), the observed digestibility (Fig. 4.2; Table 5.1) and wettability to a certain extent (Fig. 4.4) when it comes to the differences among the tested feedstocks. The physical properties of lignin seen in the extent of depolymerization is tied to the condensation of lignin [66], influenced by

$T_g$  [55,114], which can affect the ensuing redistribution after pretreatment [45,54]. Therefore the physical properties of lignin can be related to the actual extent or intensity that the lignin will play as barrier. This is especially true supposing that the chemical modification and migration of lignin during pretreatment is a dynamic process that occurred along the different range of temperatures, i.e. as the lignin melted after reaching  $T_g$ , relocated as if it were a molten glass and then redeposited during the cooling process. Therefore it is plausible that the obstruction of swelling process, i.e. access of water to cellulose microfibrils, can also be influenced by the physical changes that occurred in the lignin polymer during pretreatment. The swelling of biomass was indeed found to be tied to the  $T_g$  of lignin [198] and  $T_g$  correlated to condensation reactions [114] which is reflected in the  $M_w$  and extent of depolymerization [66,201]. Interestingly, the  $T_g$  of lignin in the biomasses are different where the  $T_g$  of WS [58,59] < *Miscanthus* and switchgrass [60,61] < hardwood [114]. Another difference related to the state of lignin condensation and polymerization is the chemical properties seen in S/G ratio. The G units are thought to readily perform more condensation reaction [30], creating cross-linked structure that yields a more potent physical barrier for the enzymes [145] and in this case potentially also for the water during pretreatment. Higher S/G ratio in poplar was recently found to correlate to lower recalcitrance [202]. In softwood lignin with almost exclusively G units [27,28], the role of lignin as barrier for both water and enzymes can then be even more potent than other biomass feedstocks. Even though the S/G ratio in this study (Fig. 5.2) did not correlate with the extent of lignin depolymerization, the pronounced presence of triclin which was suggested to retard repolymerization [31] did (Appendix A: Figures A.1-A.3; Table A.1).

All in all, this study (**Paper II**) highlighted profound connections and mechanisms which can affect greatly the recalcitrance of biomass in response to pretreatment, departing from thorough observations of hydrothermally pretreated grass biomass feedstocks. Future work will still need to find out whether the suggested inferences can be applied across a wide range of biomass

feedstocks and pretreatment methods. The future work also needs to point out more on the actual effect of redistribution of lignin following pretreatment, how to measure it and what factors might influence it. Due to the inherent dualistic role of lignin as barrier for both enzymes and water, reduction of lignin content and the potential barrier effect it creates is a plausible approach. Hence one key for efficient biomass processing is to utilize feedstocks with less surface distribution of lignin and with certain chemical and physical properties of lignin which render the ensuing relocation to be non-restricting for both water and enzymes. Considering the distinction in ASA of lignin was already noticeable from the start prior to HTP (Fig. 4.5B), it seemed that selecting or engineering feedstocks or cultivars with less lignin is the most straightforward way to circumvent the issue. Otherwise, pretreatment methods favoring delignification, such as alkali-based and organosolv pretreatments [39,41,67] can be better alternatives provided the economic feasibility. The same is true with flowthrough process configuration if HTP will still be used, although the delignification comes at the cost of high water use and diluted products [8,51]. In the end, the course of research and development of biomass processing will still be dictated by the economic needs and environmental circumstances that occur in the biosphere for the next decades to come.

## **Chapter 8 – Conclusions and future perspectives**

### ***8.1 Conclusions***

The study aimed to identify biomass properties and subsequent interaction with enzymes that affect enzymatic cellulose degradation. It was hypothesized that lignocellulose components and enzyme-lignin interactions, affect enzymatic cellulose degradation negatively. However, in general that was not proven to be the case in a strict sense:

1. Firstly, to a large extent, surface properties correlated better to the digestibility of hydrothermally pretreated grass biomass feedstocks compared to bulk composition.

The potential obstruction of cellulose by other lignocellulose components in the surface of biomass, i.e. hemicellulose and lignin was shown by ATR-FTIR analysis and supported by wettability test.

2. Secondly, the concerned induction of non-productive adsorption of cellulolytic enzymes by lignin was not shown to be critical in retarding enzymatic cellulose degradation as the enzymes were shown to bind reversibly.

The convincing evidence of reversibility was shown on cellulolytic enzyme mixture and corroborated by kinetic modelling of adsorption on lignin with monocomponent cellulases.

3. Ultimately the study showed that the role of lignin in retarding enzymatic cellulose degradation was by acting as a physical barrier for the enzymes.



This was supported by series of hydrolysis experiments and assessment of ASA of lignocellulose components which correlated to the observed digestibility and physical properties of lignin.

## ***8.2 Future perspectives***

Future research efforts should be directed to a more holistic view of biomass if HTP and other pretreatment methods which did not significantly remove or fractionate lignin will be used. In grass biomass, and conceivably any other biomass, the role of lignin as physical barrier will still exist to a certain extent. Selection or genetic engineering of cultivars with lignin properties that benefit fractionation process, create less barrier for enzymes to saccharify the carbohydrates moieties and improved lignin properties for end product application will be desirable. In that respect, development of alternative pretreatment methods that can efficiently fractionate lignocellulose components while being economic to be applied in large scale is also commendable. Additionally, further studies seeking to understand the multi-component interactions and redistributions during lignocellulosic biomass pretreatment as well as development of methods to derive quantifiable structural information from them will be valuable as inputs in designing both feedstocks properties and pretreatment methods. From the enzymes' perspectives, a straightforward potential improvement is to increase the thermostability of current ones or to continue exploration for new enzymes with improved thermostability. In that respect, the potential loss of activity incurred by lignin can be reduced and at the same time the reaction speed can be improved provided reaction at higher temperature is feasible. Another potential improvement is to engineer the enzymes to have less affinity to lignin, although discretion should be taken that in doing so, their affinity to cellulose and hence their catalytic speed will not be impaired.

## References

1. Lynd LR, Cushman JH, Nichols RJ, Wyman CE. Fuel Ethanol from Cellulosic Biomass. *Science*. 1991. p. 1318–23.
2. Cardona CA, Sanchez OJ. Fuel ethanol production: Process design trends and integration opportunities. *Bioresour Technol*. 2007;98:2415–57.
3. Larsen J, Østergaard Petersen M, Thirup L, Li HW, Iversen FK. The IBUS process - Lignocellulosic bioethanol close to a commercial reality. *Chem Eng Technol*. 2008;31:765–72.
4. Larsen J, Haven MØ, Thirup L. Inbicon makes lignocellulosic ethanol a commercial reality. *Biomass Bioenerg*. 2012;46:36–45.
5. Janssen R, Turhollow AF, Rutz D, Mergner R. Production facilities for second- generation biofuels in the USA and the EU – current status and future perspectives. *Biofuels, Bioprod Biorefining*. 2013;7:647–65.
6. Reboredo FH, Lidon FC, Ramalho JC, Pessoa MF. Perspective: The forgotten implications of low oil prices on biofuels. *Biofuels, Bioprod Biorefining*. 2017;11:625–32.
7. Mansfield SD, Mooney C, Saddler JN. Substrate and enzyme characteristics that limit cellulose hydrolysis. *Biotechnol Prog*. 1999;15:804–16.
8. Yang B, Tao L, Wyman CE. Strengths, challenges, and opportunities for hydrothermal pretreatment in lignocellulosic biorefineries. *Biofuels, Bioprod Biorefining*. 2018;12:125–38.
9. Kamm B, Kamm M. Principles of biorefineries. *Appl Microbiol Biotechnol*. 2004;64:137–45.
10. Andersen MS. An introductory note on the environmental economics of the circular economy. *Sustain Sci*. 2007;2:133–40.
11. Pauly M, Keegstra K. Cell-wall carbohydrates and their modification as a resource for biofuels. *Plant J*. 2008;54:559–68.

12. Vassilev S V., Baxter D, Andersen LK, Vassileva CG. An overview of the chemical composition of biomass. *Fuel*. 2010;89:913–33.
13. Kim S, Dale BE. Global potential bioethanol production from wasted crops and crop residues. *Biomass Bioenerg*. 2004;26:361–75.
14. Lee WC, Kuan WC. Miscanthus as cellulosic biomass for bioethanol production. *Biotechnol J*. 2015;10:840–54.
15. Robertson GP, Hamilton SK, Barham BL, Dale BE, Izaurralde RC, Jackson RD, Landis DA, Swinton SM, Thelen KD, Tiedje JM. Cellulosic biofuel contributions to a sustainable energy future: Choices and outcomes. *Science (80- )*. 2017;356:eaal2324.
16. Carpita NC. Structure and Biogenesis of the Cell Walls of Grasses. *Annu Rev Plant Physiol*. 1996;47:445–76.
17. Cosgrove DJ. Growth of the plant cell wall. *Nat Rev Mol Cell Biol*. 2005;6:850–61.
18. Vogel J. Unique aspects of the grass cell wall. *Curr Opin Plant Biol*. 2008;11:301–7.
19. Ding S-Y, Himmel ME. The maize primary cell wall microfibril: a new model derived from direct visualization. *J Agric Food Chem*. 2006;54:597–606.
20. Chundawat SPS, Beckham GT, Himmel ME, Dale BE. Deconstruction of lignocellulosic biomass to fuels and chemicals. *Annu Rev Chem Biomol Eng*. 2011;2:121–45.
21. Li M, Pu Y, Ragauskas AJ. Current understanding of the correlation of lignin structure with biomass recalcitrance. *Front Chem*. 2016;4:45.
22. Carpita NC. Update on Mechanisms of Plant Cell Wall Biosynthesis: How Plants Make Cellulose and Other (1-->4)-b-D-Glycans. *Plant Physiol*. 2011;155:171–84.
23. Sannigrahi P, Pu Y, Ragauskas A. Cellulosic biorefineries-unleashing lignin opportunities. *Curr Opin Environ Sustain*. 2010;2:383–93.
24. O’Sullivan AC. Cellulose: the structure slowly unravels. *Cellulose*. 1997;4:173–207.

25. Scheller HV, Ulvskov P. Hemicelluloses. *Annu Rev Plant Biol.* 2010;61:263–89.
26. Buranov AU, Mazza G. Lignin in straw of herbaceous crops. *Ind Crop Prod.* 2008;28:237–59.
27. Boerjan W, Ralph J, Baucher M. Lignin biosynthesis. *Annu Rev Plant Biol.* 2003;54:519–46.
28. Faix O. Classification of lignins from different botanical origins by FT-IR spectroscopy. *Holzforschung.* 1991;45:21–7.
29. Crestini C, Melone F, Sette M, Saladino R. Milled wood lignin: A linear oligomer. *Biomacromolecules.* 2011;12:3928–35.
30. Trajano HL, Engle NL, Foston M, Ragauskas AJ, Tschaplinski TJ, Wyman CE. The fate of lignin during hydrothermal pretreatment. *Biotechnol Biofuels.* 2013;6:110.
31. Jensen A, Cabrera Y, Hsieh C-W, Nielsen J, Ralph J, Felby C. 2D NMR characterization of wheat straw residual lignin after dilute acid pretreatment with different severities. *Holzforschung.* 2017;71:461–9.
32. Bidlack J, Malone M, Benson R. Molecular Structure and components integration of secondary cell walls in plants. *Proc.Okla.Acad.Sci.* 1992;75:51–6.
33. Lawoko M, Henriksson G, Gellerstedt G. Characterisation of lignin-carbohydrate complexes (LCCs) of spruce wood (*Picea abies* L.) isolated with two methods. *Holzforschung.* 2006;60:156–61.
34. Himmel ME, Ding S-Y, Johnson DK, Adney WS, Nimlos MR, Brady JW, Foust TD. Biomass recalcitrance: engineering plants and enzymes for biofuels production. *Science.* 2007;315:804–7.
35. Ragauskas AJ, Beckham GT, Biddy MJ, Chandra R, Chen F, Davis MF, Davison BH, Dixon R a, Gilna P, Keller M, Langan P, Naskar AK, Saddler JN, Tschaplinski TJ, Tuskan G a, Wyman CE. Lignin valorization: improving lignin processing in the biorefinery. *Science.* 2014;344:1246843.
36. Shevchenko SM, Bailey GW. The mystery of the lignin-carbohydrate: a computational approach complex. 1996;364:197–208.

37. Jeoh T, Ishizawa CI, Davis MF, Himmel ME, Adney WS, Johnson DK. Cellulase digestibility of pretreated biomass is limited by cellulose accessibility. *Biotechnol Bioeng.* 2007;98:112–22.
38. Meng X, Ragauskas AJ. Recent advances in understanding the role of cellulose accessibility in enzymatic hydrolysis of lignocellulosic substrates. *Curr Opin Biotech.* 2014;27:150–8.
39. Mosier N, Wyman C, Dale B, Elander R, Lee YY, Holtzapple M, Ladisch M. Features of promising technologies for pretreatment of lignocellulosic biomass. *Bioresour Technol.* 2005;96:673–86.
40. Yang B, Wyman CE. Pretreatment : the key to unlocking low-cost cellulosic ethanol. *Biofuels, Bioprod Bioref.* 2008;2:26–40.
41. Sun S, Sun S, Cao X, Sun R. The role of pretreatment in improving the enzymatic hydrolysis of lignocellulosic materials. *Bioresour Technol.* 2016;199:49–58.
42. Betarenewables website [Internet]. [cited 2016 Oct 26]. Available from: <http://www.betarenewables.com/en>
43. Ruiz HA, Rodríguez-Jasso RM, Fernandes BD, Vicente AA, Teixeira JA. Hydrothermal processing, as an alternative for upgrading agriculture residues and marine biomass according to the biorefinery concept: a review. *Renew Sust Energ Rev.* 2013;21:35–51.
44. Pedersen M, Meyer AS. Lignocellulose pretreatment severity – relating pH to biomatrix opening. *New Biotechnol.* 2010;27:739–50.
45. Kristensen JB, Thygesen LG, Felby C, Jørgensen H, Elder T. Cell-wall structural changes in wheat straw pretreated for bioethanol production. *Biotechnol Biofuels.* 2008;1:5.
46. Nitsos CK, Matis KA, Triantafyllidis KS. Optimization of hydrothermal pretreatment of lignocellulosic biomass in the bioethanol production process. *ChemSusChem.* 2013;6:110–22.
47. Overend RP, Chornet E. Fractionation of lignocellulosics by steam-aqueous pretreatments. *Philos T R Soc A.* 1987;321:523–36.

48. Jönsson LJ, Martín C. Pretreatment of lignocellulose: Formation of inhibitory by-products and strategies for minimizing their effects. *Bioresour Technol.* 2016;199:103–12.
49. Rasmussen H, Sørensen HR, Meyer AS. Formation of degradation compounds from lignocellulosic biomass in the biorefinery: sugar reaction mechanisms. *Carbohydr Res.* 2014;385:45–57.
50. Yelle DJ, Kaparaju P, Hunt CG, Hirth K, Kim H, Ralph J, Felby C. Two-dimensional NMR evidence for cleavage of lignin and xylan substituents in wheat straw through hydrothermal pretreatment and enzymatic hydrolysis. *Bioenerg Res.* 2013;6:211–21.
51. Yang B, Wyman CE. Effect of xylan and lignin removal by batch and flowthrough pretreatment on the enzymatic digestibility of corn stover cellulose. *Biotechnol Bioeng.* 2004;86:88–98.
52. Kabel MA, Bos G, Zeevalking J, Voragen AGJ, Schols HA. Effect of pretreatment severity on xylan solubility and enzymatic breakdown of the remaining cellulose from wheat straw. *Bioresour Technol.* 2007;98:2034–42.
53. Nitsos CK, Choli-Papadopoulou T, Matis KA, Triantafyllidis KS. Optimization of hydrothermal pretreatment of hardwood and softwood lignocellulosic residues for selective hemicellulose recovery and improved cellulose enzymatic hydrolysis. *ACS Sustain Chem Eng.* 2016;4:4529–44.
54. Donohoe BS, Decker SR, Tucker MP, Himmel ME, Vinzant TB. Visualizing lignin coalescence and migration through maize cell walls following thermochemical pretreatment. *Biotechnol Bioeng.* 2008;101:913–25.
55. Irvine GM. The significance of the glass transition of lignin in thermomechanical pulping. *Wood Sci Technol.* 1985;19:139–49.
56. Toledano A, Serrano L, Garcia A, Mondragon I, Labidi J. Comparative study of lignin fractionation by ultrafiltration and selective precipitation. *Chem Eng J.* 2010;157:93–9.
57. Upton BM, Kasko AM. Strategies for the Conversion of Lignin to High-Value Polymeric

Materials: Review and Perspective. *Chem Rev.* 2016;116:2275–306.

58. Stelte W, Clemons C, Holm JK, Ahrenfeldt J, Henriksen UB, Sanadi AR. Fuel Pellets from Wheat Straw: The Effect of Lignin Glass Transition and Surface Waxes on Pelletizing Properties. *Bioenerg Res.* 2012;5:450–8.

59. Ibbett R, Gaddipati S, Davies S, Hill S, Tucker G. The mechanisms of hydrothermal deconstruction of lignocellulose: New insights from thermal-analytical and complementary studies. *Bioresour Technol.* 2011;102:9272–8.

60. García A, Toledano A, Andrés MÁ, Labidi J. Study of the antioxidant capacity of *Miscanthus sinensis* lignins. *Process Biochem.* 2010;45:935–40.

61. Hosseinaei O, Harper DP, Bozell JJ, Rials TG. Role of Physicochemical Structure of Organosolv Hardwood and Herbaceous Lignins on Carbon Fiber Performance. *ACS Sustain Chem Eng.* 2016;4:5785–98.

62. Ko JK, Kim Y, Ximenes E, Ladisch MR. Effect of liquid hot water pretreatment severity on properties of hardwood lignin and enzymatic hydrolysis of cellulose. *Biotechnol Bioeng.* 2015;112:252–62.

63. Selig MJ, Viamajala S, Decker SR, Tucker MP, Himmel ME, Vinzant TB. Deposition of lignin droplets produced during dilute acid pretreatment of maize stems retards enzymatic hydrolysis of cellulose. *Biotechnol Progr.* 2007;23:1333–9.

64. Li H, Pu Y, Kumar R, Ragauskas AJ, Wyman CE. Investigation of lignin deposition on cellulose during hydrothermal pretreatment, its effect on cellulose hydrolysis, and underlying mechanisms. *Biotechnol Bioeng.* 2014;111:485–92.

65. Pu Y, Hu F, Huang F, Ragauskas AJ. Lignin Structural Alterations in Thermochemical Pretreatments with Limited Delignification. *Bioenerg Res.* 2015;8:992–1003.

66. Li J, Henriksson G, Gellerstedt G. Lignin depolymerization/repolymerization and its critical role

- for delignification of aspen wood by steam explosion. *Bioresour Technol.* 2007;98:3061–8.
67. Sipponen MH, Rahikainen J, Leskinen T, Pihlajaniemi V, Mattinen M-L, Lange H, Crestini C, Österberg M. Structural changes of lignin in biorefinery pretreatments and consequences to enzyme-lignin interactions - OPEN ACCESS. *Nord Pulp Pap Res J.* 2017;32:550–71.
68. Pu Y, Hu F, Huang F, Davison BH, Ragauskas AJ. Assessing the molecular structure basis for biomass recalcitrance during dilute acid and hydrothermal pretreatments. *Biotechnol Biofuels.* *Biotechnology for Biofuels*; 2013;6:15.
69. Hu F, Ragauskas A. Pretreatment and Lignocellulosic Chemistry. *Bioenerg Res.* 2012;5:1043–66.
70. Hall M, Bansal P, Lee JH, Realff MJ, Bommarius AS. Cellulose crystallinity - a key predictor of the enzymatic hydrolysis rate. *FEBS J.* 2010;277:1571–82.
71. Sipponen MH, Pihlajaniemi V, Pastinen O, Laakso S. Reduction of surface area of lignin improves enzymatic hydrolysis of cellulose from hydrothermally pretreated wheat straw. *RSC Adv.* *Royal Society of Chemistry*; 2014;4:36591.
72. Payne CM, Knott BC, Mayes HB, Hansson H, Himmel ME, Sandgren M, Ståhlberg J, Beckham GT. Fungal Cellulases. *Chem Rev.* 2015;115:1308–448.
73. Lynd LR, Weimer PJ, van Zyl WH, Pretorius IS. Microbial Cellulose Utilization: Fundamentals and Biotechnology. *Microbiol Mol Biol Rev.* 2002;66:739–739.
74. Häkkinen M, Arvas M, Oja M, Aro N, Penttilä M, Saloheimo M, Pakula TM. Re-annotation of the CAZy genes of *Trichoderma reesei* and transcription in the presence of lignocellulosic substrates. *Microb Cell Fact.* 2012;11:134.
75. Boraston AB, Bolam DN, Gilbert HJ, Davies GJ. Carbohydrate-binding modules: fine-tuning polysaccharide recognition. *Biochem J.* 2004;382:769–81.
76. Várnai A, Mäkelä MR, Djajadi DT, Rahikainen J, Hatakka A, Viikari L. Carbohydrate-Binding



Modules of Fungal Cellulases. Occurrence in Nature, Function, and Relevance in Industrial Biomass Conversion. *Adv Appl Microbiol.* 2014;88:103–65.

77. Gilkes NR, Henrissat B, Kilburn DG, Miller RC, Warren R a. Domains in microbial beta-1, 4-glycanases: sequence conservation, function, and enzyme families. *Microbiol Rev.* 1991;55:303–15.

78. Divne C, Ståhlberg J, Reinikainen T, Ruohonen L, Pettersson G, Knowles JK, Teeri TT, Jones T a. The three-dimensional crystal structure of the catalytic core of cellobiohydrolase I from *Trichoderma reesei*. *Science.* 1994;265:524–8.

79. Divne C, Ståhlberg J, Teeri TT, Jones T a. High-resolution crystal structures reveal how a cellulose chain is bound in the 50 Å long tunnel of cellobiohydrolase I from *Trichoderma reesei*. *J Mol Biol.* 1998;275:309–25.

80. Rouvinen J, Bergfors T, Teeri T, Knowles JKC, Jones TA. Three-Dimensional Structure of Cellobiohydrolase II from *Trichoderma reesei*. *Science (80- )*. 1990;249:380–6.

81. Kleywegt GJ, Zou JY, Divne C, Davies GJ, Sinning I, Ståhlberg J, Reinikainen T, Srisodsuk M, Teeri TT, Jones T a. The crystal structure of the catalytic core domain of endoglucanase I from *Trichoderma reesei* at 3.6 Å resolution, and a comparison with related enzymes. *J Mol Biol.* 1997;272:383–97.

82. Holtzapple M, Cognata M, Shu Y, Hendrickson C. Inhibition of *Trichoderma reesei* Cellulase by Sugars and Solvents. *Biotechnol Bioeng.* 1990;36:275–87.

83. Murphy L, Bohlin C, Baumann MJ, Olsen SN, Sørensen TH, Anderson L, Borch K, Westh P. Product inhibition of five *Hypocrea jecorina* cellulases. *Enzyme Microb Technol.* 2013;52:163–9.

84. Van Dyk JS, Pletschke BI. A review of lignocellulose bioconversion using enzymatic hydrolysis and synergistic cooperation between enzymes-Factors affecting enzymes, conversion and synergy. *Biotechnol Adv.* 2012;30:1458–80.

85. Jalak J, Väljamäe P. Mechanism of initial rapid rate retardation in cellobiohydrolase catalyzed

- cellulose hydrolysis. *Biotechnol Bioeng.* 2010;106:871–83.
86. Kurasin M, Väljamäe P. Processivity of cellobiohydrolases is limited by the substrate. *J Biol Chem.* 2011;286:169–77.
87. Jalak J, Kurašin M, Teugjas H, Väljamäe P. Endo-exo synergism in cellulose hydrolysis revisited. *J Biol Chem.* 2012;287:28802–15.
88. Ganner T, Bubner P, Eibinger M, Mayrhofer C, Plank H, Nidetzky B. Dissecting and reconstructing synergism - in situ visualization of cooperativity among cellulases. *J Biol Chem.* 2012;287:43215–22.
89. Igarashi K, Uchihashi T, Koivula A, Wada M, Kimura S, Okamoto T, Penttilä M, Ando T, Samejima M. Traffic jams reduce hydrolytic efficiency of cellulase on cellulose surface. *Science* (80- ). 2011;333:1279–82.
90. Horn SJ, Vaaje-Kolstad G, Westereng B, Eijsink VGH. Novel enzymes for the degradation of cellulose. *Biotechnol Biofuels.* 2012;5:45.
91. Cannella D, Hsieh CWC, Felby C, Jørgensen H. Production and effect of aldonic acids during enzymatic hydrolysis of lignocellulose at high dry matter content. *Biotechnol Biofuels.* 2012;5:1–10.
92. Bissaro B, Røhr ÅK, Müller G, Chylenski P, Skaugen M, Forsberg Z, Horn SJ, Vaaje-Kolstad G, Eijsink VGH. Oxidative cleavage of polysaccharides by monocopper enzymes depends on H<sub>2</sub>O<sub>2</sub>. *Nat Chem Biol.* 2017;13:1123–8.
93. Gao D, Uppugundla N, Chundawat SP, Yu X, Hermanson S, Gowda K, Brumm P, Mead D, Balan V, Dale BE. Hemicellulases and auxiliary enzymes for improved conversion of lignocellulosic biomass to monosaccharides. *Biotechnol Biofuels.* 2011;4:5.
94. Tolan JS. Iogen's process for producing ethanol from cellulosic biomass. *Clean Technol Environ Policy.* 2002;3:339–45.

95. Suurnäkki A, Tenkanen M, Siika-Aho M, Niku-Paavola ML, Viikari L, Buchert J. Trichoderma reesei cellulases and their core domains in the hydrolysis and modification of chemical pulp. *Cellulose*. 2000;7:189–209.
96. Reinikainen T, Ruohonen L, Nevanen T, Laaksonen L, Kraulis P, Jones TA, Knowles JKC, Teeri TT. Investigation of the function of mutated cellulose-binding domains of Trichoderma reesei cellobiohydrolase I. *Proteins Struct Funct Bioinforma*. 1992;14:475–82.
97. Beckham GT, Matthews JF, Bomble YJ, Bu L, Adney WS, Himmel ME, Nimlos MR, Crowley MF. Identification of amino acids responsible for processivity in a Family 1 carbohydrate-binding module from a fungal cellulase. *J Phys Chem B*. 2010;114:1447–53.
98. Liu Y-S, Baker JO, Zeng Y, Himmel ME, Haas T, Ding S-Y. Cellobiohydrolase hydrolyzes crystalline cellulose on hydrophobic faces. *J Biol Chem*. 2011;286:11195–201.
99. Alekozai EM, GhattyVenkataKrishna PK, Uberbacher EC, Crowley MF, Smith JC, Cheng X. Simulation analysis of the cellulase Cel7A carbohydrate binding module on the surface of the cellulose I $\beta$ . *Cellulose*. 2014;21:951–71.
100. Koivula A, Kinnari T, Harjunpää V, Ruohonen L, Teleman A, Drakenberg T, Rouvinen J, Jones TA, Teeri TT. Tryptophan 272: an essential determinant of crystalline cellulose degradation by Trichoderma reesei cellobiohydrolase Cel6A. *FEBS Lett*. 1998;429:341–6.
101. Igarashi K, Koivula A, Wada M, Kimura S, Penttilä M, Samejima M. High speed atomic force microscopy visualizes processive movement of Trichoderma reesei cellobiohydrolase I on crystalline cellulose. *J Biol Chem*. 2009;284:36186–90.
102. Nakamura A, Tsukada T, Auer S, Furuta T, Wada M, Koivula A, Igarashi K, Samejima M. The tryptophan residue at the active site tunnel entrance of Trichoderma reesei cellobiohydrolase Cel7A is important for initiation of degradation of crystalline cellulose. *J Biol Chem*. 2013;288:13503–10.

103. Le Costaouëc T, Pakarinen A, Várnai A, Puranen T, Viikari L. The role of carbohydrate binding module (CBM) at high substrate consistency: comparison of *Trichoderma reesei* and *Thermoascus aurantiacus* Cel7A (CBHI) and Cel5A (EGII). *Bioresour Technol.* 2013;143:196–203.
104. Várnai A, Siika-aho M, Viikari L. Carbohydrate-binding modules (CBMs) revisited : reduced amount of water counterbalances the need for CBMs. *Biotechnol Biofuels.* 2013;6:30.
105. Pakarinen A, Haven MO, Djajadi DT, Várnai A, Puranen T, Viikari L. Cellulases without carbohydrate-binding modules in high consistency ethanol production process. *Biotechnol Biofuels.* 2014;7:27.
106. Pareek N, Gillgren T, Jönsson LJ. Adsorption of proteins involved in hydrolysis of lignocellulose on lignins and hemicelluloses. *Bioresour Technol.* 2013;148:70–7.
107. Jørgensen H, Kristensen JB, Felby C. Enzymatic conversion of lignocellulose into fermentable sugars: challenges and opportunities. *Biofuels, Bioprod. Bioref.* 2007;1:119–34.
108. Saini JK, Patel AK, Adsul M, Singhanian RR. Cellulase adsorption on lignin: A roadblock for economic hydrolysis of biomass. *Renew Energy.* 2016;98:29–42.
109. Sewalt VJH, Glasser WG, Beauchemin KA. Lignin impact on fiber degradation . 3 . Reversal of inhibition of enzymatic hydrolysis by chemical modification of lignin and by additives. *J Agric Food Chem.* 1997;45:1823–8.
110. Berlin A, Balakshin M, Gilkes N, Kadla J, Maximenko V, Kubo S, Saddler J. Inhibition of cellulase, xylanase and beta-glucosidase activities by softwood lignin preparations. *J Biotechnol.* 2006;125:198–209.
111. Tu M, Pan X, Saddler JN. Adsorption of cellulase on cellulolytic enzyme lignin from lodgepole pine. *J Agric Food Chem.* 2009;57:7771–8.
112. Rahikainen J, Mikander S, Marjamaa K, Tamminen T, Lappas A, Viikari L, Kruus K. Inhibition of enzymatic hydrolysis by residual lignins from softwood - study of enzyme binding and

- inactivation on lignin-rich surface. *Biotechnol Bioeng.* 2011;108:2823–34.
113. Lai C, Tu M, Shi Z, Zheng K, Olmos LG, Yu S. Contrasting effects of hardwood and softwood organosolv lignins on enzymatic hydrolysis of lignocellulose. *Bioresour Technol.* 2014;163:320–7.
114. Ko JK, Ximenes E, Kim Y, Ladisch MR. Adsorption of enzyme onto lignins of liquid hot water pretreated hardwoods. *Biotechnol Bioeng.* 2015;112:447–56.
115. Palonen H, Tjerneld F, Zacchi G, Tenkanen M. Adsorption of *Trichoderma reesei* CBH I and EG II and their catalytic domains on steam pretreated softwood and isolated lignin. *J Biotechnol.* 2004;107:65–72.
116. Börjesson J, Engqvist M, Sipos B, Tjerneld F. Effect of poly(ethylene glycol) on enzymatic hydrolysis and adsorption of cellulase enzymes to pretreated lignocellulose. *Enzyme Microb Technol.* 2007;41:186–95.
117. Rahikainen J, Martin-Sampedro R, Heikkinen H, Rovio S, Marjamaa K, Tamminen T, Rojas OJ, Kruus K. Inhibitory effect of lignin during cellulose bioconversion: The effect of lignin chemistry on non-productive enzyme adsorption. *Bioresour Technol.* 2013;133:270–8.
118. Rahikainen J, Evans JD, Mikander S, Kalliola A, Puranen T, Tamminen T, Marjamaa K, Kruus K. Cellulase-lignin interactions-The role of carbohydrate-binding module and pH in non-productive binding. *Enzyme Microb Technol.* 2013;53:315–21.
119. Sammond DW, Yarbrough JM, Mansfield E, Bomble YJ, Hobdey SE, Decker SR, Taylor LE, Resch MG, Bozell JJ, Himmel ME, Vinzant TB, Crowley MF. Predicting enzyme adsorption to lignin films by calculating enzyme surface hydrophobicity. *J Biol Chem.* 2014;289:20960–9.
120. Kellock M, Rahikainen J, Marjamaa K, Kruus K. Lignin-derived inhibition of monocomponent cellulases and a xylanase in the hydrolysis of lignocellulosics. *Bioresour Technol.* 2017;232:183–91.
121. Kumar R, Wyman CE. Strong cellulase inhibition by mannan polysaccharides in cellulose

- conversion to sugars. *Biotechnol Bioeng.* 2014;111:1341–53.
122. Lan TQ, Lou H, Zhu JY. Enzymatic Saccharification of Lignocelluloses Should be Conducted at Elevated pH 5.2-6.2. *Bioenerg Res.* 2013;6:476–85.
123. Yu Z, Gwak K-S, Treasure T, Jameel H, Chang H, Park S. Effect of lignin chemistry on the enzymatic hydrolysis of woody biomass. *ChemSusChem.* 2014;7:1942–50.
124. Liu H, Sun J, Leu S-Y, Chen S. Toward a fundamental understanding of cellulase-lignin interactions in the whole slurry enzymatic saccharification process. *Biofuels, Bioprod Biorefining.* 2016;10:648–63.
125. Nakagame S, Chandra RP, Kadla JF, Saddler JN. The isolation, characterization and effect of lignin isolated from steam pretreated Douglas-fir on the enzymatic hydrolysis of cellulose. *Bioresour Technol.* 2011;102:4507–17.
126. Yarbrough JM, Mittal A, Mansfield E, Taylor LE, Hobdey SE, Sammond DW, Bomble YJ, Crowley MF, Decker SR, Himmel ME, Vinzant TB. New perspective on glycoside hydrolase binding to lignin from pretreated corn stover. *Biotechnol Biofuels.* 2015;8:214.
127. Nakagame S, Chandra RP, Saddler JN. The effect of isolated lignins, obtained from a range of pretreated lignocellulosic substrates, on enzymatic hydrolysis. *Biotechnol Bioeng.* 2010;105:871–9.
128. Petridis L, Pingali SV, Urban V, Heller WT, O’Neill HM, Foston M, Ragauskas A, Smith JC. Self-similar multiscale structure of lignin revealed by neutron scattering and molecular dynamics simulation. *Phys Rev E - Stat Nonlinear, Soft Matter Phys.* 2011;83:4–7.
129. Yang B, Wyman C. BSA treatment to enhance enzymatic hydrolysis of cellulose in lignin containing substrates. *Biotechnol Bioeng.* 2006;94:611–7.
130. Whitehead TA, Bandi CK, Berger M, Park J, Chundawat SPS. Negatively Supercharging Cellulases Render Them Lignin-Resistant. *ACS Sustain Chem Eng.* 2017;5:6247–52.
131. Pan X. Role of functional groups in lignin inhibition of enzymatic hydrolysis of cellulose to

glucose. *J Biobased Mater Bioenergy*. 2008;2:25–32.

132. Rahikainen J, Moilanen U, Nurmi-Rantala S, Lappas A, Koivula A, Viikari L, Kruus K. Effect of temperature on lignin-derived inhibition studied with three structurally different cellobiohydrolases. *Bioresour Technol*. 2013;146:118–25.

133. Kyriacou A, Neufeld RJ, MacKenzie CR. Reversibility and competition in the adsorption of *Trichoderma reesei* cellulase components. *Biotechnol Bioeng*. 1989;33:631–7.

134. Palonen H, Tenkanen M, Linder M. Dynamic interaction of *Trichoderma reesei* cellobiohydrolases Cel6A and Cel7A and cellulose at equilibrium and during hydrolysis. *Appl Environ Microbiol*. 1999;65:5229–33.

135. Pellegrini VOA, Lei N, Kyasaram M, Olsen JP, Badino SF, Windahl MS, Colussi F, Cruys-Bagger N, Borch K, Westh P. Reversibility of substrate adsorption for the cellulases Cel7A, Cel6A, and Cel7B from *Hypocrea jecorina*. *Langmuir*. 2014;30:12602–9.

136. Norde W. Adsorption of proteins from solution at the solid-liquid interface. *Adv Colloid Interface Sci*. 1986;25:267–340.

137. Latour RA. The Langmuir isotherm: A commonly applied but misleading approach for the analysis of protein adsorption behavior. *J Biomed Mater Res - Part A*. 2015;103:949–58.

138. Ximenes E, Kim Y, Mosier N, Dien B, Ladisch M. Deactivation of cellulases by phenols. *Enzyme Microb Technol*. 2011;48:54–60.

139. Kumar R, Hu F, Sannigrahi P, Jung S, Ragauskas AJ, Wyman CE. Carbohydrate derived-pseudo-lignin can retard cellulose biological conversion. *Biotechnol Bioeng*. 2013;110:737–53.

140. Kumar L, Arantes V, Chandra R, Saddler J. The lignin present in steam pretreated softwood binds enzymes and limits cellulose accessibility. *Bioresour Technol*. 2012;103:201–8.

141. Barsberg S, Selig MJ, Felby C. Impact of lignins isolated from pretreated lignocelluloses on enzymatic cellulose saccharification. *Biotechnol Lett*. 2013;35:189–95.

142. Lu X, Zheng X, Li X, Zhao J. Adsorption and mechanism of cellulase enzymes onto lignin isolated from corn stover pretreated with liquid hot water. *Biotechnol Biofuels*. 2016;9:118.
143. Haven MO, Jørgensen H. Adsorption of  $\beta$ -glucosidases in two commercial preparations onto pretreated biomass and lignin. *Biotechnol Biofuels*. 2013;6:165.
144. Rodrigues AC, Leitão AF, Moreira S, Felby C, Gama M. Recycling of cellulases in lignocellulosic hydrolysates using alkaline elution. *Bioresour Technol*. 2012;110:526–33.
145. Grabber JH. How do lignin composition, structure, and cross-linking affect degradability? A review of cell wall model studies. *Crop Sci*. 2005;45:820–31.
146. Pihlajaniemi V, Sipponen MH, Liimatainen H, Sirviö JA, Nyssölä A, Laakso S. Weighing the factors behind enzymatic hydrolyzability of pretreated lignocellulose. *Green Chem*. 2016;18:1295–305.
147. Várnai A, Siika-aho M, Viikari L. Restriction of the enzymatic hydrolysis of steam-pretreated spruce by lignin and hemicellulose. *Enzyme Microb Technol*. 2010;46:185–93.
148. Lu Y, Yang B, Gregg D, Saddler JN, Mansfield SD. Cellulase adsorption and an evaluation of enzyme recycle during hydrolysis of steam-exploded softwood residues. *Appl Biochem Biotech*. 2002;98–100:641–54.
149. Hansen MAT, Kristensen JB, Felby C, Jørgensen H. Pretreatment and enzymatic hydrolysis of wheat straw (*Triticum aestivum* L.) - the impact of lignin relocation and plant tissues on enzymatic accessibility. *Bioresour Technol*. 2011;102:2804–11.
150. Ju X, Engelhard M, Zhang X. An advanced understanding of the specific effects of xylan and surface lignin contents on enzymatic hydrolysis of lignocellulosic biomass. *Bioresour Technol*. 2013;132:137–45.
151. Tolbert A, Ragauskas AJ. Advances in understanding the surface chemistry of lignocellulosic biomass via time-of-flight secondary ion mass spectrometry. *Energy Sci Eng*. 2017;5:5–20.



152. Tolbert AK, Yoo CG, Ragauskas AJ. Understanding the Changes to Biomass Surface Characteristics after Ammonia and Organosolv Pretreatments by Using Time-of-Flight Secondary-Ion Mass Spectrometry (TOF-SIMS). *Chempluschem*. 2017;82:686–90.
153. Zeng Y, Himmel ME, Ding SY. Visualizing chemical functionality in plant cell walls. *Biotechnol Biofuels*. 2017;10:263.
154. Zeng Y, Zhao S, Wei H, Tucker MP, Himmel ME, Mosier NS, Meilan R, Ding SY. In situ micro-spectroscopic investigation of lignin in poplar cell walls pretreated by maleic acid. *Biotechnol Biofuels*. 2015;8:126.
155. Zhang H, Fangel JU, Willats WGT, Selig MJ, Lindedam J, Jørgensen H, Felby C. Assessment of leaf/stem ratio in wheat straw feedstock and impact on enzymatic conversion. *GCB Bioenergy*. 2014;6:90–6.
156. Sluiter A, Hames B, Ruiz R, Scarlata C, Sluiter J, Templeton D, Crocker D. Determination of structural carbohydrates and lignin in biomass. Laboratory analytical procedure (LAP). NREL/TP-510-42618. Golden, CO, USA; 2008.
157. Mansfield SD, Kim H, Lu F, Ralph J. Whole plant cell wall characterization using solution-state 2D NMR. *Nat Protoc*. 2012;7:1579–89.
158. Moller I, Sørensen I, Bernal AJ, Blaukopf C, Lee K, Øbro J, Pettolino F, Roberts A, Mikkelsen JD, Knox JP, Bacic A, Willats WGT. High-throughput mapping of cell-wall polymers within and between plants using novel microarrays. *Plant J*. 2007;50:1118–28.
159. Alonso-Simón A, Kristensen JB, Øbro J, Felby C, Willats WGT, Jørgensen H. High-throughput microarray profiling of cell wall polymers during hydrothermal pre-treatment of wheat straw. *Biotechnol Bioeng*. 2010;105:509–14.
160. Hansen MAT, Ahl LI, Pedersen HL, Westereng B, Willats WGT, Jørgensen H, Felby C. Extractability and digestibility of plant cell wall polysaccharides during hydrothermal and

- enzymatic degradation of wheat straw (*Triticum aestivum* L.). *Ind Crop Prod.* 2014;55:63–9.
161. Jensen MM, Madsen RB, Becker J, Iversen BB, Glasius M. Products of hydrothermal treatment of lignin and the importance of ortho-directed repolymerization reactions. *J Anal Appl Pyrolysis.* 2017;126:371–9.
162. Djajadi DT, Hansen AR, Jensen A, Thygesen LG, Pinelo M, Meyer AS, Jørgensen H. Surface properties correlate to the digestibility of hydrothermally pretreated lignocellulosic Poaceae biomass feedstocks. *Biotechnol Biofuels.* 2017;10:49.
163. Heiss-Blanquet S, Zheng D, Lopes Ferreira N, Lapierre C, Baumberger S. Effect of pretreatment and enzymatic hydrolysis of wheat straw on cell wall composition, hydrophobicity and cellulase adsorption. *Bioresour Technol.* 2011;102:5938–46.
164. Kristensen JB, Felby C, Jørgensen H. Yield-determining factors in high-solids enzymatic hydrolysis of lignocellulose. *Biotechnol Biofuels.* 2009;2:11.
165. Weiss ND, Thygesen LG, Felby C, Roslander C, Gourlay K. Biomass-water interactions correlate to recalcitrance and are intensified by pretreatment: an investigation of water constraint and retention in pretreated spruce using low field NMR and water retention value techniques. *Biotechnol Progr.* 2016;33:146–53.
166. Williams DL, Hodge DB. Impacts of delignification and hot water pretreatment on the water induced cell wall swelling behavior of grasses and its relation to cellulolytic enzyme hydrolysis and binding. *Cellulose.* 2014;21:221–35.
167. Cui T, Li J, Yan Z, Yu M, Li S. The correlation between the enzymatic saccharification and the multidimensional structure of cellulose changed by different pretreatments. *Biotechnol Biofuels.* 2014;7:134.
168. Shen J, Liu Z, Li J, Niu J. Wettability changes of wheat straw treated with chemicals and enzymes. *J For Res.* 2011;22:107–10.

169. Xu N, Liu W, Hou Q, Wang P, Yao Z. Effect of autohydrolysis on the wettability, absorptivity and further alkali impregnation of poplar wood chips. *Bioresour Technol.* 2016;216:317–22.
170. Weiss N, Börjesson J, Pedersen LS, Meyer AS. Enzymatic lignocellulose hydrolysis: Improved cellulase productivity by insoluble solids recycling. *Biotechnol Biofuels.* 2013;6:5.
171. Means GE, Feeney RE. Reductive alkylation of amino groups in proteins. *Biochemistry.* 1968;7:2192–201.
172. Tack BF, Dean J, Eilat D, Lorenz PE, Schechter AN. Tritium Labeling of Proteins to High Specific Radioactivity by Reductive Methylation. *J Biol Chem.* 1980;255:8842–7.
173. Vroman L, Adams AL. Findings with the recording ellipsometer suggesting rapid exchange of specific plasma proteins at liquid/solid interfaces. *Surf Sci.* 1969;16:438–46.
174. Kärcher MA, Iqbal Y, Lewandowski I, Senn T. Comparing the performance of *Miscanthus x giganteus* and wheat straw biomass in sulfuric acid based pretreatment. *Bioresour Technol.* 2015;180:360–4.
175. Zhang T, Wyman CE, Jakob K, Yang B. Rapid selection and identification of *Miscanthus* genotypes with enhanced glucan and xylan yields from hydrothermal pretreatment followed by enzymatic hydrolysis. *Biotechnol Biofuels.* 2012;5:56.
176. Lindedam J, Andersen SB, DeMartini J, Bruun S, Jørgensen H, Felby C, Magid J, Yang B, Wyman CE. Cultivar variation and selection potential relevant to the production of cellulosic ethanol from wheat straw. *Biomass Bioenerg.* 2012;37:221–8.
177. Auxenfans T, Crônier D, Chabbert B, Paës G. Understanding the structural and chemical changes of plant biomass following steam explosion pretreatment. *Biotechnol Biofuels. BioMed Central;* 2017;10:1–16.
178. Herbaut M, Zoghalmi A, Habrant A, Falourd X, Foucat L, Chabbert B, Paës G. Multimodal analysis of pretreated biomass species highlights generic markers of lignocellulose recalcitrance.

Biotechnol Biofuels. 2018;11:52.

179. Yang H, Chen Q, Wang K, Sun R-C. Correlation between hemicelluloses-removal-induced hydrophilicity variation and the bioconversion efficiency of lignocelluloses. *Bioresour Technol.* 2013;147:539–44.

180. Kabel MA, van den Borne H, Vincken JP, Voragen AGJ, Schols HA. Structural differences of xylans affect their interaction with cellulose. *Carbohydr Polym.* 2007;69:94–105.

181. Selig MJ, Thygesen LG, Felby C, Master ER. Debranching of soluble wheat arabinoxylan dramatically enhances recalcitrant binding to cellulose. *Biotechnol Lett.* 2015;37:633–41.

182. Kumar R, Bhagia S, Smith MD, Petridis L, Ong R, Cai CM, Mittal A, Himmel ME, Balan V, Dale BE, Ragauskas A, Smith JC, Wyman CE. Cellulose-Hemicellulose Interactions at Elevated Temperatures Increase Cellulose Recalcitrance to Biological Conversion. *Green Chem. Royal Society of Chemistry;* 2018;921–34.

183. Pereira CS, Silveira RL, Dupree P, Skaf MS. Effects of Xylan Side-Chain Substitutions on Xylan-Cellulose Interactions and Implications for Thermal Pretreatment of Cellulosic Biomass. *Biomacromolecules.* 2017;18:1311–21.

184. Donaldson LA, Wong KKY, Mackie KL. Ultrastructure of steam-exploded wood. *Wood Sci Technol.* 1988;22:103–14.

185. Selig MJ, Vinzant TB, Himmel ME, Decker SR. The effect of lignin removal by alkaline peroxide pretreatment on the susceptibility of corn stover to purified cellulolytic and xylanolytic enzymes. *Appl Biochem Biotech.* 2009;155:397–406.

186. Araya F, Troncoso E, Mendonça RT, Freer J. Condensed lignin structures and re-localization achieved at high severities in autohydrolysis of *Eucalyptus globulus* wood and their relationship with cellulose accessibility. *Biotechnol Bioeng.* 2015;112:1783–91.

187. Silveira RL, Stoyanov SR, Gusarov S, Skaf MS, Kovalenko A. Supramolecular interactions in

secondary plant cell walls: effect of lignin chemical composition revealed with the molecular theory of solvation. *J Phys Chem Lett.* 2015;6:206–11.

188. Langan P, Petridis L, O'Neill HM, Pingali SV, Foston M, Nishiyama Y, Schulz R, Lindner B, Hanson BL, Harton S, Heller WT, Urban V, Evans BR, Gnanakaran S, Ragauskas AJ, Smith JC, Davison BH. Common processes drive the thermochemical pretreatment of lignocellulosic biomass. *Green Chem.* 2014;16:63.

189. Linder M, Lindeberg G, Reinikainen T, Teeri TT, Pettersson G. The difference in affinity between two fungal cellulose-binding domains is dominated by a single amino acid substitution. *FEBS Lett.* 1995;372:96–8.

190. Takashima S, Ohno M, Hidaka M, Nakamura A, Masaki H, Uozumi T. Correlation between cellulose binding and activity of cellulose-binding domain mutants of *Humicola grisea* cellobiohydrolase 1. *FEBS Lett.* 2007;581:5891–6.

191. Beckham GT, Ståhlberg J, Knott BC, Himmel ME, Crowley MF, Sandgren M, Sørli M, Payne CM. Towards a molecular-level theory of carbohydrate processivity in glycoside hydrolases. *Curr Opin Biotechnol.* 2014;27:96–106.

192. Nakamura A, Watanabe H, Ishida T, Uchihashi T, Wada M, Ando T, Igarashi K, Samejima M. Trade-off between Processivity and Hydrolytic Velocity of Cellobiohydrolases at the Surface of Crystalline Cellulose. *J Am Chem Soc.* 2014;136:4584–92.

193. Taylor II LE, Knott BC, Baker JO, Alahuhta PM, Hobdey SE, Linger JG, Lunin V V, Amore A, Subramanian V, Podkaminer K, Xu Q, VanderWall TA, Schuster LA, Chaudhari YB, Adney WS, Crowley MF, Himmel ME, Decker SR, Beckham GT. Engineering enhanced cellobiohydrolase activity. *Nat Commun.* 2018;9:1186.

194. Brethauer S, Studer MH, Yang B, Wyman CE. The effect of bovine serum albumin on batch and continuous enzymatic cellulose hydrolysis mixed by stirring or shaking. *Bioresour Technol.*

2011;102:6295–8.

195. Bhagia S, Dhir R, Kumar R, Wyman CE. Deactivation of Cellulase at the Air-Liquid Interface Is the Main Cause of Incomplete Cellulose Conversion at Low Enzyme Loadings. *Sci Rep.* 2018;8:1350.

196. Wallace J, Brienzo M, García-Aparicio MP, Görgens JF. Lignin enrichment and enzyme deactivation as the root cause of enzymatic hydrolysis slowdown of steam pretreated sugarcane bagasse. *N Biotechnol.* 2016;33:361–71.

197. Dumitrache A, Tolbert A, Natzke J, Brown SD, Davison BH, Ragauskas AJ. Cellulose and lignin colocalization at the plant cell wall surface limits microbial hydrolysis of *Populus* biomass. *Green Chem. Royal Society of Chemistry;* 2017;19:2275–85.

198. Eriksson I, Haglind I, Lidbrandt O, Sahnén L. Fiber swelling favoured by lignin softening. *Wood Sci Technol.* 1991;25:135–44.

199. Mooney C, Mansfield SD, Touhy MG, Saddler JN. The effect of initial pore volume and lignin content on the enzymatic hydrolysis of softwoods. *Bioresour Technol.* 1998;64:113–9.

200. Ju X, Grego C, Zhang X. Specific effects of fiber size and fiber swelling on biomass substrate surface area and enzymatic digestibility. *Bioresour Technol.* 2013;144:232–9.

201. Wayman, M., Chua MGS. Characterization of autohydrolysis aspen (*P. tremuloides*) lignins. Part 2. Alkaline nitrobenzene oxidation studies of extracted autohydrolysis lignin. *Can J Chem.* 1979;57:2599–602.

202. Yoo CG, Dumitrache A, Muchero W, Natzke J, Akinosho HO, Li M, Sykes R, Brown SD, Davison BH, Tuskan GA, Pu Y, Ragauskas AJ. Significance of lignin S/G ratio in biomass recalcitrance of *Populus trichocarpa* variants for bioethanol production. *ACS Sustain Chem Eng.* 2018;6:2162–2168.

## Appendix A

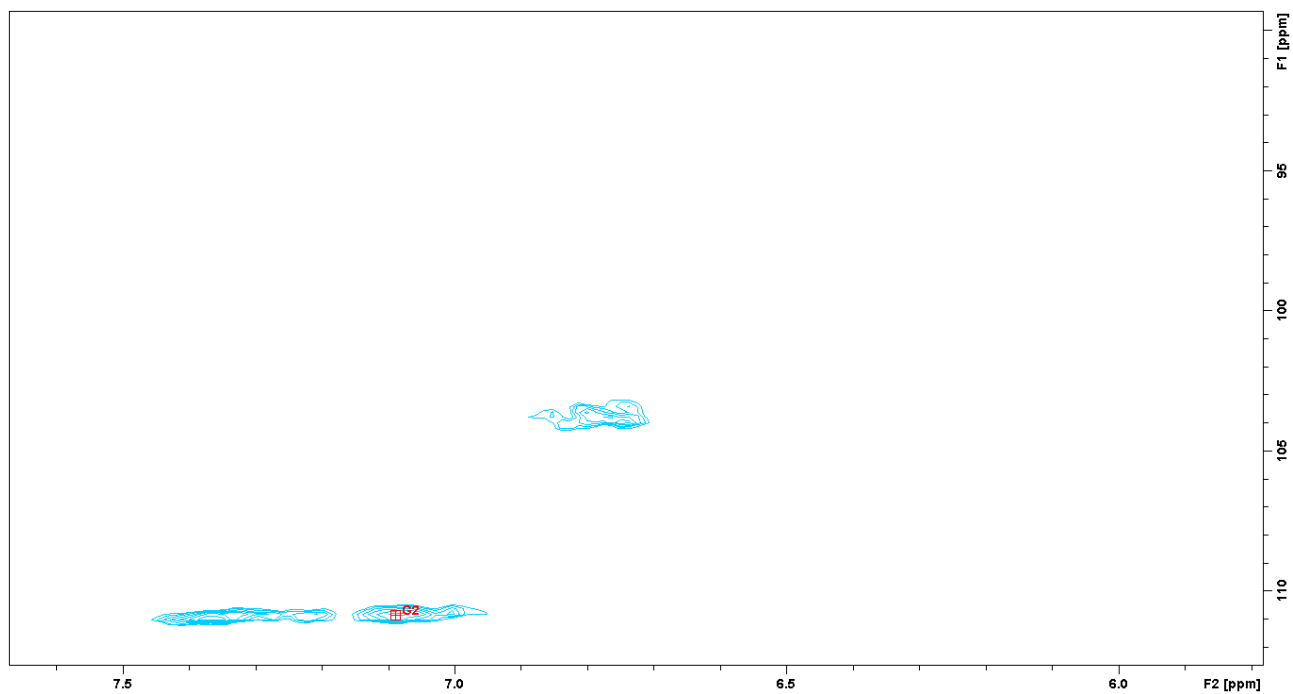


Fig. A.1  $^{13}\text{C}$ - $^1\text{H}$  HSQC (heteronuclear single quantum coherence) spectra of raw (untreated) corn stover (CS) displaying the absence of tricetin peaks relative to the G2 peak ( $\text{C}_2$ - $\text{H}_2$  correlation peak in guaiacyl subunit).

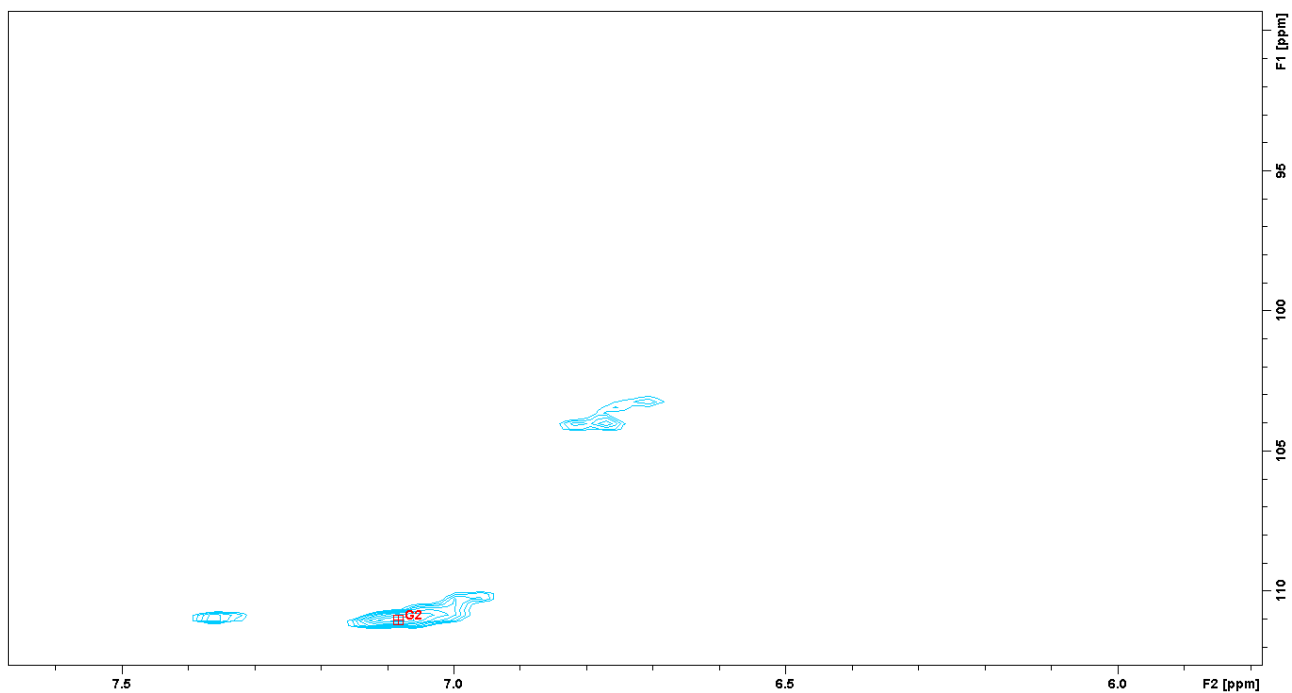


Fig. A.2  $^{13}\text{C}$ - $^1\text{H}$  HSQC (heteronuclear single quantum coherence) spectra of raw (untreated) *Miscanthus*  $\times$  *giganteus* stalks (MS) displaying the absence of tricin peaks relative to the G2 peak ( $\text{C}_2$ - $\text{H}_2$  correlation peak in guaiacyl subunit).



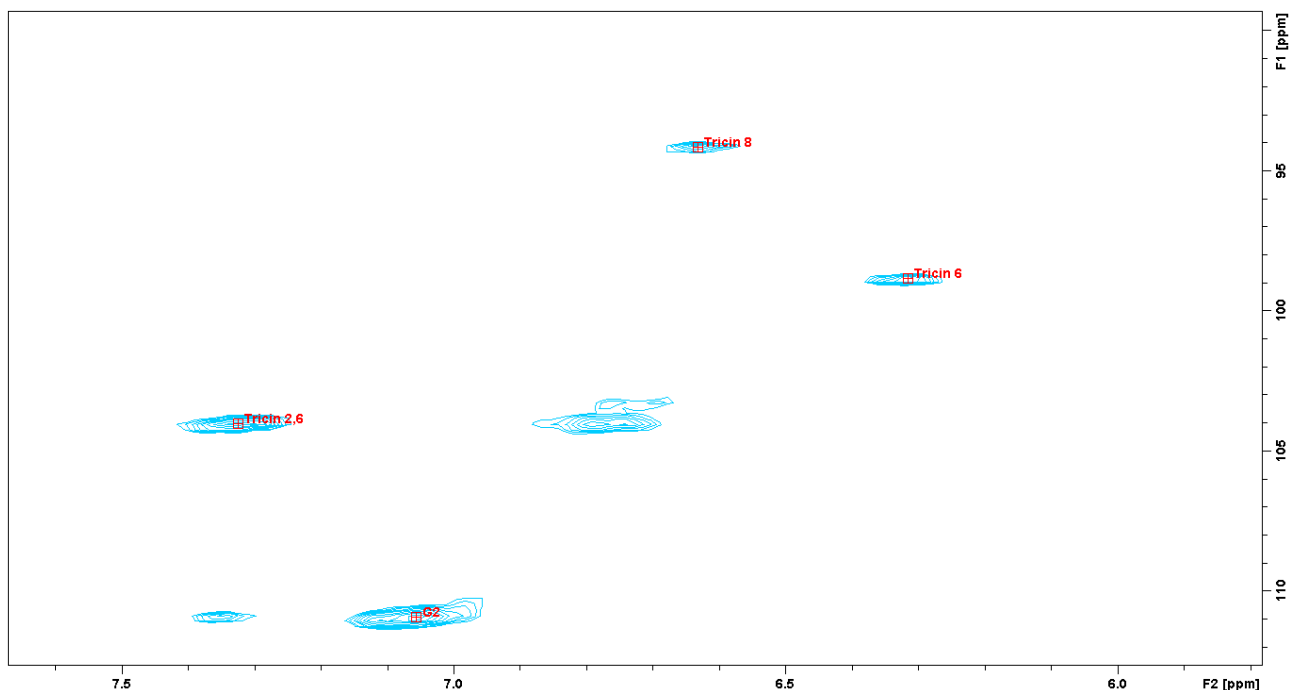


Fig. A.3  $^{13}\text{C}$ - $^1\text{H}$  HSQC (heteronuclear single quantum coherence) spectra of raw (untreated) wheat straw (WS) displaying the tricin peaks (Tricin 2,6; Tricin 6; Tricin 8) relative to the reference G2 peak ( $\text{C}_2$ - $\text{H}_2$  correlation peak in guaiacyl subunit).

Table A.1  $^{13}\text{C}$ - $^1\text{H}$  HSQC contour integration values for tricin in the raw (untreated) biomass feedstocks

Structure	CS	MS	WS
<b>G2</b>	1	1	1
<b>Tricin 2,6</b>	nd	nd	0.48
<b>Tricin 6</b>	nd	nd	0.24
<b>Tricin 8</b>	nd	nd	0.23

CS: corn stover; MS: *Miscanthus × giganteus* stalks; WS: wheat straw  
 G2:  $\text{C}_2$ - $\text{H}_2$  correlation peak in guaiacyl subunit was used as reference  
 nd: peak too small for accurate determination

## Appendix B

Table B.1 Glucose and xylose release after hydrolysis\* of lignin-rich residues using Cellic<sup>®</sup> CTec3

<b>Biomass – log <math>R_0</math></b>	<b>Glucose released (mg/l)</b>	<b>% of theoretical maximum glucose release</b>	<b>Xylose released (mg/l)</b>	<b>% of theoretical maximum xylose release</b>
<b>CS – 3.65</b>	134.3 ± 11.9	5.8 ± 0.5	51.6 ± 3.5	8.3 ± 0.6
<b>CS – 3.83</b>	69.3 ± 1.7	4.3 ± 0.1	19.4 ± 1.8	5.3 ± 0.5
<b>CS – 3.97</b>	41.5 ± 4.4	5.2 ± 0.5	3.9 ± 1.4	2.1 ± 0.8
<b>MS – 3.65</b>	81.8 ± 3.4	2.2 ± 0.1	35.6 ± 1.0	5.5 ± 0.2
<b>MS – 3.83</b>	50.3 ± 5.5	2.4 ± 0.3	13.8 ± 0.5	4.1 ± 0.1
<b>MS – 3.97</b>	41.5 ± 3.2	3.2 ± 0.2	ND	ND
<b>WS – 3.65</b>	48.9 ± 7.1	3.2 ± 0.5	25.2 ± 0.5	6.6 ± 0.1
<b>WS – 3.83</b>	22.2 ± 3.7	2.5 ± 0.4	7.7 ± 1.5	3.4 ± 0.7
<b>WS – 3.97</b>	15.5 ± 0.2	2.7 ± 0.0	ND	ND

ND: the value was not detectable since they were below the detection limit of the HPLC system.

\*: The hydrolysis of LRRs was performed with 10 mg/g dosage for 24 h at 50°C, pH 5.0 using Cellic<sup>®</sup> CTec3

## Appendix C

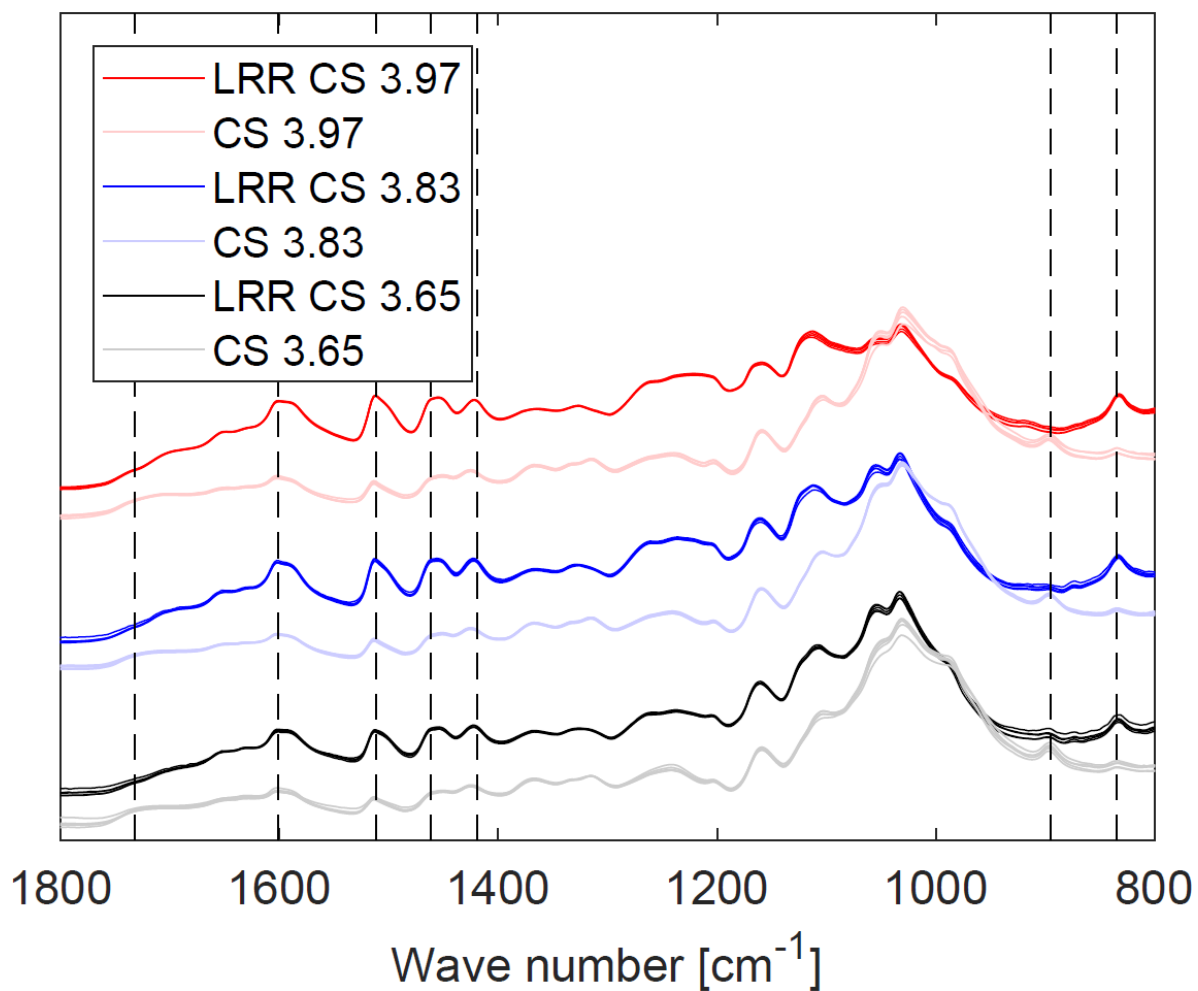


Fig. C.1 ATR-FTIR spectra of lignin-rich residues (LRRs) isolated from corn stover (CS) hydrothermally pretreated at different pretreatment severity factors ( $\log R_0$ ) and the corresponding spectra of the fiber fraction of pretreated biomass. Different lines of same colors represent five replicates of the same samples. Vertical lines mark the wave numbers 835, 895, 1419, 1432, 1512, 1601 and 1732  $\text{cm}^{-1}$ .

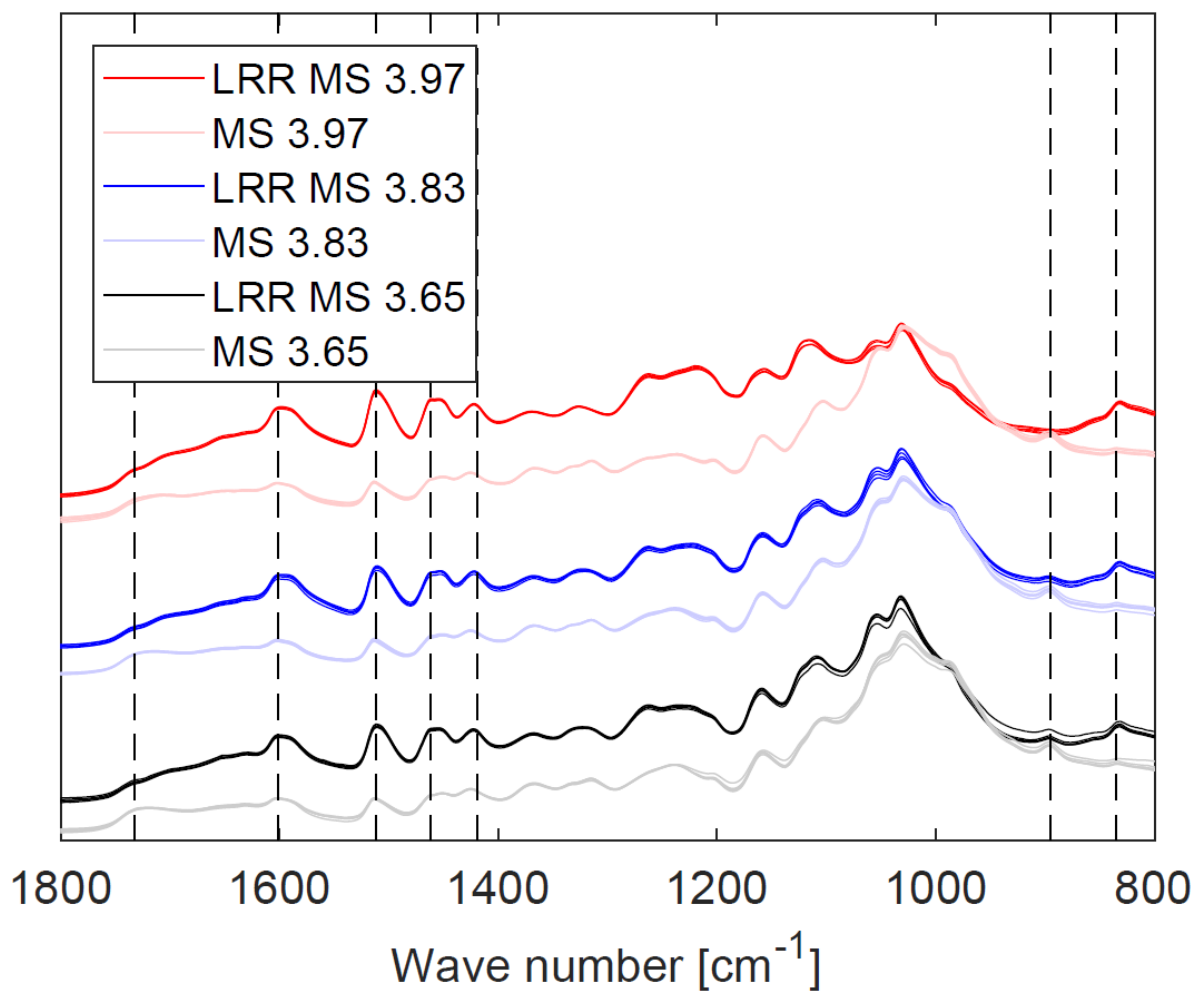


Fig. C.2 ATR-FTIR spectra of lignin-rich residues (LRRs) isolated from *Miscanthus × giganteus* stalks (MS) hydrothermally pretreated at different pretreatment severity factors ( $\log R_0$ ) and the corresponding spectra of the fiber fraction of pretreated biomass. Different lines of same colors represent five replicates of the same samples. Vertical lines mark the wave numbers 835, 895, 1419, 1432, 1512, 1601 and 1732  $\text{cm}^{-1}$ .

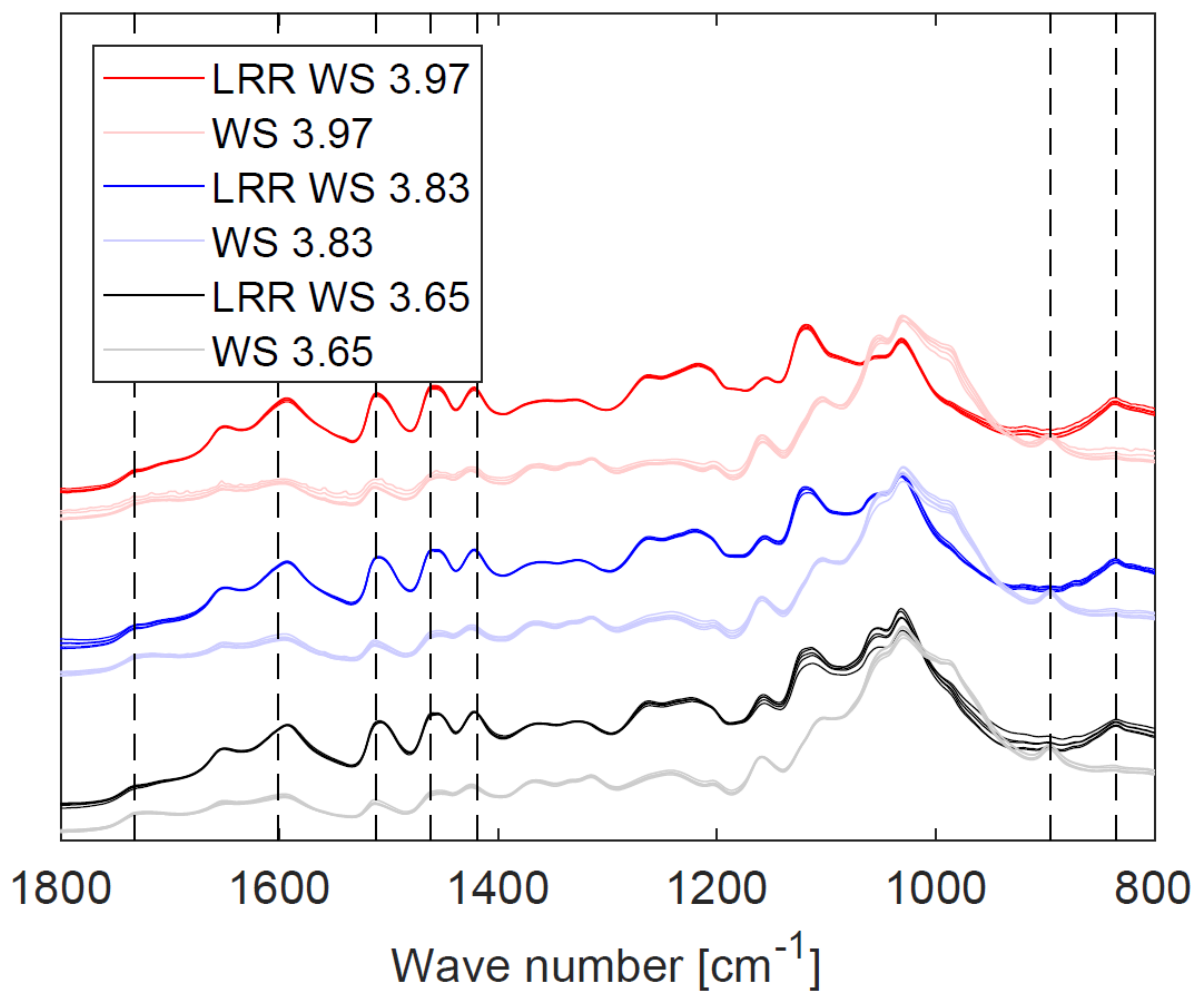


Fig. C.3 ATR-FTIR spectra of lignin-rich residues (LRRs) isolated from wheat straw (WS) hydrothermally pretreated at different pretreatment severity factors ( $\log R_0$ ) and the corresponding spectra of the fiber fraction of pretreated biomass. Different lines of same colors represent five replicates of the same samples. Vertical lines mark the wave numbers 835, 895, 1419, 1432, 1512, 1601 and 1732  $\text{cm}^{-1}$ .

## Appendix D

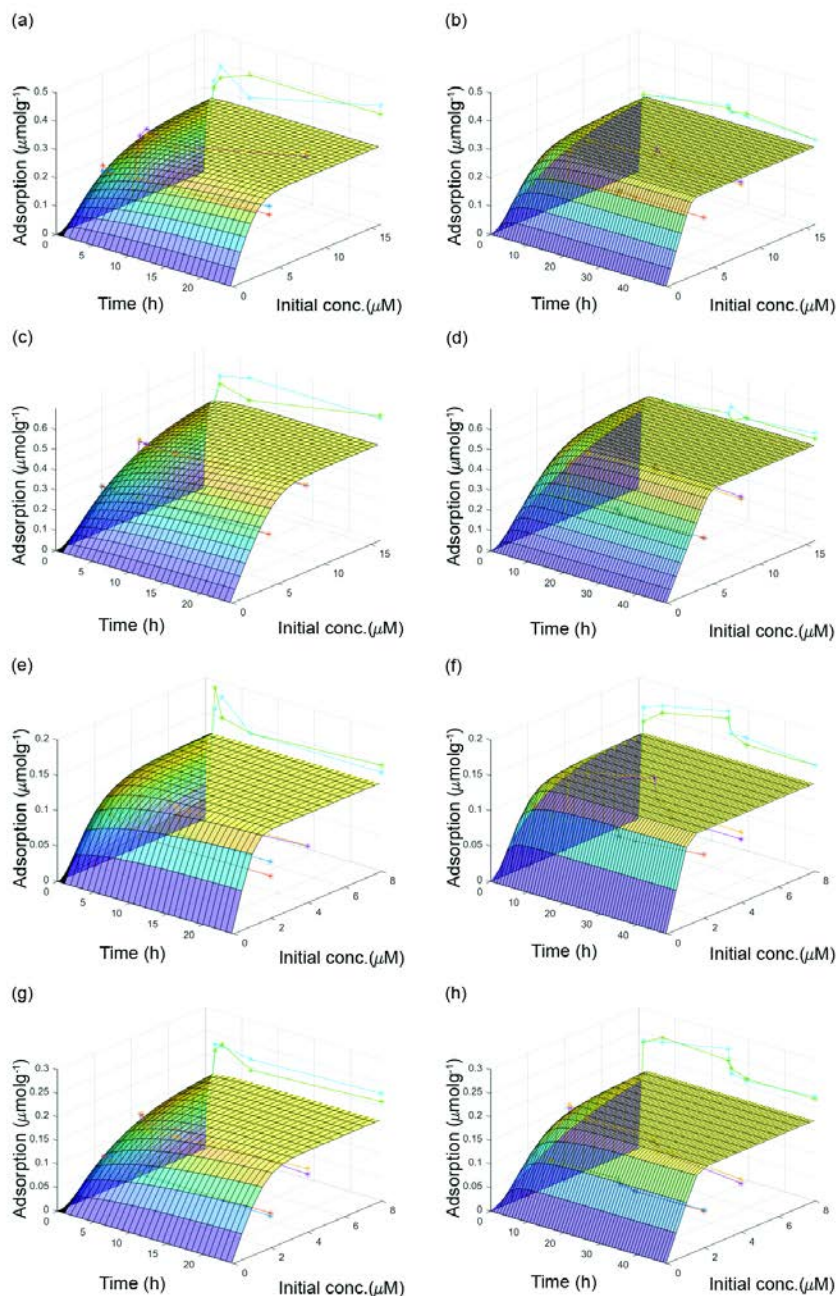


Fig. D.1 Response surface graphs displaying the fitting of experimental data on the adsorption of *TrCel6A* (a, b, e, f) & *TrCel5A* (c, d, g, h) on lignin-rich residues isolated from hydrothermally pretreated spruce (L-HPS) (a-d) & wheat straw (L-HPWS) (e-h) modelled using Model 4 (completely irreversible adsorption) with early (a, c, e, g) & late dilution (b, d, f, h).

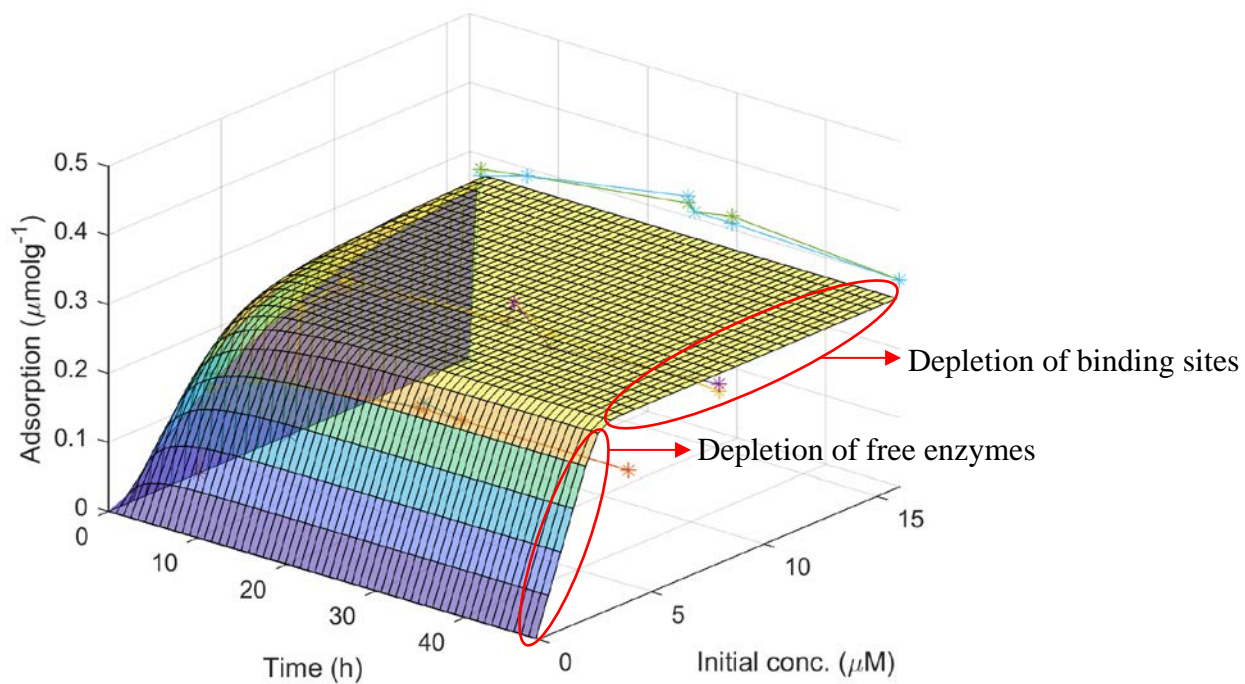


Figure D.2 Poor fit to the expected behavior of completely irreversible adsorption.

## Appendix E

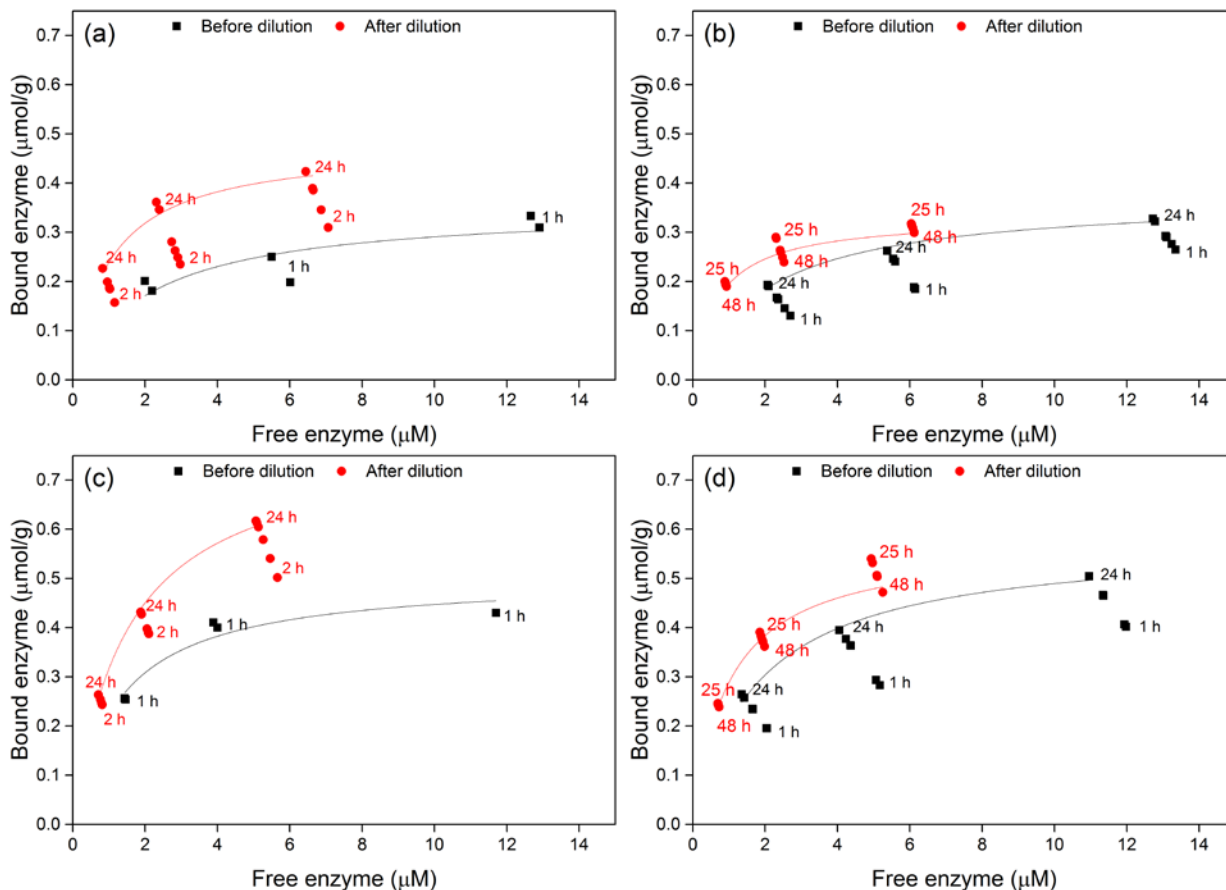


Fig. E.1 The data from dilution experiments series for kinetic modelling displayed as binding isotherm for adsorption of *TrCel6A* (a and b) and *TrCel5A* (c and d) on lignin-rich residues isolated from hydrothermally pretreated spruce (L-HPS). Different symbols and coloring were used for data points before and after dilution for Early Dilution (a and c) and Late Dilution (b and d) series. The overall progression of binding over time was presented by the corresponding text which marked the time point. Solid lines represent fitting of the Langmuir adsorption model for one binding-site to the final points before and after dilution.



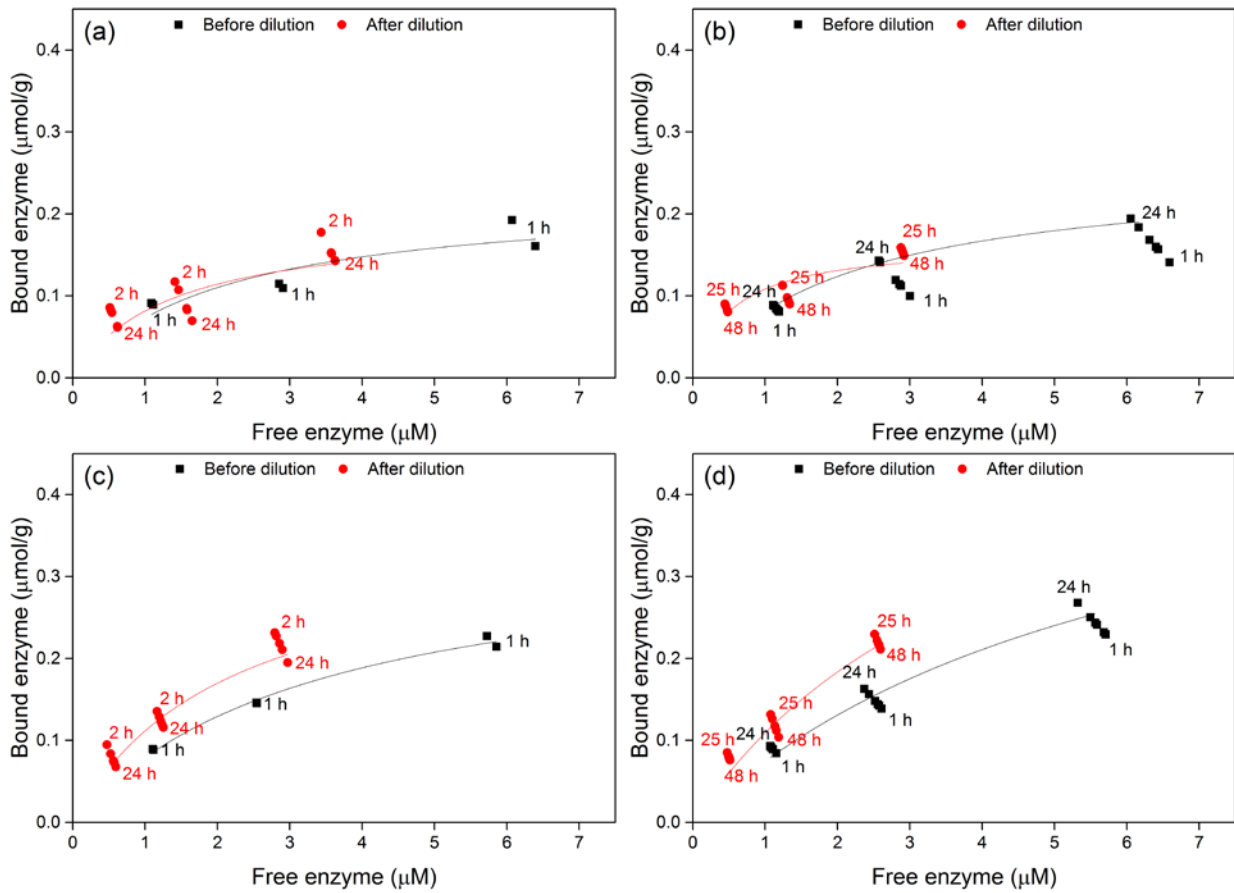


Fig. E.2 The data from dilution experiments series for kinetic modelling displayed as binding isotherm for adsorption of *TrCel6A* (a and b) and *TrCel5A* (c and d) on lignin-rich residues isolated from hydrothermally pretreated wheat straw (L-HPWS). Different symbols and coloring were used for data points before and after dilution for Early Dilution (a and c) and Late Dilution (b and d) series. The overall progression of binding over time was presented by the corresponding text which marked the time point. Solid lines represent fitting of the Langmuir adsorption model for one binding-site to the final points before and after dilution.

## PAPER I

---

Surface properties correlate to the digestibility of hydrothermally pretreated lignocellulosic Poaceae biomass feedstocks

**Djajadi DT**, Hansen AR, Jensen A, Thygesen LG, Pinelo M, Meyer AS, Jørgensen H

Biotechnol. Biofuels 2017; 10:49

© The Author(s) 2017

Reprinted under Creative Commons Attribution License 4.0

RESEARCH

Open Access



# Surface properties correlate to the digestibility of hydrothermally pretreated lignocellulosic Poaceae biomass feedstocks

Demi T. Djajadi<sup>1</sup> , Aleksander R. Hansen<sup>2</sup>, Anders Jensen<sup>3</sup>, Lisbeth G. Thygesen<sup>3</sup>, Manuel Pinelo<sup>1</sup>, Anne S. Meyer<sup>1\*</sup> , and Henning Jørgensen<sup>1,2</sup>

## Abstract

**Background:** Understanding factors that govern lignocellulosic biomass recalcitrance is a prerequisite for designing efficient 2nd generation biorefining processes. However, the reasons and mechanisms responsible for quantitative differences in enzymatic digestibility of various biomass feedstocks in response to hydrothermal pretreatment at different severities are still not sufficiently understood.

**Results:** Potentially important lignocellulosic feedstocks for biorefining, corn stover (*Zea mays* subsp. *mays* L.), stalks of *Miscanthus × giganteus*, and wheat straw (*Triticum aestivum* L.) were systematically hydrothermally pretreated; each at three different severities of 3.65, 3.83, and 3.97, respectively, and the enzymatic digestibility was assessed. Pretreated samples of *Miscanthus × giganteus* stalks were the least digestible among the biomass feedstocks producing ~24 to 66.6% lower glucose yields than the other feedstocks depending on pretreatment severity and enzyme dosage. Bulk biomass composition analyses, 2D nuclear magnetic resonance, and comprehensive microarray polymer profiling were not able to explain the observed differences in recalcitrance among the pretreated feedstocks. However, methods characterizing physical and chemical features of the biomass surfaces, specifically contact angle measurements (wettability) and attenuated total reflectance-Fourier transform infrared (ATR-FTIR) spectroscopy (surface biopolymer composition) produced data correlating pretreatment severity and enzymatic digestibility, and they also revealed differences that correlated to enzymatic glucose yield responses among the three different biomass types.

**Conclusion:** The study revealed that to a large extent, factors related to physico-chemical surface properties, namely surface wettability as assessed by contact angle measurements and surface content of hemicellulose, lignin, and wax as assessed by ATR-FTIR rather than bulk biomass chemical composition correlated to the recalcitrance of the tested biomass types. The data provide new insight into how hydrothermal pretreatment severity affects surface properties of key Poaceae lignocellulosic biomass and may help design new approaches to overcome biomass recalcitrance.

**Keywords:** Hydrothermal pretreatment, Enzymatic hydrolysis, Hemicellulose, Wettability, 2D nuclear magnetic resonance (NMR), Attenuated total reflectance-Fourier transform infrared (ATR-FTIR), Comprehensive microarray polymer profiling (CoMPP), Contact angle measurements

## Background

Pretreatment is an important process step in the processing of recalcitrant lignocellulosic biomass and is

employed to enhance the susceptibility of the biomass to enzymatic deconstruction. Among various pretreatment technologies developed and tested [1–3], hydrothermal pretreatment (HTP) has been employed in recently established demonstration and commercial scale second generation ethanol plants, i.e., the Inbicon demonstration plant in Denmark [4] and the full scale ethanol plant of Beta Renewables in Italy [5]. HTP is based on

\*Correspondence: am@kt.dtu.dk

<sup>1</sup> Department of Chemical and Biochemical Engineering, Technical University of Denmark, Søltofts Plads Building 229, 2800 Kongens Lyngby, Denmark

Full list of author information is available at the end of the article

the treatment of biomass with steam and no addition of a catalyst [4]. The advantages of HTP include that operation without catalyst addition (e.g., acids) enables the use of less expensive alloys for construction of reactors and gives lower operational costs [4]. Common to all pretreatment technologies is that they modify the cell wall structure and composition and thereby make the cellulose more susceptible to enzymatic attack.

HTP results in partial defibrillation and fractionation of the biomass due to solubilization of hemicellulose and redistribution of lignin [6, 7]. The extent of both the hemicellulose solubilization and the lignin redistribution depends on the severity of the treatment (time, temperature, particle size, and mechanical shear imposed on the material). HTP is usually performed in the range of 180–200 °C for 10–20 min, because the treatment severity is a compromise between the intention to amend the cellulose to enzymatic attack and production of cellulase inhibitors that may retard the enzymatic efficacy [4, 7, 8]. During HTP employing the conditions above, water is auto-ionized and acts as a catalyst that hydrolyzes glycosidic bonds in hemicellulose in addition to releasing notably acetic acid from the biomass which further acts to catalyze the depolymerization of hemicellulose [9, 10]. The extent of hemicellulose depolymerization is affected by the intensity of the reaction which is expressed as severity factor ( $\log R_0$ ) [10, 11], whereas the extent of cellulose hydrolysis and solubilization is minor [7, 12]. The lignin on the other hand, depending on its glass transition temperature ( $T_g$ ), turns into a fluid-like state and during the pretreatment relocates within and on the cell wall material. Redeposited droplets of recondensed lignin are frequently observed on the surface of the pretreated material [6, 13]. This relocation improves accessibility initially due to exposure of a larger cellulose area, but the lignin droplets themselves have been suggested to sterically hinder cellulolytic enzymes attack or act to unproductively bind cellulases [14, 15]. Nevertheless, the removal of hemicellulose and the redistribution of lignin during HTP are thought to render cellulose more susceptible towards enzymatic deconstruction [16–18]. Generally, there is a good correlation between severity, hemicellulose solubilization, and the degree of cellulose depolymerization, i.e., at higher severity more hemicellulose is solubilized and the cellulose hydrolysis is improved [7, 19–21], although profound differences in recalcitrance can occur within even closely related cultivars and botanical parts of the same species, as shown for, e.g., wheat straw [22, 23]. It has nevertheless been common practice to assess the removal of hemicellulose from the original material as indicator of hydrothermal pretreatment effectiveness [7, 19–21].

Recently, differences in accessibility of water to cellulose were found to partly correlate to the accessibility of

the enzymes to cellulose and thereby the cellulose convertibility [24–27]. The ability to interact with water, i.e., the wettability, represented as surface hydrophobicity through initial water contact angle measurement, has been found to improve after organosolv and steam explosion pretreatment of wheat straw; therefore suggesting a connection between digestibility and wettability [28]. Despite this recent progress the quantitative aspects of the molecular and structural mechanisms governing biomass recalcitrance of pretreated biomass are not sufficiently understood when it comes to responses to different pretreatment severities and differences across feedstocks.

The objective of this study was to obtain improved knowledge of how the chemistry, physics, and enzymatic digestibility of industrially relevant Poaceae biomass feedstocks respond to different HTP severities and notably to attempt to identify factors that correlate with the recalcitrance of a biomass with a given composition.

## Results and discussion

### Composition

The compositions of the solid fraction of the biomass feedstocks were compared among the different severity levels and with respect to the original untreated (raw) materials on a dry matter (DM) basis (Table 1). When calculated from monomeric composition assessment (using the NREL biomass analysis protocol [29]), the arabino-(galacto-)/xylan contents decreased significantly along with concomitant increase of glucan content as the pretreatment severity increased. This indicated solubilization of hemicellulose which in turn will be expected to expose cellulose and improve enzymatic digestibility [6, 7, 10]. After HTP, the lignin content was also higher than in the untreated biomass, although lignin levels remained relatively stable irrespective of severity factor in *Miscanthus × giganteus* stalks (MS) and wheat straw (WS) (Table 1). The lignin content in corn stover (CS) was lower than in the other biomass feedstocks and remained the same even after pretreatment. The carbohydrate contents of all pretreated biomass feedstocks were relatively similar among corresponding severity factors except for xylan in MS, which was lower than in CS and WS.

As mentioned, the extent of hemicellulose removal relative to the original raw material has been shown to correlate with digestibility [7, 20, 21] and cellulose accessibility [30] of pretreated lignocellulosic biomass materials. The results indicated sizeable removal of hemicellulose, assessed as degree of arabinose and xylose removal, in response to the applied severity factor, i.e., increased hemicellulose removal at elevated severity factor (Fig. 1). However, the extent of hemicellulose removal was similar across all three biomass feedstocks (Fig. 1).

**Table 1** Composition of untreated (raw) and hydrothermally pretreated (severity factor:  $\log R_0$ ) biomass feedstocks

Biomass— $\log R_0$	Arabinan (% w/w DM)	Galactan	Glucan	Xylan	Mannan	Lignin <sup>1</sup>	Ash	Extractives
Raw CS	<i>3.4 ± 0.1<sup>a</sup></i>	<i>1.4 ± 0.1<sup>a</sup></i>	<i>43.7 ± 0.7<sup>c</sup></i>	<i>23.8 ± 0.1<sup>a</sup></i>	<i>0.5 ± 0.0<sup>a</sup></i>	<i>19.4 ± 1.3<sup>c</sup></i>	<i>2.3 ± 0.1</i>	<i>6.7 ± 0.6</i>
CS—3.65	0.7 ± 0.1 <sup>d</sup>	0.4 ± 0.0 <sup>c</sup>	55.5 ± 3.1 <sup>ab</sup>	14.7 ± 0.8 <sup>c</sup>	0.2 ± 0.0 <sup>c</sup>	23.8 ± 2.3 <sup>c</sup>	4.1 ± 0.5	
CS—3.83	0.4 ± 0.0 <sup>e</sup>	0.2 ± 0.0 <sup>efg</sup>	55.7 ± 1.3 <sup>ab</sup>	11.2 ± 0.5 <sup>de</sup>	0.1 ± 0.0 <sup>d</sup>	22.4 ± 0.8 <sup>c</sup>	4.6 ± 1.2	
CS—3.97	0.2 ± 0.0 <sup>fg</sup>	0.1 ± 0.0 <sup>g</sup>	61.2 ± 1.1 <sup>a</sup>	6.4 ± 0.1 <sup>g</sup>	0.1 ± 0.0 <sup>d</sup>	19.9 ± 3.9 <sup>c</sup>	3.4 ± 0.2	
Raw MS	<i>3.0 ± 0.1<sup>b</sup></i>	<i>0.9 ± 0.0<sup>b</sup></i>	<i>38.6 ± 0.2<sup>c</sup></i>	<i>19.9 ± 0.4<sup>b</sup></i>	<i>0.3 ± 0.0<sup>b</sup></i>	<i>23.2 ± 0.2<sup>c</sup></i>	<i>2.2 ± 0.1</i>	<i>8.6 ± 0.3</i>
MS—3.65	0.6 ± 0.0 <sup>d</sup>	0.3 ± 0.0 <sup>cd</sup>	53.6 ± 2.6 <sup>b</sup>	11.3 ± 0.4 <sup>d</sup>	0.3 ± 0.0 <sup>b</sup>	32.5 ± 2.1 <sup>ab</sup>	1.1 ± 0.0	
MS—3.83	0.4 ± 0.0 <sup>e</sup>	0.2 ± 0.0 <sup>de</sup>	54.7 ± 2.8 <sup>b</sup>	7.8 ± 0.6 <sup>f</sup>	0.3 ± 0.0 <sup>b</sup>	32.2 ± 0.5 <sup>ab</sup>	1.5 ± 0.0	
MS—3.97	0.2 ± 0.0 <sup>fg</sup>	0.2 ± 0.0 <sup>ef</sup>	55.9 ± 2.1 <sup>ab</sup>	4.5 ± 0.2 <sup>h</sup>	0.3 ± 0.0 <sup>b</sup>	35.6 ± 0.3 <sup>a</sup>	1.6 ± 0.0	
Raw WS	<i>2.8 ± 0.0<sup>c</sup></i>	<i>0.9 ± 0.0<sup>b</sup></i>	<i>41.3 ± 0.2<sup>c</sup></i>	<i>24.9 ± 0.7<sup>a</sup></i>	<i>0.5 ± 0.0<sup>a</sup></i>	<i>21.4 ± 0.2<sup>c</sup></i>	<i>1.3 ± 0.0</i>	<i>10.6 ± 0.3</i>
WS—3.65	0.7 ± 0.0 <sup>d</sup>	0.3 ± 0.0 <sup>cd</sup>	54.8 ± 0.6 <sup>ab</sup>	14.7 ± 0.0 <sup>c</sup>	0.5 ± 0.0 <sup>a</sup>	29.3 ± 0.7 <sup>b</sup>	1.4 ± 0.1	
WS—3.83	0.3 ± 0.0 <sup>f</sup>	0.2 ± 0.0 <sup>def</sup>	58.2 ± 4.7 <sup>ab</sup>	9.8 ± 0.4 <sup>e</sup>	0.5 ± 0.0 <sup>a</sup>	30.8 ± 0.7 <sup>b</sup>	1.1 ± 0.2	
WS—3.97	0.1 ± 0.0 <sup>g</sup>	0.1 ± 0.0 <sup>fg</sup>	61.2 ± 2.5 <sup>a</sup>	6.5 ± 0.2 <sup>g</sup>	0.5 ± 0.0 <sup>a</sup>	30.3 ± 1.1 <sup>b</sup>	1.0 ± 0.1	

Data in italics are for untreated (raw) biomass samples

Results are average and standard deviation of triplicate measurements

Different letters indicate significant statistical difference based on ANOVA ( $P \leq 0.05$ )

CS, corn stover; MS, *Miscanthus × giganteus* stalks; WS, wheat straw

<sup>1</sup> Based on acid insoluble lignin (AIL) and acid soluble lignin (ASL) contents

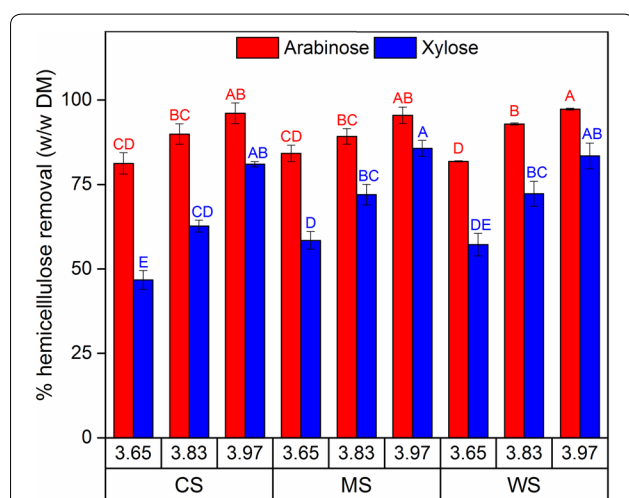


**Fig. 1** Removal of arabinose (red) and xylose (blue) relative to the untreated biomass for corn stover (CS), *Miscanthus × giganteus* stalks (MS), and wheat straw (WS) at different severity factors ( $\log R_0$ ). Data points represent average  $\pm$  standard deviation from three technical replicates. Different letters indicate significant statistical difference based on ANOVA ( $p \leq 0.05$ )

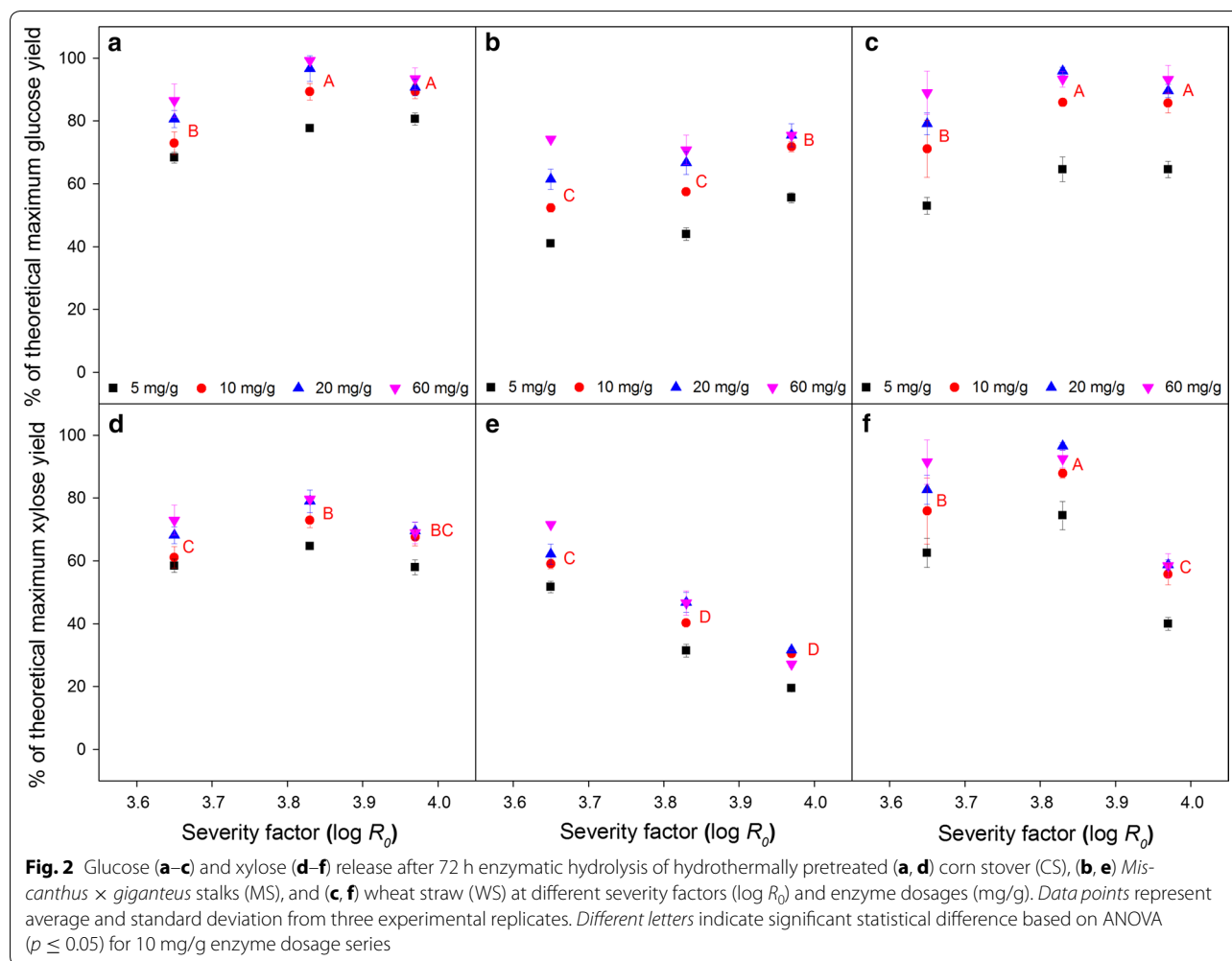
The extent of xylose removal was similar to that reported previously for corn stover [19] and wheat straw [31, 32] given the same range of severity factor.

### Enzymatic degradation

The digestibility of the three types of biomass feedstock differed in terms of glucose release after enzymatic cellulase treatment. Corn stover (CS) and wheat straw (WS)

were more digestible than *Miscanthus × giganteus* stalks (MS) as shown by a glucose release of up to 93% of maximum theoretical at the highest severity ( $\log R_0 = 3.97$ ) and enzyme dosage (60 mg protein/g biomass) tested. The corresponding value for MS was 75% (Fig. 2a–c). At other corresponding severities and enzyme dosages, the extents of glucose release from MS were also consistently lower compared to CS and WS. The three biomass feedstocks also responded differently to pretreatment severity and enzyme dosage. CS and WS were less affected by pretreatment severity as the glucose release seemed to be leveling off at  $\log R_0 = 3.83$  and 3.97; whereas in the case of MS, there was a slight tendency of increase. In terms of enzyme dosage, CS was the least responsive of the three biomass feedstocks. For CS, the increment of glucose release when increasing enzyme dosage from 5 to 60 mg protein/g DM biomass varied from 16 to 28% across the three severity levels. For MS and WS, the increments were 36–81 and 44–68%, respectively (Fig. 2a–c). Altogether, the results for glucose release revealed that MS is more recalcitrant than CS and WS. MS therefore needs higher severity pretreatment and higher enzyme dosage to obtain high cellulose conversion.

Except for corn stover, the xylose release from the pretreated biomass feedstocks tended to decrease as pretreatment severity increased, but not consistently statistically significant (Fig. 2d–f). This trend of xylose release has been observed previously for both corn stover [33] and ensiled wheat straw [31] hydrothermally pretreated at different severities. In the case of MS, the extent of xylose



release was lower than for CS and WS, particularly evident at the higher severities  $\log R_0 > 3.65$ , where the extent of xylose release achieved with the highest enzyme dosage (60 mg protein/g DM biomass) was lower than the corresponding value for CS and WS with the lowest dosage (5 mg protein/g DM biomass) (Fig. 2d–f).

To our knowledge, the apparent higher recalcitrance of MS compared to CS and WS after HTP has not been reported previously, partly due to limited number of studies comparing all three biomasses. One study comparing total hemicellulose removal during combined steam explosion and dilute sulfuric acid pretreatment found that the obtained yield for MS was slightly lower compared to wheat straw [34]. Furthermore, it took higher severity level for MS to reach the maximal yield as opposed to wheat straw [34]. However, since variation among genotypes/cultivars of *Miscanthus* [35] and wheat [22], which affects the release of sugars after HTP and enzymatic hydrolysis of the stalks/straws has been

reported, conclusions on their inherent species-related recalcitrance are not necessarily universal. The increment of xylose release (Fig. 2d–f) with increased enzyme dosage (from 5 up to 60 mg protein/g DM biomass) for each severity level varied less (19–25, 39–63, and 24–47% for CS, MS, and WS, respectively) than the corresponding glucose release (Fig. 2a–c). The data indicate that the hemicellulose remaining after increased severity pretreatment was less susceptible to the enzymes. One possible factor limiting the susceptibility of xylan to enzymes is the degree of arabinose substitution, but acetylation and diferulate cross-links may also hinder the action of xylanolytic enzymes [36]. The substitutions can persist even after pretreatment; pointing to the fact that addition of accessory enzymes such as acetyl xylan esterase [37] and arabinofuranosidases [38] may be needed to further improve the enzymatic hydrolysis. 2D NMR and CoMPP were performed to investigate the decorations of hemicellulose in the biomasses.

## 2D Nuclear magnetic resonance (NMR)

$^{13}\text{C}$ - $^1\text{H}$  HSQC (Heteronuclear single quantum coherence) spectra (Additional file 1: Figures S1–S12) were used for data analysis. The lowest contour peak integration values showed substantial reduction of acetylated positions (2-*O*-Ac- $\beta$ -D-Xylp and 3-*O*-Ac- $\beta$ -D-Xylp) in the fiber fraction of biomasses as a result of HTP. The values decreased as the pretreatment severity increased (Table 2). This is in accordance with previous observations showing that acetylated groups are cleaved during HTP [10, 39]. The results also indicated that acetyl groups once belonging to the hemicellulose moieties of MS and WS were removed substantially to the same extent. However, the values for CS were not able to be processed since the phenylcoumaran structure (Additional file 1: Figure S13) used as reference was not present [40] (Additional file 1: Figures S1–S4). For WS, a substantial reduction of uronic acid (4-*O*-methyl glucuronosyl) was observed after HTP and increased severity (Table 2). Even though the presence of 4-*O*-methyl glucuronosyl residues in arabinoxylans is known to be prominent in the vegetative parts of grasses [41], it was not detected for MS.

### Comprehensive microarray polymer profiling (CoMPP)

CoMPP analysis was performed to infer whether there are particular structural polysaccharides that are more preferentially removed in some biomasses compared to others, thus possibly explaining the contribution towards recalcitrance. Based on several models of cell walls in grasses [42–44], the cellulose microfibrils can be covered and/or tethered by structures like arabinoxylan (AX), mixed linked glucan (MLG), and xyloglucan (XG). The signals derived from antibodies binding to MLG, xylan, and AX (LM10 and LM11) had high intensity in all of the untreated biomass and they dropped significantly after pretreatment (Fig. 3). The effect seemed to correlate with the applied severity and the observed hemicellulose removal (Fig. 1). LM10 is known to preferably bind to unsubstituted or low-substituted xylans, whereas LM11 binds to arabinoxylan as well as unsubstituted xylan [45, 46]. This is in accordance with the observed significant

removal of arabinose and xylose after HTP (Fig. 1). The signals derived from binding of LM23, on the other hand, were increased after HTP for all biomass feedstocks (Fig. 3). Since LM23 is known to bind to unsubstituted and non-acetylated xylans [47], the increase of signals can be expected to happen due to removal of acetyl groups. This is in accordance with the 2D NMR observation of decreased acetylation (Table 2).

The signals derived from antibodies binding to xyloglucans (LM15 and LM25) and mannans (LM21 and BS-400-4) remained relatively stable after HTP, which was in agreement with the mannan content (Table 1). In general, the findings are also in agreement with previous results on wheat straw [44] in which XG and mannans were suggested to be bound more tightly to the microfibrils in the cell wall matrix. On the contrary, MLG and AX were found to be rather loosely bound in the cell wall matrix, shielding the cellulose microfibrils from enzymatic attack until released after pretreatment [44, 48]. The CoMPP results thus revealed that these changes in plant cell wall structural polysaccharides composition, which was previously observed only in WS [44, 48], also applied to CS and MS. Regardless of this, the quantitative composition data coupled with the CoMPP and 2D NMR indicated that hemicellulose decoration or substitution was likely not the factor conferring higher recalcitrance in MS compared to CS and WS.

### Wettability of biomass

Since even detailed chemical assessment of the bulk biomass did not fully explain the observed differences in enzymatic digestibility in response to different pretreatment severities and notably between the different feedstocks, we hypothesized that surface hydrophobicity might play a role, and in turn that assessment of physical properties of the biomass surface might provide quantitative clues to explain the observed differences in biomass digestibility. Interaction between biomass and water as shown using NMR analysis [49] and water retention value [25, 26] has been found to correlate well with cellulose accessibility, adsorption of cellulases, and biomass digestibility.

**Table 2**  $^{13}\text{C}$ - $^1\text{H}$  HSQC NMR contour integration values for acetylated xylosyl and uronic acid relative to phenylcoumaran- $\alpha$

Structure	MS				WS			
	Raw	3.65	3.83	3.97	Raw	3.65	3.83	3.97
Phenylcoumaran- $\alpha$	1	1	1	1	1	1	1	1
2- <i>O</i> -Ac- $\beta$ -D-Xylp	38.38	9.99	5.45	3.60	31.26	8.74	4.92	2.38
3- <i>O</i> -Ac- $\beta$ -D-Xylp	20.76	9.20	5.42	3.10	27.56	10.36	5.41	2.58
4- <i>O</i> -MeGlcA	<sup>a</sup>	<sup>a</sup>	<sup>a</sup>	<sup>a</sup>	4.32	1.40	0.73	0.07

2-*O*-Ac- $\beta$ -D-Xylp and 3-*O*-Ac- $\beta$ -D-Xylp: acetylated xylosyl

4-*O*-MeGlcA: uronic acid

<sup>a</sup> Peaks were too small for accurate determination

Antibodies	(1,3)-(1,4)- $\beta$ -D-glucan	(1,4)- $\beta$ -D-xylan (unsubstituted or low-substituted)	(1,4)- $\beta$ -D-xylan /arabinoxylan	(1,4)- $\beta$ -D-xylan (unsubstituted and non-acetylated)	Xyloglucan (unsubstituted)	Xyloglucan (galactosylated)	(1,4)- $\beta$ -D-mannan /galactomannan /glucomannan	(1,4)- $\beta$ -D-mannan /galactomannan
	BS-400-3	LM10	LM11	LM23	LM15	LM25	LM21	BS-400-4
Raw CS	100	57	91	0	13	31	0	5
CS - 3.65	67	33	40	13	22	24	0	6
CS - 3.83	49	24	27	12	23	21	0	7
CS - 3.97	24	25	27	11	16	19	0	0
Raw MS	74	52	95	0	13	23	11	30
MS - 3.65	24	21	27	10	14	18	0	11
MS - 3.83	22	28	36	17	21	27	6	23
MS - 3.97	10	26	29	15	14	22	0	15
Raw WS	74	60	99	0	25	43	16	35
WS - 3.65	67	30	41	23	25	26	7	19
WS - 3.83	39	31	37	23	21	24	0	14
WS - 3.97	21	28	31	16	22	23	0	11

**Fig. 3** CoMPP results for untreated (raw) and hydrothermally pretreated corn stover (CS), *Miscanthus × giganteus* stalks (MS), and wheat straw (WS) at different severity factors ( $\log R_p$ ) after extraction with CDTA and 4 M NaOH in 0.1% (w/v)  $\text{NaBH}_4$

Biomass–water interaction can also be evaluated using water contact angle measurement (CAM), which depicts the wettability of the solids' surface through relative measurement of surface hydrophobicity. The higher the contact angle, the more hydrophobic the surface of the material is, and the lower wettability it has [50, 51]. Measurement of the initial (instantaneous) water contact angle of milled biomass particles pressed into a tablet showed significantly lower initial water contact angles of the hydrothermally pretreated biomass materials compared to the raw materials for all three Poaceae biomasses (Fig. 4a). This is in accordance with previous studies that found the reduction of initial water contact angle after steam explosion and organosolv treatment of wheat straw [28], after autohydrolysis of poplar wood chips [52], as well as after chemical and enzymatic treatments of wheat straw [53].

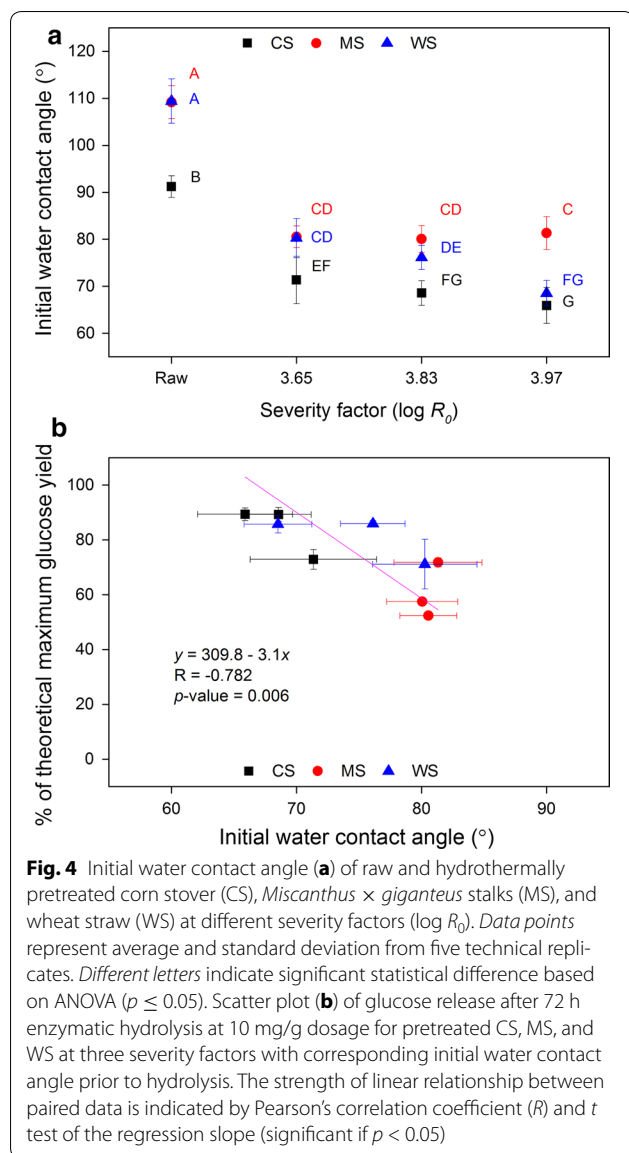
In general, the initial water contact angle had a negative correlation ( $R = -0.782$ ;  $p = 0.006$ ) with the glucose release after 72 h at 10 mg protein/g DM biomass dosage (Fig. 4b). However, this negative correlation was more pronounced for CS and WS than for MS (the contact angle values for MS after HTP varied less in response to increased pretreatment severity than those for CS and WS) (Fig. 4a, b). Furthermore, the initial water contact angle values after HTP were lower for CS and WS

compared to the MS values (Fig. 4a), which correlated negatively to the overall observed higher glucose (Fig. 2a–c) and xylose (Fig. 2d–f) release across severities for CS and WS compared to MS. Wettability assessment using contact angle measurement has been shown previously to correlate negatively with hydrolysis rate and digestibility of pure cellulose [51, 54] as well as adsorption of cellulases onto pretreated wheat straw samples [28]. The results obtained here appear to distinguish MS from the other biomass feedstocks CS and WS. As the initial water contact angle assesses the chemical and/or physical properties of the surface of biomass materials, the data suggest that differences in surface properties of pretreated *Miscanthus × giganteus* stalks rather than bulk chemical composition traits play a role in the observed higher recalcitrance of MS when compared to the recalcitrance of CS and WS. Additionally, these observations also indicated that assessment of surface wettability may be able to predict biomass digestibility across different hydrothermally pretreated feedstocks.

#### Attenuated total reflectance-Fourier transform infrared (ATR-FTIR) spectroscopy

Similar to the CAM, ATR-FTIR reflects the chemical composition of the surface (estimated penetration depth





of 0.57–1.85  $\mu\text{m}$ ) of the milled biomass samples. Therefore, it is likely that ATR-FTIR data (Additional file 1: Figures S14–S16) can reveal information about chemical and/or physical features causing the change in observed wettability and hence digestibility. The ATR-FTIR results revealed significant differences that again distinguished MS significantly from CS and WS. Based on the hemicellulose/holocellulose peak area ratio (1732/895  $\text{cm}^{-1}$ ) (Fig. 5a), MS initially had the highest apparent surface abundance of hemicellulose relative to holocellulose (ASA-H/C) compared to the corresponding untreated (raw) CS and WS samples. After HTP, the ASA-H/C levels decreased as the severity increased for all three Poaceae biomass feedstocks; a result which is in line with the hemicellulose (arabinose and xylose) removal

observed through composition analysis (Fig. 1). However, for each pretreatment severity level, the values of ASA-H/C were consistently higher in MS compared to CS and WS (Fig. 5a). CS had the lowest ASA-H/C among the three feedstocks, which might imply why it had higher overall digestibility (glucose release) relative to the others (Fig. 2a–c). This difference among the materials was not apparent based on the composition analysis, which yielded similar hemicellulose content for all three biomass feedstocks at each corresponding severity factor (Table 1). Accordingly, the digestibility of biomass correlated strongly and negatively to ASA-H/C; a correlation which was not evident from bulk hemicellulose (arabino-/xylan) composition or hemicellulose (arabinose and xylose) removal after pretreatment (Table 3; Additional file 1: Figures S17, S21, S23).

It is also noteworthy that the surface hemicellulose content (ASA-H/C) had a strong positive correlation with the initial water contact angle (negative with respect to wettability) (Table 3; Additional file 1: Figure S24). This indicated that hemicellulose plays a role in preventing the enzymatic cellulose depolymerization. This can be either by shielding cellulose for enzymatic attack via sterical hindrance or indirectly using other mechanisms. However, the correlation with wettability was not evident when bulk hemicellulose (arabino-/xylan) composition and hemicellulose (arabinose and xylose) removal were considered (Table 3; Additional file 1: Figures S28, S30). Treatment of wheat straw with sodium hydroxide and xylanase which removed hemicellulose was previously reported to reduce the water contact angle, but the correlation to enzymatic cellulose digestibility was not examined [53]. In this study, cellulose digestibility increased after HTP in response to increased severity (Fig. 2a–c) and had negative correlation with the initial water contact angle (positive with respect to wettability) (Fig. 4b). Accordingly, both cellulose digestibility (glucose release) and initial water contact angle (wettability) correlated well with bulk cellulose (glucan) content (Table 3; Additional file 1: Figures S20, S27).

The hydrothermal pretreatment preferentially removes the highly branched hydrophilic hemicellulose moieties thus presumably contributing to reduced digestibility due to reduction of hydrophilicity [55]. It is thus tempting to infer that the residual hemicellulose may not be hydrophilic and actually may adhere strongly to cellulose. In this study, composition analysis (Fig. 1), NMR (Table 2) and CoMPP (Fig. 3) showed major removal of hemicellulose substitutions. Accordingly, hemicellulose with less substitution adsorbed stronger to cellulose compared to more substituted hemicellulose which further provides recalcitrance [56, 57]. Therefore, semi-quantitative assessment of surface hemicellulose and wettability

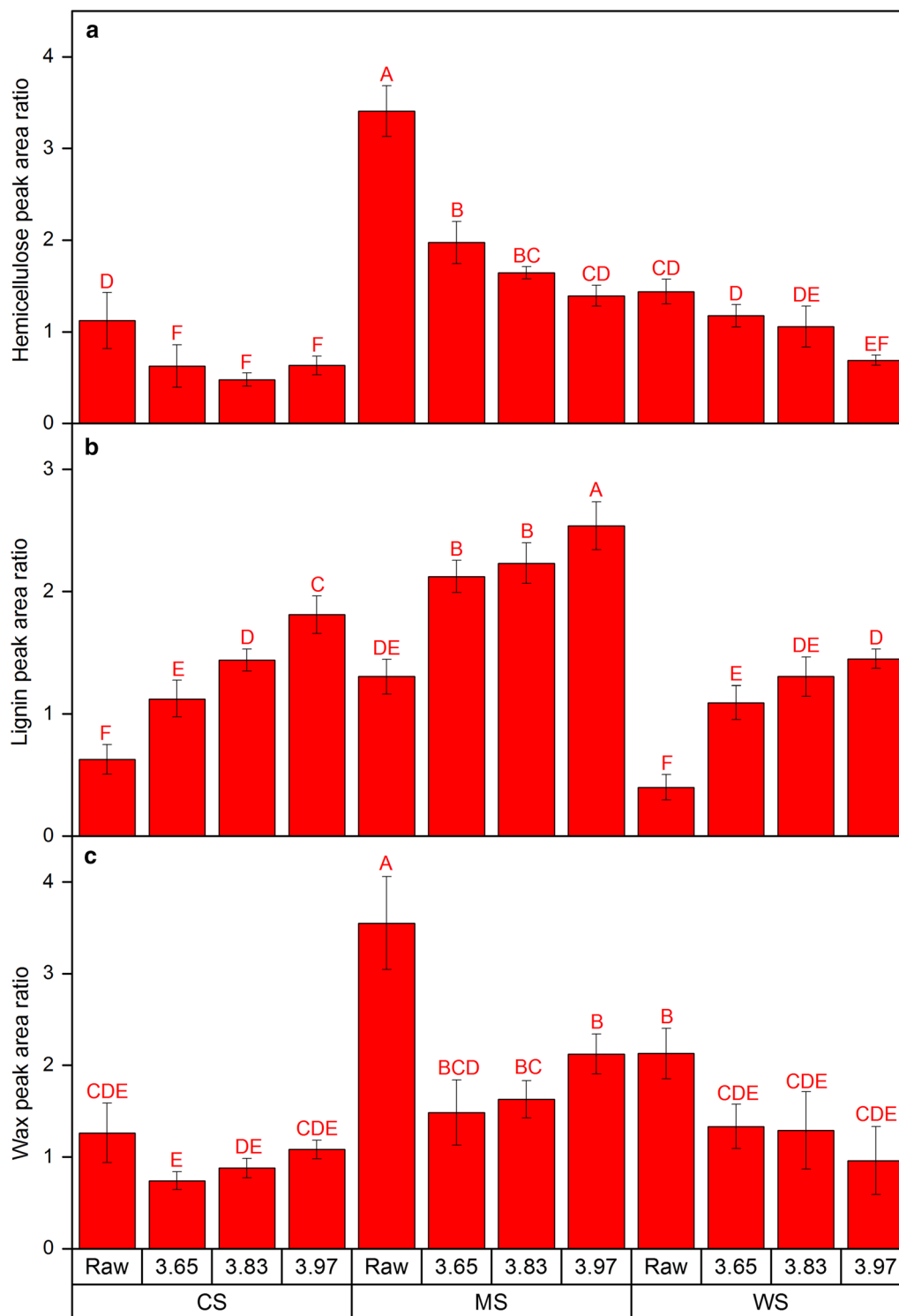


**Fig. 5** ATR-FTIR peak area ratio of wavenumbers representing **a** hemicellulose ( $1732\text{ cm}^{-1}$ ), **b** lignin ( $1508\text{ cm}^{-1}$ ), and **c** wax ( $2918\text{ cm}^{-1}$ ) each relative to that of holocellulose ( $895\text{ cm}^{-1}$ ) for raw and hydrothermally pretreated corn stover (CS), *Miscanthus x giganteus* stalks (MS), and wheat straw (WS) at different severity factors ( $\log R_0$ ). Data points represent average and standard deviation from five technical replicates. Different letters indicate significant statistical difference based on ANOVA ( $p \leq 0.05$ )

**Table 3** Linear regression parameters of surface and bulk composition with digestibility and wettability of pretreated biomass

Parameters	% of theoretical maximum glucose yield <sup>a</sup>					Initial water contact angle (°)				
	t test of regression <sup>b</sup>		Pearson's correlation			t test of regression <sup>b</sup>		Pearson's correlation		
	p value	Trend	R	Trend	p value	Trend	R	Trend		
Surface <sup>c</sup>	Hemicellulose	<0.001	Strong	-0.883	Strong negative relationship	0.003	Strong	0.876	Strong positive relationship	
	Lignin	0.034	Weak	-0.477	Possible negative relationship	0.076	None	0.431	No significant relationship	
	Wax	0.081	None	-0.521	Possible negative relationship	0.007	Strong	0.801	Strong positive relationship	
Bulk <sup>d</sup>	Cellulose	0.025	Weak	0.760	Strong positive relationship	0.018	Weak	-0.723	Strong negative relationship	
	Hemicellulose	0.086	None	-0.215	No significant relationship	0.652	None	0.104	No significant relationship	
	Lignin	0.044	Weak	-0.586	Possible negative relationship	0.008	Strong	0.829	Strong positive relationship	
	Hemicellulose removal	0.072	None	0.347	No significant relationship	0.427	None	-0.136	No significant relationship	

<sup>a</sup> Based on glucose release after 72 h enzymatic hydrolysis at 10 mg/g dosage

<sup>b</sup> t test of the regression slope is significant if p value <0.05

<sup>c</sup> Based on ATR-FTIR data (peak area ratio relative to holocellulose)

<sup>d</sup> Based on composition analysis data (% w/w DM) for glucan (cellulose), arabino-/xylo- (hemicellulose), lignin (AIL and ASL), and arabinose + xylose (hemicellulose) removal

may predict recalcitrance of pretreated biomass materials. Based on the lignin/holocellulose peak area ratio ( $1508/895\text{ cm}^{-1}$ ), the apparent surface abundance of lignin relative to holocellulose (ASA-L/C) showed a general trend of increase after HTP in response to increasing severity factor (Fig. 5b). Regardless of this, when comparing the data across all three biomasses, both bulk and surface lignin only had a weak possible negative correlation ( $R \approx -0.5$ ;  $p \approx 0.05$ ) with digestibility (Table 3; Additional file 1: Figures S18, S22). It is important to note, however, that unlike the significant increase in ASA-L/C (Fig. 5b), the bulk lignin content for each biomass did not vary across the HTP severity levels (Table 1).

The deposition of lignin in the surface of biomass after dilute acid and hydrothermal pretreatment as seen by microscopic observations [6, 13, 14] was indeed thought to improve enzymatic hydrolysis by providing access to cellulose microfibrils [6, 13]. Later work, however, indicated that during the later stages of enzymatic hydrolysis of hydrothermally pretreated biomass, the lignin droplets accumulated and retarded the glucose release [58]. This is especially true since the droplets have also been found to be inhibitory towards enzymatic hydrolysis [14, 15]. Furthermore, at higher pretreatment severity, the extent of lignin redistribution can be more pronounced [59]. The data obtained thus indicated that within each individual type of biomass, the redistribution of lignin after hydrothermal pretreatment *increased* the lignin abundance at the surface (ASA-L/C) of each biomass with increased pretreatment severity (Fig. 5b). This increased ASA-L/C

correlated *positively* to increased glucose release as the pretreatment severity was increased for each biomass (Fig. 2a–c). In contrast, when assessing the ASA-L/C versus glucose release across all three biomasses and across all pretreatments, the correlation changed to become *negative*, and the MS data dominated the model because the overall low glucose release was connected to the highest ASA-L/C values in the dataset (Fig. 5b). Taken together with the data for hemicellulose (Table 3) and contemplating the available knowledge [6, 13, 14, 58, 59], this paradox, i.e., that lignin abundance at the biomass surface (ASA-L/C) correlated *positively* to cellulose digestibility (and pretreatment severity) when each of the biomasses were assessed individually (Fig. 5b), but *negatively* when all three biomasses were compared (across all three severities) (Table 3), led to a suggestion that the positive correlation found between ASA-L/C and cellulose digestibility for the individual biomasses in this study is an artifact. This artifact may be a result of the elevated ASA-L/C with increased pretreatment severity being accompanied by a presumed more significant improvement in cellulose digestibility resulting directly from the effect of hydrothermal pretreatment on the biomass material with increased pretreatment severity in each individual biomass.

Weighing the effect of lignin towards inhibition of cellulose hydrolysis has been difficult to measure since it both obstructs the enzymes and non-productively adsorbs them which has led to different interpretations [16–18]. Studying the inhibitory effect of lignin usually

requires an isolation step, which can change the properties of lignin, and this also moves the investigation away from the actual plant cell wall surface, thus removing relevant structural and spatial arrangements. Moreover, the inhibitory effect of isolated lignin to cellulases can also depend on biomass. In softwood (spruce), lignin was reported to be inhibitory [60], whereas in grasses (corn stover and wheat straw) no inhibitory effect was reported [61]. Furthermore the role of lignin as steric hindrance is also known to be affected by the presence of hemicellulose since the direct relationship between lignin redistribution/removal and biomass digestibility was only present when it was coupled to hemicellulose removal [62–64].

Concerning wettability, bulk lignin had a strong positive relation with initial water contact angle (negative with respect to wettability), whereas the surface lignin content did not have it (Table 3; Additional file 1: Figures S25, S29). The bulk composition represents physical existence of lignin, which is generally regarded as hydrophobic. Thus, samples with higher lignin content will have higher initial contact angle as previously reported [28]. However, it is worth noticing again that the bulk lignin content for each biomass did not vary across the HTP severity levels (Table 1), whereas there was a constant trend of increase in ASA-L/C (Fig. 5b). As the ASA-L/C increased, the wettability decreased (increased initial water contact angle) for CS and WS, whereas the wettability remained constant in MS along with increased ASA-L/C (Fig. 4a). This indicates that the relationship between surface lignin and wettability can potentially be strongly negative in some biomass, but not the others. MS indeed had higher ASA-L/C compared to CS and WS already when it had not been pretreated and it increased to even higher extent than the others for each corresponding severity levels.

ATR-FTIR data therefore revealed higher extent of both the original lignin surface distribution and the lignin redistribution (or rather aptly termed resurfacing) after HTP in MS compared to CS and WS which was not apparent using bulk lignin content (Table 1). This correlated negatively with the overall observed lower glucose (Fig. 2a–c) and xylose (Fig. 2d–f) release in MS compared to CS and WS after enzymatic hydrolysis. Investigating the effect of lignin towards wettability might require separate focused studies since other components in biomass can also affect the overall surface properties. Using simulation with molecular theory of solvation, it was shown that lignin and hemicellulose form supramolecular assembly with hydrophobic interaction, which covers cellulose microfibril and expels water from it, thus contributing to recalcitrance altogether [65]. Another simulation

study with molecular probes also showed the access of water to cavities in plant cell wall matrix improved after hemicellulose is hydrolyzed and separated from lignin [66].

The wax content has been rarely highlighted in published reports even though it has been considered as one of the structural factors that contributes to lignocellulosic biomass recalcitrance [67]. Correspondingly, wax removal using supercritical CO<sub>2</sub> on *Miscanthus × giganteus* stalks [68] as well as hydrothermal pretreatment [6] and plasma-assisted pretreatment [69] on wheat straw have been shown to correlate with improved hydrolysis yield. Based on the wax/holocellulose peak area ratio (2918/895 cm<sup>-1</sup>), the apparent surface abundance of wax relative to holocellulose (ASA-W/C) decreased significantly after pretreatment, but the level remained relatively stable irrespective of severity (Fig. 5c). Even though it had no strong correlation with digestibility (Table 3; Additional file 1: Figure S19) as with other ATR-FTIR data it also displayed differences among the tested feedstocks. In general, MS had higher ASA-W/C compared to CS and WS for each corresponding severity level. These findings correlated with the overall glucose (Fig. 2a–c) and xylose (Fig. 2d–f) release, which showed that MS was the least digestible. The ASA-W/C had strong positive correlation with the wettability (Table 3; Additional file 1: Figure S26) which can be expected due to its hydrophobic nature and the observation of its removal after extraction [28]. Nevertheless, it was not the only factor affecting wettability after pretreatment since the trend of increase in wettability (decrease of initial water contact angle) was also observed in the materials that were previously solvent-extracted to remove wax [28].

Altogether, investigation of surface properties using ATR-FTIR and contact angle measurement showed that the wettability and hence the observed recalcitrance of biomass are the result of different multi-component interactions on the surface. Even though strong correlation across pretreated biomass feedstocks was seen in connection to surface hemicellulose, overall collective forces from other components, i.e., lignin and wax also pinpointed clues to the particular observed recalcitrance of *Miscanthus × giganteus* stalks used in this study. In order to fully understand the changes, future studies need to be directed to investigate the distribution of the different biomass components with respect to ultrastructural architecture of plant cell wall and to take into account changes in physical and/or structural factors. Systematic study focusing on different biomass components will be required to assess their interaction which might not always be linear.

## Conclusions

The study established that characterization of bulk biomass composition based on wet chemical methods cannot explain differences in enzymatic biomass digestibility in response to differences in pretreatment severity and notably cannot provide unequivocal clues to explain differences in enzymatic digestibility (recalcitrance to enzymatic digestion) among different types of lignocellulosic biomass feedstocks—even among three types of stalk or stover biomass. Methods characterizing physical and chemical features of the biomass surface were more successful, namely contact angle measurement (wettability) and attenuated total reflectance-Fourier transform infrared (ATR-FTIR) spectroscopy (surface biopolymer composition). Higher surface content of hemicellulose, lignin, and wax promoted lower wettability (as seen by higher contact angle) therefore restraining the transport of water and enzyme and thus decreasing digestibility. Consequently, to a large extent, factors related to surface physical and/or chemical properties rather than bulk chemical composition seem to determine recalcitrance of biomass feedstocks of the types studied here. This conclusion emphasizes the fact that since the first contact of enzymes with biomass material is on the surface; studying the interaction between biomass and enzymes also requires understanding of

Chornet [11]. Wheat straw was mixed with water and pre-conditioned in plastic bags over night at room temperature to obtain 40% dry matter (DM). Other biomass feedstocks were used directly due to high moisture content. After pretreatment, the biomass is pressed inside the reactor to obtain a solid fraction with around 35–40% DM and a liquid fraction. For each biomass and pretreatment condition, a minimum of three batches were done, each with a biomass loading of 1 kg DM. After pretreatment, the solid material from all three (or more) batches were mixed and then immediately frozen.

$$\log R_0 = \log \left[ t(\text{min}) \times \left( \frac{T(^{\circ}\text{C}) - 100}{14.75} \right) \right] \quad (1)$$

## Compositional analysis

Composition of biomass fiber fraction was determined using strong acid hydrolysis procedure [29]. Solvent extraction was performed on untreated biomass whereas the pretreated biomass feedstocks were washed with distilled water prior to strong acid hydrolysis.

The percentage removal of hemicellulose from the fiber fraction was determined by taking into account the chemical composition (i.e., content of arabinose and xylose calculated as dehydrated moieties) and the dry amount of biomass before and after pretreatment (Eq. 2):

$$\% \text{ removal} = \frac{\text{hemicellulose in raw biomass (g DM)} - \text{hemicellulose in pretreated biomass (g DM)}}{\text{hemicellulose in raw biomass (g DM)}} \times 100 \quad (2)$$

multi-component interactions on the surface level. The molecular mechanisms and quantitative enzymatic conversion rate kinetics underlying these variations in surface properties need to be investigated further in order to understand lignocellulosic biomass recalcitrance better as well as to develop approaches to overcome it.

## Methods

### Biomass feedstocks

Wheat straw (*Triticum aestivum* L.) (WS) and *Miscanthus × giganteus* stalks (MS) were harvested at Aarhus University (AU) Foulum in autumn 2014. Corn stover (*Zea mays* subsp. *mays* L.) (CS) was harvested at AU Jyndevad in autumn 2014. CS and MS were stored frozen due to high moisture content. WS was dried on the field and stored dry at room temperature.

### Pretreatment conditions

HTP was performed using the Mini-IBUS equipment (Technical University of Denmark, Risø Campus). The biomass feedstocks were used as provided—no further milling or drying. The details of materials and pretreatment conditions are listed in Table 4. The severity factor  $\log R_0$  (Eq. 1) is calculated according to Overend and

## Enzymatic hydrolysis

The pretreated biomass feedstocks were washed using distilled water prior to hydrolysis experiments and stored frozen until use. The washed pretreated biomass feedstocks were then homogenized in a blender BL-1200 (AS Wilfa, Skytta, Norway) for 3 min at medium setting with the corresponding buffer solution used in the hydrolysis

**Table 4** HTP conditions used

Biomass feedstock	Pretreatment conditions		
	Temperature (°C)	Time (min)	Severity factor ( $\log R_0$ )
CS	190	10	3.65
	190	15	3.83
	195	15	3.97
MS	190	10	3.65
	190	15	3.83
	195	15	3.97
WS	190	10	3.65
	190	15	3.83
	195	15	3.97

CS, corn stover; MS, *Miscanthus × giganteus* stalks; WS, wheat straw

experiment. The dry matter content of the slurry was adjusted to 1% DM based on measurement of DM (using a Moisture Content Analyzer HR83, Mettler Toledo GmbH, Greifensee, Switzerland). The slurry was always prepared fresh for every experiment.

Enzymatic hydrolysis of pretreated biomass feedstocks was performed in triplicates at 1% DM in 0.05 M acetate buffer pH 5.0 at 50 °C with Cellic<sup>®</sup> CTec3 (Novozymes A/S, Bagsværd, Denmark). The hydrolysis experiment was carried out in 2 ml Protein LoBind<sup>®</sup> tubes (Eppendorf AG, Hamburg, Germany) and agitated with vortex mixing at 1250 RPM using ThermoMixer Comfort (Eppendorf AG, Hamburg, Germany). Dosage response curve experiments were performed at a constant duration of 72 h with enzyme dosage of 5, 10, 20, and 60 mg protein/g DM biomass. Reactions were halted by boiling samples for 10 min. After centrifugation, reaction mixture supernatants were analyzed for monosaccharides and corrected with biomass and enzyme blanks as reference.

#### Analysis of monosaccharides

Monosaccharides were quantified by high performance anion exchange chromatography with pulsed amperometric detection (HPAEC-PAD) using a Dionex ICS-5000 system (Dionex Corp, Sunnyvale, CA, USA) equipped with a CarboPac PA1 analytical column (250 × 4 mm) and a CarboPac PA1 guard column (250 × 4 mm) operated at a flow rate of 1 ml/min. Isocratic elution took place at 25 °C, with water, for 30 min. The column was then washed for 10 min with 500 mM NaOH and equilibrated with water for 10 min. Detection was done by post-column addition of 500 mM NaOH at 0.2 ml/min. Standards of D-glucose, D-xylose, L-arabinose, D-galactose, and D-mannose were used for quantification.

#### 2D Nuclear magnetic resonance (NMR)

Untreated and fiber fraction of pretreated biomass feedstocks was prepared in DMSO-d<sub>6</sub>/pyridine-d<sub>5</sub> (4:1, v/v) according to a protocol for whole plant cell wall characterization [40]. Heteronuclear single quantum coherence (HSQC) experiments of samples were performed using a 600 MHz Avance III HD (Bruker, Billerica, MA, USA) equipped with a cryogenically cooled 5 mm dual probe optimized for <sup>13</sup>C and <sup>1</sup>H. For <sup>13</sup>C-<sup>1</sup>H HSQC NMR, 16 scans of the Bruker pulse sequence hsqcetpg was applied with a fixed spectral width of 220 ppm for <sup>13</sup>C and 13 ppm for <sup>1</sup>H. The NMR spectra were analyzed and processed using Bruker's Topspin 3.5 software. The central DMSO solvent peaks were used as internal reference ( $\delta_H/\delta_C = 2.50/39.50$ ). Peak assignment was done according to previously reported peaks [40] and contour volume integration was done at lowest contour level method.

#### Comprehensive microarray polymer profiling (CoMPP)

The procedure is performed based on previously established works [44, 48, 70]. Alcohol insoluble residue (AIR) was prepared from untreated and solid fraction of pretreated biomass feedstocks by freeze-drying and ball-milling. Milled tissue was washed five times in pre-warmed 70% v/v ethanol, shaking for 10 min and pelleted by centrifugation, followed by washing with acetone. For the CoMPP analysis, the liquid fractions of pretreated biomass feedstocks were used directly, while the solid fractions were sequentially extracted.

The extraction was performed first with 50 mM diamino-cyclohexanetetraacetic acid (CDTA) for predominant pectin extraction, then with alkaline 4 M NaOH in 0.1% (w/v) NaBH<sub>4</sub> that extracts mainly hemicelluloses. Both liquid and extracted samples were spotted using a microarray robot (Sprint, Arrayjet, Roslin, UK). Once printed, arrays were blocked with phosphate-buffered saline (PBS) containing 5% (w/v) low fat milk powder (MPBS). Arrays were washed with PBS and probed with antibodies (PlantProbes, Leeds University, UK) in 5% MPBS. The antibodies used were BS-400-3 that targets mixed linked glucan (MLG); LM10, LM11, and LM23 that target xylans; LM15 and LM25 that target xyloglucans; LM21 and BS-400-4 that target mannans [45, 46].

Subsequently, the arrays were washed in PBS and incubated with anti-rat secondary antibody conjugated to alkaline phosphatase (Sigma, St. Louis, USA) in 5% (w/v) MPBS 1/5000. Arrays were developed in a solution containing 5-bromo-4-chloro-3-indolylphosphate and nitro blue tetrazolium in alkaline phosphatase buffer (100 mM NaCl, 5 mM MgCl<sub>2</sub>, 100 mM diethanolamine, pH 9.5). Developed microarrays were scanned at 2400 dpi (CanoScan 8800 F, Canon, Søborg, Denmark) and converted to TIFFs. Antibody signals were measured using appropriate software (Array-Pro Analyzer 6.3, Media Cybernetics, Rockville, USA). Data were presented as two datasets where maximal spot signal was set to 100 and all other values normalized accordingly with color intensity is correlating with mean spot signal value.

#### Wettability test

Wettability of biomass feedstocks was assessed by measuring initial water contact angle according to Heiss-Blanquet et al. [28]. The untreated and pretreated biomass feedstocks were air-dried at room temperature and milled using a MF 10 microfine grinder (IKA<sup>®</sup> Werke GmbH & Co. KG, Staufen, Germany) to obtain particles that pass a 0.5 mm sieve. The milled biomass samples (2 g DM) were then pressed at tonnage load of 10 Mg for 5 min using an Atlas Manual 25 T Hydraulic Press (Specac Ltd., Kent, UK), yielding a tablet with diameter of 4 cm. Ultrapure water was used for the sessile drop method at controlled

**Table 5** ATR-FTIR assignments of wavenumbers used to measure peak area

Wavenumber (cm <sup>-1</sup> )	Assignment <sup>a</sup>	Estimated penetration depth <sup>a</sup> (μm)
895	Holocellulose Anomeric C-groups, C <sub>1</sub> -H deformation, ring valence vibration (cellulose, wood, holocellulose) [71]	1.85
1508	Lignin Aromatic skeletal vibrations [71, 72]	1.10
1732	Hemicellulose C=O stretch in unconjugated carbonyl groups of carbohydrate origin (side chain acetylation in mannan, carboxylic acid side chain in xylan, and ester groups in lignin-carbohydrate complexes) [71, 72]	0.96
2918	Wax Asymmetric CH <sub>2</sub> stretching from cuticular waxes [73]	0.57

<sup>a</sup> Calculated based on the formula (Eq. 3):

$$d_p = \frac{\lambda}{2\pi n_1 \sqrt{\sin^2 \theta - (n_2/n_1)^2}}, \quad (3)$$

where  $d_p$ ,  $\lambda$ ,  $\theta$ ,  $n_1$ , and  $n_2$  are penetration depth, wavelength, incident angle, ATR crystal refractive index, and sample refractive index, respectively. The values of  $\theta$  and  $n_1$  are known specifically to be 45° and 2.40, respectively, for diamond ATR. The refractive index of biomass samples is estimated to be 1.4 which is a common value for organic polymer, e.g., in wood cell wall [74]

working temperature of 22.0 °C using OCA 20 instrument (DataPhysics Instruments GmbH, Filderstadt, Germany). The water drop (15 μl) was deposited to the surface of the pellet using a computer-controlled syringe and the images were recorded at 2.5 frames per second. The images of drop shape were analyzed using SCA 20 software (DataPhysics Instruments GmbH, Filderstadt, Germany) to calculate the initial contact angle using Young–Laplace fitting mode. The wettability test was performed with five replicates for each tablet.

#### Attenuated total reflectance-Fourier transform infrared (ATR-FTIR) spectroscopy

Air-dried untreated and pretreated biomass feedstocks were milled using a MF 10 microfine grinder (IKA® Werke GmbH & Co. KG, Staufen, Germany) to obtain particles that passed 0.5 mm sieve. ATR-FTIR measurements were performed with five replicates using a Nicolet 6700 FT-IR, Pike Technologies GladiATR diamond spectrometer (Thermo Scientific, Waltham, MA, USA), with a working temperature of 25 °C. The spectral range included was 4000–600 cm<sup>-1</sup> and spectra were obtained using 64 scans (128 for the background) and a resolution of 4.0 cm<sup>-1</sup>. Peak areas were estimated based on the trapz algorithm as implemented in Matlab R2014A (The Mathworks Inc., Natick, MA, USA). Individual linear baselines were applied for each peak. The peaks included are listed in Table 5. In order to provide semi-quantitative analysis of the surface chemical composition, ratios of peak areas were calculated for 1508/895 cm<sup>-1</sup> corresponding to lignin/holocellulose, 1732/895 cm<sup>-1</sup> corresponding to hemicellulose/holocellulose and 2918/895 cm<sup>-1</sup> corresponding to wax/holocellulose. Therefore, the peak area ratios represent apparent surface abundance (ASA) of the corresponding components, i.e., apparent surface abundance of lignin relative to holocellulose (ASA-L/C), hemicellulose relative to holocellulose (ASA-H/C) and wax relative to holocellulose (ASA-W/C).

#### Statistical analysis

One-way analysis of variance (ANOVA) was performed using JMP 12 (SAS Institute Inc., Cary, NC, USA) with post hoc analysis using Tukey–Kramer's Honestly Significant Difference (HSD) test at  $p \leq 0.05$ . Least-squares linear regression analyses of the scatter plots were performed using OriginPro 2016 (OriginLab Corp., Northampton, MA, USA) using York linear fitting to account for errors in both  $x$ - and  $y$ -axes. The trend and significance of the relationship between the data were validated using Pearson's correlation coefficient ( $R$ ) and  $t$  test for the slope value where significant relationship is indicated by  $p$  value <0.05.

#### Additional file

**Additional file 1: Figures S1–S12.** <sup>13</sup>C-<sup>1</sup>H HSQC (heteronuclear single quantum coherence) spectra of untreated (raw) and hydrothermally pretreated (log  $R_0$  = 3.65, 3.83 and 3.97) corn stover, *Miscanthus × giganteus* stalks and wheat straw. **Figure S13.** Phenylcoumaran structure. **Figures S14–S16.** Selected ATR-FTIR spectra each representing sample from untreated (raw) and hydrothermally pretreated (log  $R_0$  = 3.65, 3.83 and 3.97) corn stover, *Miscanthus × giganteus* stalks and wheat straw. **Figures S17–S30.** Scatter plot of surface and bulk chemical composition with glucose release and wettability test of hydrothermally pretreated (log  $R_0$  = 3.65, 3.83 and 3.97) corn stover, *Miscanthus × giganteus* stalks and wheat straw.

#### Abbreviations

ANOVA: one-way analysis of variance; ASA-H/C: apparent surface abundance of hemicellulose relative to holocellulose; ASA-L/C: apparent surface abundance of lignin relative to holocellulose; ASA-W/C: apparent surface abundance of wax relative to holocellulose; ATR-FTIR: attenuated total reflectance-Fourier transform infrared (spectroscopy); AX: arabinoxylan; <sup>13</sup>C-<sup>1</sup>H HSQC: heteronuclear single quantum coherence (spectra); CAM: contact angle measurement; CoMPP: comprehensive microarray polymer profiling; CS: corn stover; DM: dry matter; HTP: hydrothermal pretreatment; MLG: mixed linked glucan; MS: *Miscanthus × giganteus* stalks; NMR: nuclear magnetic resonance; WS: wheat straw; XG: xyloglucan.

#### Authors' contributions

DTD, MP, AM, HJ planned the study, analyzed the results, and wrote the manuscript. DTD performed experiments, analyzed data, and drafted the

manuscript. ARH performed CoMPP and participated in CoMPP data analysis. AJ acquired 2D NMR spectra and participated in NMR data analysis. LGT participated in the analysis of ATR-FTIR spectra. HJ arranged the collection and pretreatment of biomass feedstocks. All authors read and approved the final manuscript.

#### Author details

<sup>1</sup> Department of Chemical and Biochemical Engineering, Technical University of Denmark, Søtofts Plads Building 229, 2800 Kongens Lyngby, Denmark.

<sup>2</sup> Present Address: Department of Plant and Environmental Sciences, University of Copenhagen, Thorvaldsensvej 40, 1871 Kongens Lyngby, Denmark.

<sup>3</sup> Department of Geosciences and Natural Resource Management, University of Copenhagen, Rolighedsvej 23, 1958 Frederiksberg C, Denmark.

#### Acknowledgements

Søren S. Pedersen is acknowledged for providing the biomass feedstocks. Thomas Fernqvist is acknowledged for the operation of the Mini-IBUS for biomass pretreatment. Danish Polymer Centre is acknowledged for providing access to contact angle measurement.

#### Competing interests

The authors declare that they have no competing interests.

#### Availability of data and materials

All data generated and analyzed during this study are included in the manuscript in form of graphs and tables.

#### Consent for publication

All authors agree to the submission.

#### Funding

This study was funded by the BioValue SPIR, Strategic Platform for Innovation and Research on value added products from biomass, which is co-funded by The Innovation Fund Denmark, Case No: 0603-00522B.

Received: 11 January 2017 Accepted: 10 February 2017

Published online: 23 February 2017

#### References

- Yang B, Wyman CE. Pretreatment: the key to unlocking low-cost cellulosic ethanol. *Biofuels Bioprod Bioref*. 2008;2:26–40.
- Sun S, Sun S, Cao X, Sun R. The role of pretreatment in improving the enzymatic hydrolysis of lignocellulosic materials. *Bioresour Technol*. 2016;199:49–58.
- Dominguez De María P, Grande PM, Leitner W. Current trends in pretreatment and fractionation of lignocellulose as reflected in industrial patent activities. *Chem-Ing-Tech*. 2015;87:1686–95.
- Larsen J, Haven MØ, Thirup L. Inbicon makes lignocellulosic ethanol a commercial reality. *Biomass Bioenergy*. 2012;46:36–45.
- Betarenewables website. <http://www.betarenewables.com/en>. Accessed 26 Oct 2016.
- Kristensen JB, Thygesen LG, Felby C, Jørgensen H, Elder T. Cell-wall structural changes in wheat straw pretreated for bioethanol production. *Biotechnol Biofuels*. 2008;1:5.
- Nitsos CK, Matis KA, Triantafyllidis KS. Optimization of hydrothermal pretreatment of lignocellulosic biomass in the bioethanol production process. *ChemSusChem*. 2013;6:110–22.
- Rasmussen H, Sørensen HR, Meyer AS. Formation of degradation compounds from lignocellulosic biomass in the biorefinery: sugar reaction mechanisms. *Carbohydr Res*. 2014;385:45–57.
- Pedersen M, Meyer AS. Lignocellulose pretreatment severity—relating pH to biomatrix opening. *New Biotechnol*. 2010;27:739–50.
- Ruiz HA, Rodríguez-Jasso RM, Fernandes BD, Vicente AA, Teixeira JA. Hydrothermal processing, as an alternative for upgrading agriculture residues and marine biomass according to the biorefinery concept: a review. *Renew Sust Energ Rev*. 2013;21:35–51.
- Overend RP, Chornet E. Fractionation of lignocellulosics by steam-aqueous pretreatments. *Philos T R Soc A*. 1987;321:523–36.
- Xiao X, Bian J, Li MF, Xu H, Xiao B, Sun R. Enhanced enzymatic hydrolysis of bamboo (*Dendrocalamus giganteus* Munro) culm by hydrothermal pretreatment. *Bioresour Technol*. 2014;159:41–7.
- Donohoe BS, Decker SR, Tucker MP, Himmel ME, Vinzant TB. Visualizing lignin coalescence and migration through maize cell walls following thermochemical pretreatment. *Biotechnol Bioeng*. 2008;101:913–25.
- Selig MJ, Viamajala S, Decker SR, Tucker MP, Himmel ME, Vinzant TB. Deposition of lignin droplets produced during dilute acid pretreatment of maize stems retards enzymatic hydrolysis of cellulose. *Biotechnol Prog*. 2007;23:1333–9.
- Li H, Pu Y, Kumar R, Ragauskas AJ, Wyman CE. Investigation of lignin deposition on cellulose during hydrothermal pretreatment, its effect on cellulose hydrolysis, and underlying mechanisms. *Biotechnol Bioeng*. 2014;111:485–92.
- Leu S-Y, Zhu JY. Substrate-related factors affecting enzymatic saccharification of lignocelluloses: our recent understanding. *Bioenerg Res*. 2013;6:405–15.
- Meng X, Ragauskas AJ. Recent advances in understanding the role of cellulose accessibility in enzymatic hydrolysis of lignocellulosic substrates. *Curr Opin Biotech*. 2014;27:150–8.
- Pihlajaniemi V, Sipponen MH, Liimatainen H, Sirviö JA, Nyssölä A, Laakso S. Weighing the factors behind enzymatic hydrolyzability of pretreated lignocellulose. *Green Chem*. 2016;18:1295–305.
- Yang B, Wyman CE. Effect of xylan and lignin removal by batch and flowthrough pretreatment on the enzymatic digestibility of corn stover cellulose. *Biotechnol Bioeng*. 2004;86:88–98.
- Kabel MA, Bos G, Zeevalking J, Voragen AGJ, Schols HA. Effect of pretreatment severity on xylan solubility and enzymatic breakdown of the remaining cellulose from wheat straw. *Bioresour Technol*. 2007;98:2034–42.
- Nitsos CK, Choli-Papadopoulou T, Matis KA, Triantafyllidis KS. Optimization of hydrothermal pretreatment of hardwood and softwood lignocellulosic residues for selective hemicellulose recovery and improved cellulose enzymatic hydrolysis. *ACS Sustain Chem Eng*. 2016;4:4529–44.
- Lindedam J, Andersen SB, DeMartini J, Bruun S, Jørgensen H, Felby C, Magid J, Yang B, Wyman CE. Cultivar variation and selection potential relevant to the production of cellulosic ethanol from wheat straw. *Biomass Bioenergy*. 2012;37:221–8.
- Zhang H, Fangel JU, Willats WGT, Selig MJ, Lindedam J, Jørgensen H, Felby C. Assessment of leaf/stem ratio in wheat straw feedstock and impact on enzymatic conversion. *GCB Bioenergy*. 2014;6:90–6.
- Zhang H, Thygesen LG, Mortensen K, Kádár Z, Lindedam J, Jørgensen H, Felby C. Structure and enzymatic accessibility of leaf and stem from wheat straw before and after hydrothermal pretreatment. *Biotechnol Biofuels*. 2014;7:74.
- Weiss ND, Thygesen LG, Felby C, Roslander C, Gourlay K. Biomass-water interactions correlate to recalcitrance and are intensified by pretreatment: an investigation of water constraint and retention in pretreated spruce using low field NMR and water retention value techniques. *Biotechnol Progr*. 2016. doi:10.1002/btpr.2398.
- Williams DL, Hodge DB. Impacts of delignification and hot water pretreatment on the water induced cell wall swelling behavior of grasses and its relation to cellulolytic enzyme hydrolysis and binding. *Cellulose*. 2014;21:221–35.
- Jeoh T, Ishizawa CI, Davis MF, Himmel ME, Adney WS, Johnson DK. Cellulase digestibility of pretreated biomass is limited by cellulose accessibility. *Biotechnol Bioeng*. 2007;98:112–22.
- Heiss-Blanquet S, Zheng D, Lopes Ferreira N, Lapiere C, Baumberger S. Effect of pretreatment and enzymatic hydrolysis of wheat straw on cell wall composition, hydrophobicity and cellulase adsorption. *Bioresour Technol*. 2011;102:5938–46.
- Sluiter A, Hames B, Ruiz R, Scarlata C, Sluiter J, Templeton D, Crocker D. Determination of structural carbohydrates and lignin in biomass. Laboratory Analytical Procedure (LAP). NREL/TP-510-42618. Golden; 2008.
- Chandra RP, Arantes V, Saddler J. Steam pretreatment of agricultural residues facilitates hemicellulose recovery while enhancing enzyme accessibility to cellulose. *Bioresour Technol*. 2015;185:302–7.
- Ambye-Jensen M, Thomsen S, Kádár Z, Meyer AS. Ensilage of wheat straw decreases the required temperature in hydrothermal pretreatment. *Biotechnol Biofuels*. 2013;6:116.
- Petersen MØ, Larsen J, Thomsen MH. Optimization of hydrothermal pretreatment of wheat straw for production of bioethanol at low



- water consumption without addition of chemicals. *Biomass Bioenergy*. 2009;33:834–40.
33. Zhang J, Viikari L. Impact of xylan on synergistic effects of xylanases and cellulases in enzymatic hydrolysis of lignocelluloses. *Appl Biochem Biotechnol*. 2014;174:1393–402.
  34. Kärcher MA, Iqbal Y, Lewandowski I, Senn T. Comparing the performance of *Miscanthus × giganteus* and wheat straw biomass in sulfuric acid based pretreatment. *Bioresour Technol*. 2015;180:360–4.
  35. Zhang T, Wyman CE, Jakob K, Yang B. Rapid selection and identification of *Miscanthus* genotypes with enhanced glucan and xylan yields from hydrothermal pretreatment followed by enzymatic hydrolysis. *Biotechnol Biofuels*. 2012;5:56.
  36. Meyer AS, Rosgaard L, Sørensen HR. The minimal enzyme cocktail concept for biomass processing. *J Cereal Sci*. 2009;50:337–44.
  37. Zhang J, Siika-aho M, Tenkanen M, Viikari L. The role of acetyl xylan esterase in the solubilization of xylan and enzymatic hydrolysis of wheat straw and giant reed. *Biotechnol Biofuels*. 2011;4:60.
  38. Gao D, Uppugundla N, Chundawat SP, Yu X, Hermanson S, Gowda K, Brumm P, Mead D, Balan V, Dale BE. Hemicellulases and auxiliary enzymes for improved conversion of lignocellulosic biomass to monosaccharides. *Biotechnol Biofuels*. 2011;4:5.
  39. Yelle DJ, Kaparaju P, Hunt CG, Hirsh K, Kim H, Ralph J, Felby C. Two-dimensional NMR evidence for cleavage of lignin and xylan substituents in wheat straw through hydrothermal pretreatment and enzymatic hydrolysis. *Bioenergy Res*. 2013;6:211–21.
  40. Mansfield SD, Kim H, Lu F, Ralph J. Whole plant cell wall characterization using solution-state 2D NMR. *Nat Protoc*. 2012;7:1579–89.
  41. Scheller HV, Ulvskov P. Hemicelluloses. *Annu Rev Plant Biol*. 2010;61:263–89.
  42. Buckeridge MS, Rayon C, Urbanowicz B, Tiné MAS, Carpita NC. Mixed linkage (1 → 3), (1 → 4)-β-D-glucans of grasses. *Cereal Chem*. 2004;81:115–27.
  43. Park YB, Cosgrove DJ. A revised architecture of primary cell walls based on biomechanical changes induced by substrate-specific endoglucanases. *Plant Physiol*. 2012;158:1933–43.
  44. Hansen MAT, Ahl LI, Pedersen HL, Westereng B, Willats WGT, Jørgensen H, Felby C. Extractability and digestibility of plant cell wall polysaccharides during hydrothermal and enzymatic degradation of wheat straw (*Triticum aestivum* L.). *Ind Crop Prod*. 2014;55:63–9.
  45. McCartney L, Marcus SE, Knox JP. Monoclonal antibodies to plant cell wall xylans and arabinoxylans. *J Histochem Cytochem*. 2005;53:543–6.
  46. Pedersen HL, Fangel JU, McCleary B, Ruzanski C, Rydahl MG, Ralet MC, Farkas V, Von Schantz L, Marcus SE, Andersen MCF, Field R, Ohlin M, Knox JP, Clausen MH, Willats WGT. Versatile high resolution oligosaccharide microarrays for plant glycobiology and cell wall research. *J Biol Chem*. 2012;287:39429–38.
  47. Zhang X, Rogowski A, Zhao L, Hahn MG, Avci U, Knox JP, Gilbert HJ. Understanding how the complex molecular architecture of mannan-degrading hydrolases contributes to plant cell wall degradation. *J Biol Chem*. 2014;289:2002–12.
  48. Alonso-Simón A, Kristensen JB, Øbro J, Felby C, Willats WGT, Jørgensen H. High-throughput microarray profiling of cell wall polymers during hydrothermal pre-treatment of wheat straw. *Biotechnol Bioeng*. 2010;105:509–14.
  49. Meng X, Foston M, Leisen J, DeMartini J, Wyman CE, Ragauskas AJ. Determination of porosity of lignocellulosic biomass before and after pretreatment by using Simons' stain and NMR techniques. *Bioresour Technol*. 2013;144:467–76.
  50. Hsieh Y-L, Yu B. Liquid wetting, transport, and retention properties of fibrous assemblies. Part I: water wetting properties of woven fabrics and their constituent single fibers. *Text Res J*. 1992;62:677–85.
  51. Cui T, Li J, Yan Z, Yu M, Li S. The correlation between the enzymatic saccharification and the multidimensional structure of cellulose changed by different pretreatments. *Biotechnol Biofuels*. 2014;7:134.
  52. Xu N, Liu W, Hou Q, Wang P, Yao Z. Effect of autohydrolysis on the wettability, absorbability and further alkali impregnation of poplar wood chips. *Bioresour Technol*. 2016;216:317–22.
  53. Shen J, Liu Z, Li J, Niu J. Wettability changes of wheat straw treated with chemicals and enzymes. *J For Res*. 2011;22:107–10.
  54. Stauner T, Silva IB, El Seoud OA, Frollini E, Petri DFS. Cellulose loading and water sorption value as important parameters for enzymatic hydrolysis of cellulose. *Cellulose*. 2013;20:1109–19.
  55. Yang H, Chen Q, Wang K, Sun R-C. Correlation between hemicelluloses-removal-induced hydrophilicity variation and the bioconversion efficiency of lignocelluloses. *Bioresour Technol*. 2013;147:539–44.
  56. Kabel MA, van den Borne H, Vincken JP, Voragen AGJ, Schols HA. Structural differences of xylans affect their interaction with cellulose. *Carbohydr Polym*. 2007;69:94–105.
  57. Selig MJ, Thygesen LG, Felby C, Master ER. Debranching of soluble wheat arabinoxylan dramatically enhances recalcitrant binding to cellulose. *Biotechnol Lett*. 2015;37:633–41.
  58. Hansen MAT, Kristensen JB, Felby C, Jørgensen H. Pretreatment and enzymatic hydrolysis of wheat straw (*Triticum aestivum* L.)—the impact of lignin relocation and plant tissues on enzymatic accessibility. *Bioresour Technol*. 2011;102:2804–11.
  59. Zhang M, Chen G, Kumar R, Xu B. Mapping out the structural changes of natural and pretreated plant cell wall surfaces by atomic force microscopy single molecular recognition imaging. *Biotechnol Biofuels*. 2013;6:147.
  60. Rahikainen J, Mikander S, Marjamaa K, Tamminen T, Lappas A, Viikari L, Kruus K. Inhibition of enzymatic hydrolysis by residual lignins from softwood—study of enzyme binding and inactivation on lignin-rich surface. *Biotechnol Bioeng*. 2011;108:2823–34.
  61. Barsberg S, Selig MJ, Felby C. Impact of lignins isolated from pretreated lignocelluloses on enzymatic cellulose saccharification. *Biotechnol Lett*. 2013;35:189–95.
  62. Donaldson LA, Wong KKY, Mackie KL. Ultrastructure of steam-exploded wood. *Wood Sci Technol*. 1988;22:103–14.
  63. Selig MJ, Vinzant TB, Himmel ME, Decker SR. The effect of lignin removal by alkaline peroxide pretreatment on the susceptibility of corn stover to purified cellulolytic and xylanolytic enzymes. *Appl Biochem Biotechnol*. 2009;155:397–406.
  64. Araya F, Troncoso E, Mendonça RT, Freer J. Condensed lignin structures and re-localization achieved at high severities in autohydrolysis of Eucalyptus globulus wood and their relationship with cellulose accessibility. *Biotechnol Bioeng*. 2015;112:1783–91.
  65. Silveira RL, Stoyanov SR, Gusarov S, Skaf MS, Kovalenko A. Supramolecular interactions in secondary plant cell walls: effect of lignin chemical composition revealed with the molecular theory of solution. *J Phys Chem Lett*. 2015;6:206–11.
  66. Langan P, Petridis L, O'Neill HM, Pingali SV, Foston M, Nishiyama Y, Schulz R, Lindner B, Hanson BL, Harton S, Heller WT, Urban V, Evans BR, Gnanakaran S, Ragauskas AJ, Smith JC, Davison BH. Common processes drive the thermochemical pretreatment of lignocellulosic biomass. *Green Chem*. 2014;16:63.
  67. Himmel ME, Ding S-Y, Johnson DK, Adney WS, Nimlos MR, Brady JW, Foust TD. Biomass recalcitrance: engineering plants and enzymes for biofuels production. *Science*. 2007;315:804–7.
  68. Attard TM, McElroy CR, Gammons RJ, Slattery JM, Supanchaiyamat N, Kamei CLA, Dolstra O, Trindade LM, Bruce NC, McQueen-Mason SJ, Shimizu S, Hunt AJ. Supercritical CO<sub>2</sub> extraction as an effective pretreatment step for wax extraction in a *Miscanthus* biorefinery. *ACS Sustain Chem Eng*. 2016;4:5979–88.
  69. Kádár Z, Schultz-Jensen N, Jensen JS, Hansen MAT, Leipold F, Bjerre A-B. Enhanced ethanol production by removal of cutin and epicuticular waxes of wheat straw by plasma assisted pretreatment. *Biomass Bioenergy*. 2015;81:26–30.
  70. Moller I, Sørensen I, Bernal AJ, Blaukopf C, Lee K, Øbro J, Pettolino F, Roberts A, Mikkelsen JD, Knox JP, Bacic A, Willats WGT. High-throughput mapping of cell-wall polymers within and between plants using novel microarrays. *Plant J*. 2007;50:1118–28.
  71. Schwanninger M, Rodrigues JC, Pereira H, Hinterstoisser B. Effects of short-time vibratory ball milling on the shape of FT-IR spectra of wood and cellulose. *Vib Spectrosc*. 2004;36:23–40.
  72. Faix O. Classification of lignins from different botanical origins by FT-IR spectroscopy. *Holzforschung*. 1991;45:21–7.
  73. Merk S, Blume A, Riederer M. Phase behaviour and crystallinity of plant cuticular waxes studied by Fourier transform infrared spectroscopy. *Planta*. 1998;204:44–53.
  74. Baas P. Interference microscopic studies on wood plastic and cell wall-liquid interactions in beech. *J Microsc*. 1975;104:83–90.

## PAPER II

---

Lignin from hydrothermally pretreated grass biomass retards enzymatic cellulose degradation by acting as a physical barrier rather than by inducing non-productive adsorption of enzymes

**Djajadi DT**, Jensen MM, Oliveira M, Jensen A, Thygesen LG, Pinelo M, Glasius M, Jørgensen H, Meyer AS

Biotechnol. Biofuels 2018; 11:85

© The Author(s) 2018


Reprinted under Creative Commons Attribution License 4.0

RESEARCH

Open Access



# Lignin from hydrothermally pretreated grass biomass retards enzymatic cellulose degradation by acting as a physical barrier rather than by inducing nonproductive adsorption of enzymes

Demi T. Djajadi<sup>1</sup>, Mads M. Jensen<sup>2</sup>, Marlene Oliveira<sup>1</sup>, Anders Jensen<sup>3</sup>, Lisbeth G. Thygesen<sup>3</sup>, Manuel Pinelo<sup>1</sup>, Marianne Glasius<sup>2</sup>, Henning Jørgensen<sup>1,4</sup> and Anne S. Meyer<sup>1\*</sup> 

## Abstract

**Background:** Lignin is known to hinder efficient enzymatic conversion of lignocellulose in biorefining processes. In particular, nonproductive adsorption of cellulases onto lignin is considered a key mechanism to explain how lignin retards enzymatic cellulose conversion in extended reactions.

**Results:** Lignin-rich residues (LRRs) were prepared via extensive enzymatic cellulose degradation of corn stover (*Zea mays* subsp. *mays* L.), *Miscanthus × giganteus* stalks (MS) and wheat straw (*Triticum aestivum* L.) (WS) samples that each had been hydrothermally pretreated at three severity factors ( $\log R_0$ ) of 3.65, 3.83 and 3.97. The LRRs had different residual carbohydrate levels—the highest in MS; the lowest in WS. The residual carbohydrate was not traceable at the surface of the LRRs particles by ATR-FTIR analysis. The chemical properties of the lignin in the LRRs varied across the three types of biomass, but monolignols composition was not affected by the severity factor. When pure cellulose was added to a mixture of LRRs and a commercial cellulolytic enzyme preparation, the rate and extent of glucose release were unaffected by the presence of LRRs regardless of biomass type and severity factor, despite adsorption of the enzymes to the LRRs. Since the surface of the LRRs particles were covered by lignin, the data suggest that the retardation of enzymatic cellulose degradation during extended reaction on lignocellulosic substrates is due to physical blockage of the access of enzymes to the cellulose caused by the gradual accumulation of lignin at the surface of the biomass particles rather than by nonproductive enzyme adsorption.

**Conclusions:** The study suggests that lignin from hydrothermally pretreated grass biomass retards enzymatic cellulose degradation by acting as a physical barrier blocking the access of enzymes to cellulose rather than by inducing retardation through nonproductive adsorption of enzymes.

**Keywords:** Lignin, Cellulases, Adsorption, Inhibition, Enzymatic hydrolysis, S/G ratio,  $\beta$ -O-4 linkage, Apparent surface abundance, Depolymerization, Physical barrier

\*Correspondence: am@kt.dtu.dk

<sup>1</sup> Department of Chemical and Biochemical Engineering, Technical University of Denmark, Søltofts Plads Building 229, 2800 Kongens Lyngby, Denmark

Full list of author information is available at the end of the article

## Background

Optimal utilization of lignocellulosic biomass is vital for sustainable production of food, feed, fuels, chemicals, and materials. Hydrothermal pretreatment (HTP) and other types of physicochemical pretreatment methods are used to overcome the recalcitrance of the lignocellulosic biomass feedstocks to allow efficient enzymatic and biological processing [1, 2]. HTP of lignocellulosic biomass is known to remove parts of the hemicellulose fraction, thereby resulting in a cellulose-enriched fiber fraction which is more amenable to cellulase-catalyzed saccharification; depending on the pretreatment severity [3].

On the other hand, the presence of lignin in hydrothermally pretreated lignocellulosic biomass has also been considered as an important limiting factor in the enzymatic hydrolysis of cellulose [4, 5]. Lignin has thus been reported to promote nonproductive adsorption of the enzymes through charged and noncharged interactions and it may also act as a physical barrier that blocks the access of cellulolytic enzymes to cellulose [6–8]. Notably, nonproductive adsorption of cellulases to lignin has been considered as a key factor that limits the enzymatic conversion of pretreated biomass [4, 6, 9].

Available studies [10–18] have consistently shown that the enzymes are bound to isolated lignin materials from various biomasses and consequently the enzymes' activity and/or the rate and extent of saccharification of model cellulose substrate in the presence of the isolated lignin were reduced. Observation of the latter has contributed to the use of the term “inhibitory effect” of lignin to enzymatic hydrolysis of cellulose in scientific literature.

Investigating the role of lignin as a physical barrier, however, can be difficult and complicated. Primarily this is due to modification of the lignin structure [19, 20] and its redistribution in the cell wall matrix [21, 22] after hydrothermal or dilute acid pretreatment. Advanced microscopy and imaging techniques have been developed to visualize components of lignocellulosic biomass, although extracting quantitative information can sometimes be difficult [23].

Recently, we have published a systematic study where industrially relevant Poaceae biomass feedstocks, namely corn stover, *Miscanthus × giganteus* stalks and wheat straw were hydrothermally pretreated at different severity levels. Via utilizing several quantitative and semiquantitative approaches, we proposed that surface properties, including apparent surface abundance of lignin as semiquantitatively determined by attenuated total reflectance Fourier transform infrared (ATR-FTIR) spectroscopy were correlated to the digestibility of biomass [24].

The objective of the present study was to further elucidate the role of lignin in retarding enzymatic cellulose

degradation. This was done by simultaneously studying both enzyme–lignin interaction and the physicochemical properties and apparent surface abundance of lignocellulose components. The experimental approach was performed in three steps. Firstly, lignin-rich residues (LRRs) from the abovementioned biomass feedstocks were isolated through extensive enzymatic hydrolysis and characterized comprehensively. The ensuing profile of the LRRs is expected to resemble the actual bioprocess residues from lignocellulosic ethanol/biorefinery plants and the procedure is also expected to only exert minimal changes to the lignin structure. Secondly, the LRRs were assessed for their effect on the activity of state-of-the-art commercial cellulolytic enzyme mixture using relevant dosage. Thirdly, the data obtained in previous steps were extrapolated to explain what seemed to have occurred during actual extended enzymatic biomass hydrolysis reaction.

## Results and discussion

### Composition of lignin-rich residues

The composition of LRRs was assessed after repeated rounds of cellulase treatment at high enzyme loading followed by protease treatment to remove the enzymes adsorbed. In this way, the lignin isolation method also serves as exaggerated version of enzymatic cellulose degradation. As expected, the results revealed that the composition of the LRRs varied across biomass and pretreatment severities (Table 1). The LRRs from wheat straw (WS) had significantly higher lignin content than those from corn stover (CS) and *Miscanthus × giganteus* stalks (MS) at corresponding severities. In all LRRs from the three biomasses, it was observed that the lignin content increased relative to the carbohydrate content with elevated pretreatment severity (Table 1). The significantly higher residual carbohydrates content in the LRRs of MS is in agreement with our previous finding that MS was more recalcitrant compared to CS and WS [24] even though the starting compositions of the materials at corresponding pretreatment severities were similar (Table 1).

In order to investigate the accessibility of the residual carbohydrates, further enzymatic hydrolysis was done on the LRRs. The results showed that only negligible amounts of monosaccharides were released (Additional file 1: Table S1). This indicated that the remaining cellulose and hemicellulose fractions were not accessible to the enzymes; most likely due to the surface coverage by lignin. Therefore it can be assumed that adsorption of the enzymes onto residual cellulose is negligible.

In order to assess the apparent surface abundance of lignocellulose components in the LRRs, ATR-FTIR spectroscopy was utilized as described previously [24]. However, when using the semiquantitative approach, the

**Table 1** Composition of pretreated biomass feedstocks and their resulting isolated lignin-rich residues

Biomass—log $R_0$	Pretreated biomass feedstocks			Lignin-rich residues		
	Glucan	Xylan	Lignin <sup>1</sup>	Glucan	Xylan	Lignin <sup>1</sup>
	(% w/w DM)					
CS—3.65	55.5 ± 3.1 <sup>ab</sup>	14.7 ± 0.8 <sup>a</sup>	23.8 ± 2.3 <sup>cd</sup>	20.9 ± 0.5 <sup>b</sup>	5.4 ± 0.2 <sup>a</sup>	60.4 ± 1.3 <sup>f</sup>
CS—3.83	55.7 ± 1.3 <sup>ab</sup>	11.2 ± 0.5 <sup>b</sup>	22.4 ± 0.8 <sup>d</sup>	14.5 ± 0.1 <sup>d</sup>	3.2 ± 0.1 <sup>bc</sup>	75.4 ± 0.9 <sup>de</sup>
CS—3.97	61.2 ± 1.1 <sup>a</sup>	6.4 ± 0.1 <sup>e</sup>	19.9 ± 3.9 <sup>d</sup>	7.2 ± 0.2 <sup>f</sup>	1.6 ± 0.0 <sup>e</sup>	79.5 ± 1.6 <sup>bc</sup>
MS—3.65	53.6 ± 2.6 <sup>b</sup>	11.3 ± 0.4 <sup>b</sup>	32.5 ± 2.1 <sup>ab</sup>	33.9 ± 0.7 <sup>a</sup>	5.7 ± 0.1 <sup>a</sup>	58.5 ± 0.7 <sup>f</sup>
MS—3.83	54.7 ± 2.8 <sup>ab</sup>	7.8 ± 0.6 <sup>d</sup>	32.2 ± 0.5 <sup>ab</sup>	18.9 ± 0.6 <sup>c</sup>	3.0 ± 0.1 <sup>c</sup>	73.1 ± 0.8 <sup>e</sup>
MS—3.97	55.9 ± 2.1 <sup>ab</sup>	4.5 ± 0.2 <sup>f</sup>	35.6 ± 0.3 <sup>a</sup>	11.7 ± 0.5 <sup>e</sup>	1.4 ± 0.0 <sup>e</sup>	81.9 ± 0.3 <sup>b</sup>
WS—3.65	54.8 ± 0.6 <sup>ab</sup>	14.7 ± 0.0 <sup>a</sup>	29.3 ± 0.7 <sup>bc</sup>	13.7 ± 0.6 <sup>d</sup>	3.4 ± 0.1 <sup>b</sup>	77.7 ± 0.7 <sup>cd</sup>
WS—3.83	58.2 ± 4.7 <sup>ab</sup>	9.8 ± 0.4 <sup>c</sup>	30.8 ± 0.7 <sup>ab</sup>	7.9 ± 0.0 <sup>f</sup>	2.0 ± 0.0 <sup>d</sup>	86.2 ± 0.1 <sup>a</sup>
WS—3.97	61.2 ± 2.5 <sup>a</sup>	6.5 ± 0.2 <sup>e</sup>	30.3 ± 1.1 <sup>b</sup>	5.3 ± 0.1 <sup>g</sup>	1.1 ± 0.0 <sup>f</sup>	87.8 ± 1.0 <sup>a</sup>

Results are average and standard deviation of triplicate measurements

CS corn stover, MS *Miscanthus × giganteus* stalks, WS wheat straw

Different letters indicate significant statistical difference based on ANOVA ( $P \leq 0.05$ )

<sup>1</sup> Based on acid insoluble lignin (AIL) and acid soluble lignin (ASL) contents

peak area values of the carbohydrates in the lignin-rich residues (LRRs) were too low for reasonable quantification. Upon examination of the ATR-FTIR spectra (Additional file 1: Figures S1–S3), apparently this was due to the diminishing intensity of carbohydrate peaks corresponding to cellulose ( $895\text{ cm}^{-1}$ ) and hemicellulose ( $1732\text{ cm}^{-1}$ ) after extensive enzymatic hydrolysis process. On the other hand, the peaks corresponding to lignin ( $835$ ,  $1419$ ,  $1432$ ,  $1508$  and  $1601\text{ cm}^{-1}$ ) increased greatly after hydrolysis. Since ATR-FTIR wavenumbers have limited depth of penetration (Table 3), these observations confirmed the previous observations and inference (Additional file 1: Table S1) that the carbohydrates in the lignin-rich residues were not present in the surface, conceivably due to being engulfed by lignin. A likely scenario therefore was that as cellulose hydrolysis progressed, the work of the enzymes was halted due to the increasing presence of lignin in the surface of the biomass particles which acted as physical barrier. However, since lignin has been reported to promote retardation through nonproductive adsorption, the interaction between lignin and LRRs should also be investigated.

#### Interaction between enzymes and lignin-rich residues

In order to directly assess the interaction between the LRRs from the pretreated biomass with a commercial cellulolytic enzyme mixture (Cellic<sup>®</sup> CTec3), an adsorption experiment was performed. No consistent trends were evident across all LRRs regardless whether it was based on biomass feedstocks or severity factors. Approximately 34–47% of total protein in the enzyme mixture was adsorbed in all cases (Fig. 1).

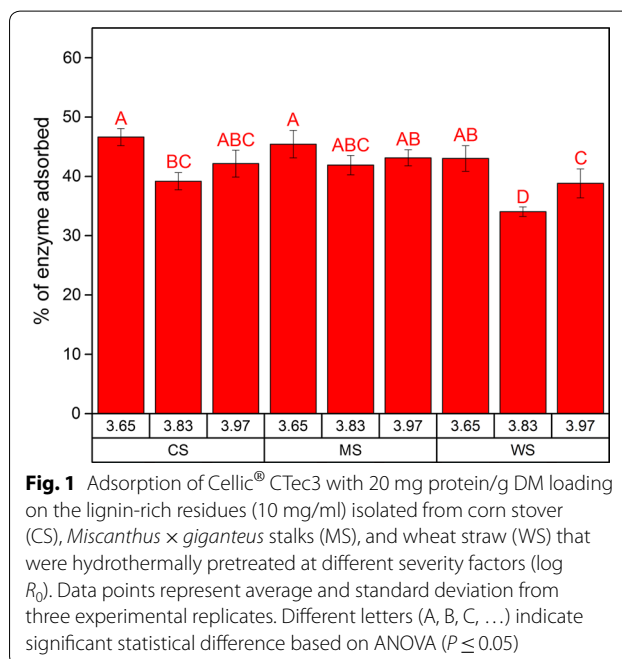


**Fig. 1** Adsorption of Cellic<sup>®</sup> CTec3 with 20 mg protein/g DM loading on the lignin-rich residues (10 mg/ml) isolated from corn stover (CS), *Miscanthus × giganteus* stalks (MS), and wheat straw (WS) that were hydrothermally pretreated at different severity factors (log  $R_0$ ). Data points represent average and standard deviation from three experimental replicates. Different letters (A, B, C, ...) indicate significant statistical difference based on ANOVA ( $P \leq 0.05$ )

Several studies on the adsorption of cellulases on lignin materials isolated from various biomasses have found that adsorption of cellulases (or their adsorption parameters modeled with Langmuir isotherms) increase slightly with elevated severity factor [15, 25, 26], although one study found the opposite [27]. In one study on lignin isolated from corn stover that had been hydrothermally pretreated at different severities, it was found that there were only minor differences in the binding capacity of

cellulases, with only 6% of increase with severity factor ( $\log R_0$ ) of 3.6–3.9 [26]. These results imply that the applied severity factor during pretreatment does not always warrant a significant increase in adsorption of cellulolytic enzymes. However, separate tests need to be conducted to assess whether adsorption of enzymes has direct impact on their performance.

Therefore, in order to further study the interaction of the LRRs with cellulolytic enzymes, the effect of LRRs on activity of the enzymes was examined. The assessment was performed in two sets of experiments. In the first experiment (Experiment I), an Avicel (cellulose) suspension was added to the mixture of preincubated Cellic<sup>®</sup> CTec3 and LRRs to directly assess both nonproductive adsorption and any consequent “inhibitory” effect of the LRRs. In the second experiment (Experiment II), each supernatant after preincubation of Cellic<sup>®</sup> CTec3 and LRRs was added to an Avicel suspension to assess the

significance of the adsorption of enzymes onto LRRs on cellulolytic activity. The results of Experiment I did not show any significant difference in the degree of Avicel hydrolysis between enzymes incubated with or without LRRs or any difference due to the severity factor and/or botanical origin of the LRRs (Fig. 2a–c). On the contrary, the results of Experiment II showed that the glucose release from Avicel was reduced after preincubation with LRRs (Fig. 2d–f); corroborating that some of the enzymes were adsorbed to the insoluble fraction, leaving reduced activity in the supernatant. The reductions were around 19–28, 30–57 and 31–52% for LRRs from CS, MS and WS, respectively across all time points and severity factors; although there was no significant difference among the LRRs in response to the degree of severity factor (Fig. 2d–f).

In Experiment I, despite the adsorption of enzymes from the commercial cellulolytic enzyme mixture on

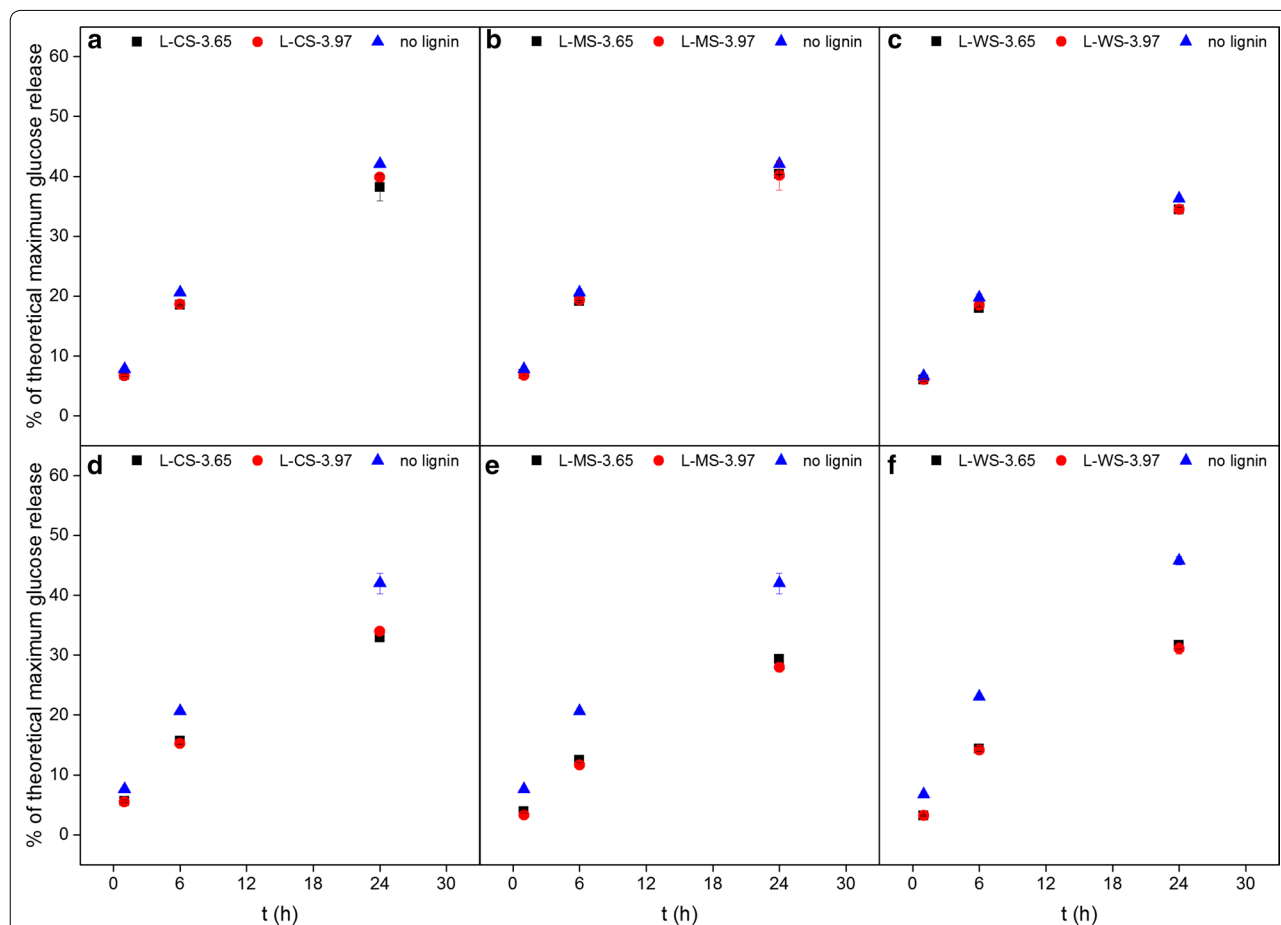


**Fig. 2** Glucose release from 2% DM Avicel hydrolysis after adsorption experiment of Cellic<sup>®</sup> CTec3 in the presence of lignin-rich residues (LRRs) as in Experiment I (**a–c**) or by supernatant containing unbound enzymes after incubation with LRRs in Experiment II (**d–f**—Pyrolysis-GC–MS characterization of forage materials). LRRs were isolated from corn stover (L-CS) (**a** and **d**), *Miscanthus × giganteus* stalks (L-MS) (**b** and **e**), and wheat straw (L-WS) (**c** and **f**) that were hydrothermally pretreated at severity factors ( $\log R_0$ ) 3.65 and 3.97. Data points represent average and standard deviation from two replicates

LRRs (Fig. 1), there was no reduction of enzymatic activity in saccharifying cellulose (Fig. 2a–c). Since the final enzyme dosage in the hydrolysis reaction was low (10 mg protein/g DM cellulose) and on par with that being used in large-scale process [28], it is less likely that the absence of any retardation of the glucose release was due to the excess of unbound enzymes. Furthermore, in Experiment II, the activity of unbound enzymes after adsorption was studied in a scenario as if the binding of the enzymes on lignin were irreversible by performing solid–liquid separation. The results showed that the activity of unbound enzymes alone (with reductions of 19–57% for the different LRRs across all time points) was not enough to degrade the added Avicel to the same rate and extent as that accomplished by the free enzymes that were not adsorbed on LRRs (Fig. 2d–f). This absence of retardation in Experiment I therefore indicated that the LRR-adsorbed cellulose degrading enzymes in the mixture were still active on the added cellulose despite the adsorption. The phenomenon has been shown previously where the enzymes adsorbed on insoluble lignin-rich solids obtained after hydrolysis of dilute acid pretreated corn stover can be recycled by adding fresh substrate to the residue [29]. The finding thus led to two possibilities.

One possibility is that the enzymes were still active despite being bound on lignin [30, 31], likely since the binding occurred without impeding the active site of the enzymes. However, if this was the sole case, a pronounced decrease in cellulose hydrolysis should still be observed since adsorbed or immobilized cellulases were reported to have decreased activity [31, 32]. In contrary, Experiment I showed negligible effect of the presence of LRRs on enzymatic cellulose hydrolysis (Fig. 2a–c). Experiment I has been designed to expand the assessment of enzyme–lignin interaction. On the one hand, the preadsorption of the enzymes on lignin provided more difficulty for the enzymes to degrade the cellulose. On the other hand, the latter introduction of cellulose allowed the enzymes to display whether the binding on lignin is reversible. Therefore, by showing negligible difference in the Avicel hydrolysis (Fig. 2a–c), the results gave strong indication on the reversible binding nature of the enzymes on lignin, i.e. the more likely was the possibility that the adsorbed enzymes desorbed from the LRRs and then re-adsorbed onto Avicel and catalyzed the degradation. This is also supported by the previous findings that cellulases have higher affinity to cellulose or lignocellulosic biomass compared to lignin [16, 33]. The adsorption and desorption kinetics of individual monocomponent cellulases on lignin hence deserve further investigation in order to corroborate this hypothesis.

It is also important to note that the trend of the effect of LRRs on the enzymes was consistent throughout the

tested grass biomass (Fig. 2a–c). In a previous study, LRR from hydrothermally pretreated spruce was found to reduce the rate and extent of Avicel hydrolysis by cellulases after incubation at 45 °C [13]. In this work, there was no reduction discernible as a result of the presence of LRRs during reaction at 50 °C (Fig. 2a–c). The difference between the data in this study and the previously reported data on spruce is likely due to botanical origin of the lignin material. Hence this present work, along with other studies using LRRs from hydrothermally pretreated grasses, showed that the LRRs did not reduce the rate and extent of enzymatic cellulose hydrolysis despite some degree of enzyme adsorption on the LRRs [26, 34, 35].

Experiment II nevertheless validated that a portion of the commercial cellulolytic enzyme mixture did get adsorbed onto LRRs and thus was not recovered when the supernatant was transferred, thereby reducing the extent of Avicel hydrolysis (Fig. 2d–f). Since glucose release was compromised in Experiment II, it is plausible that the fraction of the adsorbed enzyme consisted of  $\beta$ -glucosidases (BGLs). Accordingly, BGL was reported previously to have the highest affinity toward lignin from steam-pretreated corn stover compared to other components of Cellic<sup>®</sup> CTec2 [36]. However, the difference in the reduction of Avicel hydrolysis in Experiment II may be a result of the different affinities of other various enzyme components in the mixture to the different LRRs, as there was no distinct pattern in the overall protein adsorption (Fig. 1). Since the LRRs did not exert nonproductive adsorption and reduction of activity that distinguished them from one another, it can be expected that there were only minor changes in the chemical composition of the lignin.

#### Physical and chemical characterization of the lignin-rich residues

A series of physical and chemical characterizations were performed on the LRRs to assess any physicochemical changes in the lignin after HTP at different severity factors and to understand the role of lignin as a physical barrier. Firstly, nuclear magnetic resonance (NMR) spectroscopy was performed mainly to assess the relative abundance of inter-unit linkages in the lignin polymer of the LRRs after pretreatment at different severities. The <sup>13</sup>C-<sup>1</sup>H HSQC (heteronuclear single quantum coherence) spectra (Additional file 1: Figures S4–S12) revealed that there was a slight decrease of  $\beta$ -O-4 linkage in all biomasses with each elevated severity level. The C–C bonds ( $\beta$ -5 and  $\beta$ - $\beta$ ) however, remained relatively stable except for a slight increase of  $\beta$ -5 in MS (Table 2).

The reduction of ether  $\beta$ -O-4 linkages intensity is expected to occur as a result of increasing pretreatment

**Table 2**  $^{13}\text{C}$ - $^1\text{H}$  HSQC contour integration values for inter-unit linkages in the lignin polymer of the lignin-rich residues

Structure	CS			MS			WS		
	3.65	3.83	3.97	3.65	3.83	3.97	3.65	3.83	3.97
G2	1	1	1	1	1	1	1	1	1
$\beta$ -O-4	*	0.46	0.40	0.49	0.44	0.41	0.63	0.57	0.55
$\beta$ -5	n/a	n/a	n/a	0.08	0.10	0.18	0.08	0.10	0.10
$\beta$ - $\beta$	n/a	n/a	n/a	nd	0.005	nd	0.010	0.010	nd

G2: C<sub>2</sub>-H<sub>2</sub> correlation peak in guaiacyl subunit was used as reference

n/a: not applicable, structure does not exist

nd: peak too small for accurate determination

\* Contour integration was not possible

severity as it is the most susceptible linkage to break during thermochemical treatment [19, 37–39]. However, the cleavage of  $\beta$ -O-4 was not significant with only 4–13% signal reduction in the contour integration values across biomass and severity levels (Table 2). In another study, an increase of HTP severity factor ( $\log R_0$ ) from 2.76 (160 °C for 10 min) to 3.65 (190 °C for 10 min) resulted in a 700% drop of the relative abundance of  $\beta$ -O-4 linkages in wheat straw lignin [39]. The minimal change in  $\beta$ -O-4 cleavage observed in this study therefore can be attributed to the narrower range of the HTP severity factor ( $\log R_0$ ) being used (from 3.65 to 3.97). Stable contour integration values of covalent C–C bonds have also been reported across elevated severity either due to increase of temperature or addition of acid [39]. Overall, the 2D NMR results suggested that the lignin in the LRRs did not undergo significant chemical changes within the tested severity factors.

Py-GC–MS analysis was performed in order to assess the composition of the monolignols of the different lignin-rich residues (LRRs) from corn stover (CS), *Miscanthus × giganteus* stalks (MS) and wheat straw (WS). The results revealed no differences on the relative monolignols contents after pretreatment with different severities and their corresponding ratios in the case of each biomass (Fig. 3). However, there were differences of relative monolignols contents among biomass feedstocks. LRRs from CS had higher content of syringyl (S) and *p*-hydroxyphenyl (H) units while lower content of guaiacyl (G) unit compared to the other biomasses (Fig. 3a), which resulted in higher S/G ratio of CS compared to MS and WS (Fig. 3b).

Attenuated total reflectance—Fourier Transform Infrared (ATR-FTIR) spectroscopy has also been used to estimate monolignols ratios, although it has been done in different ways in different studies [40–43]. Py-GC–MS and NMR are more commonly used to assess S/G ratio [38, 44]. In this study, H/G and S/G

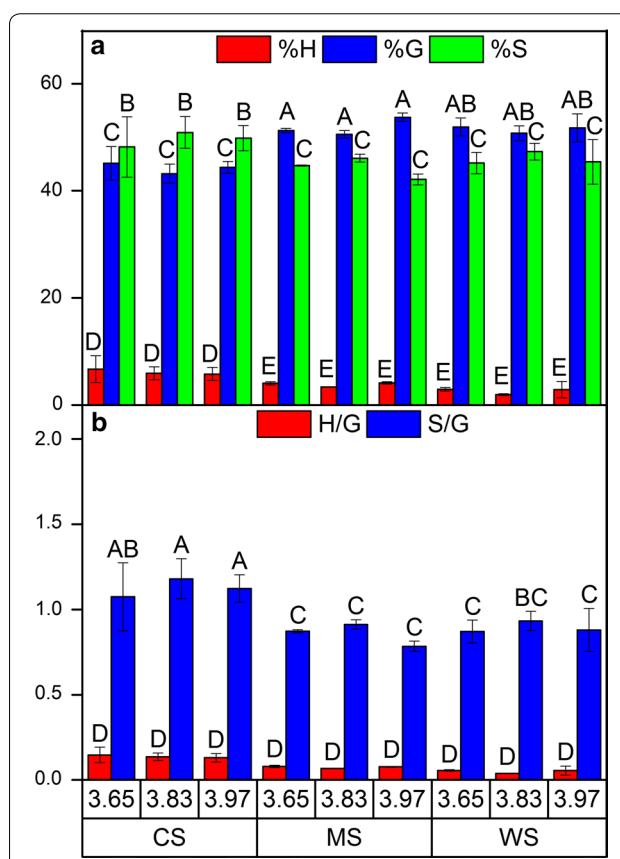


**Fig. 3** The relative abundance of monolignols, namely *p*-hydroxyphenyl (H), guaiacyl (G), and syringyl (S) units (a), and the corresponding monolignols ratio (b), based on Py-GC–MS results of the lignin-rich residues (LRRs) from corn stover (CS), *Miscanthus × giganteus* stalks (MS), and wheat straw (WS). Data points represent average and standard deviation from two replicates. Different letters (A, B, C, ...) indicate significant statistical difference based on ANOVA ( $P \leq 0.05$ )

ratios were assessed by calculating the ratio of estimated peak areas of 835/1508 and 1601/1508  $\text{cm}^{-1}$ , respectively (Additional file 1: Figures S1–S3). The wavenumbers 835, 1508, and 1601  $\text{cm}^{-1}$  each

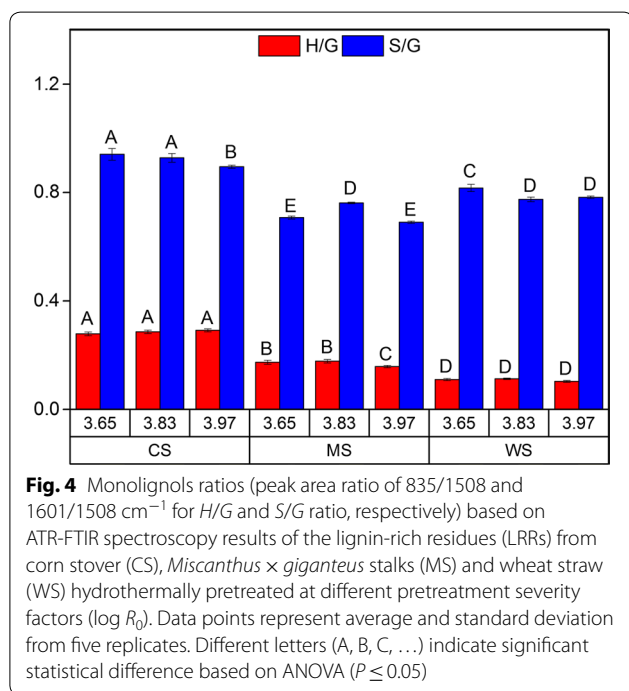


**Table 3** ATR-FTIR assignments of wavenumbers used to measure peak area

Wavenumber (cm <sup>-1</sup> )	Assignment <sup>a</sup>	Estimated penetration depth <sup>a</sup> (μm)
835	Lignin	C–H out-of-plane in all position of H and in positions 2 and 6 of S units [40]
895	Holocellulose	Anomeric C-groups, C <sub>1</sub> -H deformation, ring valence vibration (cellulose, wood, holocellulose) [63]
1419; 1432	Lignin	Aromatic skeletal vibrations combined with C–H in-plane deformation [40]
1508	Lignin	Aromatic skeletal vibrations; G > S [40, 63]
1601	Lignin	Aromatic skeletal vibrations plus C=O stretch; S > G [40, 63]
1732	Hemicellulose	C=O stretch in unconjugated carbonyl groups of carbohydrate origin (side chain acetylation in mannan, carboxylic acid side chain in xylan and ester groups in lignin-carbohydrate complexes) [40, 63]

<sup>a</sup> Calculated based on the formula (Eq. 1):  $d_p = \frac{\lambda}{2\pi n_1 \sqrt{\sin^2 \theta - (n_2/n_1)^2}}$  (1) where  $d_p$ ,  $\lambda$ ,  $\theta$ ,  $n_1$  and  $n_2$  are penetration depth, wavelength, incident angle, ATR crystal

refractive index and sample refractive index respectively. The values of  $\theta$  and  $n_1$  are specifically known to be 45° and 2.40 respectively for diamond ATR. The refractive index of biomass samples is estimated to be 1.4 which is a common value for an organic polymer, e.g. in wood cell walls [64]



corresponds to a signal from H, G, and S units, respectively (Table 3) [40]. The calculated monolignols ratio (Fig. 4) resembled those determined by Py-GC-MS (Fig. 3b) both in terms of number and trend, which confirms that no changes in the monolignols ratio took place as a result of the increased pretreatment severity, but distinct differences were evident due to the inherent differences among the biomass feedstocks. The work indicates that the ATR-FTIR spectroscopy approach can be used as a fast method to estimate monolignols' ratio of lignin from grasses. In retrospect, the finding

also showed that the chemical composition of the lignin on the surface of the LRRs (using ATR-FTIR) was the same as that of the bulk of the LRRs (using Py-GC-MS). This congruence of results between ATR-FTIR and Py-GC-MS on the chemical composition of the lignin corroborated the aforementioned notion that the residual carbohydrates in the LRRs (Table 1) were engulfed by the same lignin which covered the surface of the LRR particles.

Other studies assessing biomass resulting from hydrothermal or dilute acid pretreated biomass have found that increasing pretreatment severity results in higher release of S units compared to G units in GS type lignin, thus reducing the S/G ratio [19, 45, 46]. However, it has also been reported that the S/G ratio is unaffected by pretreatment severity level [44, 47]. Apparently, the botanical origin of lignin as well as pretreatment method affect the S/G ratio. Since cleavage of β-O-4 linkages in the LRRs was minimum across the applied severity levels in this study (Table 2), it is conceivable that the S/G ratio did not change as β-O-4 linkage constitutes a significant fraction of linkages with syringyl units [19]. Even though the monolignols content, especially the S/G ratio of lignin, may be related to biomass recalcitrance, the exact contribution is not clearly defined as conflicting trends across different feedstocks and pretreatment methods have been reported [7].

In this work, the results from Experiment II showed that the LRRs from CS had higher S/G ratio compared to the others (Figs. 3b and 4) and also gave less reduction of Avicel hydrolysis compared to LRRs from MS and WS (Fig. 2d–f). Accordingly, another study on isolated lignins from hardwood found that there were less adsorption on substrate with higher S/G ratio [48]. However, this was not apparent from the adsorption

experiment since the binding of total protein on LRRs from CS was not significantly lower than others (Fig. 1). Regardless, relative monolignols contents (Figs. 3 and 4) indicated that the chemical composition of the lignin did not change significantly across the tested hydrothermal pretreatment severity levels.

Gel permeation chromatography (GPC) analysis was performed to assess changes in the physical parameter of lignin, namely molecular weight ( $M_w$ ) distribution. The absorbance of the compounds at 280 nm was normalized to show the relative changes of  $M_w$  as pretreatment severity was increased. The results of GPC revealed negligible changes in the  $M_w$  fractions of LRRs from CS and MS as the severity increased, except the appearance of low  $M_w$  fractions at the highest severity level tested in this study. However in the case of LRRs from WS, there were substantial increase of fractions with lower  $M_w$  as the severity level was increased (Fig. 5).

During HTP, the cleavage of inter-unit linkages such as  $\beta$ -O-4 bonds can occur, which will result in depolymerization of lignin polymer and subsequent decrease of  $M_w$ . On the other hand, at increased severity, condensation reactions can also occur due to the formation of new covalent bonds (C-C) which will result in lignin repolymerization and subsequent increase of  $M_w$ . Both reactions can occur competitively or either one can dominate [37, 39, 49–51], most likely subject to the botanical origin of the lignin as well as employed pretreatment method and severity factors. The GPC results therefore suggested that there were significantly more depolymerization reaction in the LRRs of WS across severity factors compared to that of CS and MS (Fig. 5).

Based on the 2D NMR results, depolymerization should be likely to have occurred although not to a great extent due to only minor reduction of  $\beta$ -O-4 linkage across the tested severity levels in the LRRs (Table 2). The slight increase in the  $\beta$ -5 bond of LRRs from MS (Table 2) can give indication of repolymerization reactions although it can be difficult to confirm. In any case, it is possible that competing repolymerization reactions might have occurred in the lignin polymers of LRRs from CS and MS which resulted in relatively stable distribution of molecular weight fractions across the severity levels. Alternatively, it has been known that guaiacyl (G) units tend to start condensation reaction more easily than the syringyl (S) units during thermochemical pretreatment and therefore are harder to remove [19, 45, 48, 49, 51]. Based on Py-GC-MS and ATR-FTIR, LRRs of MS and WS had lower S/G ratio than that of CS (Figs. 3b and 4); meaning that they had more G units. However, GPC results showed differently in which lignin

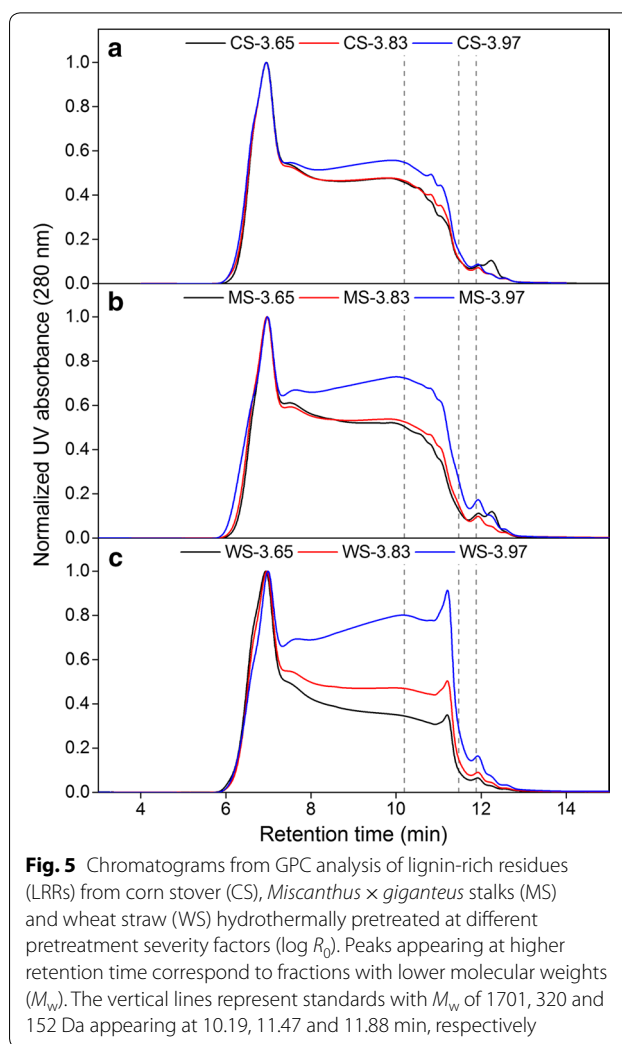
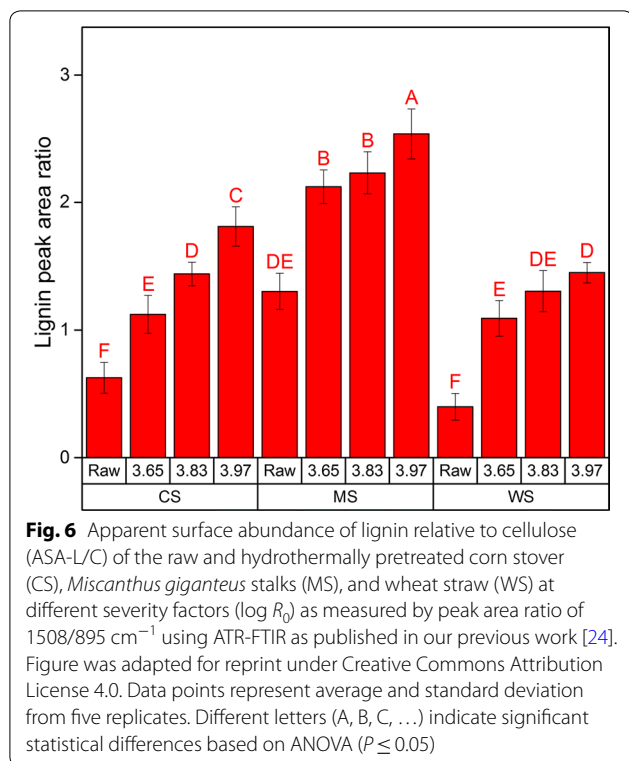


**Fig. 5** Chromatograms from GPC analysis of lignin-rich residues (LRRs) from corn stover (CS), *Miscanthus × giganteus* stalks (MS) and wheat straw (WS) hydrothermally pretreated at different pretreatment severity factors ( $\log R_0$ ). Peaks appearing at higher retention time correspond to fractions with lower molecular weights ( $M_w$ ). The vertical lines represent standards with  $M_w$  of 1701, 320 and 152 Da appearing at 10.19, 11.47 and 11.88 min, respectively

depolymerization occurred to a greater extent in the LRRs of WS than others (Fig. 5).

Recently, Jensen et al. hypothesized that the presence of triclin, an electron-rich aromatic compound can retard repolymerization reactions [39]. NMR analysis of raw (untreated) biomass revealed more pronounced presence of triclin in WS compared to CS and MS (Additional file 1: Figures S13–S15, Table S2). This can explain the observed reduction of  $M_w$  in the LRRs of WS (Fig. 5), namely due to better prevention of repolymerization reactions and thus the higher extent of lignin depolymerization compared to the LRRs of CS and MS. Accordingly, an effort in gene silencing which reduced the synthesis of triclin in corn revealed that the resulting plant obtained increased recalcitrance due to higher lignin content with covalent interunit linkages [52]. In our previous work, the lignin content of pretreated WS at the three severities was not lower compared to CS and MS (Table 1) [24]. However,



our previous finding also pointed that the apparent surface abundance of lignin in the pretreated biomass was the highest on MS for each corresponding severity factor (Fig. 6), which correlated to its lowest glucose release after enzymatic hydrolysis [24]. Therefore, it is likely that the explanation of the role of lignin in retarding enzymatic cellulose degradation lies in the inherent properties and/or subsequent lignin surface coverage after HTP.

This work showed that when viewing the LRRs as an exaggerated version of extensive cellulose hydrolysis, the residual carbohydrates contents were highest in the LRRs of MS (Table 1). The low extent of hydrolysis of MS correlated to our previous finding, where using ATR-FTIR, we previously showed that MS had the highest initial relative abundance of lignin in the surface prior to pretreatment (Fig. 6) [24]. Following HTP, the apparent surface abundance of lignin in the biomass prior to enzymatic treatment increased with increasing severity factor although it was consistently lower in WS compared to CS and MS for each corresponding severity (Fig. 6) [24]. Extrapolation of the insight from our previous finding to the present study suggests that as extensive cellulose hydrolysis progressed, the advance was retarded earlier in CS and MS which had higher apparent surface abundance of lignin than WS. This lower apparent surface abundance of lignin in pretreated WS (Fig. 6) corresponded to a greater

extent of depolymerization of lignin in the LRRs of WS (Fig. 5). In contrast, the lignin in pretreated CS and MS with higher apparent surface abundance (Fig. 6) corresponded to lesser extent of lignin depolymerization (Fig. 5); indicating the possibility that lignin properties can affect its subsequent distribution. Therefore, it can be suggested that the lignin in pretreated CS and MS has become a more potent physical barrier that shielded the carbohydrates after pretreatment than the lignin in pretreated WS. This proposition is supported by the fact that the remaining carbohydrates in the LRRs (Table 1) were not accessible for release by enzymes (Additional file 1: Table S1) and that ATR-FTIR revealed increased presence of lignin in the surface but almost negligible carbohydrates (Additional file 1: Figures S1–S3). All in all, this study along with our previous work [24] and recent works by other groups [53–55] have emphasized the role of lignin as a physical barrier which hinders the accessibility of enzymes to the cellulose in lignocellulosic biomass during extended enzymatic treatment.

## Conclusions

The study showed that enzymes from a commercial cellulolytic mixture adsorbed onto lignin-rich residues (LRRs) isolated from hydrothermally pretreated grass biomass. Although the adsorption reduced the free activity in the supernatant, the performance of the enzymes was not affected by the presence of LRRs. The applied pretreatment severity levels did not significantly affect lignin's chemical composition, and while there were differences across biomass feedstocks, the differences had no impact on the adsorption of enzymes and their ability to saccharify cellulose. On the other hand, even though there was a positive correlation between the lignin content of the LRRs with severity level and biomass digestibility, the residual carbohydrates were not accessible due to physical obstruction by lignin. We suggest that the lignin surface coverage, plausibly due to its inherent physicochemical and structural properties, determines the degree of retardation of enzymatic cellulose degradation in lignocellulosic biomass feedstocks. Therefore, the role of lignin in impeding enzymatic degradation of cellulose can be defined more as a physical barrier which obstructs the access of enzymes to cellulose rather than acting as an "inhibitor" that promotes the loss of activity through nonproductive adsorption. This points to the need to better understand pretreatment and hydrolysis of biomass particles at the physical level where among others, the migration of lignin can be monitored both within micro- and ultrastructural scales of the plant cell wall. Based on the results obtained in the present study,

it is also important to investigate the dynamics of non-productive binding of cellulases and its monocomponent enzymes on lignin in order to assess if the adsorption of individual enzymes differs with various substrates.

## Methods

### Biomass feedstocks

Corn stover (*Zea mays* subsp. *mays* L.) (CS), *Miscanthus* × *giganteus* stalks (MS), and wheat straw (*Triticum aestivum* L.) (WS) were each hydrothermally pretreated at three severity factors ( $\log R_0$ ): 3.65 (190 °C, 10 min), 3.83 (190 °C, 15 min), and 3.97 (195 °C, 15 min) as described previously [24]. Composition of biomass fiber fraction was determined using strong acid hydrolysis procedure based on the protocol of the National Renewable Energy Laboratory (NREL) [56].

### Isolation of lignin-rich residues (LRRs)

Isolation of the LRRs was performed according to Rahikainen et al. [13] with modifications. Extensive cellulose hydrolysis of the biomass was performed using Cellic<sup>®</sup> CTec3 (Novozymes, Bagsværd, Denmark) with a dosage of 60 mg protein/g DM biomass in 0.05 M sodium citrate buffer pH 5.0 at 50 °C with 7.5% DM solids loading for 72 h. After every 24 h of hydrolysis, the whole suspension was centrifuged, and then, fresh amount of buffer and enzyme were added as in the original amount. After 72 h, the suspension was sieved using 500- $\mu$ m mesh and washed thrice using ultrapure water pH 2.50 acidified with HCl, freeze-dried, and then protease treated. The protease treatment of the residue was done using commercial protease from *Bacillus licheniformis* (Sigma-Aldrich, St. Louis, MO, USA) at 37 °C for 24 h at 5% DM solids loading and enzyme loading of 20 mg protein/g DM residue in 0.5 M NaHCO<sub>3</sub>/Na<sub>2</sub>CO<sub>3</sub> buffer pH 9.60. After protease treatment, the LRRs were freeze-dried, ground, and used for analyses and experiments. Composition of the LRRs was determined using strong acid hydrolysis procedure [56]. Elemental analysis was performed on the LRRs to confirm the removal of adsorbed proteins using an EA3000 element analyzer with acetanilide as standard (Euro Vector Instruments & Software, Milan, Italy). After protease treatment, the nitrogen content was significantly reduced, indicating that the remaining adsorbed enzymes after extensive hydrolysis had been removed (Additional file 1: Table S3).

### Adsorption experiment

Adsorption experiment was performed using Cellic<sup>®</sup> CTec3 (Novozymes A/S, Bagsværd, Denmark) with protein loading of 20 mg/g DM. The experiments were performed in triplicates at 1% DM lignin-rich residues

in 0.05 M sodium citrate buffer pH 5.0 in 2 ml Protein LoBind<sup>®</sup> tubes (Eppendorf AG, Hamburg, Germany). The tubes were agitated using a tube revolver (Thermo Fisher Scientific Inc., Waltham, MA, USA) for 2 h at 15 RPM and incubated at 50 °C. After the experiments, liquid fractions were separated by centrifugation and stored frozen prior to analysis. The protein concentration in the liquid fraction was analyzed using ninhydrin method with bovine serum albumin (BSA) as standard [57, 58].

### Effect of lignin-rich residues (LRRs) on the hydrolysis of cellulose

The effect of the isolated LRRs on the enzymatic hydrolysis of cellulose was assessed in two experiments. In Experiment I, 1 ml of 0.2 mg protein/ml Cellic<sup>®</sup> CTec3 (Novozymes A/S, Bagsværd, Denmark) was incubated with 1% DM LRRs as in the previous adsorption experiment study for 2 h at 50 °C. Then 0.5 ml suspension of 6% DM Avicel PH-101 (Sigma-Aldrich, St. Louis, MO, USA) was added into the mixture which resulted in final total solids concentration of 2.67% DM. The final enzyme dosage being used in Experiment I therefore was 6.7 mg protein/g DM total solids (LRR and Avicel) or equivalent to 10 mg protein/g DM cellulose (Avicel). As a control, the same amount of enzyme was incubated without LRRs. In Experiment II, 1 ml of 0.2 mg protein/ml Cellic<sup>®</sup> CTec3 (Novozymes A/S, Bagsværd, Denmark) was also incubated with 1% DM LRRs as in the previous adsorption experiment study for 2 h at 50 °C. The suspension was then centrifuged, and 0.75 ml of the supernatant was mixed with 0.375 ml of 6% DM Avicel PH-101 (Sigma-Aldrich, St. Louis, MO, USA) suspension which resulted in final solids concentration of 2% DM. As a control, the same amount of liquid was taken from the same amount of enzyme that was incubated without the LRRs. In both experiments, the hydrolysis of added Avicel was performed in ThermoMixer Comfort (Eppendorf AG, Hamburg, Germany) at 50 °C and agitation of 1250 RPM with samples being taken after 1, 6 and 24 h. Samples for each time points were boiled for 10 min, centrifuged, and the supernatant was analyzed for glucose using Dionex ICS-5000 system (DionexCorp, Sunnyvale, CA, USA) as explained previously [24]. Both experiments were performed in duplicate and enzyme and substrate blanks were used for correction.

### Pyrolysis-gas chromatography-mass spectrometry (Py-GC-MS)

The lignin-rich residues were pyrolyzed in duplicates according to Jensen et al. [59] with modifications. The samples were prepared by transferring about 100–200  $\mu$ g to a pyrolysis tube. Pyrolysis was performed under a He flow of 100 ml/min at 500 °C (calibrated as sample

received temperature). The pyrolysis temperature was held for 20 s by the PYRO pyrolysis unit (GERSTEL, Mülheim an der Ruhr, Germany). The transfer line was held at 320 °C and pyrolysates were carried onto the chromatographic column with a 100:1 split in the inlet held at 300 °C. The pyrolysates were separated and detected using 7890B GC and 5977A MSD series GC–MS (Agilent, St. Clara, CA, USA) equipped with an VF-5 ms (60 m, 0.25 mm, 0.25 μm) (Agilent, St. Clara, CA, USA) column. All compounds used for calculating monolignol ratios were identified by standards or published mass spectra [60]. The compounds were grouped according to methoxylation into *H*, *G* or *S* (Additional file 1: Table S4). Monolignol ratios were calculated as the peak area of the specific monolignol in proportion to the total peak area of the three monolignols.

### Gel permeation chromatography (GPC)

The molecular weight ( $M_w$ ) distribution of aromatic compounds in the LRR samples was determined by gel permeation chromatography (GPC) using a procedure adapted from a previous study [59]. Separation of compounds was performed on a PolarSil column (300 × 8 mm, 5 μm, 100 Å) (PSS Polymer Standards Service, Mainz, Germany) at 70 °C in a 9:1 (v/v) dimethyl sulfoxide/water eluent with 0.05 M LiBr. The LRR samples were dissolved in the eluent at concentrations of 2 g/l with sonication and overnight mixing. Detection was performed using UV–Vis detector at 280 nm. Tannic acid (1701 Da), β-O-4 dimer (320 Da) and vanillin (152 Da) were used as standards to approximate the molecular weight distribution in the chromatograms.

### 2D Nuclear magnetic resonance (NMR)

The lignin-rich residues were prepared in DMSO- $d_6$ /pyridine- $d_5$  for whole plant cell wall characterization and were analyzed through heteronuclear single quantum coherence (HSQC) experiments according to the established protocol [61] as reported previously [24].

### Attenuated total reflectance-Fourier transform infrared (ATR-FTIR) spectroscopy

ATR-FTIR measurements were performed on the lignin-rich residues with five technical replicates using a Nicolet 6700 FT-IR, Pike Technologies GladiATR diamond spectrometer (Thermo Scientific, Waltham, MA, USA) as described previously [24]. The IR spectra (Additional file 1: Figures S1–S3) were normalized using Standard Normal Variate [62]. The peaks included are listed in Table 3. Monolignols ratios of syringyl (*S*), guaiacyl (*G*) and *p*-hydroxyphenyl (*H*) units of lignin, namely *H/G* and *S/G* ratios, were assessed by calculating the ratio of

estimated peak areas of 835/1508 and 1601/1508  $\text{cm}^{-1}$  respectively.

### Statistical analysis

One-way analysis of variance (ANOVA) was performed using JMP 13 (SAS Institute Inc., Cary, NC, USA) with post hoc analysis using Tukey–Kramer's Honestly Significant Difference (HSD) test at  $P \leq 0.05$ . Connecting letters were used to report the significant statistical difference among the mean values where different letters indicate that the compared mean values are significantly different. For example, values with the letters “A,” “B,” and “C” are significantly different from one another, whereas those with the letter “A” are not significantly different.

### Additional file

**Additional file 1: Table S1.** Glucose and xylose release after hydrolysis of lignin-rich residues using Cellic<sup>®</sup> CTec3. **Figures S1–S3.** ATR-FTIR spectra of lignin-rich residues (LRRs) isolated from hydrothermally pretreated (log  $R_0 = 3.65, 3.83$  and  $3.97$ ) corn stover (CS), *Miscanthus × giganteus* stalks (MS) and wheat straw (WS) and the corresponding spectra of the fiber fraction of pretreated biomass. **Figures S4–S12.**  $^{13}\text{C}$ - $^1\text{H}$  HSQC (heteronuclear single quantum coherence) spectra of lignin-rich residues (LRRs) isolated from hydrothermally pretreated (log  $R_0 = 3.65, 3.83$  and  $3.97$ ) corn stover (CS), *Miscanthus × giganteus* stalks (MS) and wheat straw (WS). **Figures S13–S15.**  $^{13}\text{C}$ - $^1\text{H}$  HSQC (heteronuclear single quantum coherence) spectra of raw (untreated) corn stover (CS), *Miscanthus × giganteus* stalks (MS) and wheat straw (WS). **Table S2.**  $^{13}\text{C}$ - $^1\text{H}$  HSQC contour integration values for triclin in the raw (untreated) biomass feedstocks. **Table S3.** Nitrogen content of the pretreated biomass feedstocks and their corresponding lignin-rich residues (LRRs) after hydrolysis and protease treatment. **Table S4.** Py-GC-MS relative peak areas (%) of compounds used for calculation of monolignol ratios of the lignin-rich residues.

### Authors' contributions

DTD, MP, HJ, and AM planned the study, analyzed the results, and wrote the manuscript. DTD performed experiments, analyzed data, and drafted the manuscript. MMJ and MG performed Py-GC–MS and GPC and participated in the corresponding data analysis. MO participated in the preparation and compositional analysis of the lignin-rich residues and adsorption experiment. AJ acquired 2D NMR spectra and participated in NMR data analysis. LGT directed the ATR-FTIR data acquisition and participated in the analysis of the spectra. All the authors read and approved the final manuscript.

### Author details

<sup>1</sup> Department of Chemical and Biochemical Engineering, Technical University of Denmark, Søtofts Plads Building 229, 2800 Kongens Lyngby, Denmark. <sup>2</sup> Department of Chemistry, Aarhus University, Langelandsgade 140, 8000 Aarhus C, Denmark. <sup>3</sup> Department of Geosciences and Natural Resource Management, University of Copenhagen, Rolighedsvej 23, 1958 Frederiksberg C, Denmark. <sup>4</sup> Present Address: Department of Plant and Environmental Sciences, University of Copenhagen, Thorvaldsensvej 40, 1871 Frederiksberg C, Denmark.

### Acknowledgements

The Combustion and Harmful Emission Control research center is thanked for providing access to elemental analyzer. René Thrane is thanked for assistance in freeze-drying.

### Competing interests

The authors declare that they have no competing interest.

**Availability of data and materials**

All data generated and analyzed during this study are included in the manuscript and its additional file in form of graphs and tables.

**Consent for publication**

All authors agree to the submission.

**Ethics approval and consent to participate**

Not applicable.

**Funding**

This study was funded by the BioValue SPIR, Strategic Platform for Innovation and Research on value added products from biomass, which is co-funded by The Innovation Fund Denmark, Case No: 0603-00522B.

**Publisher's Note**

Springer Nature remains neutral with regard to jurisdictional claims in published maps and institutional affiliations.

Received: 3 February 2018 Accepted: 17 March 2018

Published online: 02 April 2018

**References**

- Larsen J, Haven MØ, Thirup L. Inbicon makes lignocellulosic ethanol a commercial reality. *Biomass Bioenerg*. 2012;46:36–45.
- Yang B, Tao L, Wyman CE. Strengths, challenges, and opportunities for hydrothermal pretreatment in lignocellulosic biorefineries. *Biofuels Bioprod Biorefining*. 2018;12:125–38.
- Ruiz HA, Rodríguez-Jasso RM, Fernandes BD, Vicente AA, Teixeira JA. Hydrothermal processing, as an alternative for upgrading agriculture residues and marine biomass according to the biorefinery concept: a review. *Renew Sustain Energy Rev*. 2013;21:35–51.
- Mansfield SD, Mooney C, Saddler JN. Substrate and enzyme characteristics that limit cellulose hydrolysis. *Biotechnol Prog*. 1999;15:804–16.
- Himmel ME, Ding S-Y, Johnson DK, Adney WS, Nimlos MR, Brady JW, Foust TD. Biomass recalcitrance: engineering plants and enzymes for biofuels production. *Science*. 2007;315:804–7.
- Jørgensen H, Kristensen JB, Felby C. Enzymatic conversion of lignocellulose into fermentable sugars: challenges and opportunities. *Biofuels Bioprod Biorefining*. 2007;1:119–34.
- Li M, Pu Y, Ragauskas AJ. Current understanding of the correlation of lignin structure with biomass recalcitrance. *Front Chem*. 2016;4:45.
- Sipponen MH, Rahikainen J, Leskinen T, Pihlajaniemi V, Mattinen M-L, Lange H, Crestini C, Östberg M. Structural changes of lignin in biorefinery pretreatments and consequences to enzyme-lignin interactions—OPEN ACCESS. *Nord Pulp Pap Res J*. 2017;32:550–71.
- Saini JK, Patel AK, Adsul M, Singhania RR. Cellulase adsorption on lignin: a roadblock for economic hydrolysis of biomass. *Renew Energy*. 2016;98:29–42.
- Sewalt VJH, Glasser WG, Beauchemin KA. Lignin impact on fiber degradation. 3. Reversal of inhibition of enzymatic hydrolysis by chemical modification of lignin and by additives. *J Agric Food Chem*. 1997;45:1823–8.
- Berlin A, Balakshin M, Gilkes N, Kadla J, Maximenko V, Kubo S, Saddler J. Inhibition of cellulase, xylanase and beta-glucosidase activities by softwood lignin preparations. *J Biotechnol*. 2006;125:198–209.
- Tu M, Pan X, Saddler JN. Adsorption of cellulase on cellulolytic enzyme lignin from lodgepole pine. *J Agric Food Chem*. 2009;57:7771–8.
- Rahikainen J, Mikander S, Marjamaa K, Tamminen T, Lappas A, Viikari L, Kruus K. Inhibition of enzymatic hydrolysis by residual lignins from softwood - study of enzyme binding and inactivation on lignin-rich surface. *Biotechnol Bioeng*. 2011;108:2823–34.
- Lai C, Tu M, Shi Z, Zheng K, Olmos LG, Yu S. Contrasting effects of hardwood and softwood organosolv lignins on enzymatic hydrolysis of lignocellulose. *Bioresour Technol*. 2014;163:320–7.
- Ko JK, Ximenes E, Kim Y, Ladisch MR. Adsorption of enzyme onto lignins of liquid hot water pretreated hardwoods. *Biotechnol Bioeng*. 2015;112:447–56.
- Palonen H, Tjerneld F, Zacchi G, Tenkanen M. Adsorption of *Trichoderma reesei* CBH I and EG II and their catalytic domains on steam pretreated softwood and isolated lignin. *J Biotechnol*. 2004;107:65–72.
- Börjesson J, Engqvist M, Sipos B, Tjerneld F. Effect of poly(ethylene glycol) on enzymatic hydrolysis and adsorption of cellulase enzymes to pretreated lignocellulose. *Enzyme Microb Technol*. 2007;41:186–95.
- Kellock M, Rahikainen J, Marjamaa K, Kruus K. Lignin-derived inhibition of monocomponent cellulases and a xylanase in the hydrolysis of lignocelluloses. *Bioresour Technol*. 2017;232:183–91.
- Trajano HL, Engle NL, Foston M, Ragauskas AJ, Tschaplinski TJ, Wyman CE. The fate of lignin during hydrothermal pretreatment. *Biotechnol Biofuels*. 2013;6:110.
- Yelle DJ, Kaparaju P, Hunt CG, Hirth K, Kim H, Ralph J, Felby C. Two-dimensional NMR evidence for cleavage of lignin and xylan substituents in wheat straw through hydrothermal pretreatment and enzymatic hydrolysis. *Bioenerg Res*. 2013;6:211–21.
- Donohoe BS, Decker SR, Tucker MP, Himmel ME, Vinzant TB. Visualizing lignin coalescence and migration through maize cell walls following thermochemical pretreatment. *Biotechnol Bioeng*. 2008;101:913–25.
- Kristensen JB, Thygesen LG, Felby C, Jørgensen H, Elder T. Cell-wall structural changes in wheat straw pretreated for bioethanol production. *Biotechnol Biofuels*. 2008;1:5.
- Zeng Y, Himmel ME, Ding SY. Visualizing chemical functionality in plant cell walls. *Biotechnol Biofuels*. 2017;10:263.
- Djajadi DT, Hansen AR, Jensen A, Thygesen LG, Pinelo M, Meyer AS, Jørgensen H. Surface properties correlate to the digestibility of hydrothermally pretreated lignocellulosic Poaceae biomass feedstocks. *Biotechnol Biofuels*. 2017;10:49.
- Nakagame S, Chandra RP, Kadla JF, Saddler JN. The isolation, characterization and effect of lignin isolated from steam pretreated Douglas-fir on the enzymatic hydrolysis of cellulose. *Bioresour Technol*. 2011;102:4507–17.
- Lu X, Zheng X, Li X, Zhao J. Adsorption and mechanism of cellulase enzymes onto lignin isolated from corn stover pretreated with liquid hot water. *Biotechnol Biofuels*. 2016;9:118.
- Ooshima H, Burns DS, Converse AO. Adsorption of cellulase from *Trichoderma reesei* on cellulose and lignin residue in wood pretreated by dilute sulfuric acid with explosive decompression. *Biotechnol Bioeng*. 1990;36:446–52.
- Larsen J, Øtergaard Petersen M, Thirup L, Li HW, Iversen FK. The IBUS process—lignocellulosic bioethanol close to a commercial reality. *Chem Eng Technol*. 2008;31:765–72.
- Weiss N, Börjesson J, Pedersen LS, Meyer AS. Enzymatic lignocellulose hydrolysis: improved cellulase productivity by insoluble solids recycling. *Biotechnol Biofuels*. 2013;6:5.
- Rodrigues AC, Leitão AF, Moreira S, Felby C, Gama M. Recycling of cellulases in lignocellulosic hydrolysates using alkaline elution. *Bioresour Technol*. 2012;110:526–33.
- Lu X, Wang C, Li X, Zhao J, Zhao X. Studying nonproductive adsorption ability and binding approach of cellobiohydrolase to lignin during bioconversion of lignocellulose. *Energy Fuels*. 2017;31:14393–400.
- Tébéka IRM, Silva AGL, Petri DFS. Hydrolytic activity of free and immobilized cellulase. *Langmuir*. 2009;25:1582–7.
- Li Y, Sun Z, Ge X, Zhang J. Effects of lignin and surfactant on adsorption and hydrolysis of cellulases on cellulose. *Biotechnol Biofuels*. 2016;9:20.
- Nakagame S, Chandra RP, Saddler JN. The effect of isolated lignins, obtained from a range of pretreated lignocellulosic substrates, on enzymatic hydrolysis. *Biotechnol Bioeng*. 2010;105:871–9.
- Barsberg S, Selig MJ, Felby C. Impact of lignins isolated from pretreated lignocelluloses on enzymatic cellulose saccharification. *Biotechnol Lett*. 2013;35:189–95.
- Yarbrough JM, Mittal A, Mansfield E, Taylor LE, Hobdley SE, Sammond DW, Bomble YJ, Crowley MF, Decker SR, Himmel ME, Vinzant TB. New perspective on glycoside hydrolase binding to lignin from pretreated corn stover. *Biotechnol Biofuels*. 2015;8:214.
- Li J, Henriksson G, Gellerstedt G. Lignin depolymerization/repolymerization and its critical role for delignification of aspen wood by steam explosion. *Bioresour Technol*. 2007;98:3061–8.
- del Río JC, Rencoret J, Prinsen P, Martínéz ÁT, Ralph J, Gutiérrez A. Structural characterization of wheat straw lignin as revealed by analytical pyrolysis, 2D-NMR, and reductive cleavage methods. *J Agric Food Chem*. 2012;60:5922–35.

39. Jensen A, Cabrera Y, Hsieh C-W, Nielsen J, Ralph J, Felby C. 2D NMR characterization of wheat straw residual lignin after dilute acid pretreatment with different severities. *Holzforschung*. 2017;71:461–9.
40. Faix O. Classification of lignins from different botanical origins by FT-IR spectroscopy. *Holzforschung*. 1991;45:21–7.
41. Santos JJ, Martín-sampedro R, Fillat Ú, Oliva JM, Negro MJ, Ballesteros M, Eugenio ME, Ibarra D. Evaluating lignin-rich residues from biochemical ethanol production of wheat straw and olive tree pruning by FTIR and 2D-NMR. *Int J Polym Sci*. 2015;2015:11.
42. Huang Y, Wang L, Chao Y, Nawawi DS, Akiyama T, Yokoyama T, Matsumoto Y. Analysis of lignin aromatic structure in wood based on the IR spectrum. *J Wood Chem Technol*. 2012;32:294–303.
43. Derkacheva OY. Estimation of aromatic structure contents in hardwood lignins from IR absorption spectra. *J Appl Spectrosc*. 2013;80:670–6.
44. Tana T, Zhang Z, Moghaddam L, Rackemann DW, Rencoret J, Gutiérrez A, del Río JC, Doherty WOS. Structural changes of sugar cane bagasse lignin during cellulosic ethanol production process. *ACS Sustain Chem Eng*. 2016;4:5483–94.
45. Wayman M, Chua MGS. Characterization of autohydrolysis aspen (*P. tremuloides*) lignins. Part 2. Alkaline nitrobenzene oxidation studies of extracted autohydrolysis lignin. *Can J Chem*. 1979;57:2599–602.
46. Li C, Knierim B, Manisseri C, Arora R, Scheller HV, Auer M, Vogel KP, Simmons BA, Singh S. Comparison of dilute acid and ionic liquid pretreatment of switchgrass: biomass recalcitrance, delignification and enzymatic saccharification. *Bioresour Technol*. 2010;101:4900–6.
47. Li M, Cao S, Meng X, Studer M, Wyman CE, Ragauskas AJ, Pu Y. The effect of liquid hot water pretreatment on the chemical—structural alteration and the reduced recalcitrance in poplar. *Biotechnol Biofuels*. 2017;10:237.
48. Yu Z, Gwak K-S, Treasure T, Jameel H, Chang H, Park S. Effect of lignin chemistry on the enzymatic hydrolysis of woody biomass. *Chemschem*. 2014;7:1942–50.
49. Samuel R, Pu Y, Raman B, Ragauskas AJ. Structural characterization and comparison of switchgrass ball-milled lignin before and after dilute acid pretreatment. *Appl Biochem Biotechnol*. 2010;162:62–74.
50. Pu Y, Hu F, Huang F, Davison BH, Ragauskas AJ. Assessing the molecular structure basis for biomass recalcitrance during dilute acid and hydrothermal pretreatments. *Biotechnol Biofuels*. 2013;6:15.
51. Pielhop T, Larrazábal GO, Studer MH, Brethauer S, Seidel C-M, Rudolf von Rohr P. Lignin repolymerisation in spruce autohydrolysis pretreatment increases cellulase deactivation. *Green Chem R Soc Chem*. 2015;17:3521–32.
52. Eloy NB, Voorend W, Lan W, de Saleme MLS, Cesarino I, Vanholme R, Smith RA, Goeminne G, Pallidis A, Morreel K, Nicomedes J, Ralph J, Boerjan W. Silencing chalcone synthase in maize impedes the incorporation of tricin into lignin and increases lignin content. *Plant Physiol*. 2017;173:998–1016.
53. Ju X, Engelhard M, Zhang X. An advanced understanding of the specific effects of xylan and surface lignin contents on enzymatic hydrolysis of lignocellulosic biomass. *Bioresour Technol*. 2013;132:137–45.
54. Wallace J, Brienzo M, García-Aparicio MP, Görgens JF. Lignin enrichment and enzyme deactivation as the root cause of enzymatic hydrolysis slowdown of steam pretreated sugarcane bagasse. *N Biotechnol*. 2016;33:361–71.
55. Dumitrache A, Tolbert A, Natzke J, Brown SD, Davison BH, Ragauskas AJ. Cellulose and lignin colocalization at the plant cell wall surface limits microbial hydrolysis of Populus biomass. *Green Chem R Soc Chem*. 2017;19:2275–85.
56. Sluiter A, Hames B, Ruiz R, Scarlata C, Sluiter J, Templeton D, Crocker D. Determination of structural carbohydrates and lignin in biomass. Golden: Laboratory analytical procedure (LAP), NREL/TP-510-42618; 2008.
57. Starcher B. A ninhydrin-based assay to quantitate the total protein content of tissue samples. *Anal Biochem*. 2001;292:125–9.
58. Tu M, Chandra RP, Saddler JN. Recycling cellulases during the hydrolysis of steam exploded and ethanol pretreated lodgepole pine. *Biotechnol Prog*. 2007;23:1130–7.
59. Jensen MM, Madsen RB, Becker J, Iversen BB, Glasius M. Products of hydrothermal treatment of lignin and the importance of ortho-directed repolymerization reactions. *J Anal Appl Pyrolysis*. 2017;126:371–9.
60. Ralph J, Hatfield RD. Pyrolysis-GC-MS characterization of forage materials. *J Agric Food Chem*. 1991;39:1426–37.
61. Mansfield SD, Kim H, Lu F, Ralph J. Whole plant cell wall characterization using solution-state 2D NMR. *Nat Protoc*. 2012;7:1579–89.
62. Barnes RJ, Dhanoa MS, Lister SJ. Standard normal variate transformation and de-trending of near-infrared diffuse reflectance spectra. *Appl Spectrosc*. 1989;43:772–7.
63. Schwanninger M, Rodrigues JC, Pereira H, Hinterstoesser B. Effects of short-time vibratory ball milling on the shape of FT-IR spectra of wood and cellulose. *Vib Spectrosc*. 2004;36:23–40.
64. Baas P. Interference microscopic studies on wood plastic and cell wall-liquid interactions in beech. *J Microsc*. 1975;104:83–90.

Submit your next manuscript to BioMed Central and we will help you at every step:

- We accept pre-submission inquiries
- Our selector tool helps you to find the most relevant journal
- We provide round the clock customer support
- Convenient online submission
- Thorough peer review
- Inclusion in PubMed and all major indexing services
- Maximum visibility for your research

Submit your manuscript at  
[www.biomedcentral.com/submit](http://www.biomedcentral.com/submit)



## PAPER III

---

Cellulases adsorb reversibly on biomass lignin

**Djajadi DT†, Pihlajaniemi V†, Rahikainen J, Kruus K, Meyer AS**

Submitted to *Biotechnol. Bioeng.* (2018)

†: Equal contribution



1 Cellulases adsorb reversibly on biomass lignin

2

3 Demi T. Djajadi<sup>1†</sup>, Ville Pihlajaniemi<sup>2†</sup>, Jenni Rahikainen<sup>2</sup>, Kristiina Kruus<sup>2</sup>, Anne S.

4 Meyer<sup>1\*</sup>

5

6 Affiliations:

7 1: Department of Chemical and Biochemical Engineering, Søtofts Plads Building 229,

8 Technical University of Denmark, 2800 Kongens Lyngby, Denmark.

9 2: VTT Technical Research Center of Finland Ltd, P.O. Box 1000, 02044 VTT, Finland.

10

11 \*Corresponding author:

12 Anne S. Meyer

13 Address: Søtofts Plads Building 229, Technical University of Denmark, 2800 Kongens

14 Lyngby, Denmark

15 Phone: +45-45252909

16 Email: [am@kt.dtu.dk](mailto:am@kt.dtu.dk)

17

18 †: Equal contribution

19

20 Short running title: Cellulases adsorb reversibly on biomass lignin

21

22 Grant numbers

23 0603-00522B

24

25

26 Abstract

27 Adsorption of cellulases on lignin is considered a major factor in retarding enzymatic  
28 cellulose degradation. However, the adsorption mechanisms and kinetics are not well  
29 understood for individual cellulases. This study examines the binding affinity, kinetics of  
30 adsorption, and competition of monocomponent cellulases during adsorption on lignin.  
31 *TrCel7A*, *TrCel6A*, *TrCel7B* and *TrCel5A* were radiolabeled for adsorption experiments on  
32 lignin-rich residues (LRRs) isolated from hydrothermally pretreated spruce (L-HPS) and  
33 wheat straw (L-HPWS), respectively. Based on adsorption isotherms fitted to the Langmuir  
34 model, the ranking of binding affinities was  $TrCel5A > TrCel6A > TrCel7B > TrCel7A$  on  
35 both LRRs. The enzymes had higher affinity on L-HPS than on L-HPWS. Adsorption  
36 experiments with dilution after 1 h and 24 h and kinetic modelling were performed to  
37 quantify any irreversible binding over time. Models with reversible binding parameters fitted  
38 well and can explain the results. The adsorption constants obtained from the reversible  
39 models agreed with the fitted Langmuir isotherms and suggested that reversible adsorption-  
40 desorption existed at equilibrium. Competitive binding experiments showed that individual  
41 types of cellulases competed for binding sites on lignin and the adsorption data fitted well  
42 with Langmuir model. Overall, the data strongly indicates that the adsorption of cellulases on  
43 lignin is reversible.

44

45 Key words: cellulase, lignin, biomass, adsorption, reversible, competition

46

47

48

49

50

51 Introduction

52 Lignin has been considered as one of the major obstructions in biorefinery operations aiming  
53 to enzymatically convert mainly cellulose from lignocellulosic biomass into glucose prior to  
54 further downstream processing (Li, Pu, & Ragauskas, 2016). Non-productive adsorption of  
55 cellulases on lignin is considered an important mechanism in inducing retardation of  
56 enzymatic cellulose degradation (Liu, Sun, Leu, & Chen, 2016; Saini, Patel, Adsul, &  
57 Singhania, 2016; Sipponen et al., 2017). Studies have reported adsorption of cellulases on  
58 lignin isolated from various biomass feedstocks and thus have correlated it with the observed  
59 retardation of enzymatic degradation of pure model cellulose in the presence of the isolated  
60 lignin (Kellock, Rahikainen, Marjamaa, & Kruus, 2017; Rahikainen et al., 2011; Tu, Pan, &  
61 Saddler, 2009). Hydrophobic interaction (Sammond et al., 2014; Tu et al., 2009), electrostatic  
62 interaction (Lan, Lou, & Zhu, 2013; Yarbrough et al., 2015), and hydrogen bonding (Sewalt,  
63 Glasser, & Beauchemin, 1997; Yu et al., 2014) have been attributed as the cause of the non-  
64 productive binding, although there can be several simultaneous interactions among the  
65 different chemical groups in the lignin and enzymes (Liu et al., 2016; Nakagame, Chandra,  
66 Kadla, & Saddler, 2011; Rahikainen, Evans, et al., 2013; Sipponen et al., 2017).

67           Accordingly, several mitigating efforts by including additives such as BSA and  
68 surfactants in the hydrolysis reaction (Börjesson, Engqvist, Sipos, & Tjerneld, 2007; Yang &  
69 Wyman, 2006), engineering the charge of the enzymes (Whitehead, Bandi, Berger, Park, &  
70 Chundawat, 2017) or changing the pH of the reaction (Lan et al., 2013) have been employed  
71 with varying degrees of success. However, the precise mechanism in the enzyme-lignin  
72 interaction that leads to reduced recoverable activity or cellulose conversion is not well  
73 understood, especially with respect to individual enzymes in a cellulolytic mixture. There are  
74 also studies reporting that isolated lignin neither retarded the enzymatic cellulose degradation  
75 (Barsberg, Selig, & Felby, 2013; Djajadi et al., 2018) nor reduced the recoverable activity

76 after adsorption (Rodrigues, Leitão, Moreira, Felby, & Gama, 2012). These studies suggested  
77 that the binding of the enzymes on lignin is reversible by nature. However, such phenomenon  
78 has not been investigated up to date as the loss of enzyme activity due to non-productive  
79 adsorption on lignin has been considered as irreversible (Saini et al., 2016).

80           Generally, adsorption of protein on solid surface is known as a dynamic process  
81 involving partial exchange of adsorbed and desorbed states. During the process however, the  
82 constant conformational rearrangements between the two states can compromise the  
83 structural integrity of the protein, leading to irreversible structural change(s) that can affect  
84 subsequent adsorption behavior (Norde, 1986). This denaturation due to protein unfolding  
85 has been suggested as the cause of reduced enzymatic cellulose degradation in the presence  
86 of lignin (Rahikainen et al., 2011; Sammond et al., 2014), especially at elevated temperature  
87 (Börjesson et al., 2007; Rahikainen et al., 2011). Consequently, cellulose hydrolysis by  
88 thermostable enzymes was affected less by lignin compared to that performed by enzymes  
89 with lesser thermostability (Rahikainen, Moilanen, et al., 2013). In this study, well-  
90 characterized monocomponent cellulases were studied to assess their binding affinity on  
91 lignin-rich residues from different biomass feedstocks, to distinguish reversible and  
92 irreversible bindings over extended reaction time using kinetic experiments and modelling, as  
93 well as to assess their competition with one another during adsorption on lignin.

94

95 **Materials and methods**

96 *Biomass pretreatment and lignin isolation*

97 Lignin-rich residues (LRRs) were obtained from extensive enzymatic hydrolysis of  
98 hydrothermally pretreated spruce (HPS) and wheat straw (HPWS) followed by protease  
99 treatment optimized from previous method (Rahikainen et al., 2011). The hydrothermal  
100 pretreatment (HTP) conditions were 195°C for 15 min ( $\log R_0 = 3.97$ ) for wheat straw

101 (Djajadi et al., 2017) and 200°C for 10 min ( $\log R_0 = 3.94$ ) for spruce. The composition of the  
102 LRRs have been determined using the National Renewable Energy Laboratory (NREL)  
103 protocol (Sluiter et al., 2008). The LRRs contained 82.3% and 83.7% total lignin for lignin  
104 from hydrothermally pretreated spruce (L-HPS) and wheat straw (L-HPWS), respectively.

105

#### 106 *Enzyme purification and characterization*

107 Monocomponent cellulases, i.e. cellobiohydrolases (CBHs: *TrCel7A* and *TrCel6A*) and  
108 endoglucanases (EGs: *TrCel7B* and *TrCel5A*) were produced from *Trichoderma reesei*  
109 (Teleomorph *Hypocrea jecorina*) at VTT and were purified according to previous work  
110 (Suurnäkki et al., 2000). The molecular weights ( $M_{ws}$ ), isoelectric point (pI) and  
111 hydrophobic surface characteristics (patch score) of the enzymes have been determined  
112 previously (Kellock et al., 2017; Várnai, Siika-aho, & Viikari, 2013). Final protein purity and  
113 protein concentration were determined using SDS-PAGE analysis with Criterion Imaging  
114 System and Detergent Compatible (DC) Protein assay (Bio-Rad Laboratories Inc., CA,  
115 USA), respectively. The details of the enzymes used in this study are presented in Table I.

116

#### 117 *Radiolabeling of the enzymes through reductive methylation*

118 The enzymes (*TrCel7A*, *TrCel6A*, *TrCel7B* and *TrCel5A*) were radiolabeled with tritium  
119 through reductive methylation using tritiated sodium borohydride ( $[^3\text{H}]\text{NaBH}_4$ ) and  
120 formaldehyde ( $\text{CH}_2\text{O}$ ) (Means & Feeney, 1968; Tack, Dean, Eilat, Lorenz, & Schechter,  
121 1980) with modifications according to previous works (Rahikainen, Evans, et al., 2013;  
122 Wahlström, Rahikainen, Kruus, & Suurnäkki, 2014). For the reaction, 3 mg enzyme was  
123 buffer-exchanged in 0.2 M sodium borate buffer pH 8.5 at 4°C and was incubated on ice.  
124 Formaldehyde solution (Sigma–Aldrich Co., MO, USA) was added in 5-fold molar excess of  
125 the molar concentration of free amino groups in the enzyme.  $[^3\text{H}]\text{NaBH}_4$  with 100 mCi

126 activity (5–15 Ci/mmol, PerkinElmer, MA, USA) was dissolved in 0.01 M NaOH (1 Ci/ml)  
127 and added to the reaction. After 60 min, the reaction was stopped by transferring the mixture  
128 to Econo-Pac 10 DC gel filtration column (Bio-Rad Laboratories Inc., CA, USA) and eluting  
129 it with 0.05 M sodium acetate buffer pH 5.0 to exchange the buffer solution. The protein-rich  
130 fractions were pooled and transferred to another gel filtration column. The specific  
131 radioactivities as determined by liquid scintillation counting (LSC) and protein concentration  
132 assay were 0.5, 0.5, 1.7, and 2.8 Ci/mmol for *TrCel7A*, *TrCel6A*, *TrCel7B* and *TrCel5A*  
133 respectively. Accordingly, in the subsequent adsorption experiments, the <sup>3</sup>H-labeled enzymes  
134 were mixed in 1:20 (for *TrCel7A* and *TrCel6A*) and 1:50 dilution ratio (for *TrCel7B* and  
135 *TrCel5A*) with their non-radiolabeled counterparts to allow accurate detection as done  
136 previously (Rahikainen, Evans, et al., 2013; Wahlström et al., 2014). SDS-PAGE analysis  
137 indicated that there was no degradation of the radiolabeled enzymes (Figure S1).

138

#### 139 *Adsorption experiments and liquid scintillation counting (LSC)*

140 All of the enzyme adsorption experiments were performed in 0.05 M sodium acetate buffer  
141 pH 5.0 at substrate concentration of 1% DM and temperature of 45°C with moderate mixing.  
142 After 1 h incubation, the experiment was terminated by centrifugation and the supernatant  
143 was collected for determination of unbound enzymes using LSC. The supernatant was mixed  
144 with Ultima Gold™ XR liquid scintillation cocktail (PerkinElmer, MA, USA) and the counts  
145 per minute values of the <sup>3</sup>H-labeled enzymes were measured using Tri-Carb 2810 TR liquid  
146 scintillation counter (PerkinElmer, MA, USA) with 15 min counting time. Enzyme blanks  
147 were used to determine the fraction of bound enzyme. Adsorption isotherms were established  
148 at initial protein concentration range of 2-16 µM for L-HPS and 1-8 µM for L-HPWS in  
149 triplicates for each concentration. The adsorption isotherms data were fitted to the one  
150 binding-site Langmuir adsorption model (Eq. 1).

$$B = B_{max} \frac{K_{ads}[F]}{1 + K_{ads}[F]} \quad (1)$$

151 Where B is the amount of bound enzyme,  $B_{max}$  is the maximum adsorption capacity,  $K_{ads}$  is  
152 the Langmuir affinity constant and [F] is the concentration of unbound enzyme.

153

#### 154 *Reversibility test and kinetic modeling of adsorption*

155 The reversibility test was conducted at similar conditions as with adsorption isotherms. The  
156 experiment was performed using *TrCel5A* and *TrCel6A* on both L-HPS and L-HPWS. The  
157 enzymes were incubated with 1% DM LRRs at concentrations of 4, 8, 16  $\mu\text{M}$  for L-HPS and  
158 2, 4, 8  $\mu\text{M}$  for L-HPWS. Subsamples were taken at different time points, centrifuged and  
159 measured to determine the amount of enzyme bound. There were two sets of reaction in  
160 which two-fold buffer dilution was performed at different time points. In the first set of  
161 reaction, the “Early Dilution”, the samples were incubated for 1 h, after which a subsample  
162 was taken and dilution was performed. After dilution, the binding of the enzyme was then  
163 followed after 1, 5 and 23 h by taking subsamples. In the second set of reaction, the “Late  
164 Dilution”, the samples were incubated for 24 h during which subsamples were taken after 1, 6  
165 and 24 h incubation. After 24 h, buffer dilution was performed and subsamples were taken  
166 after 1, 5 and 23 h to follow the binding of the enzymes. The experiments were performed in  
167 duplicates and enzyme blanks were used to determine the amount of the enzyme bound.

168 Kinetic modelling was performed by using Matlab R2015a (The Mathworks  
169 Inc., MA, USA). The differential equations of a kinetic model were solved by numerical  
170 integration using *ode15s* ordinary differential equation solver. The resulting time curves were  
171 simultaneously fitted to the combined data from the Early Dilution and Late Dilution  
172 experiments of an enzyme-lignin pair by nonlinear regression using *lsqcurvefit*. The fitting  
173 parameters included the rate constants of reversible adsorption  $k_{Rev}$ , desorption  $k_{-Rev}$ , and  
174 irreversible adsorption  $k_{Ir}$  and the maximum adsorption capacity of lignin,  $B_{max}$ . In order to

175 find the global maximum for the iterative fitting procedure, the fitting was repeated with a  
176 full factorial set of initial value combinations with five different initial values (10, 1, 0.01,  
177 0.0001 and 0) for each rate constant and two initial values for the adsorption capacity  $B_{\max}$ ,  
178 including the maximum observed adsorption and its double. For three rate constants and a  
179 single  $B_{\max}$  this meant 250 repetitions of fitting. The identifiability of the parameters was  
180 assessed statistically according to previous work (Pihlajaniemi, Sipponen, Kallioinen,  
181 Nyssölä, & Laakso, 2016), by determining the relative standard deviation (RSD) of each  
182 parameter from the set of best fitting parameters, including the sets with the  $R^2$  at least 99%  
183 of the highest  $R^2$ .

184

#### 185 *Competitive binding experiment*

186 Competitive binding experiments were performed similarly as with the adsorption isotherms  
187 experiments, except that an equimolar amount of another enzyme type was added on top of  
188 the other prior to the experiments to establish adsorption isotherms. *TrCel5A* and *TrCel6A*  
189 were chosen in this experiment, so that in one experiment a radiolabeled *TrCel5A* was  
190 accompanied with non-radiolabeled *TrCel6A* and vice versa. The isotherms were established  
191 at the ranges of 2-16  $\mu\text{M}$  for L-HPS and 1-8  $\mu\text{M}$  for L-HPWS using triplicates for each  
192 concentration. Enzyme blanks were used to determine the fraction of bound enzyme.

193

#### 194 *Statistical analysis*

195 One-way analysis of variance (ANOVA) was performed using JMP 12 (SAS Institute Inc.,  
196 NC, USA) with post hoc analysis using Tukey–Kramer’s Honestly Significant Difference  
197 (HSD) test at  $p \leq 0.05$ . Fitting of isotherms data to one-site Langmuir adsorption model was  
198 performed using OriginPro 2016 (OriginLab Corporation, MA, USA).

199



200 Results and discussion

201 *Binding of monocomponent cellulases on lignin-rich residues*

202 Adsorption isotherms of *TrCel7A*, *TrCel6A*, *TrCel7B* and *TrCel5A* on lignin-rich residues  
203 (LRRs) isolated from hydrothermally pretreated spruce (L-HPS) and wheat straw (L-HPWS)  
204 were established to determine their binding affinity in hydrolytic conditions (pH 5.0 and  
205 45°C). The isotherms revealed that *TrCel5A* had the highest affinity on both L-HPS and L-  
206 HPWS (Figure 1). In the adsorption on L-HPS, the binding of *TrCel5A* was noticeably higher  
207 compared to the other enzymes, although less pronounced in the case of binding on L-HPWS.  
208 Visually, the order of the enzymes' affinity was more distinct on L-HPWS compared to L-  
209 HPS where the following order of decreasing value can be made: *TrCel5A* > *TrCel6A* >  
210 *TrCel7B* > *TrCel7A*. In general, the enzymes had higher affinity on L-HPS compared to L-  
211 HPWS as previously shown in the case of *MaCel45A* (Rahikainen, Evans, et al., 2013).

212           One binding-site Langmuir adsorption model was fitted to the isotherms data to  
213 provide quantitative parameters of the binding. The Langmuir adsorption model has  
214 previously been used to model the binding of cellulases to lignin (Börjesson et al., 2007;  
215 Rahikainen, Evans, et al., 2013; Tu et al., 2009) due to its simplicity and versatility despite  
216 the inadequacy and shortcomings to depict the adsorption of proteins on solid surface  
217 (Latour, 2015; Rabe, Verdes, & Seeger, 2011). The relative association constant ( $\alpha$ ) in  
218 particular has been shown to reflect the relative affinity during the initial slope of the  
219 isotherm (Gilkes et al., 1992; Nidetzky, Steiner, Hayn, & Claeysens, 1994; Rahikainen,  
220 Evans, et al., 2013). Accordingly, the order of affinity based on  $\alpha$  values (Table 2) fits with  
221 the visual observation noticed in the isotherms curve for both L-HPS and L-HPWS (Figure 1)  
222 and confirmed the previously mentioned ranking of binding affinity: *TrCel5A* > *TrCel6A* >  
223 *TrCel7B* > *TrCel7A*.

224 Alternatively, analyzing adsorption at the lower concentration range of an  
225 isotherm also provides information on the affinity of the enzyme in non-saturated conditions.  
226 At low initial protein concentration, the ratio of unbound compared to bound enzyme is very  
227 low. Therefore the fraction of the bound enzyme reflects the initial affinity towards the  
228 substrate without oversaturation of the surface of the adsorbent or excessive interaction  
229 among adsorbate molecules. The fraction of bound enzyme at initial protein concentration of  
230 2  $\mu\text{M}$  after 1 h showed that *TrCel5A* had the highest binding with 88 and 55 % of enzymes  
231 adsorbed on both L-HPS and L-HPWS, respectively (Figure 2). The degree of binding  
232 affinity based on the fraction of bound enzyme both on L-HPS and L-HPWS (Figure 2) was:  
233  $TrCel5A > TrCel6A > TrCel7A = TrCel7B$ . To a certain extent, this also confirmed the  
234 similar previously established order based on visual observation of the isotherms curve  
235 (Figure 1) and fitted  $\alpha$  values (Table II).

236 The results in this work evidently showed that *TrCel5A* had the highest binding  
237 affinity compared to all the tested enzymes, both in L-HPS and L-HPWS (Figures 1 and 2).  
238 In a recent study where the same set of enzymes were subjected to binding with model  
239 surface lignin isolated from HPS and HPWS on quartz crystal microbalance with dissipation  
240 monitoring (QCM-D), *TrCel7B* had the highest binding (Kellock et al., 2017). The finding is  
241 in contrast with this study where *TrCel7B* had the second lowest affinity (Table II). However,  
242 based on maximum adsorption capacity ( $B_{\text{max}}$ ), the values of *TrCel7B* and *TrCel5A* were in  
243 the same magnitude both in L-HPS and L-HPWS (Table II) which can explain the  
244 discrepancy of the finding in the two works. Regardless, direct comparison between the  
245 previous QCM-D work (Kellock et al., 2017) and this current work will be difficult due to  
246 different underlying mechanisms in the methods and even properties of the isolated lignin  
247 (Rahikainen, Martin-Sampedro, et al., 2013). Both current work (Figures 1 and 2, Table II)

248 and previous study (Kellock et al., 2017) nevertheless agreed that *TrCel6A* had the second  
249 highest affinity and *TrCel7A* had the lowest affinity from the four tested enzymes.

250           The binding affinity of the enzymes was compared with their intrinsic  
251 properties in order to find correlation between the two. *TrCel5A*, which bound the highest,  
252 has the lowest molecular weight ( $M_w$ ) of the tested monocomponent cellulases (Table I).  
253 However, the trend is not consistent across the enzymes since *TrCel7A*, which had the lowest  
254 affinity, had the second highest  $M_w$ . The highest affinity of *TrCel5A* and *TrCel6A* correlated  
255 to their pI values, which are above the experimental pH value of 5.0. This rendered them to  
256 be positively charged and therefore increased the tendency to bind to isolated lignin-rich  
257 residues from hydrothermally pretreated spruce and wheat straw which were previously  
258 found to be negatively-charged in the experimental pH (Rahikainen, Evans, et al., 2013).  
259 However, the trend is not consistent since the pI value of the dominant band was lower in  
260 *TrCel5A* compared to *TrCel6A* (Table I). Estimated hydrophobic patch score did not provide  
261 a clear trend either since both the overall and carbohydrate binding module (CBM) scores  
262 were both second highest in the case of *TrCel7A* (Table I), which had the lowest affinity  
263 (Figure 1). At this point, correlating the affinity of the enzymes with their properties was not  
264 feasible, yet the enzymes displayed similar ranking of affinity in the two substrates.  
265 Experiments at longer duration will be needed to assess the nature of the binding.

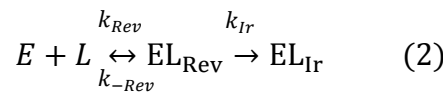
266

### 267 *Reversibility test and kinetic modeling of adsorption*

268 Kinetic modelling was applied for studying the proportions and potential mechanisms of  
269 reversible and irreversible adsorption of *TrCel6A* and *TrCel5A* on L-HPS and L-HPWS.  
270 First, the time course of adsorption and subsequent desorption after dilution of the system by  
271 a factor of two were determined. The dilution was performed either after 1 h (early dilution)  
272 or 24 h of adsorption (late dilution). Three initial enzyme concentrations were used, covering

293 the linear and saturated areas of the adsorption isotherms (Figure 1). The aim was to quantify  
 294 the proportion of irreversible binding from the difference in desorption after early and late  
 295 dilution, and to provide data for distinguishing the different models. The idea was that the  
 296 longer incubation prior to the late dilution would allow irreversible binding to advance  
 297 further and lead to lower desorption of enzymes compared to the early dilution, which would  
 298 allow quantification of the proportion and the rate constant of irreversible binding.

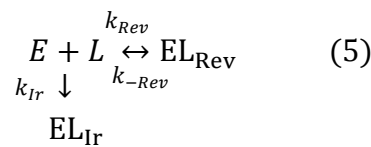
299 Four different kinetic models were studied. Model 1 (Eq. 2) describes reversible  
 300 adsorption which may turn into irreversible by a further 1<sup>st</sup> order reaction, resulting in kinetic  
 301 equations Eq. 3 and Eq. 4, where E stands for free enzymes, L for free binding sites and EL  
 302 for bound enzymes, and the subscripts <sub>Rev</sub> and <sub>Ir</sub> refer to reversible and irreversible binding  
 303 and the corresponding rate constants k. The concentration of free sites is the proportion of  
 304 unoccupied sites multiplied by lignin concentration,  $[L] = (B_{\max} - (EL_{\text{Rev}} + EL_{\text{Ir}})) * [\text{lignin}]$ .



$$\frac{dEL_{\text{Rev}}}{dt} = k_{\text{Rev}}[E][L] - (k_{-Rev} + k_{\text{Ir}})[EL_{\text{Rev}}] \quad (3)$$

$$\frac{dEL_{\text{Ir}}}{dt} = k_{\text{Ir}}[EL_{\text{Rev}}] \quad (4)$$

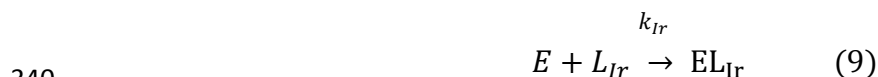
308 Model 2 (Eq. 5) describes separate reversible and irreversible binding on the same binding  
 309 sites, representing a situation where binding may occur differently, depending on e.g.  
 310 orientation; therefore following the Langmuir-kinetics of reversible adsorption (Eq. 6) and a  
 311 2<sup>nd</sup> order reaction of irreversible binding (Eq. 7) in parallel.



$$\frac{dEL_{\text{Rev}}}{dt} = k_{\text{Rev}}[E][L] - k_{-Rev}[EL_{\text{Rev}}] \quad (6)$$

336 
$$\frac{dEL_{Ir}}{dt} = k_{Ir}[E][L] \quad (7)$$

337 Models 3 and 4 represent completely reversible (Langmuirian) (Eq. 8) and completely  
 338 irreversible (Eq. 9) adsorption, each follows the kinetics of Eq. 6 and Eq. 7, respectively.



341 The models were fitted to the experimental data and compared in terms of  $R^2$  and parameter  
 342 identifiability. Identifiability describes whether the parameter value could be determined  
 343 exclusively, displaying importance for the fit, or whether it can adopt an arbitrary value,  
 344 deeming it irrelevant. The identifiability was described as relative standard deviation (RSD)  
 345 of each parameter at the optimum fit, determined from the set of repetitions reaching at least  
 346 99% of the best fit, according to  $R^2$ .

347 Majority of adsorption occurred during the first hour, after which only minor  
 348 changes were observed (Figure 3); indicating that equilibrium was reached within 1 h of  
 349 adsorption. *TrCel6A* and *TrCel5A* showed similar adsorption patterns, whereas they differed  
 350 on L-HPS and L-HPWS (Figures S2-S5). After dilution, minor or no release of enzymes  
 351 occurred from L-HPS, whereas considerable desorption from L-HPWS-lignin was observed.  
 352 The lack of desorption from L-HPS appears to suggest irreversible binding, but on a closer  
 353 look this conclusion turns out to be premature. In fact, completely irreversible adsorption  
 354 fitted poorly to the data (Figure S6) with  $R^2$  below 0.78 in each case (Table III). Given the  
 355 high initial rate of adsorption, the long incubation should have easily allowed completion of  
 356 irreversible binding, thus leading to either depletion of free enzymes or complete saturation  
 357 of binding sites. However, such behavior was not observed and instead, equilibrium was  
 358 reached at each concentration between free and adsorbed enzymes and the endpoints

316 followed a Langmuir isotherm (Figure S6). By definition, both the dynamic equilibrium and  
317 Langmuirian behavior indicate reversible adsorption.

318           Displaying the data from the dilution experiments as binding isotherms revealed  
319 that most of the points after dilution returned to the original point prior to dilution (Figures S7  
320 and S8). In other words, the ascending isotherm (prior to dilution) overlaps with the  
321 descending isotherm (after dilution), displaying no hysteresis. This behavior has also been  
322 described as a display of fully reversible binding during studies on the binding of  
323 monocomponent cellulases on cellulose (Palonen, Tenkanen, & Linder, 1999; Pellegrini et  
324 al., 2014). The Langmuir constants  $K_{ads} = \frac{k_{Rev}}{k_{-Rev}}$  and  $B_{max}$  determined from the kinetic  
325 modelling (Table III) and those determined from the adsorption isotherms data (Table II) are  
326 found to be in agreement with one another (Figure S9). These observations further gave  
327 strong indication of reversible binding on lignin. The adsorption constant ( $K_{ads}$ ) of *TrCel6A*  
328 and *TrCel5A* were lower on L-HPWS compared to L-HPS both in the adsorption isotherms  
329 fitting (Table II) and modelling data (Table III). This indicated lower binding affinity of  
330 cellulases on L-HPWS than L-HPS which is in accordance with the high desorption on L-  
331 HPWS following dilution (Figure 3). The difference in affinity can offer explanation on the  
332 previous observations where L-HPS was found to retard the enzymatic hydrolysis of model  
333 cellulose more than L-HPWS (Kellock et al., 2017; Rahikainen, Moilanen, et al., 2013).

334           For L-HPS, the Models 1 and 2 showed a similar fit ( $R^2$  of 0.896–0.923) and  
335 parameter values as completely reversible adsorption and poor identifiability was observed  
336 for the irreversible adsorption rate constant  $k_{Ir}$  (RSD from 140 % to  $4.8 \times 10^7$  %), indicating  
337 that reversible adsorption behavior can fully explain the results. No quantifiable irreversible  
338 binding was observed and the reason for low desorption was high affinity of L-HPS (Table  
339 III). For L-HPWS, a higher amount of desorption provided a higher resolution for  
340 determining irreversible binding. Model 1 showed a slightly better fit for both enzymes ( $R^2$  of

341 0.945 and 0.967) compared to reversible binding (0.936 and 0.965) with a relevant  
342 irreversible binding rate (RSD of  $k_{Ir}$  lower than that of  $k_{Rev}$  and  $k_{-Rev}$ ), whereas Model 2  
343 neither provided improvement in fit nor relevance of  $k_{Ir}$  (Table III). This suggested partial  
344 irreversible binding on L-HPWS and that the enzymes are first bound reversibly, which is  
345 then followed by further interactions leading to irreversible binding. This is in line with the  
346 idea of protein unfolding taking place after binding on lignin (Rahikainen et al., 2011;  
347 Rahikainen, Moilanen, et al., 2013; Sammond et al., 2014).

348           The overall good fitting of the Models 1-3, coupled with good identifiability of  
349 reversible adsorption constants, especially in Model 3 (completely reversible adsorption)  
350 nevertheless pointed out that the adsorption of monocomponent cellulases on lignin is  
351 reversible by nature. Although in some ways the statement might seem contradictory to  
352 previous understanding, this points the need to redefine the term irreversibility and not to  
353 confuse it with high binding affinity. Furthermore, this also points the need to understand the  
354 precise mechanism leading to the loss of enzyme activity. Model 1 in this work confirmed  
355 and slightly explained the previous finding and suggestion (Rahikainen et al., 2011). Initially  
356 the enzymes constantly change structural conformation as they adsorb and desorb reversibly.  
357 Incubation at elevated temperature increases the rate of the process and thus the binding  
358 affinity. As the process continues, eventually the protein structure unfolds and renders the  
359 enzymes to be bound irreversibly at a certain extent, losing activity. It remains to be seen by  
360 future work whether the loss of enzyme activity and the change to irreversible binding on  
361 lignin occurred sequentially, separately or simultaneously. Finally, it is important to stress  
362 that while the binding is reversible, the loss of activity due to denaturation is irreversible.  
363

364 *Competitive binding of cellulases*

365 Competitive binding study was performed to find if there is competition between selected  
366 monocomponent cellulases *TrCel6A* and *TrCel5A* which had the highest binding affinity  
367 based on the adsorption isotherms (Figures 1 and 2, Table II). In this experimental setup, only  
368 the binding of radiolabeled enzyme was recorded. In the equimolar presence of one another,  
369 the enzymes showed competitive binding in the isotherms (Figure 4). The presence of  
370 *TrCel6A* reduced the binding of labeled *TrCel5A* significantly, whereas the presence of  
371 *TrCel5A* had less pronounced effect on the binding of labeled *TrCel6A*. The reduction of the  
372 binding was clearly visible in both L-HPS (Figure 4a) and L-HPWS (Figure 4b).

373           Fitting of one binding-site Langmuir adsorption model to the competitive  
374 adsorption isotherms still showed good fit in general (Table IV). The maximum adsorption  
375 capacity ( $B_{\max}$ ) of *TrCel6A* was less affected by *TrCel5A*, whereas the  $B_{\max}$  of *TrCel5A* was  
376 reduced more significantly by *TrCel6A* both in L-HPS and L-HPWS (Table IV). The  $B_{\max}$   
377 values of the mixture constituted by the two enzymes were nevertheless almost similar in  
378 magnitude (Table IV). This indicated that both enzymes competed for similar binding sites  
379 and *TrCel6A* predominated the competitive binding albeit lower  $B_{\max}$  value. Previously it  
380 was suggested that Vroman effect was present in a cellulolytic enzyme mixture where  
381 enzymes of greater affinity displaced others of lesser affinity (Yarbrough et al., 2015). In this  
382 study, affinity seemed to be not the factor since *TrCel5A* had higher if not similar affinity as  
383 *TrCel6A* based on both  $\alpha$  and  $K_{\text{ads}}$  (Table IV). However, in the original study that coined the  
384 Vroman effect, it was shown that proteins with larger size ( $M_w$ ) displaced the smaller ones  
385 (Vroman & Adams, 1969). Accordingly, *TrCel6A* is indeed larger than *TrCel5A* (Table I),  
386 therefore suggesting size as a plausible factor that governs competitive binding.

387           The presence of competitive binding between two enzymes showed that  
388 monitoring the adsorption of a multi-component system such as cellulases can be difficult to



389 perform. Nevertheless, the presence of competition and good fitting to Langmuir model also  
390 suggest that the binding of cellulases on lignin is exchangeable and thus reversible by nature.  
391 The finding thus supports the previous observations in this work and points that the binding  
392 of cellulases on lignin is both reversible and competitive as in the case of the binding of  
393 cellulases on cellulose (Kyriacou, Neufeld, & MacKenzie, 1989; Pellegrini et al., 2014).

394

## 395 Conclusions

396 The present work indicates that despite differences in the binding affinity of individual  
397 monocomponent cellulases, the binding is reversible by nature. Modelling of kinetic  
398 experiments suggests the possibility of previously reversible binding turning to irreversible  
399 which can explain the previous observations on retardation of enzymatic cellulose conversion  
400 in the presence of lignin. Due to reversible nature of binding, the negative effect of lignin can  
401 plausibly be alleviated by including additives in the reaction. Given the indication that the  
402 binding turns irreversible hence losing activity due to structural unfolding over time,  
403 engineering or finding novel enzymes with improved thermostability can be an avenue to  
404 pursue. Future studies should be directed into deciphering the underlying mechanism and  
405 factors that govern the deactivation of the enzyme by lignin. The competition among  
406 cellulases in the adsorption on lignin highlights the necessity to develop methods able to  
407 distinguish the binding and activity of individual enzymes in a mixture in order to identify  
408 and selectively improve the necessary enzyme component.

409

## 410 Nomenclature

411  $B_{\max}$ : maximum adsorption constant ( $\mu\text{mol/g}$ )

412  $K_{\text{ads}}$ : Langmuir adsorption constant ( $1/\mu\text{mol}$ )

413  $\alpha$ : relative association constant ( $1/\text{g}$ )

414 E: free enzymes ( $\mu\text{mol/l}$ )  
415 L: free binding sites in lignin-rich residues (g/l)  
416 EL: bound enzymes ( $\mu\text{mol/g}$ )  
417  $k_{\text{Rev}}$ : reversible adsorption constant ( $\text{l}^2/\mu\text{mol g h}$ )  
418  $k_{-\text{Rev}}$ : reversible desorption constant ( $\text{l/g h}$ )  
419  $k_{\text{Ir}}$ : irreversible adsorption constant ( $\text{l/g h}$  in Model 1; otherwise  $\text{l}^2/\mu\text{mol g h}$  in other models)

420

#### 421 Acknowledgments

422 PhD study of DTD is funded by the BioValue SPIR, Strategic Platform for Innovation and  
423 Research on value added products from biomass, which is co-funded by The Innovation Fund  
424 Denmark, Case No: 0603-00522B. Miriam Kellock is thanked for preparing the L-HPS.

425

#### 426 References

427 Barsberg, S., Selig, M. J., & Felby, C. (2013). Impact of lignins isolated from pretreated  
428 lignocelluloses on enzymatic cellulose saccharification. *Biotechnology Letters*, *35*(2),  
429 189–195. <https://doi.org/10.1007/s10529-012-1061-x>

430 Börjesson, J., Engqvist, M., Sipos, B., & Tjerneld, F. (2007). Effect of poly(ethylene glycol)  
431 on enzymatic hydrolysis and adsorption of cellulase enzymes to pretreated  
432 lignocellulose. *Enzyme and Microbial Technology*, *41*(1–2), 186–195.  
433 <https://doi.org/10.1016/j.enzmictec.2007.01.003>

434 Djajadi, D. T., Hansen, A. R., Jensen, A., Thygesen, L. G., Pinelo, M., Meyer, A. S., &  
435 Jørgensen, H. (2017). Surface properties correlate to the digestibility of hydrothermally  
436 pretreated lignocellulosic Poaceae biomass feedstocks. *Biotechnology for Biofuels*,  
437 *10*(1), 49. <https://doi.org/10.1186/s13068-017-0730-3>

438 Djajadi, D. T., Jensen, M. M., Oliveira, M., Jensen, A., Thygesen, L. G., Pinelo, M., ...  
439 Meyer, A. S. (2018). Lignin from hydrothermally pretreated grass biomass retards  
440 enzymatic cellulose degradation by acting as a physical barrier rather than by inducing  
441 nonproductive adsorption of enzymes. *Biotechnology for Biofuels*, 11(1), 85.  
442 <https://doi.org/10.1186/s13068-018-1085-0>

443 Gilkes, N. R., Jervis, E., Henrissat, B., Tekant, B., Miller, R. C., Warren, R. A. J., & Kilburn,  
444 D. G. (1992). The adsorption of a bacterial cellulase and its two isolated domains to  
445 crystalline cellulose. *Journal of Biological Chemistry*, 267(10), 6743–6749.

446 Kellock, M., Rahikainen, J., Marjamaa, K., & Kruus, K. (2017). Lignin-derived inhibition of  
447 monocomponent cellulases and a xylanase in the hydrolysis of lignocellulosics.  
448 *Bioresource Technology*, 232, 183–191. <https://doi.org/10.1016/j.biortech.2017.01.072>

449 Kyriacou, A., Neufeld, R. J., & MacKenzie, C. R. (1989). Reversibility and competition in  
450 the adsorption of *Trichoderma reesei* cellulase components. *Biotechnology and*  
451 *Bioengineering*, 33(5), 631–637. <https://doi.org/10.1002/bit.260330517>

452 Lan, T. Q., Lou, H., & Zhu, J. Y. (2013). Enzymatic Saccharification of Lignocelluloses  
453 Should be Conducted at Elevated pH 5.2-6.2. *Bioenergy Research*, 6, 476–485.  
454 <https://doi.org/10.1007/s12155-012-9273-4>

455 Latour, R. A. (2015). The Langmuir isotherm: A commonly applied but misleading approach  
456 for the analysis of protein adsorption behavior. *Journal of Biomedical Materials*  
457 *Research - Part A*, 103(3), 949–958. <https://doi.org/10.1002/jbm.a.35235>

458 Li, M., Pu, Y., & Ragauskas, A. J. (2016). Current understanding of the correlation of lignin  
459 structure with biomass recalcitrance. *Frontiers in Chemistry*, 4, 45.  
460 <https://doi.org/10.3389/fchem.2016.00045>

461 Liu, H., Sun, J., Leu, S.-Y., & Chen, S. (2016). Toward a fundamental understanding of  
462 cellulase-lignin interactions in the whole slurry enzymatic saccharification process.  
463 *Biofuels, Bioproducts and Biorefining*, 10, 648–663. <https://doi.org/10.1002/bbb>

464 Means, G. E., & Feeney, R. E. (1968). Reductive alkylation of amino groups in proteins.  
465 *Biochemistry*, 7(1965), 2192–2201. <https://doi.org/10.1021/bi00846a023>

466 Nakagame, S., Chandra, R. P., Kadla, J. F., & Saddler, J. N. (2011). The isolation,  
467 characterization and effect of lignin isolated from steam pretreated Douglas-fir on the  
468 enzymatic hydrolysis of cellulose. *Bioresource Technology*, 102(6), 4507–4517.  
469 <https://doi.org/10.1016/j.biortech.2010.12.082>

470 Nidetzky, B., Steiner, W., Hayn, M., & Claeysens, M. (1994). Cellulose hydrolysis by the  
471 cellulases from *Trichoderma reesei*: a new model for synergistic interaction. *The*  
472 *Biochemical Journal*, 298(1994), 705–710.

473 Norde, W. (1986). Adsorption of proteins from solution at the solid-liquid interface.  
474 *Advances in Colloid and Interface Science*, 25(C), 267–340.  
475 [https://doi.org/10.1016/0001-8686\(86\)80012-4](https://doi.org/10.1016/0001-8686(86)80012-4)

476 Palonen, H., Tenkanen, M., & Linder, M. (1999). Dynamic interaction of *Trichoderma reesei*  
477 cellobiohydrolases Cel6A and Cel7A and cellulose at equilibrium and during hydrolysis.  
478 *Applied and Environmental Microbiology*, 65(12), 5229–5233.

479 Pellegrini, V. O. A., Lei, N., Kyasaram, M., Olsen, J. P., Badino, S. F., Windahl, M. S., ...  
480 Westh, P. (2014). Reversibility of substrate adsorption for the cellulases Cel7A, Cel6A,  
481 and Cel7B from *Hypocrea jecorina*. *Langmuir*, 30(42), 12602–12609.  
482 <https://doi.org/10.1021/la5024423>

483 Pihlajaniemi, V., Sipponen, M. H., Kallioinen, A., Nyssölä, A., & Laakso, S. (2016). Rate-

484       constraining changes in surface properties, porosity and hydrolysis kinetics of  
485       lignocellulose in the course of enzymatic saccharification. *Biotechnology for Biofuels*,  
486       9(1), 18. <https://doi.org/10.1186/s13068-016-0431-3>

487       Rabe, M., Verdes, D., & Seeger, S. (2011). Understanding protein adsorption phenomena at  
488       solid surfaces. *Advances in Colloid and Interface Science*, 162(1–2), 87–106.  
489       <https://doi.org/10.1016/j.cis.2010.12.007>

490       Rahikainen, J., Evans, J. D., Mikander, S., Kalliola, A., Puranen, T., Tamminen, T., ...  
491       Kruus, K. (2013). Cellulase-lignin interactions-The role of carbohydrate-binding module  
492       and pH in non-productive binding. *Enzyme and Microbial Technology*, 53(5), 315–321.  
493       <https://doi.org/10.1016/j.enzmictec.2013.07.003>

494       Rahikainen, J., Martin-Sampedro, R., Heikkinen, H., Rovio, S., Marjamaa, K., Tamminen, T.,  
495       ... Kruus, K. (2013). Inhibitory effect of lignin during cellulose bioconversion: The  
496       effect of lignin chemistry on non-productive enzyme adsorption. *Bioresource*  
497       *Technology*, 133, 270–278. <https://doi.org/10.1016/j.biortech.2013.01.075>

498       Rahikainen, J., Mikander, S., Marjamaa, K., Tamminen, T., Lappas, A., Viikari, L., & Kruus,  
499       K. (2011). Inhibition of enzymatic hydrolysis by residual lignins from softwood - study  
500       of enzyme binding and inactivation on lignin-rich surface. *Biotechnology and*  
501       *Bioengineering*, 108(12), 2823–2834. <https://doi.org/10.1002/bit.23242>

502       Rahikainen, J., Moilanen, U., Nurmi-Rantala, S., Lappas, A., Koivula, A., Viikari, L., &  
503       Kruus, K. (2013). Effect of temperature on lignin-derived inhibition studied with three  
504       structurally different cellobiohydrolases. *Bioresource Technology*, 146, 118–125.  
505       <https://doi.org/10.1016/j.biortech.2013.07.069>

506       Rodrigues, A. C., Leitão, A. F., Moreira, S., Felby, C., & Gama, M. (2012). Recycling of  
507       cellulases in lignocellulosic hydrolysates using alkaline elution. *Bioresource*

508        *Technology*, 110, 526–533. <https://doi.org/10.1016/j.biortech.2012.01.140>

509     Saini, J. K., Patel, A. K., Adsul, M., & Singhania, R. R. (2016). Cellulase adsorption on  
510        lignin: A roadblock for economic hydrolysis of biomass. *Renewable Energy*, 98, 29–42.  
511        <https://doi.org/10.1016/j.renene.2016.03.089>

512     Sammond, D. W., Yarbrough, J. M., Mansfield, E., Bomble, Y. J., Hobdey, S. E., Decker, S.  
513        R., ... Crowley, M. F. (2014). Predicting enzyme adsorption to lignin films by  
514        calculating enzyme surface hydrophobicity. *Journal of Biological Chemistry*, 289(30),  
515        20960–20969. <https://doi.org/10.1074/jbc.M114.573642>

516     Sewalt, V. J. H., Glasser, W. G., & Beauchemin, K. a. (1997). Lignin impact on fiber  
517        degradation . 3 . Reversal of inhibition of enzymatic hydrolysis by chemical  
518        modification of lignin and by additives. *Journal of Agricultural and Food Chemistry*,  
519        45, 1823–1828. <https://doi.org/10.1021/jf9608074>

520     Sipponen, M. H., Rahikainen, J., Leskinen, T., Pihlajaniemi, V., Mattinen, M.-L., Lange, H.,  
521        ... Österberg, M. (2017). Structural changes of lignin in biorefinery pretreatments and  
522        consequences to enzyme-lignin interactions - OPEN ACCESS. *Nordic Pulp and Paper*  
523        *Research Journal*, 32(4), 550–571. [https://doi.org/10.3183/NPPRJ-2017-32-04-p550-](https://doi.org/10.3183/NPPRJ-2017-32-04-p550-571)  
524        571

525     Sluiter, A., Hames, B., Ruiz, R., Scarlata, C., Sluiter, J., Templeton, D., & Crocker, D.  
526        (2008). *Determination of structural carbohydrates and lignin in biomass. Laboratory*  
527        *analytical procedure (LAP). NREL/TP-510-42618*. Golden, CO, USA.

528     Suurnäkki, A., Tenkanen, M., Siika-Aho, M., Niku-Paavola, M. L., Viikari, L., & Buchert, J.  
529        (2000). Trichoderma reesei cellulases and their core domains in the hydrolysis and  
530        modification of chemical pulp. *Cellulose*, 7(2), 189–209.  
531        <https://doi.org/10.1023/A:1009280109519>

532 Tack, B. F., Dean, J., Eilat, D., Lorenz, P. E., & Schechter, A. N. (1980). Tritium Labeling of  
533 Proteins to High Specific Radioactivity by Reductive Methylation. *Journal of Biological*  
534 *Chemistry*, 255(18), 8842–8847.

535 Tu, M., Pan, X., & Saddler, J. N. (2009). Adsorption of cellulase on cellulolytic enzyme  
536 lignin from lodgepole pine. *Journal of Agricultural and Food Chemistry*, 57(17), 7771–  
537 7778. <https://doi.org/10.1021/jf901031m>

538 Várnai, A., Siika-aho, M., & Viikari, L. (2013). Carbohydrate-binding modules (CBMs)  
539 revisited : reduced amount of water counterbalances the need for CBMs. *Biotechnology*  
540 *for Biofuels*, 6, 30. <https://doi.org/10.1186/1754-6834-6-30>

541 Várnai, A., Viikari, L., Marjamaa, K., & Siika-aho, M. (2011). Adsorption of  
542 monocomponent enzymes in enzyme mixture analyzed quantitatively during hydrolysis  
543 of lignocellulose substrates. *Bioresource Technology*, 102(2), 1220–1227.  
544 <https://doi.org/10.1016/j.biortech.2010.07.120>

545 Vroman, L., & Adams, A. L. (1969). Findings with the recording ellipsometer suggesting  
546 rapid exchange of specific plasma proteins at liquid/solid interfaces. *Surface Science*, 16,  
547 438–446. [https://doi.org/10.1016/0039-6028\(69\)90037-5](https://doi.org/10.1016/0039-6028(69)90037-5)

548 Wahlström, R., Rahikainen, J., Kruus, K., & Suurnäkki, A. (2014). Cellulose hydrolysis and  
549 binding with *Trichoderma reesei* Cel5A and Cel7A and their core domains in ionic  
550 liquid solutions. *Biotechnology and Bioengineering*, 111(4), 726–733.  
551 <https://doi.org/10.1002/bit.25144>

552 Whitehead, T. A., Bandi, C. K., Berger, M., Park, J., & Chundawat, S. P. S. (2017).  
553 Negatively Supercharging Cellulases Render Them Lignin-Resistant. *ACS Sustainable*  
554 *Chemistry and Engineering*, 5(7), 6247–6252.  
555 <https://doi.org/10.1021/acssuschemeng.7b01202>

556 Yang, B., & Wyman, C. (2006). BSA treatment to enhance enzymatic hydrolysis of cellulose  
557 in lignin containing substrates. *Biotechnology and Bioengineering*, 94(5), 611–617.  
558 <https://doi.org/10.1002/bit>

559 Yarbrough, J. M., Mittal, A., Mansfield, E., Taylor, L. E., Hobdey, S. E., Sammond, D. W.,  
560 ... Vinzant, T. B. (2015). New perspective on glycoside hydrolase binding to lignin  
561 from pretreated corn stover. *Biotechnology for Biofuels*, 8(1), 214.  
562 <https://doi.org/10.1186/s13068-015-0397-6>

563 Yu, Z., Gwak, K.-S., Treasure, T., Jameel, H., Chang, H., & Park, S. (2014). Effect of lignin  
564 chemistry on the enzymatic hydrolysis of woody biomass. *ChemSusChem*, 7, 1942–  
565 1950. <https://doi.org/10.1002/cssc.201400042>

566

567

568

569

570

571

572

573

574

575

576



577 Tables

578 **Table I.** Summary of the characteristics of monocomponent cellulases used in this study

Enzymes	Old name	EC number	Domain architecture	M <sub>w</sub> (kDa) <sup>1</sup>	pI <sup>2</sup>	Hydrophobic patch score <sup>2</sup>		
						Core	CBM	Total
<i>TrCel7A</i>	CBHI	3.2.1.91	GH7- CBM1	56.0	3.6- <u>4.3</u>	6.7	6.6	13.3
<i>TrCel6A</i>	CBHII	3.2.1.91	GH6- CBM1	56.7	5.4- <u>6.2</u>	14.1	1.9	16.0
<i>TrCel7B</i>	EGI	3.2.1.4	GH7- CBM1	51.9	4.5-4.9, <u>4.7</u>	6.2	0.8	7.0
<i>TrCel5A</i>	EGII	3.2.1.4	GH5- CBM1	48.2	<u>5.6</u>	2.6	7.0	9.6

579 1: Based on (Várnai et al., 2013)

580 2: Based on (Kellock et al., 2017); major isoform in pI measurement is underlined

581

582

583

584

585

586

587

588

589 **Table II.** Langmuir isotherm parameters from the fitted adsorption data of monocomponent  
 590 cellulases on isolated lignin-rich residues

Adsorbent	Enzyme	$10 \times B_{\max}$ ( $\mu\text{mol/g}$ )	$10 \times K_{\text{ads}}$ ( $l/\mu\text{mol}$ )	$10 \times \alpha$ ( $l/\text{g}$ )	$R^2$
L-HPS	<i>TrCel7A</i>	$3.34 \pm 0.28$	$5.48 \pm 0.82$	$1.83 \pm 0.31$	0.957
	<i>TrCel6A</i>	$3.66 \pm 0.33$	$8.58 \pm 1.86$	$3.14 \pm 0.74$	0.926
	<i>TrCel7B</i>	$7.94 \pm 1.29$	$1.42 \pm 0.47$	$1.13 \pm 0.42$	0.972
	<i>TrCel5A</i>	$9.13 \pm 0.61$	$8.94 \pm 1.32$	$8.16 \pm 1.32$	0.984
L-HPWS	<i>TrCel7A</i>	$0.84 \pm 0.06$	$6.02 \pm 0.96$	$0.51 \pm 0.09$	0.975
	<i>TrCel6A</i>	$1.72 \pm 0.15$	$6.57 \pm 1.28$	$1.13 \pm 0.24$	0.974
	<i>TrCel7B</i>	$4.27 \pm 1.64$	$0.62 \pm 0.28$	$0.26 \pm 0.16$	0.967
	<i>TrCel5A</i>	$3.07 \pm 0.24$	$4.66 \pm 0.61$	$1.43 \pm 0.22$	0.991

591  $B_{\max}$ : maximum adsorption capacity;  $K_{\text{ads}}$ : Langmuir adsorption constant;  $\alpha$ : relative  
 592 association constant ( $B_{\max} \times K_{\text{ads}}$ ).

593

594

595

596

597

598

599

600

601

602 **Table III.** The values and identifiability of fitting parameters of kinetic modelling

LRRs	Enzyme	Model	Fit	Parameters				
			R <sup>2</sup>	k <sub>Rev</sub> l <sup>2</sup> /(μmol g h)	k <sub>-Rev</sub> l/(g h)	k <sub>Ir</sub> <sup>*</sup>	B <sub>max</sub> μmol/g	K <sub>ads</sub> l/μmol
HPS	<i>TrCel6A</i>	Model 1	0.896	0.0157	0.0163	3.82E-10	0.356	0.959
HPS	<i>TrCel6A</i>	Model 2	0.896	0.0120	0.0166	3.64E-03	0.357	0.723
HPS	<i>TrCel6A</i>	Reversible	0.896	0.0157	0.0164		0.356	0.957
HPS	<i>TrCel6A</i>	Irreversible	0.772			0.0217	0.272	
HPS	<i>TrCel5A</i>	Model 1	0.923	0.0165	0.0171	1.45E-07	0.562	0.962
HPS	<i>TrCel5A</i>	Model 2	0.923	0.0154	0.0167	7.81E-04	0.562	0.921
HPS	<i>TrCel5A</i>	Reversible	0.923	0.0160	0.0167		0.562	0.958
HPS	<i>TrCel5A</i>	Irreversible	0.784			0.0158	0.471	
HPWS	<i>TrCel6A</i>	Model 1	0.945	0.0397	0.0855	1.18E-03	0.223	0.464
HPWS	<i>TrCel6A</i>	Model 2	0.936	0.0311	0.0515	3.01E-04	0.217	0.603
HPWS	<i>TrCel6A</i>	Reversible	0.936	0.0314	0.0518		0.217	0.606
HPWS	<i>TrCel6A</i>	Irreversible	0.640			0.0743	0.124	
HPWS	<i>TrCel5A</i>	Model 1	0.967	0.0202	0.0626	4.05E-04	0.385	0.322
HPWS	<i>TrCel5A</i>	Model 2	0.965	0.0140	0.0512	4.49E-03	0.378	0.274
HPWS	<i>TrCel5A</i>	Reversible	0.965	0.0188	0.0525		0.379	0.357
HPWS	<i>TrCel5A</i>	Irreversible	0.570			0.0332	0.170	

LRRs	Enzyme	Model	Fit	Identifiability (RSD at optimum fit)			
			R <sup>2</sup>	k <sub>Rev</sub>	k <sub>-Rev</sub>	k <sub>Ir</sub>	B <sub>max</sub>
HPS	<i>TrCel6A</i>	Model 1	0.896	9%	9%	4.86E+07%	3%
HPS	<i>TrCel6A</i>	Model 2	0.896	46%	10%	140%	3%
HPS	<i>TrCel6A</i>	Reversible	0.896	4%	10%		3%
HPS	<i>TrCel6A</i>	Irreversible	0.772			9%	1%
HPS	<i>TrCel5A</i>	Model 1	0.923	19%	23%	2.35E+05%	4%
HPS	<i>TrCel5A</i>	Model 2	0.923	28%	11%	513%	4%
HPS	<i>TrCel5A</i>	Reversible	0.923	10%	10%		5%
HPS	<i>TrCel5A</i>	Irreversible	0.784			0%	0%
HPWS	<i>TrCel6A</i>	Model 1	0.945	71%	65%	9%	4%
HPWS	<i>TrCel6A</i>	Model 2	0.936	30%	8%	3.03E+03%	3%
HPWS	<i>TrCel6A</i>	Reversible	0.936	3%	10%		4%
HPWS	<i>TrCel6A</i>	Irreversible	0.640			31%	3%
HPWS	<i>TrCel5A</i>	Model 1	0.967	78%	71%	49%	10%
HPWS	<i>TrCel5A</i>	Model 2	0.965	55%	10%	159%	13%
HPWS	<i>TrCel5A</i>	Reversible	0.965	25%	8%		13%
HPWS	<i>TrCel5A</i>	Irreversible	0.570			0%	0%

603 \*) k<sub>Ir</sub> is a 1<sup>st</sup> order rate constant with the unit l/(g h) in Model 1 and a 2<sup>nd</sup> order rate constant  
604 with the unit l<sup>2</sup>/(μmol g h) in other models.

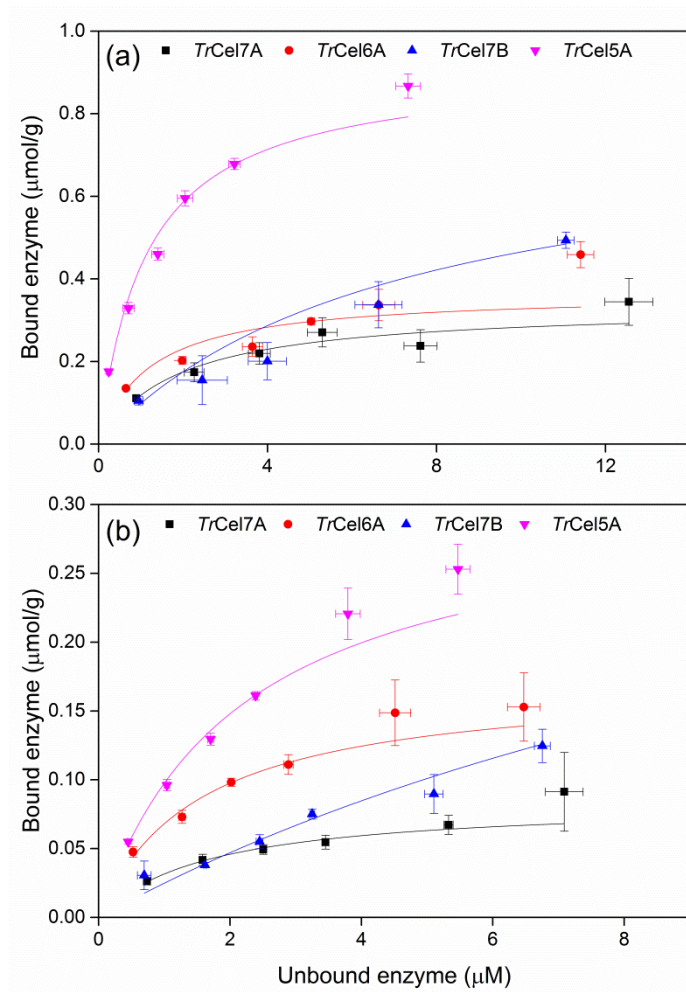
605

606 **Table IV.** Langmuir isotherm parameters from the fitted adsorption data of competitive  
 607 binding of *TrCel6A* and *TrCel5A* on isolated lignin-rich residues

Adsorbent	Enzyme	$10 \times B_{\max}$ ( $\mu\text{mol/g}$ )	$10 \times K_{\text{ads}}$ ( $l/\mu\text{mol}$ )	$10 \times \alpha$ ( $l/\text{g}$ )	$R^2$
L-HPS	<i>TrCel6A</i> -[ $^3\text{H}$ ]	$3.66 \pm 0.33$	$8.58 \pm 1.86$	$3.14 \pm 0.74$	0.926
	<i>TrCel6A</i> -[ $^3\text{H}$ ]	$2.11 \pm 0.05$	$16.3 \pm 2.87$	$3.43 \pm 0.61$	0.948
	+ <i>TrCel5A</i>				
	<i>TrCel5A</i> -[ $^3\text{H}$ ]	$9.13 \pm 0.61$	$8.94 \pm 1.32$	$8.16 \pm 1.32$	0.984
	<i>TrCel5A</i> -[ $^3\text{H}$ ]	$3.64 \pm 0.12$	$5.66 \pm 0.45$	$2.06 \pm 0.18$	0.992
	+ <i>TrCel6A</i>				
L-HPWS	<i>TrCel6A</i> -[ $^3\text{H}$ ]	$1.72 \pm 0.15$	$6.57 \pm 1.28$	$1.13 \pm 0.24$	0.974
	<i>TrCel6A</i> -[ $^3\text{H}$ ]	$1.17 \pm 0.11$	$15.4 \pm 3.17$	$1.80 \pm 0.41$	0.898
	+ <i>TrCel5A</i>				
	<i>TrCel5A</i> -[ $^3\text{H}$ ]	$3.07 \pm 0.24$	$4.66 \pm 0.61$	$1.43 \pm 0.22$	0.991
	<i>TrCel5A</i> -[ $^3\text{H}$ ]	$1.38 \pm 0.09$	$7.79 \pm 1.29$	$1.08 \pm 0.19$	0.979
	+ <i>TrCel6A</i>				

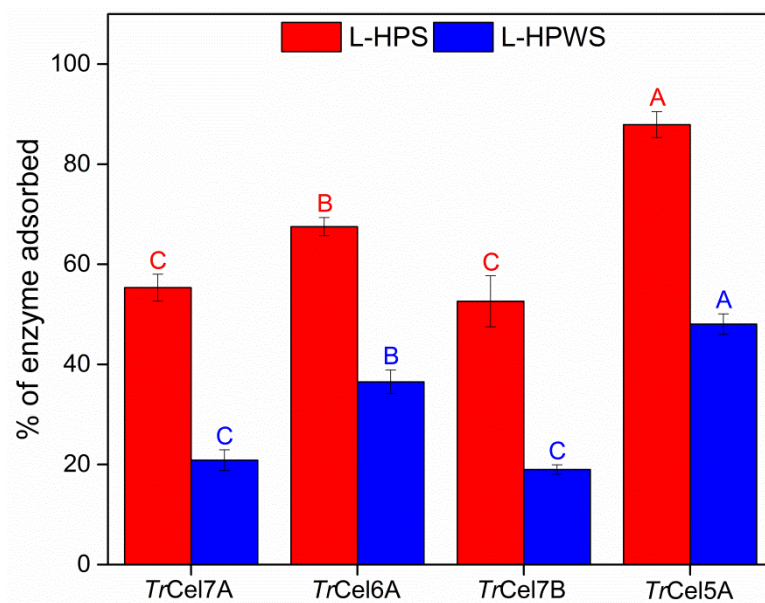
608  $B_{\max}$ : maximum adsorption capacity;  $K_{\text{ads}}$ : Langmuir adsorption constant;  $\alpha$ : relative

609 association constant ( $B_{\max} \times K_{\text{ads}}$ ).



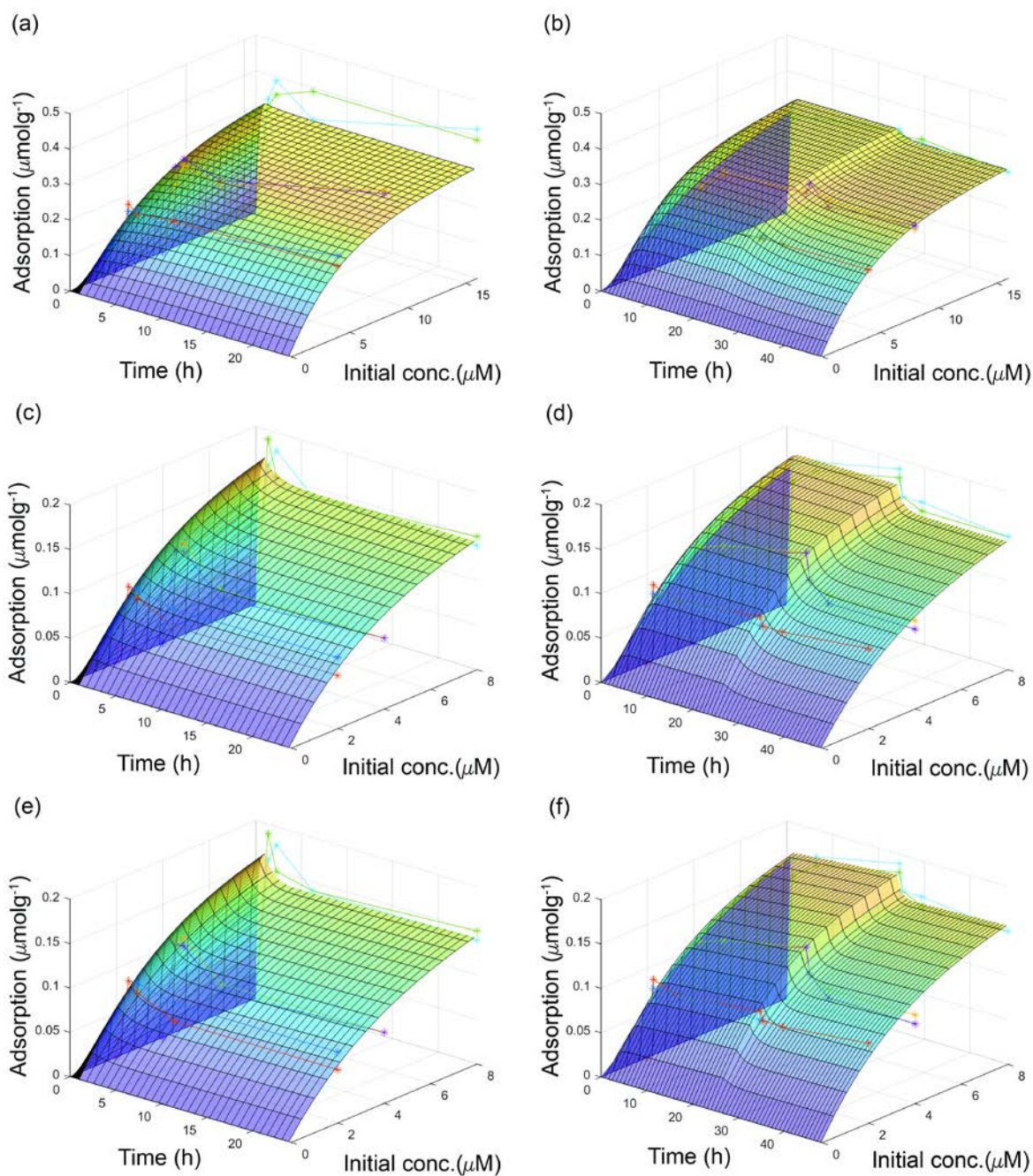
611

612 **Figure 1.** Adsorption isotherms of radiolabeled *TrCel7A*, *TrCel6A*, *TrCel7B* and *TrCel5A*  
 613 on lignin-rich residues isolated from hydrothermally pretreated (a) spruce (L-HPS) and (b)  
 614 wheat straw (L-HPWS) at 45°C, pH 5.0 after 1 h. Solid lines represent fitting of the  
 615 Langmuir adsorption model for one binding-site to the isotherms.



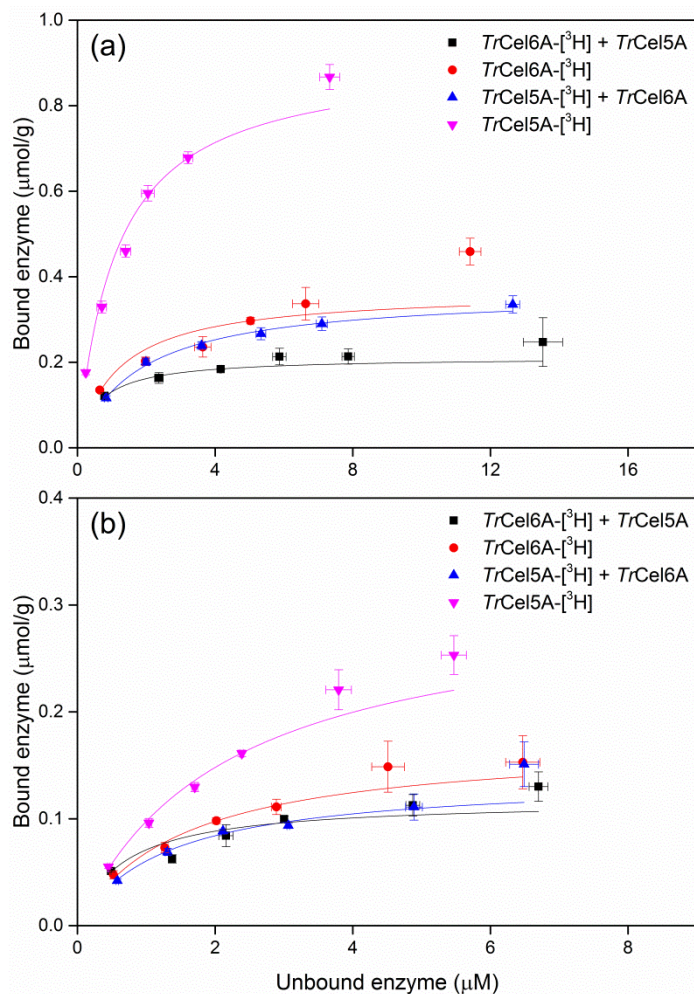
616

617 **Figure 2.** Adsorption of monocomponent cellulases to lignin-rich residues isolated from  
 618 hydrothermally pretreated spruce (L-HPS) and hydrothermally pretreated wheat straw (L-  
 619 HPWS) at initial protein concentration of 2  $\mu$ M after 1 h at 45°C. Different letters indicate  
 620 significant statistical difference based on ANOVA ( $p \leq 0.05$ ).



621

622 **Figure 3.** Response surface graphs displaying the fitting of experimental data of *TrCel6A*  
 623 adsorption on lignin-rich residues isolated from hydrothermally pretreated spruce (L-HPS) (a  
 624 & b) and hydrothermally pretreated wheat straw (L-HPWS) (c-f) modelled as reversible  
 625 adsorption (a-d) and using Model 1 (e & f) with early (a, c & e) and late dilution (b, d & f).



626

627 **Figure 4.** Competitive binding isotherms of *TrCel6A* and *TrCel5A* on lignin-rich residues  
 628 isolated from hydrothermally pretreated (a) spruce (L-HPS) and (b) wheat straw (L-HPWS)  
 629 at 45°C, pH 5.0 after 1 h. The tritium symbol ([<sup>3</sup>H]) indicates radiolabeled enzyme. Solid  
 630 lines represent fitting of the Langmuir adsorption model for one binding-site to the isotherms.

631